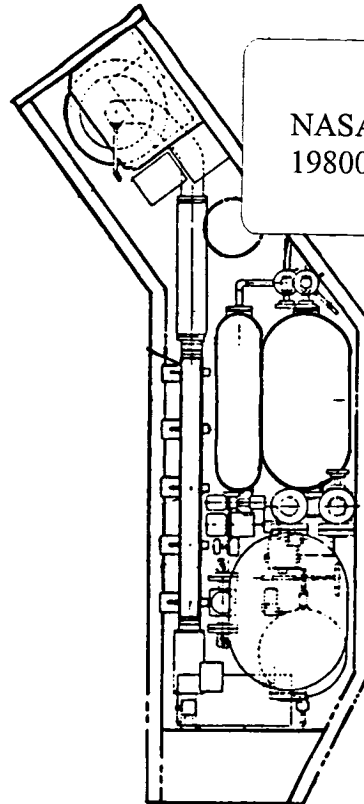
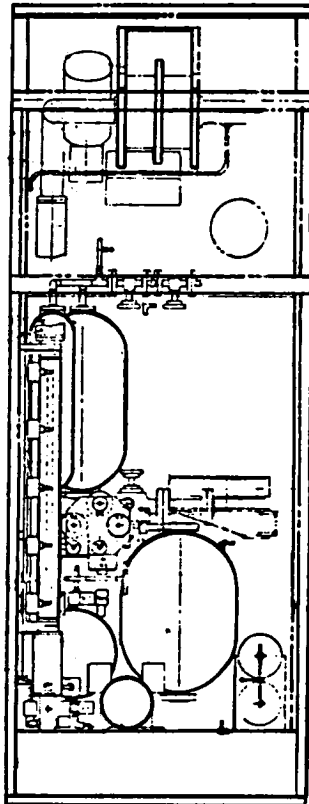




NASA CR-159,810

NASA CR-159810  
GDC-CRAD-80-002



NASA-CR-159810  
19800018902

# CONCEPTUAL DESIGN OF TWO-PHASE FLUID MECHANICS AND HEAT TRANSFER FACILITY FOR SPACELAB

**LIBRARY COPY**

JUL 31 1980

LIBRARY RESEARCH CENTER  
LIBRARY, NASA  
HAMPTON, VIRGINIA

**GENERAL DYNAMICS**  
*Convair Division*



NASA CR-159810  
GDC-CRAD-80-002

**CONCEPTUAL DESIGN OF TWO-PHASE  
FLUID MECHANICS AND HEAT TRANSFER  
FACILITY FOR SPACELAB**

June 1980

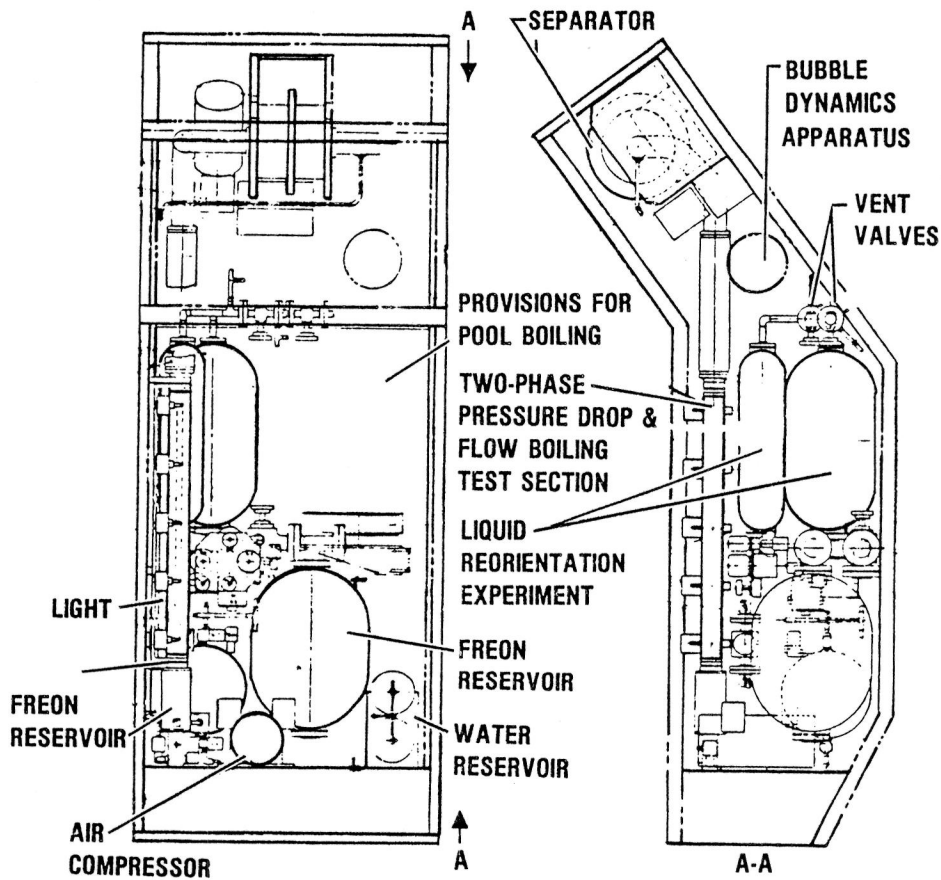
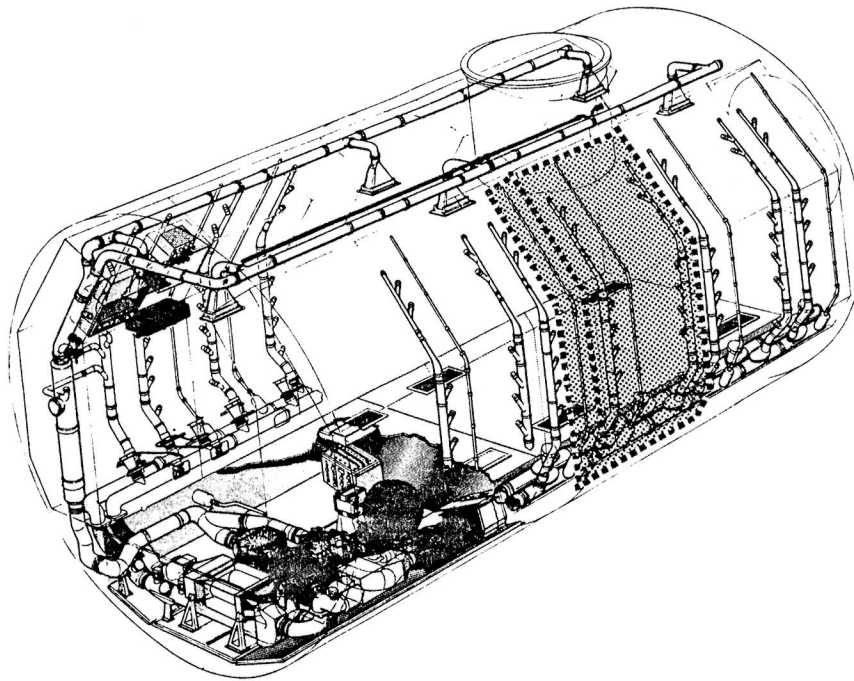
Prepared by  
B.F. North  
M.E. Hill

Prepared for  
National Aeronautics and Space Administration  
LEWIS RESEARCH CENTER  
21000 Brookpark Road  
Cleveland, Ohio 44135

Prepared Under  
Contract NAS3-21750

Prepared by  
GENERAL DYNAMICS CONVAIR DIVISION  
P.O. Box 80847  
San Diego, California 92138

*N80-27403 #*



*Five experiments are hard mounted in one double rack aboard the Spacelab*

1. Report No. NASA CR-159810	2. Government Accession No.	3. Recipient's Catalog No.	
4. Title and Subtitle Conceptual Design of Two-Phase Fluid Mechanics and Heat Transfer Facility For Spacelab		5. Report Date June 1980	
		6. Performing Organization Code	
7. Author(s) B. F. North and M. E. Hill		8. Performing Organization Report No. GDC-CRAD-80-002	
9. Performing Organization Name and Address General Dynamics/Convair Division P.O. Box 80847 San Diego, CA 92138		10. Work Unit No.	
		11. Contract or Grant No. NAS3-21750	
12. Sponsoring Agency Name and Address National Aeronautics and Space Administration Washington, D.C. 20546		13. Type of Report and Period Covered Contract Report	
		14. Sponsoring Agency Code	
15. Supplementary Notes Project Manager, E.P. Symons, Space Propulsion & Power Division NASA Lewis Research Center, Cleveland, Ohio 44135			
16. Abstract Five specific experiments were analyzed to provide definition of experiments designed to evaluate two-phase fluid behavior in low-gravity. The conceptual design represents a fluid mechanics and heat transfer facility for a double rack in Spacelab. The five experiments are two-phase flow patterns and pressure drop, flow boiling, pool boiling, liquid reorientation and interface bubble dynamics. Hardware was sized, instrumentation and data recording requirements defined and the five experiments were installed as an integrated experimental package. Applicable available hardware was selected in the experiment design and total experiment program costs were defined.			
17. Key Words (Suggested by Author(s)) Two-Phase Flow Boiling Reduced Gravity Spacelab		Settling Bubbles	18. Distribution Statement  Unclassified — Unlimited
19. Security Classif. (of this report) Unclassified	20. Security Classif. (of this page) Unclassified	21. No. of Pages 194	22. Price*

\* For sale by the National Technical Information Service, Springfield, Virginia 22161



## FOREWORD

This report was prepared by the Convair Division of General Dynamics (GDC) under Contract NAS 3-21750 to the National Aeronautics and Space Administration for the Lewis Research Center. This documents the work performed beginning with five experiment concepts described in the contract statement of work and ending with the definition of integration, installation, and operation of the experiment in a Spacelab double experiment rack. The purpose of all the experiments is to allow the study of the behavior of two-phase fluid mixtures in a controlled, low and near zero gravity environment.

The technical monitor for this contract was E. P. Symons. The principal members of the GDC study team were B. F. North as Program Manager, M. Hill as technical analyst, R. E. Bradley, economic analysis, and J. Ivan and L. Siden as design engineers. Consultants who performed critiques of the analytical models and provided guidance in experiment design were:

Professor Walter Frost, University of Tennessee Space Institute  
Experiments 1 and 2 - Two-Phase Flow Isothermal Flow  
Pattern and Pressure Drop, and Two-Phase Flow Boiling

Professors John Lienhard and Robert Peck, University of Kentucky  
Experiment 3 - Pool Boiling in Low Gravity

Professor Tom Bowman, Florida Institute of Technology  
Experiment 4 - Liquid Reorientation and Settling

Dr. Tom Labus, National Aeronautics and Space Administration,  
Lewis Research Center  
Experiment 5 - Bubble Interface Dynamics

The period of performance for this work was November 1978 through May 1980.



## TABLE OF CONTENTS

	<u>Page</u>
LIST OF FIGURES	vii
LIST OF TABLES	ix
SUMMARY	xi
1 INTRODUCTION	1-1
2 INTERFACE DATA	2-1
2.1 ORBITER	2-1
2.2 SPACELAB	2-6
3 TEST PROGRAM MODEL	3-1
4 EXPERIMENTS 1 AND 2, DESIGN DEFINITION	4-1
4.1 ISOTHERMAL FLOW PATTERN AND PRESSURE DROP	4-1
4.1.1 Description	4-1
4.1.2 Method of Operation	4-1
4.2 TWO-PHASE FLOW BOILING	4-5
4.2.1 Description	4-5
4.2.2 Method of Operation	4-5
4.3 INSTRUMENTATION	4-6
4.4 COMPONENTS	4-10
4.4.1 Pump	4-10
4.4.2 Blower	4-10
4.4.3 Separator	4-10
4.4.4 Tanks	4-11
4.5 ANALYSIS	4-11
4.5.1 Pressure Drop for Air/Water Experiment 1	4-11
4.5.2 Pressure Drop for Flow Boiling, Experiment 2	4-15
4.5.3 Presentation and Discussion of Calculations	4-16
4.5.4 Wall Temperature Calculations for Flow Boiling Experiment	4-19
5 POOL BOILING EXPERIMENT 3	
5.1 DESCRIPTION	5-1
5.2 METHOD OF OPERATION	5-1
5.3 INSTRUMENTATION	5-4
5.4 ANALYSIS TO PREDICT FLUID TEMPERATURE GRADIENTS	5-5

## TABLE OF CONTENTS, Contd

		<u>Page</u>
6	LIQUID REORIENTATION, EXPERIMENT 4	6-1
6.1	DESCRIPTION	6-1
6.2	METHOD OF OPERATION	6-1
6.3	INSTRUMENTATION	6-5
6.4	COMPONENTS	6-5
6.5	ANALYSES, LIQUID REORIENTATION TIME	6-7
6.5.1	Constant Acceleration	6-8
6.5.2	Impulsive Settling	6-12
7	BUBBLE DYNAMICS, EXPERIMENT 5	7-1
7.1	DESCRIPTION	7-1
7.2	METHOD OF OPERATION	7-2
7.3	INSTRUMENTATION AND COMPONENTS	7-4
7.4	ANALYSIS OF BUBBLE TERMINAL VELOCITY	7-4
7.4.1	Force Balance With a Submerged Gas Bubble	7-4
7.4.2	Normal Gravity Calculations	7-6
7.4.3	Reduced Gravity Calculations	7-7
7.4.4	Discussion of Results	7-10
8	PHOTOGRAPHIC DATA RECORDING	8-1
8.1	CAMERA REQUIREMENTS	8-1
8.2	LIGHTING	8-4
8.3	DATA RECORDING	8-4
9	DISCUSSION AND CONCLUSIONS	9-1
10	EXPERIMENT FACILITY COSTS	10-1
10.1	ESTIMATING METHODOLOGY	10-1
10.2	GROUND RULES AND ASSUMPTIONS	10-2
10.3	COST ESTIMATE	10-3
11	REFERENCES	11-1
APPENDIX A	INSTRUMENTATION/COMPONENT HARDWARE DESCRIPTIONS	A-1
APPENDIX B	LIQUID PROPELLANT REORIENTATION VELOCITY INCREMENTS - A CLOSED-FORM METHOD OF SOLUTION	B-1
APPENDIX C	DISTRIBUTION LIST - CONTRACT NAS3-21750	C-1

## LIST OF FIGURES

<u>Figure</u>		<u>Page</u>
2-1	Orbiter Axis Reference Definition	2-2
2-2	Effect of Atmospheric Drag on Orbiter in Drift Mode	2-3
2-3	Reaction Control Subsystem	2-4
2-4	RCS Propellant Feed Schematics	2-5
2-5	Spacelab Configuration, Double and Single Experiment Rack Location	2-7
2-6	Spacelab Module Frontal View	2-8
2-7	Rack Dimensions Per Spacelab Accommodation Handbook	2-9
2-8	Spacelab Venting Provisions, Layout of Forward Feed-Through Plate	2-10
2-9	Spacelab Venting Provisions	2-10
2-10	Spacelab Venting Provisions	2-11
2-11	Spacelab Venting Provisions	2-12
4-1	Flow Schematic - Experiments 1 and 2, Flow Pattern and Pressure Drop, and Flow Boiling	4-2
4-2	Layout, Flow Pattern and Pressure Drop Experiment	4-3
4-3	Layout, Flow Boiling Experiment	4-7
4-4	Pressure Loss as a Function of Quality for Isothermal Air Water System	4-17
4-5	Pressure Loss as a Function of Inlet Quality for Flow Boiling System	4-18
4-6	Regions of Heat Transfer in Convective Boiling	4-20
4-7	Values of F and S as Used in Equations 14 and 15	4-21
4-8	Wall Temperature as a Function of Position Along Tube for Various Experimental Conditions	4-24
5-1	Pool Boiling Test Cell, Large Box Illustrated	5-2
5-2	Pool Boiling Layout	5-3
5-3	Test Cell Configuration	5-6
5-4	Fluid Temperature Distribution After Eight Hours of Heating	5-7

## LIST OF FIGURES, (Cont.)

<u>Figure</u>		<u>Page</u>
6-1	Liquid Reorientation Schematic, Experiment 4	6-2
6-2	Liquid Reorientation Experiment Layout	6-3
6-3	Tank Geometries for Liquid Reorientation Analysis	6-7
6-4	Settling Weber Number Versus Bond Number for Various Fill Levels and Fineness Ratios	6-13
6-5	Acceleration and Burn Times for Impulsive Settling	6-14
7-1	Instrumentation Schematic - Experiment 5 Bubble Dynamics	7-2
7-2	Bubble Dynamics Experiment Layout	7-3
7-3	Terminal Velocities for Various Acceleration Levels	7-8
7-4	Drag Coefficient for Various Acceleration Levels	7-9
8-1	Candidate Photographic Equipment	8-2
8-2	Photographic Data Recording	8-3
8-3	IRIG Standard Format Time Codes	8-4
9-1	General Installation of Five Experiments in Spacelab Double Rack	9-2
9-2	Primary Thruster ON-OFF Pulse	9-3
9-3	Primary Thruster ON-OFF Pulse	9-3

## LIST OF TABLES

<u>Table</u>		<u>Page</u>
2-1	Accelerative G-Levels and Sources	2-3
2-2	Typical Orbital RCS Maximum Acceleration Levels	2-6
2-3	Typical RCS Propellant Survey	2-7
2-4	Spacelab Venting Provisions	2-13
2-5	Spacelab Venting Provisions	2-13
2-6	Spacelab Accommodation Features	2-13
3-1	Experiment Acceleration and RCS Propellant Requirements	3-2
4-1	Experiments 1 and 2 - Tests and Test Conditions	4-5
4-2	Instrumentation/Component Requirements for Experiments 1 and 2, Flow Patterns and Flow Boiling	4-8
4-3	Heat Fluxes for Wall Temperature Calculations	4-23
5-1	Test Parameters for Pool Boiling Experiment	5-4
5-2	Instrumentation/Component Requirements - Experiment 3, Pool Boiling	5-5
5-3	Thermal Analysis Results	5-7
6-1	Test Parameters for Liquid Reorientation, Experiment 4	6-1
6-2	Instrumentation/Component Requirements - Experiment 4, Liquid Reorientation	6-6
7-1	Instrument/Component Requirements - Experiment Versus Bubble Dynamics	7-4
8-1	Photosonics Camera Model 16 mm - 1 PL	8-5
8-2	Photographic Data Recording	8-6
10-1	Preliminary Experiment Hardware Cost Estimate Experiment 1 and 2	10-4
10-2	Preliminary Experiment Hardware Cost Estimate Experiment 3	10-4
10-3	Preliminary Experiment Hardware Cost Estimate Experiment 4	10-5
10-4	Preliminary Experiment Hardware Cost Estimate Experiment 5	10-5

LIST OF TABLES (Cont.)

<u>Table</u>		<u>Page</u>
10-5	Preliminary Two Phase Fluid Mechanics and Heat Transfer Facility Project Cost	10-6
10-6	Cost Estimate Range	10-6

## SUMMARY

Five specific experiments were analyzed to provide definition of experiments designed to evaluate two-phase fluid behavior in low-g. Analytical methods were selected or developed to predict the significant variables to be observed in each experiment and the probable range of physical characteristics to be measured. From these studies, equipment was sized and selection criteria established which were necessary to provide the desired conditions for observation of fluid behavior. These individually defined experiment requirements were then developed into system concepts and all five experiments configured and packaged to fit within a Spacelab double experiment rack. Instrumentation requirements were defined and integrated with each experiment with appropriate attention given to compatibility with the Spacelab Data Management Subsystem.

Flow schematics for each experiment are provided along with a description of the operation of the experiment, definition of instrumentation, ranges anticipated for the significant parameters, and a design drawing showing the installation of the experiment within the rack. A top drawing is also provided showing the five experiments to be physically compatible with the dimensional constraints of the rack.

The Orbiter/Spacelab/Experiment Facility interfaces have been defined and the facility has been designed to conform to those interfaces. Two problem areas have been defined by this study. The first is the total mission Reaction Control System (RCS) fuel required to perform all of the experiments. There is adequate fuel for this facility but none extra for other Spacelab requirements. The second is the limited range, and discreet thrust level available with the RCS. It is possible that the lower gravity level desired for the pool boiling experiment may not be practical without special consideration of attaining the desired level independently with an experiment peculiar thrusting system. Definition of such a system was not within the scope of this contract.

With the exceptions noted above, it is concluded that the five selected experiments can be successfully integrated into a Spacelab double rack and used during future Spacelab missions to provide experimental verification or basis for modifications of analytical models used to predict two-phase fluid behavior in low gravity. A cost estimate for hardware, development, and overall program cost is presented. The total program cost is estimated to range from \$2.44M for a minimum program with optimistic projection to \$5.2M for a highly conservative program estimate.



# 1

## INTRODUCTION

The purpose of this study was to provide a conceptual design of a two-phase fluid mechanics and heat transfer facility for Spacelab. To do this, five experiments were defined and analyzed with respect to fluid behavior in low gravity. These were:

1. Two-phase isothermal flow pattern and pressure drop
2. Two-phase flow boiling
3. Pool boiling
4. Liquid reorientation and settling
5. Bubble dynamics

Specific objectives of the study were to provide the basis for fluid selection, equipment sizing and selection, definition of instrumentation and supporting equipment requirements, and overall program costs including hardware and engineering development.

This report presents the conceptual design of each experiment, the analysis, and analytical results supporting the design. The Orbiter/Spacelab interfaces affecting the design are presented and ramifications of such interfaces are discussed. The fluid flow schematics, instrumentation type and location, and design and installation drawings of each experiment are shown along with equipment lists, instrumentation lists, and a test run summary. The cost estimate detailing equipment, development, and program costs are presented with the assumption that total costs are predicated on the five experiments being flown as an integrated experiment package.

The lead scientists' contributions to this study have been incorporated to achieve a well-defined test program to obtain experimental verification of analytical models used to predict two-phase fluid behavior in low gravity conditions.



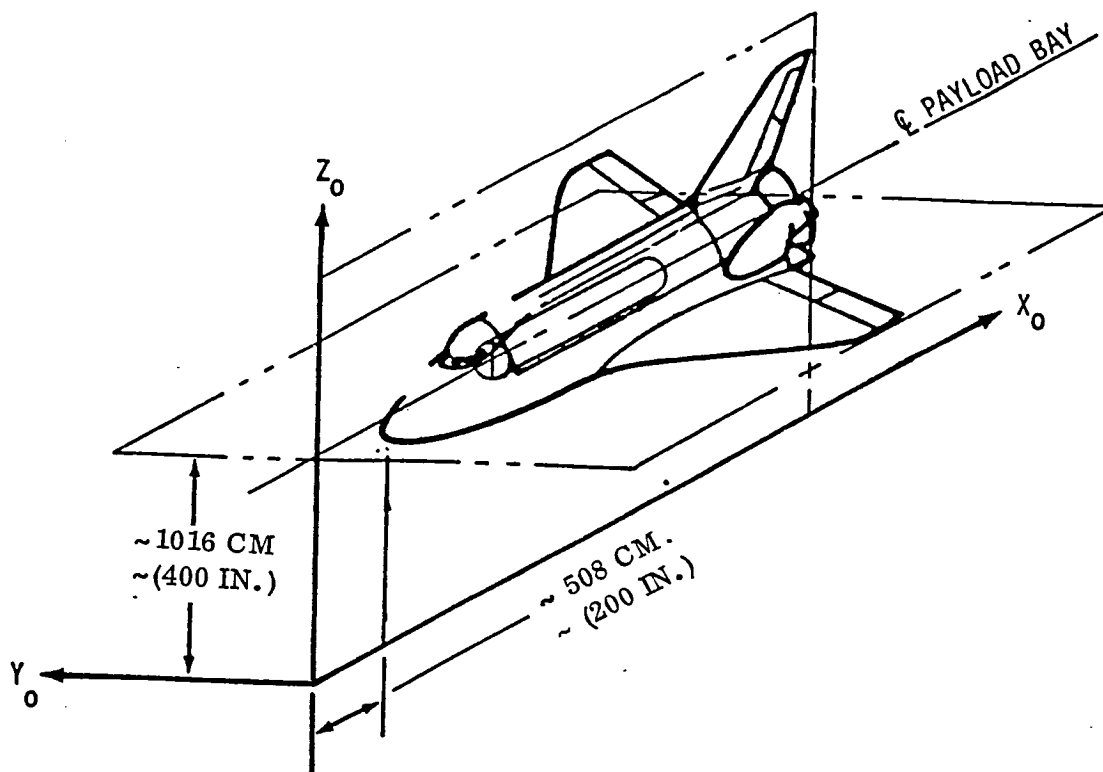
# 2

## INTERFACE DATA

### 2.1 ORBITER

The Orbiter provides for transportation of Spacelab to and from earth orbits. Launch can be accomplished from either of two launch sites. The Eastern Test Range (ETR) at Cape Canaveral is used for low inclination orbits. The Western Test Range (WTR) is used for high inclination or polar orbits. Boost to suborbital velocity is accomplished by two solid rocket boosters and the orbiter main engine. The Orbiter Orbital Maneuvering Subsystem (OMS) is used to achieve orbital velocity and the desired orbit, perform orbit corrections, orbit transfer, rendezvous, and deorbit maneuvers. The Orbiter Reaction Control Subsystem (RCS) provides on-orbit thrusting for attitude correction, pointing ability and station-keeping. The RCS is proposed for experiment use to provide the controlled, sustained acceleration required for low gravity testing of the defined experiments. Figure 2-1 presents the Orbiter axis reference definition for later use in defining experiment location and orientation in the rack. The inherent gravity level induced by atmospheric drag on the Orbiter in drift mode is presented in Figure 2-2 for the reference axes of Figure 2-1. In addition to this basic, uncontrollable gravity level to which everything is subject, there is another, somewhat inherent, set of forces resulting in g-jitter which is a transient acceleration imposed by crew member activity. An estimate of these accelerations and the activities causing them are presented in Table 2-1 from Reference 14.

The RCS used to provide the controlled g-level for testing is shown in Figure 2-3. The significant information provided by this figure is the fact that there are two thruster systems (main and vernier). They are located in a manner such that two or more must be fired to provide translating motion, and only one discreet thrust level is obtained per thruster. This introduces two requirements. The first is the programming necessary to achieve translation along the required axis. A schematic of the RCS as shown in Figure 2-4 shows this to be possible as each of the thrusters is capable of being independently fired. The software necessary to provide the proper motion necessary for these experiments would have to account for the CG shift during the mission or, by pre-mission planning, assure that the shift is within an acceptable range to prevent excessive angular motion with attendant effect on experiment results. The second requirement is the ability to achieve the desired acceleration level with the RCS. Table 2-2 gives typical RCS maximum acceleration levels. As will be seen later in examining the acceleration levels desired for the experiments, the RCS has adequate magnitude at acceleration to meet experiment requirements but lacks variability and adjustment to low levels.



TYPE: ROTATING, ORBITER REFERENCED

ORIGIN: APPROXIMATELY 508 CM (200 IN) AHEAD OF THE NOSE AND APPROXIMATELY 1016 CM (400 IN) BELOW THE CENTERLINE OF THE PAYLOAD BAY

ORIENTATION AND LABELING: THE X AXIS IS PARALLEL TO THE CENTERLINE OF THE PAYLOAD BAY, NEGATIVE IN THE DIRECTION OF LAUNCH

THE Z AXIS IS POSITIVE UPWARD IN LANDING ATTITUDE

THE Y COMPLETES THE RIGHT-HAND SYSTEM

THE STANDARD SUBSCRIPT IS 0

Figure 2-1. Orbiter Axis Reference Definition

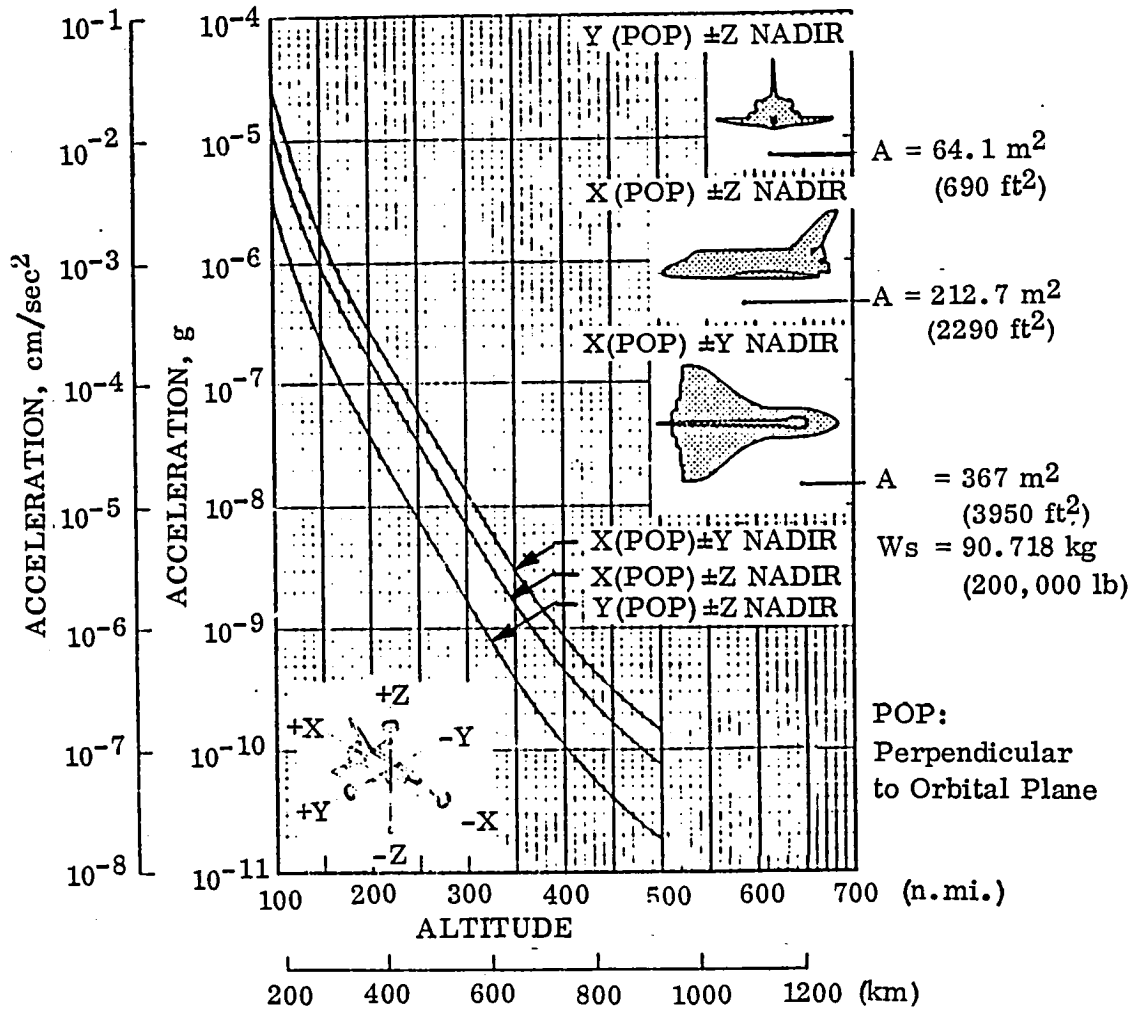


Figure 2-2. Effect of Atmospheric Drag on Orbiter in Drift Mode

Table 2-1. Accelerative G-Levels and Sources

SOURCE	DISTURBANCE VALUE (g)
GRAVITY GRADIENT	$8 \times 10^{-7}$
AERODYNAMIC DRAG	$2 \times 10^{-7}$
LEFT, RIGHT FLASH EVAPORATORS	$2.5 \times 10^{-7}$
BOTH FLASH EVAPORATORS	$1 \times 10^{-7}$
WATER DUMP	$8 \times 10^{-6}$
VFR SPIN-UP	$7 \times 10^{-7}$
THRUSTERS	$6 \times 10^{-5} - 6 \times 10^{-4}$
CREW MOTION	
BREATHING	$10^{-5} - 10^{-4}$
COUGHING	$5 \times 10^{-5} - 2 \times 10^{-4}$
SNEEZING	$2 \times 10^{-5} - 3 \times 10^{-4}$
CONSOLE OPERATION	$10^{-5} - 3 \times 10^{-5}$
BODY BENDING	$9 \times 10^{-5} - 3 \times 10^{-4}$
ARM ROTATION (90°)	$4 \times 10^{-5} - 2 \times 10^{-4}$
LEG ROTATION (45°)	$7 \times 10^{-5} - 2 \times 10^{-4}$
CROUCH AND STAND	$3 \times 10^{-4} - 5 \times 10^{-4}$

FREQUENCY BAND: 0.3 TO 2 HERTZ

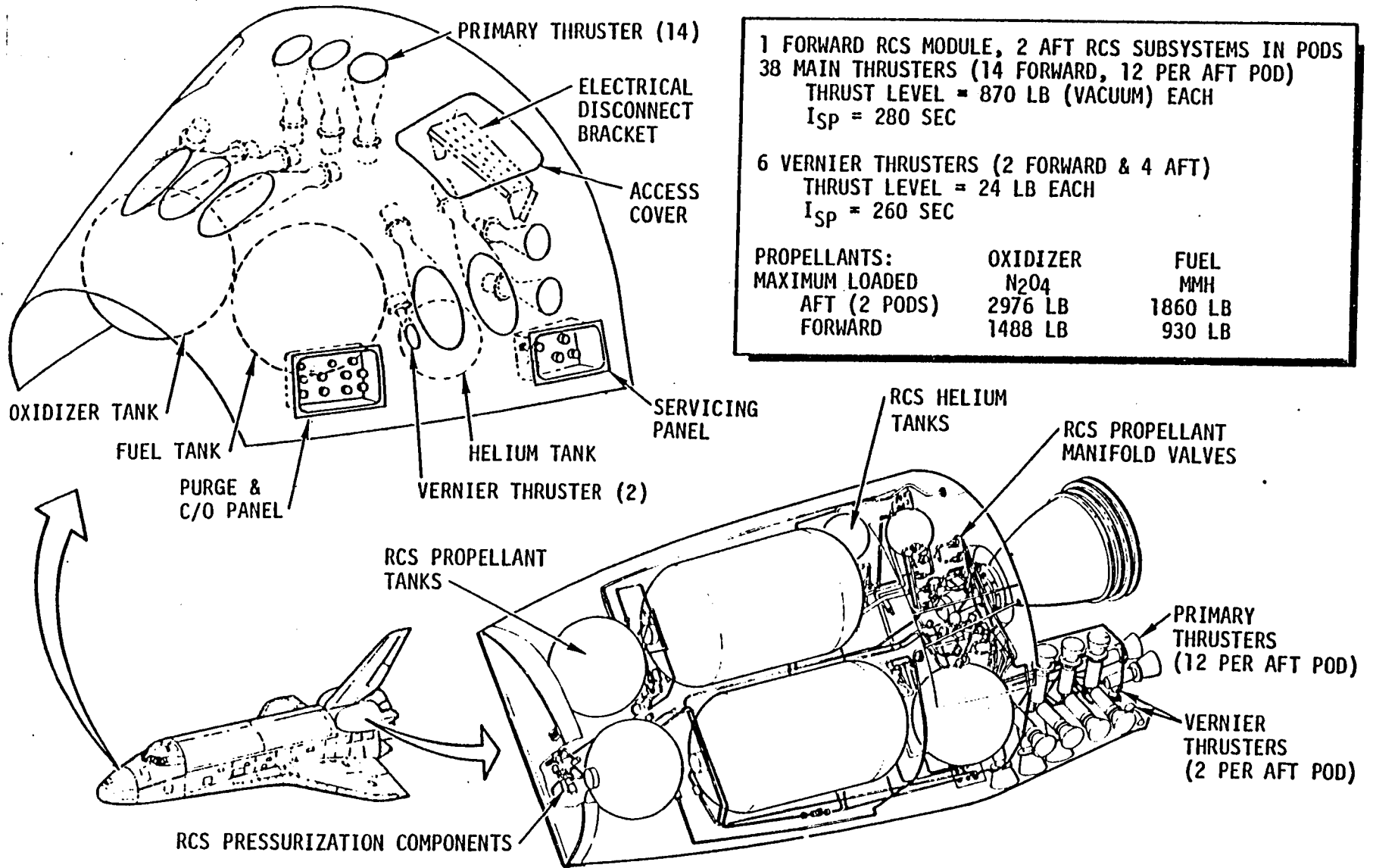


Figure 2-3. Reaction Control Subsystem

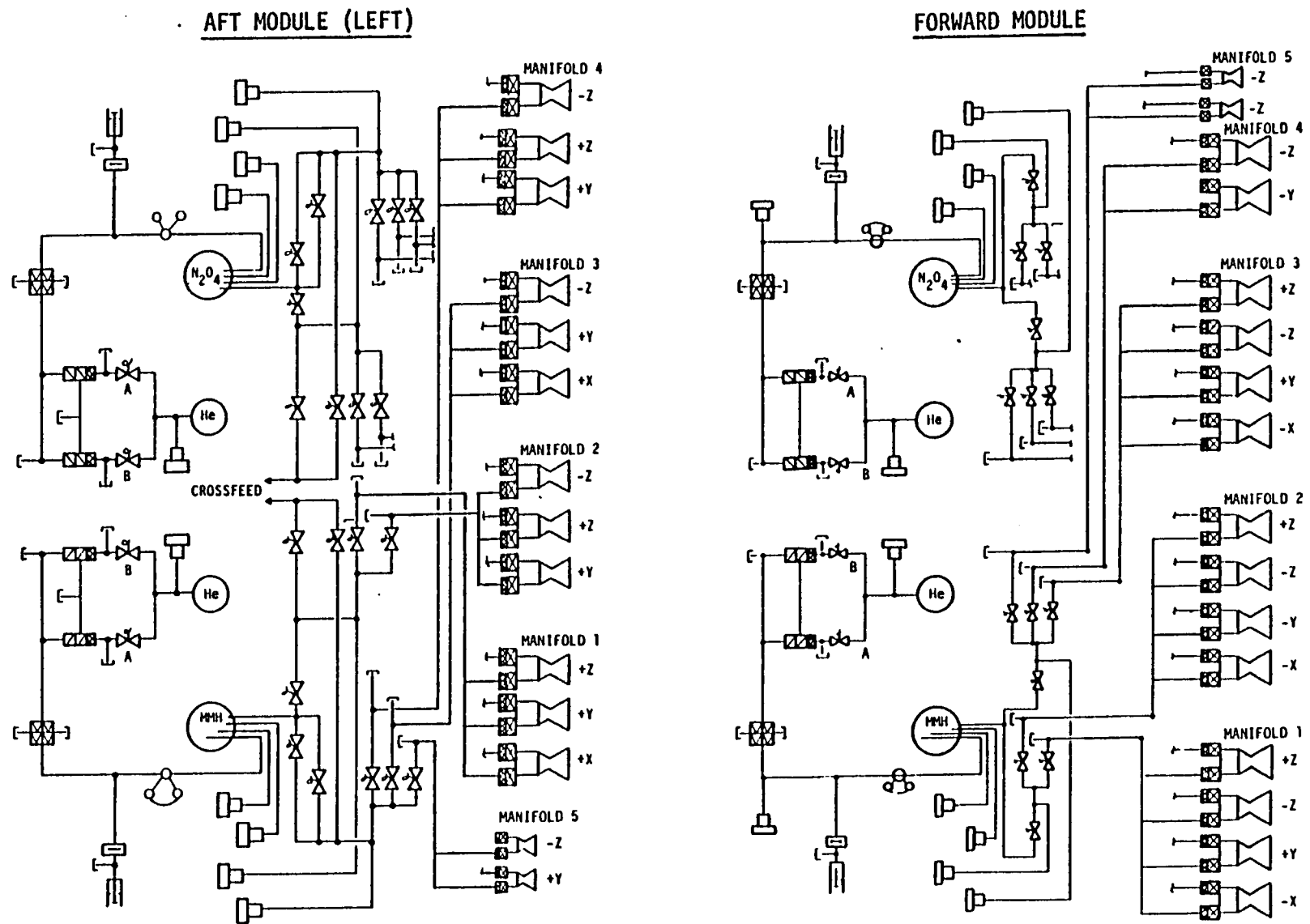


Figure 2-4. RCS Propellant Feed Schematics.

Table 2-2. Typical Orbital RCS Maximum Acceleration Levels

DIRECTION	TRANSLATIONAL ACCELERATION FT/SEC <sup>2</sup> (MPS <sup>2</sup> )					ROTATIONAL ACCELERATION DEG/SEC <sup>2</sup>			
	RCS SYSTEM	+X	-X	±Y	+Z	-Z	± $\ddot{\phi}$	+ $\ddot{\theta}$	- $\ddot{\theta}$
Primary Thruster	0.554 (0.169)	0.424 (0.129)	0.695 (0.212)	1.251 (0.381)	1.014 (0.309)	1.168	1.320	1.482	0.738
Vernier Thruster	0 0	0 0	0.0070 (0.0021)	0 0	0.0080 (0.0024)	0.037	0.024	0.017	0.019

Based on mass properties from Shuttle Operational Data Book, Volume II, Revision A, Amendment 1, for Orbiter at pre-deorbit with 32K lb (14515 Kg) cargo.

A typical representation of the RCS propellant budget is shown in Table 2-3. It is seen that about 1815 kg<sub>m</sub> (4000 lb<sub>m</sub>) of propellant is available for payload support. It will be shown later that this is very nearly that required to accomplish the experiments proposed for the fluid mechanics and heat transfer facility.

## 2.2 SPACELAB

A cutaway of the Spacelab configuration is shown in Figure 2-5. This picture shows the single and double rack locations and the shaded area depicts one possible location of a double rack which might be chosen for the fluid and heat transfer facility. The cabin air recirculating and the closed loop avionics cooling air distribution systems are shown. Although not deemed necessary at this time, it is seen that cooling capability is available in the rack if so desired. Figure 2-6 shows a view looking aft down the aisle of Spacelab and shows the access available to the payload specialist to monitor and run the facility. The dimensions of the double rack in which the experiment is to be housed is shown in Figure 2-7. The shaded areas shown are those areas in which access must be granted, if required, for passthrough of elements from other experiments or Spacelab required connections. These areas are to be evaluated on a case by case basis and will be peculiar to the specific Spacelab mission which transports the experiment facility. In general the design installation shown does not interfere in these areas. Where interference may be a problem will not be known until this experiment is integrated in a defined mission.

Because it is not permitted to contaminate the interior of Spacelab, venting provisions are provided in the basic Spacelab design. These provisions are detailed in Tables 2-4 and 2-5. Since these provisions are available to all of the on-board experiments, scheduling between experiments will probably be required to avoid overloading this system. The location of the venting system and details of connector interfaces to permit connection with the rack experiments are shown in Figures 2-8 through 2-11. The experiment design will accommodate mating features to be compatible with these interface features. In general, Spacelab provides several special accommodations available to the experiment without payload penalty. These features are shown in Table 2-6 and indicate that, in addition to flexibility in mounting

in the rack and plug-in power features, small articles required for the experiment can be stowed separately from the experiment. This is important when considering storage of film or film cartridges, camera lenses, experiment expendables, and possible plug-in sensors to accommodate wide readout ranges.

An extremely important interface is the Spacelab Command and Data Management Subsystem (CDMS). The CDMS provides adequate means to evaluate the test or experiment environment and offers extensive data management capability. The following data regarding the CDMS was extracted from the "Life Sciences Guide to the Space Shuttle and Spacelab Experiments' Handbook."

Table 2-3. Typical RCS Propellant Survey

	<u>lb<sub>m</sub></u>	<u>kg<sub>m</sub></u>
Total RCS Loadable	7,391	3,353
Unavailable (Incl. Residuals + Tank Loading Tolerances)	<u>-806</u>	<u>366</u>
	6,585	2,987
Required for Insertion	<u>-228</u>	<u>103</u>
	6,357	2,883
Required for Orbital Adjustment	<u>-899</u>	<u>408</u>
	5,458	2,476
Required for Entry	<u>-1,164</u>	<u>528</u>
	4,294	1,948
On-Orbit Dispersions and Contingencies	<u>-301</u>	<u>136</u>
Available for Payload Support	3,993	1,811

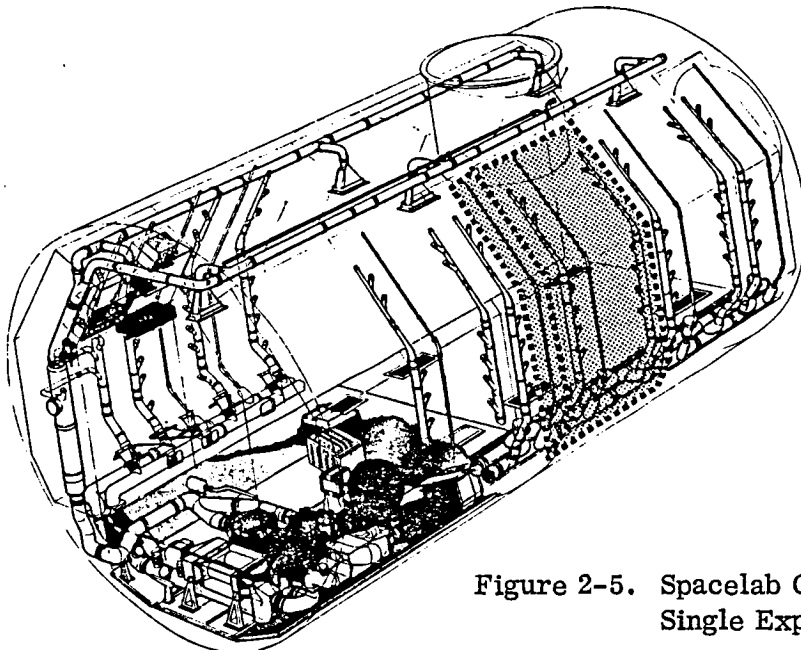


Figure 2-5. Spacelab Configuration, Double and Single Experiment Rack Locations

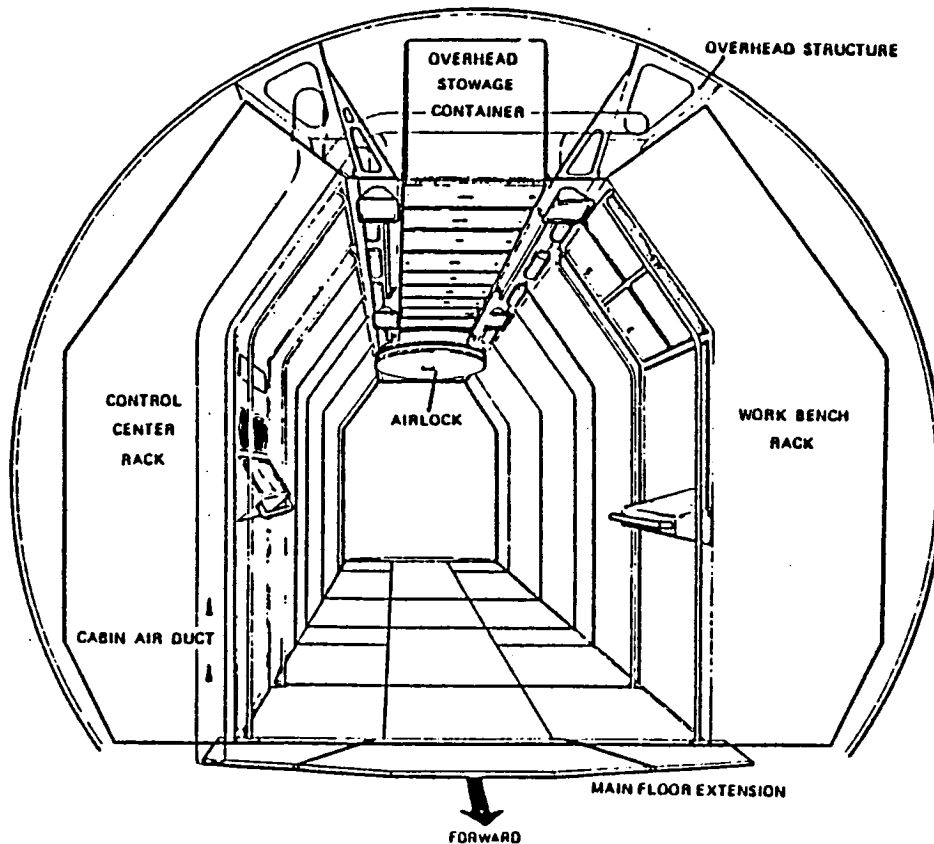


Figure 2-6. Spacelab Module Frontal View

### DIGITAL DATA

The Spacelab module's data management system enables the collection, processing, recording, on-board display, and transmission of low-rate digital data (including digitized analog) received from the flight experiments at 1 Mb/sec or less. Experiment-produced data with rates between 1 Mb/sec and 16 Mb/sec can be stored and/or transmitted to the ground, but these data cannot be processed or displayed on-board the spacecraft.

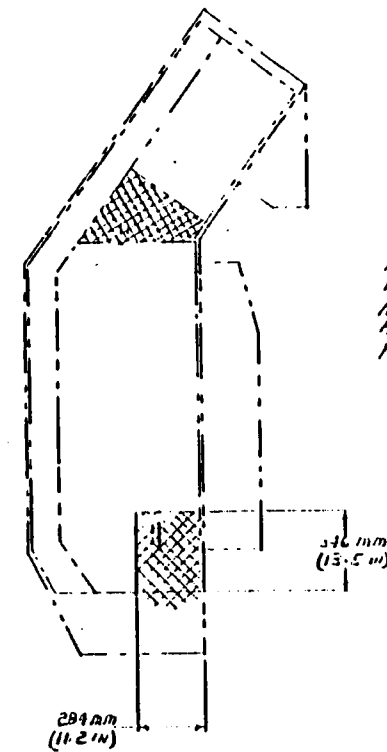
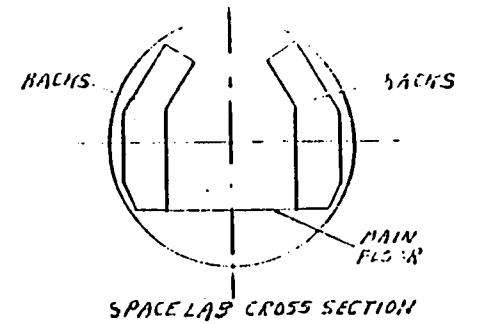
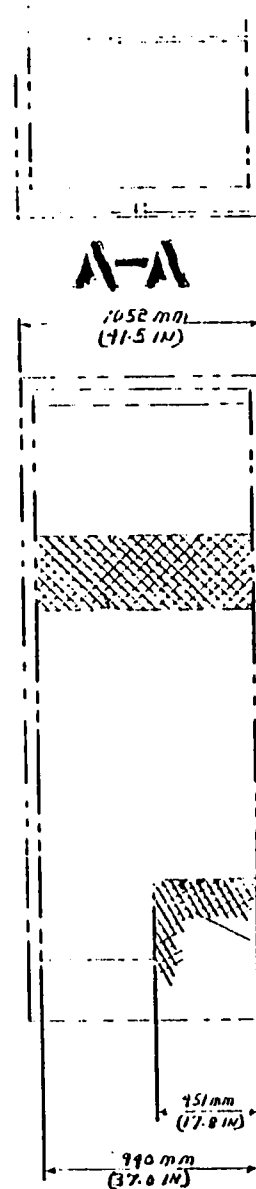
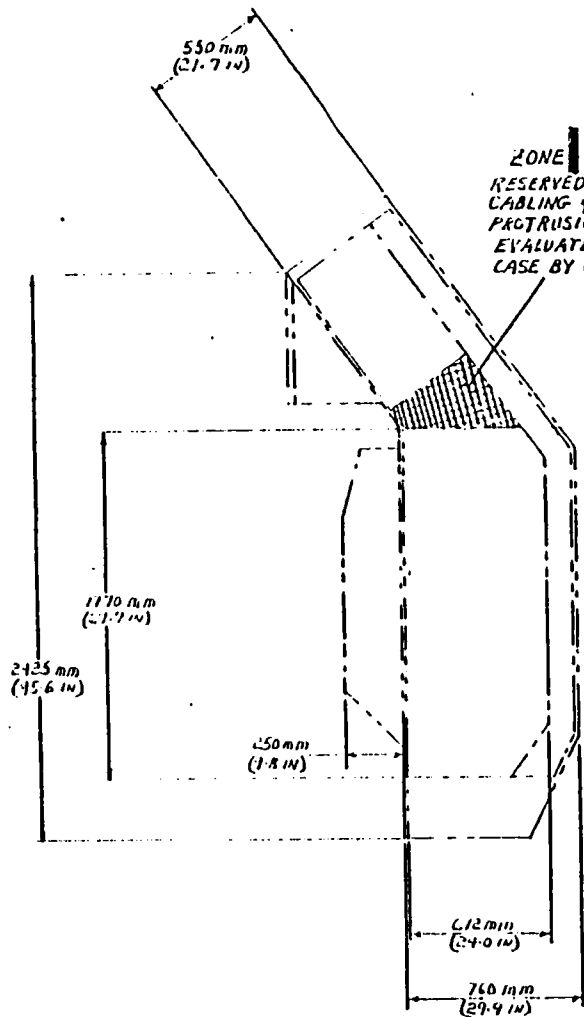
Low-rate digital data can be processed and analyzed on-board. These data may be formatted and displayed for review and analysis by the payload specialist while on-board or recorded on data tapes, or transmitted to the ground. The data may also be annotated with voice recording and/or time marks.

### ANALOG DATA

If feasible, analog data should be digitized to take full advantage of the SPACELAB's extensive digital data recording, processing, and transmission capabilities. Analog data which cannot be digitized may be recorded on-board and/or transmitted to the ground. Planned capabilities include:

- a. Analog to digital conversion. Data may be stored, transmitted to the ground, or processed and displayed on-board the spacecraft. Conversion rates are programmable at 1, 10, and 100 samples/sec.

2-9



RACK DIMENSIONS PER SPACE LAB ACCOMMODATION HANDBOOK SUP/2124 PAGES 4-1-8 THRU 4-1-17.

J. E. ... MAY 24, 1977

Figure 2-7. Rack Dimensions Per Spacelab Accommodation Handbook

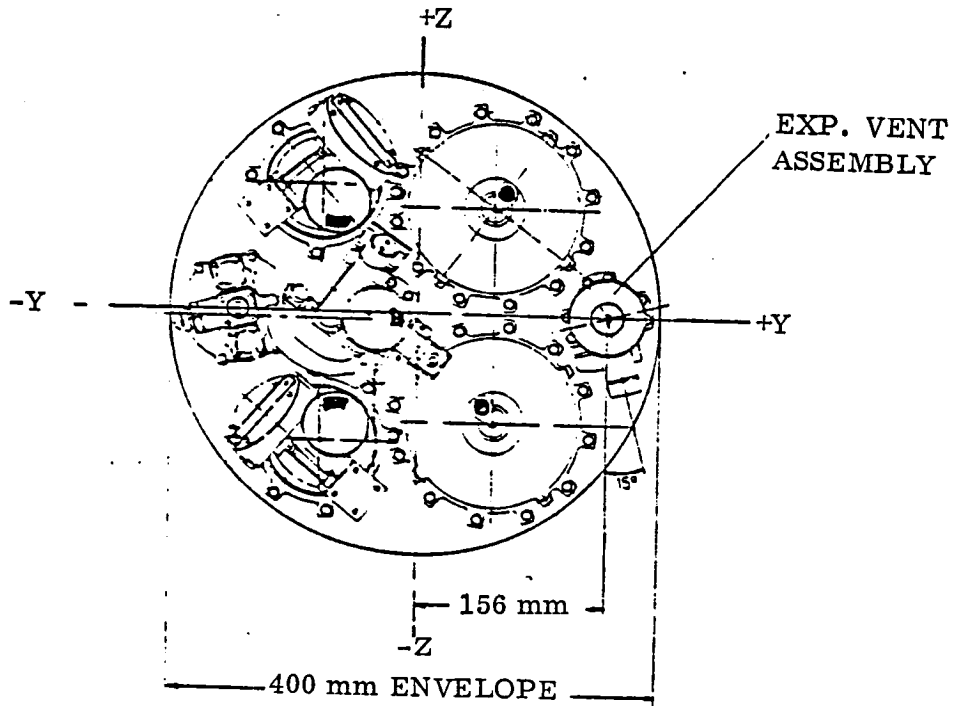


Figure 2-8. Spacelab Venting Provisions, Layout of Forward Feed-Through Plate

LOCATION: Vent assembly is located in upper part of top

forward end cone.

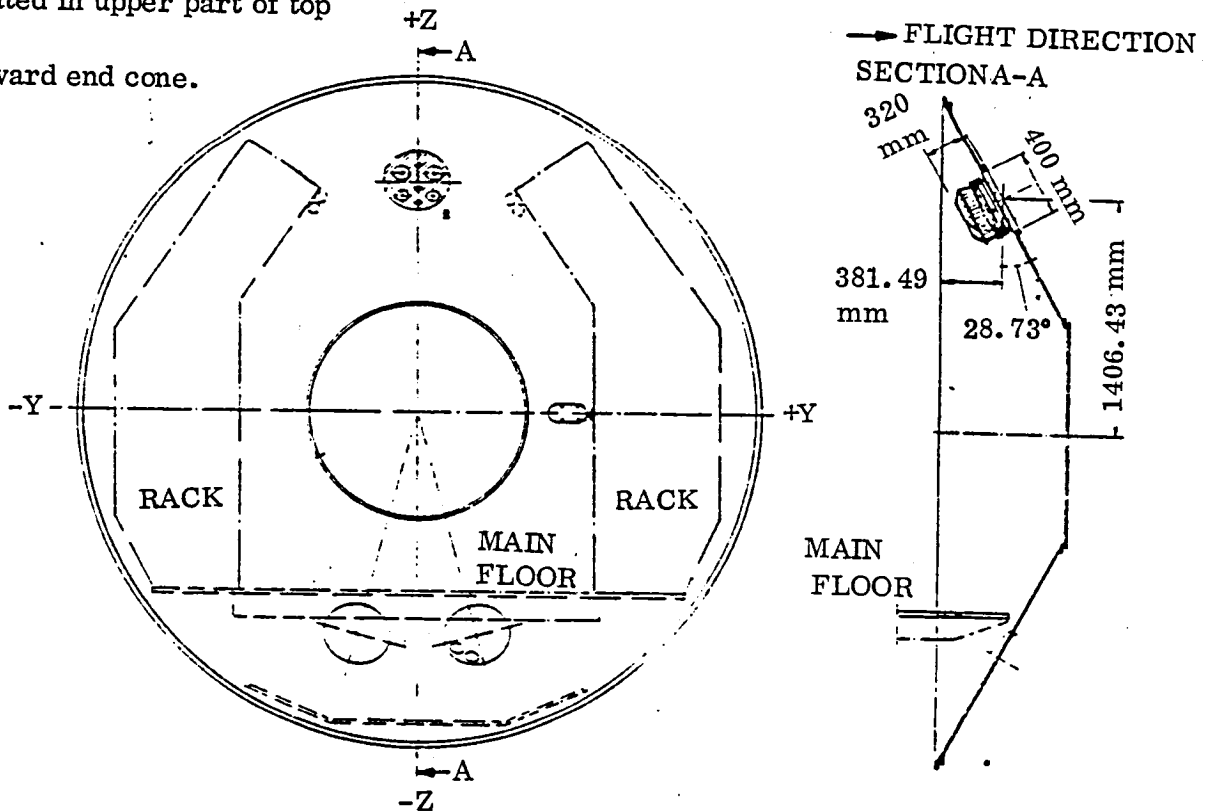


Figure 2-9. Spacelab Venting Provisions

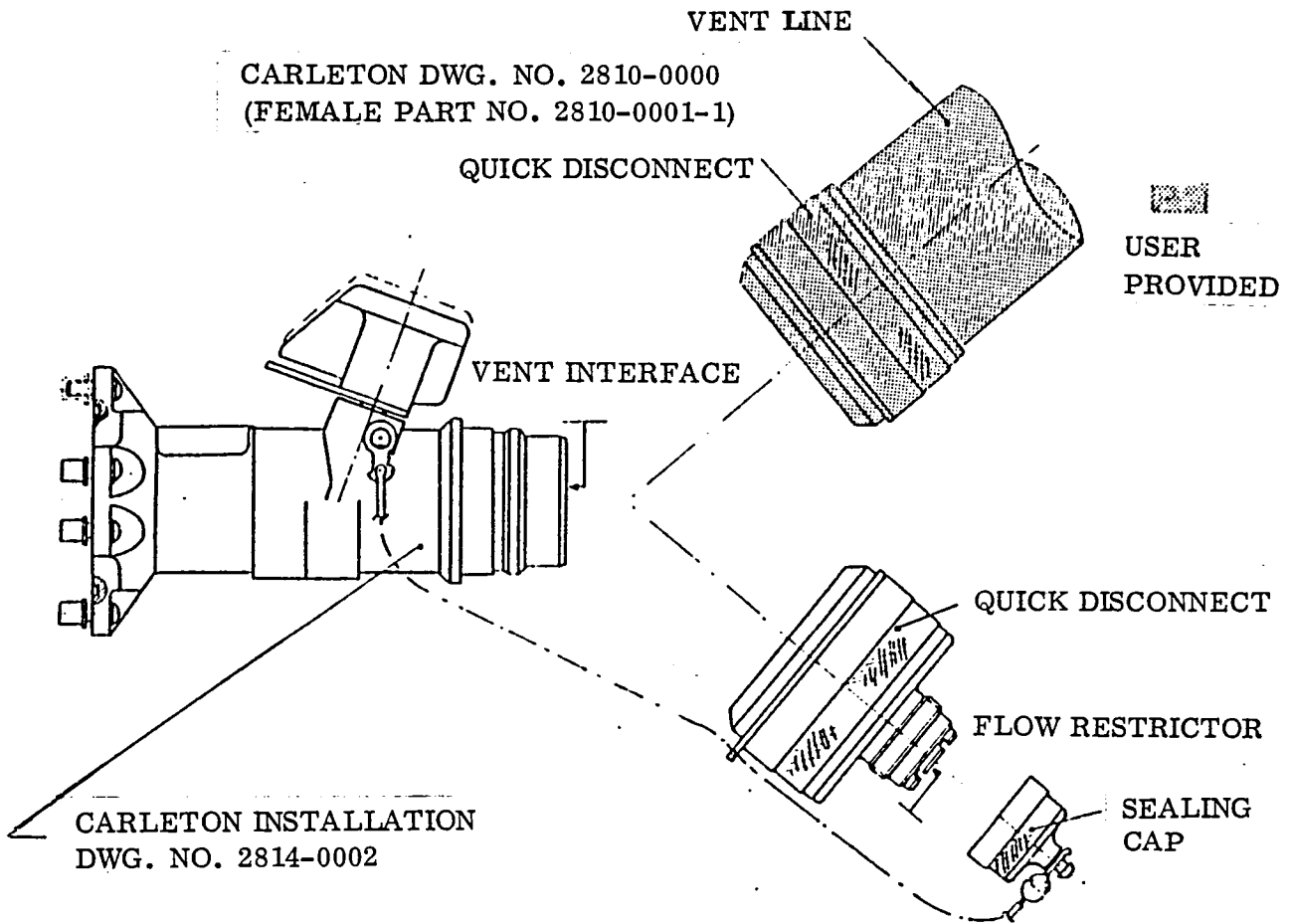


Figure 2-10. Spacelab Venting Provisions

REFERENCE: SPACELAB PAYLOAD ACCOMMODATION HANDBOOK  
SLP/2104, 30 JUNE 1977

PURPOSE: TO PROVIDE SPACELAB USERS WITH CAPABILITY TO VENT  
OR EVACUATE SCIENTIFIC EXPERIMENT CHAMBER

OPERATION: EXPERIMENT VENT ASSEMBLY IS MANUALLY OPERATED  
WITH BUTTERFLY VALVE CAPABLE OF TWO PRECALIBRATED  
FIXED POSITIONS BETWEEN CLOSED AND FULL OPEN

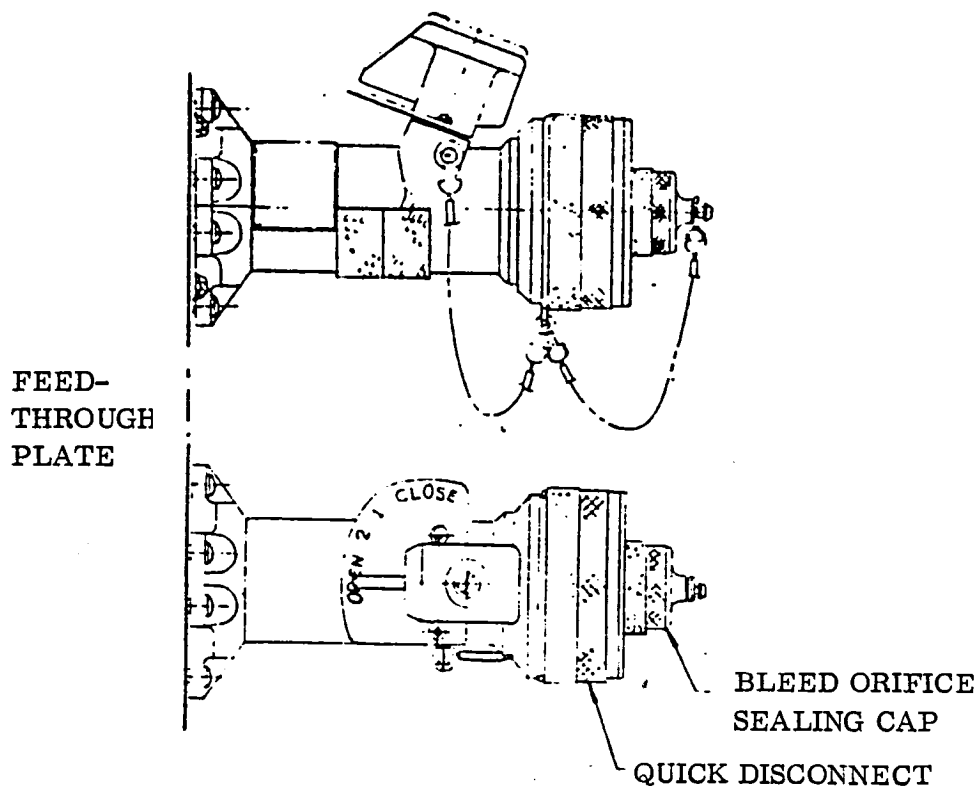


Figure 2-11. Spacelab Venting Provisions

Table 2-4. Spacelab Venting Provisions

<u>Vent Assembly Characteristics</u>	
Pressure	
Operating	0 to 110 kN/m <sup>2</sup>
Proof	165 kN/m <sup>2</sup>
Burst	220 kN/m <sup>2</sup>
Temperature	-74 to +71C
Valve Orifice Flow Area	11.4 cm <sup>2</sup>
Mass Flow Rate at 21C and ΔP =	101.3 kN/m <sup>2</sup>
Full Open	0.18 kg/sec
Position 1	0.12 kg/sec
Position 2	0.06 kg/sec
<u>Note:</u> Mass flow rate is for air and for vent valve assembly only. User provided female quick disconnect plus line loss from experiment to valve assembly will modify available rate.	

Table 2-5. Spacelab Venting Provisions

<u>Compatible Gases</u>
Compatibility of vented gases with the vent assembly is essentially determined by their compatibility with the valve assembly seals.
Seals are silicone rubber (two types): Silastic 675 and Silastic L5-53.
Freon is not considered compatible with seals without testing specific Freon at expected temperatures, pressures and durations. An investigation of compatible seal materials shows that either Buna-N or Viton A would be satisfactory for both F-11 and F-113. Hypalon or polysulphide would be satisfactory for F-11 but questionable for F-113. Nitrile rubber, neoprene, or polyurethane would be satisfactory with F-113 but not with F-11. Metal seals would also be compatible but would not be suitable for repeated connect/disconnect service.
Vent valve seal modification possible if required but is chargeable to experiment.

Table 2-6. Spacelab Accommodation Features

● Rack accessories include: Interfaces with Spacelab data collection/processing/transmission systems; power outlets; connectors for forced-air cooling of flight experiment equipment.	
● Equipment unsuitable for rack mounting can be mounted directly to the floor of the Spacelab.	
● Small experiment articles can be kept in any of several stowage containers located throughout the module.	
● Electrical power:	28V DC; 115/200V AC @ 400 HZ/3 phase
● Power conditioning equipment.	
● Power available for payload and mission-dependent equipment in the module or on a pallet is payload dependent.	
Ascent/Descent:	1 KW (Continuous) 1.5 KW (Peak)
On-Orbit (All Module Configurations):	2.6 to 3.5 KW (Continuous) 7.2 to 8.1 KW (Peak) 160 to 300 KWH or Energy Available/Mission
● Spacelab electrical power is routed to flight experiments through experiment switching panels which can be mounted to individual racks, or under the Spacelab floor to service floor-mounted to individual racks, or under the Spacelab floor to service floor-mounted equipment.	

- b. Analog down-link transmission for up to 85% of the mission. Data may be real-time or tape records (3 hz to 4.2 Mhz).

LOW RATE ( $\leq 1$  Mb/sec) or High Rate (62.5Kb/sec to  $\pm 6$  Mb/sec)

Remote Acquisition Units (RAU's) receive experiment data and deliver them to the Spacelab data management system for computer processing, display, storage, and/or transmission to the ground. RAU's may be mounted in equipment racks, under the Spacelab floor, and inside an Airlock. The RAU data acquisition function is under experiment-supplied software control. They provide an 8-bit resolution, analog-to-digital conversion, and can accept serial digital data. Signal conditioning equipment will be available to interface experiment equipment with the RAU.

A data processing computer (Mitra 125 S, 64K core, 16 bitwords,  $3.5 \times 10^5$  operations/sec) which can analyze experiment data on-board the spacecraft, data for on-board display, and format data for transmission to the ground will be on-board. A mass memory unit for storage of software will be on-board. A data display unit and keyboard which permit on-board review of experiment data will be available on-board. Data may be stored on tape or transmitted to the ground at up to 64 Kb/sec.

VIDEO DATA

An Orbiter-to-Spacelab interface has been provided that enables the collection, monitoring, and recording of black-and-white and color video signals. Also, black-and-white video data can be transmitted to the ground, one channel at a time, through this interface. Spacelab video capabilities currently under consideration include:

- Black-and-white video cameras
- Black-and-white video monitor
- Black-and-white video tape recorder plus tapes
- Camera Control - Provides automatic and manual camera/recorder/monitor switching and tags video records with time and experiment identification
- Camera Timer - Provides automatic time-controlled activation/deactivation of cameras and recorders
- Accessories - Mounting brackets, lens assortments, cabling, and remote controls
- Color video camera
- Color video monitor
- Color video tape recorders plus tapes

# 3

## TEST PROGRAM MODEL

As a basis for analytical considerations necessary for equipment design and test configuration definition, an overall program was defined. The preliminary definition of this program was contained in the contract statement of work and embellished and finalized following the program kick-off meeting between the NASA, GDC, and lead scientists participating in the study. From the ensuing program and establishment of number of tests, test times, gravity levels, and RCS performance, a minimum weight of RCS propellant was defined. A summary of test conditions to be analyzed for each experiment is presented in Table 3-1. As shown, the table represents a significant departure from the acceleration levels originally proposed, particularly in the Bubble Dynamics experiment which were decreased considerably. It was fortunate that such redefinition was possible as the RCS propellant requirements to meet the original conditions were beyond that available from the RCS tankage. After the redefinition, it is seen that the program is still rather ambitious in that nearly all the propellant available for payload use (see Table 2-3) will be required for this experiment package alone. This does not account for inefficient propellant usage resulting from the inability to achieve pure translational motion at the desired level by firing the thrusters at a thrust commensurate with the desired acceleration. This difficulty and the consequent affect on the experiment program will be discussed in a later section. The conditions of Table 3-1, therefore, defined the starting point for the analytical effort performed during this study. The analyses defined the pertinent parameters involved in each experiment and quantified the physical measurements and range of such measurements to allow component sizing and selection, and instrumentation definition. Analyses completed were documented by internal GDC memoranda and distributed to program personnel during the course of the study. These documents are listed in the reference section of this report. Parts of these analyses are also included in this report to provide a single point of reference tying together all the parts of the study.

Table 3-1. Experiment Acceleration & RCS Propellant Requirements

Experiment	Test Identification (Times are at accel. level)*	No. of Tests	Acceleration, cm/sec (g)	Total Accel. Times, sec	Propellants, kg/sec	Total, kg
I. Two-Phase Patterns and Pressure Drop	Air H <sub>2</sub> O - Constant Quality Isothermal Runs (20 sec/test)(0.0001g)	80	0.098 (10 <sup>-4</sup> )	1600	0.0316	51
	Isothermal Runs (20 sec/test)(0.005g)	10	4.9 (5×10 <sup>-3</sup> )	200	1.58	316
II. Two-Phase Flow Boiling	Freon-Variable Quality Heater (40 sec/test)(0.0001g)	28	0.098 (10 <sup>-4</sup> )	1120	0.0316	35
	(10 sec/test) (0.0033g)	10	3.26 (3.33×10 <sup>-3</sup> )	400	1.053	421
III. Pool Boiling	Various Container and Rod Sizes Low-Gravity (15 sec/test) (0.0001g)	9	0.098 (10 <sup>-4</sup> )	405	0.0316	13
	Medium Gravity (45 sec/test)(0.0033g)	9	3.26(3.33×10 <sup>-3</sup> )	405	1.053	427
IV. Liquid Settling	Constant Acceleration Tank 1 (5 liquid levels)	5	0.18 to 0.25 (1.8 × 10 <sup>-4</sup> to 2.6 × 10 <sup>-4</sup> )	400	0.057-0.082	28
	Tank 2 (5 liquid levels)	5	0.54 to 0.76 (5.5 × 10 <sup>-4</sup> to 7.8 × 10 <sup>-4</sup> )	400	0.174-0.247	84
	Impulsive Acceleration Tank 1 (5 liquid levels)	5	9.8 (10 <sup>-2</sup> )	1.5	3.16	5
	Tank 2 (5 liquid levels)	5	4.9 (5 × 10 <sup>-3</sup> )	6.0	1.58	9
V. Bubble Dynamics	Vary Bubble Size 0.05 - 5 cm	3	.98 (10 <sup>-3</sup> )	180	.316	57
	60 sec each	6	.49 (5×10 <sup>-4</sup> )	360	.158	57

\* Does not account for time for flow and camera adjustments between points

Total: 1503 kg

# 4

## EXPERIMENTS 1 AND 2, DESIGN DEFINITION

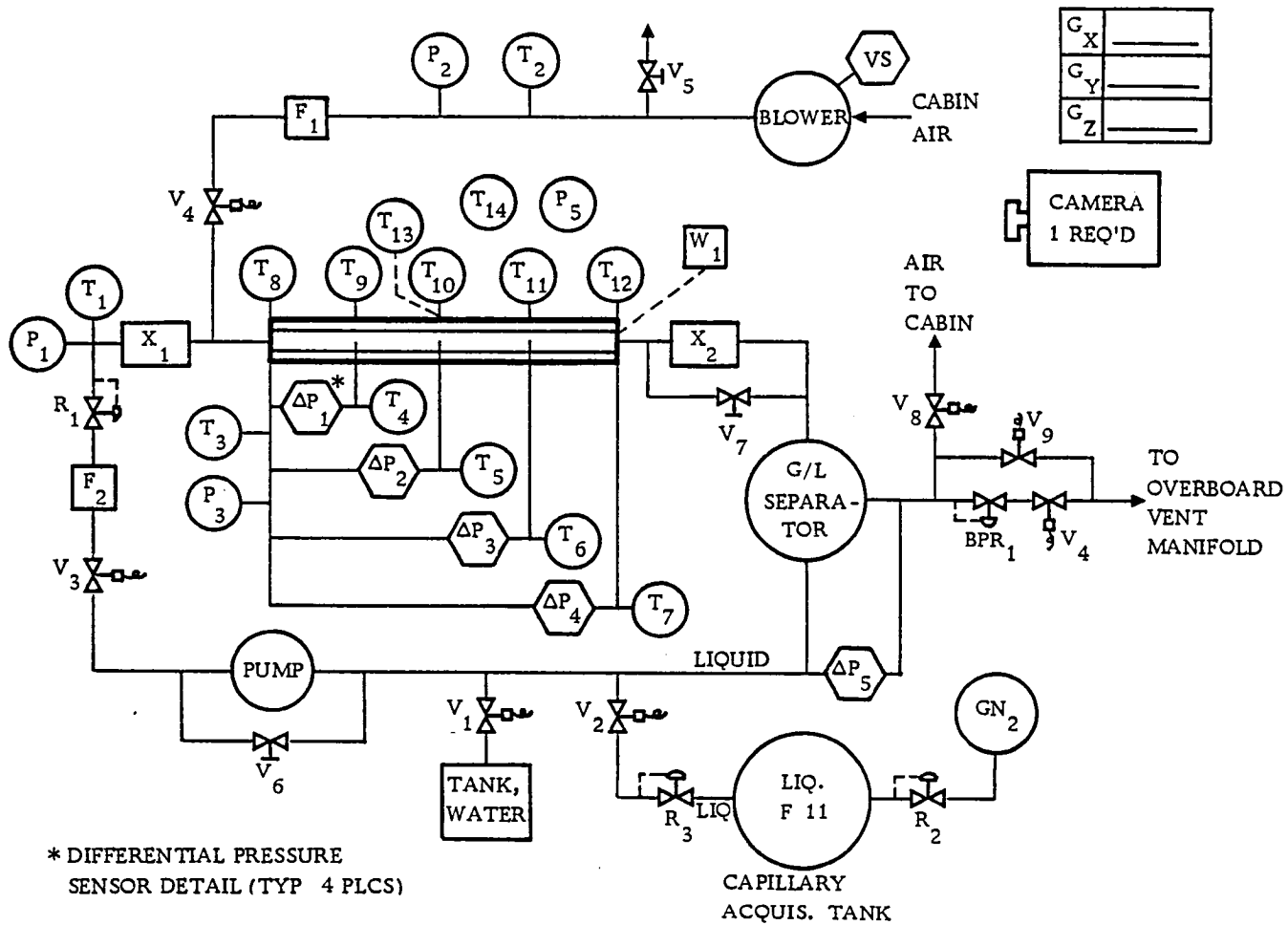
### 4.1 ISOTHERMAL FLOW PATTERN AND PRESSURE DROP

4.1.1 DESCRIPTION. The objective of this experiment is to define the effect of gravity level on flow pattern and pressure drop in an isothermal, two-phase fluid in pipe flow. These variables are to be observed over a range of fluid quality and flow rates sufficient to observe discrete regimes of fluid flow anticipated for lower gravity levels. This will be an extension of the work performed and described in Reference 1. It is recognized that the "g" dependency is not reflected in the equations used. The calculations provide an estimate of the  $\Delta P$  range to consider for instrumentation to obtain low-g data to correlate with 1-g data. Following the lead of this earlier work, the proposed flow schematic for this test is shown in Figure 4-1. This experiment lends itself to integration with Experiment 2 for flow boiling and Figure 4-1 reflects this integration by showing all of the components required for both tests. Components have been identified and weight and volume defined. The weight summary of components is given in Figure 4-2. The volume is compatible with the rack dimensions as shown in the design layout of Figure 4-2. The tests and test conditions for this experiment are given in Table 4-1.

4.1.2 METHOD OF OPERATION. In this test, water and air form the two-phase fluid flow under consideration. With no heat addition in the test section and being in the controlled temperature environment of Spacelab, the flow may be considered isothermal. Cabin air is introduced into the test section by the variable speed blower. Flow is controlled by means of the blower speed and the by-pass valve  $V_5$ . It is monitored by flowmeter  $F_1$ . The air is mixed with circulating water flow provided by the pump and measured by  $F_2$ . The mixture flows through the test section and into the gas liquid separator via a by-pass line (valve  $V_7$ ) to avoid the pressure drop of the quality meter,  $X_2$ . This minimizes the inlet pressure at the entrance to the test section, and also minimizes the blower  $\Delta P$  requirement.

A small water storage reservoir is included in the liquid loop in the event that water is accidentally vented overboard. The bypass valve  $V_6$  provides adjustment of water flow and pressure to the regulator R-1, which is set to control flow through the test section.

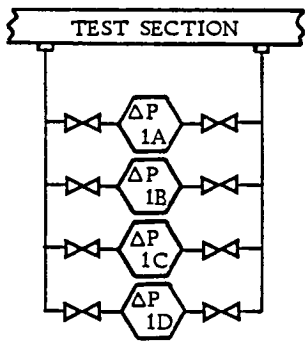
Liquid carryover into the air return is a function of separator efficiency and although efficiency is expected to be high, a liquid carryover problem still may exist to some degree. This can be overcome if necessary with a wicking type coalescer in the air return. This is not considered necessary at this time.



G <sub>X</sub>	_____
G <sub>Y</sub>	_____
G <sub>Z</sub>	_____

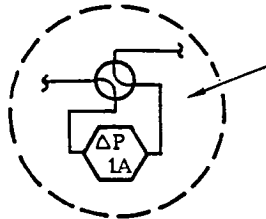
CAMERA  
1 REQ'D

\* DIFFERENTIAL PRESSURE  
SENSOR DETAIL (TYP 4 PLCS)



SENSOR RANGES

- $\Delta P_{1A} = 0-0.345 \text{ kN/m}^2 \text{ (0-0.05 psid)}$
- $\Delta P_{1B} = 0.345-1.72 \text{ kN/m}^2 \text{ (0.05-0.25 psid)}$
- $\Delta P_{1C} = 1.72-6.9 \text{ kN/m}^2 \text{ (0.25-1.0 psid)}$
- $\Delta P_{1D} = 6.9-34.5 \text{ kN/m}^2 \text{ (1.0-5.0 psid)}$



ALTERNATIVE TWO-WAY  
VALVE ARRANGEMENT  
(ISOLATES ΔP SENSOR OR  
PUTS IT IN LINE)

NOTE: SENSORS TO BE  
BLED MANUALLY

Figure 4-1. Flow Schematic - Experiments 1 and 2, Flow Pattern and Pressure Drop, and Flow Boiling

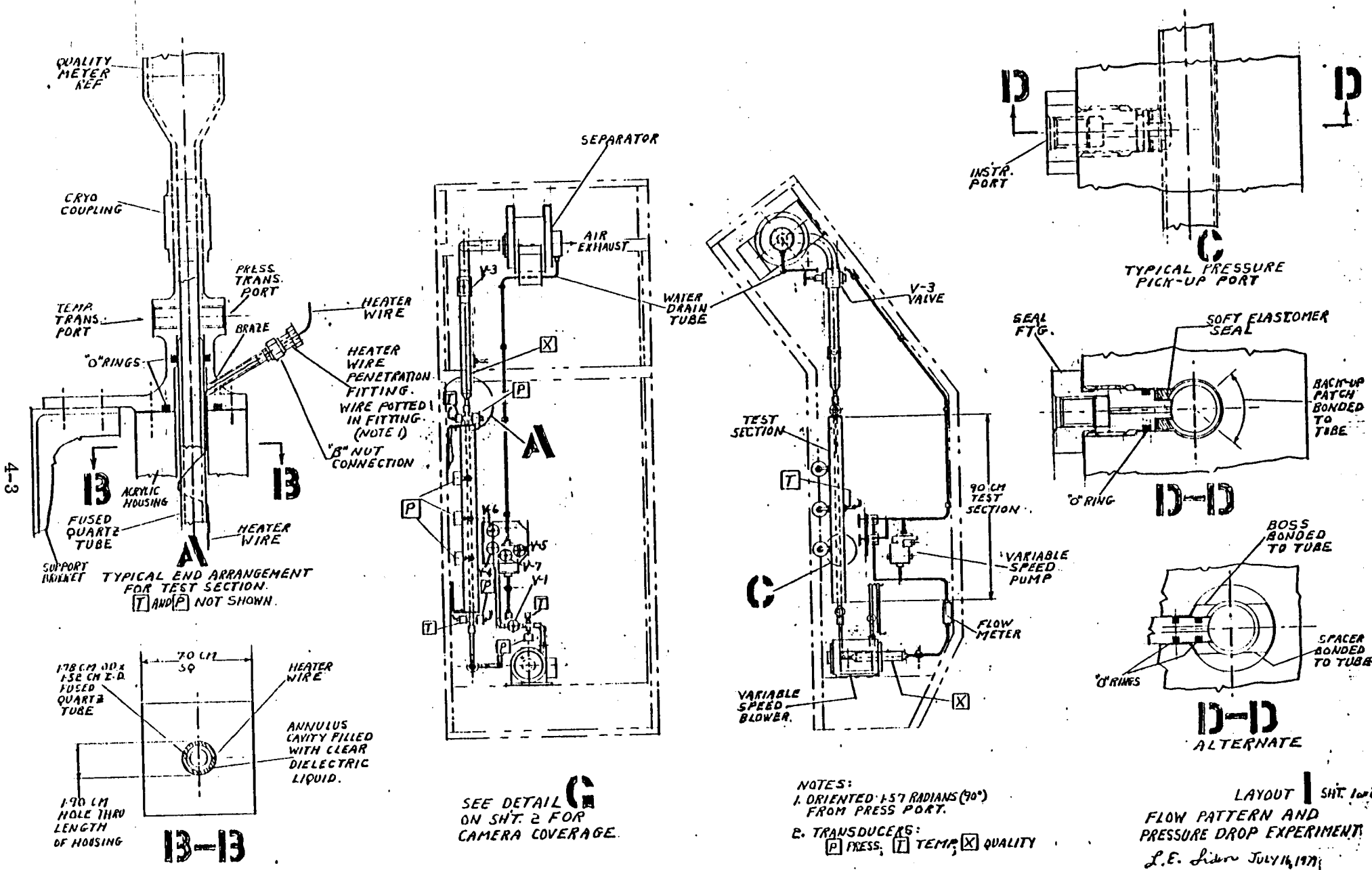
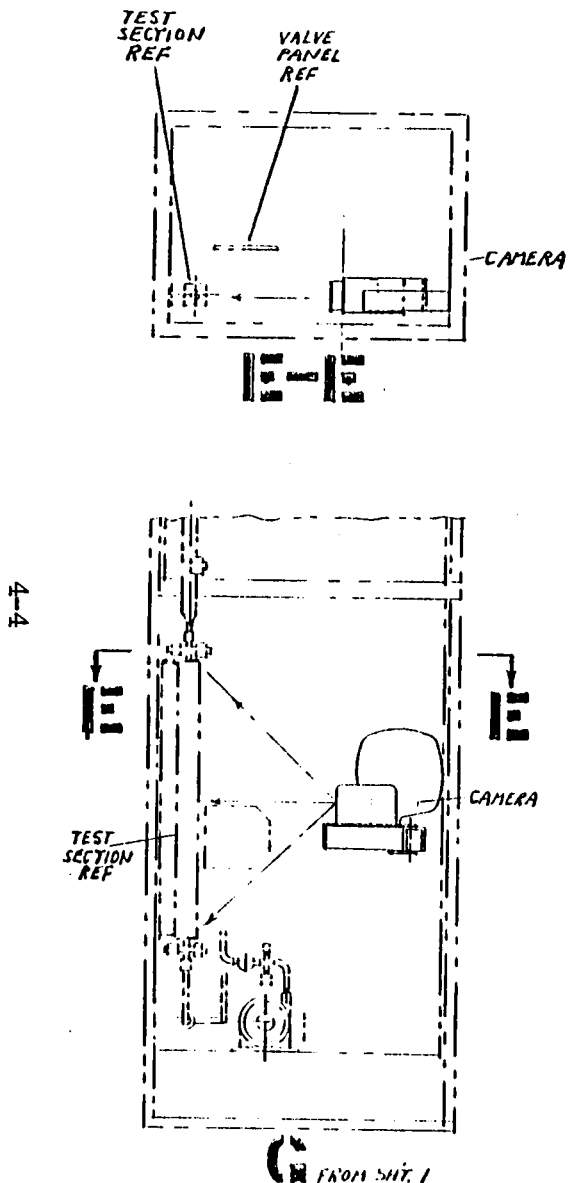


Figure 4-2. Layout, Sheet 1 of 2 - Flow Pattern and Pressure Drop Experiment



ITEM	NO SCALE	WT. Kg (LBS)
	VALVES	3.63 (8.0)
	PRESSURE TRANSDUCERS	4.99 (11.0)
	TEMPERATURE TRANSDUCERS	0.68 (1.5)
	CRES PRESS. & TEMP TRANSDUCER SEAL FTGS. 4 REQD.	0.36 (.8)
	ELECTRICAL HARNESSES	4.08 (9.0)
	BLOWER	5.90 (13.0)
	MISC NUTS, BOLTS, CLIPS & COUPLINGS.	1.36 (3.0)
	TEST SECTION LIGHTS	2.04 (4.5)
	10% CONTINGENCIES	4.76 (10.5)
	TOTAL	51.8 (114.1)

ITEM	NO SCALE	WT. Kg (LBS)
	ACRYLIC TEST SECTION HOUSING	6.12 (13.5)
	FUSED QUARTZ TEST SECTION TUBE	.14 (.3)
	CRES TEST SECTION END FITTINGS. TWO REQD.	1.68 (3.7)
	ALALY TEST SECTION SUPPORT BRACKET	0.91 (2.0)
	CRES QUALITY METERS TWO REQD.	1.81 (4.0)
	CRES SEPARATOR INLET TUBING	1.81 (4.0)
	ALALY SEPARATOR INCL. SUPPORTS	5.44 (12.0)
	CRES PLUMBING FOR WATER FROM SEPARATOR	1.36 (3.0)
	ALALY PUMP	1.27 (2.8)
	CRES FLOW METER	0.59 (1.3)
	CRES BLOWER PLUMBING	1.22 (2.7)
	VALVE PANEL & PUMP SUPPORTS	1.59 (3.5)

LAYOUT | SHIT. 2 OF 2  
FLOW PATTERN AND  
PRESSURE DROP EXPERIMENT.

L. E. Sider July 12, 1979

Figure 4-2. Layout, Sheet 2 of 2 - Flow Pattern and Pressure Drop Experiment

Table 4-1. Experiments 1 and 2 - Tests and Test Conditions

No. of Runs	Duration Ea. Run	G-Level	Mass Vel., G (kg/m <sup>2</sup> -S)	Quality, X, (m <sub>g</sub> /m <sub>m</sub> )	Gas Flow lpm(kg/hr)	Liquid Flow lpm(kg/m)	Total Flow lpm(kg/hr)	Test Section ΔP, kN/m <sup>2</sup>
Experiment I - Flow Pattern and Pressure Drop Experiment Fluids = Air/Water @ 21.1°C - 1014 mbars								
80	20 sec.	10 <sup>-4</sup> g	10	0.01	0.883 (0.064)	0.105 (6.30)	0.988 (6.36)	0.0019 (min.)
10	20 sec.	5×10 <sup>-3</sup> g	10	0.64	56.6 (4.07)	0.040 (2.29)	56.6 (6.36)	0.064
			640	0.01	56.6 (4.07)	6.74 (403)	63.4 (407)	3.37
			640	0.08	453.0 (32.6)	6.26 (375)	459.0 (407)	23.8 (max.)
Experiment II - Flow Boiling Tests at -3.3, 4.4, 12.2 and 20.0°C Fluid = Freon 11								
28	40 sec.	10 <sup>-4</sup> g	10	0.005	0.102 (0.032)	0.071 (6.33)	0.173 (6.36)	0.0013 (min.)
10	40 sec.	3.3×10 <sup>-3</sup> g	10	0.10	4.90 (0.636)	0.062 (5.73)	4.96 (6.36)	0.036
			640	0.005	6.57 (2.04)	4.53 (405)	11.1 (407)	3.89
			640	0.10	314.0 (40.7)	3.96 (367)	318.0 (407)	48.3 (max.)
			10	0.005	0.102 (0.032)	0.53 (6.33)	0.63 (6.36)	
Flow Prop. at 20.0°C (Min. Vol. Flow Case)								

## 4.2 TWO-PHASE FLOW BOILING

4.2.1 DESCRIPTION. The object of this experiment is to verify or develop analytical expressions regarding two-phase flow boiling in low gravity. Several conditions which might be examined are discussed in Reference 1. The fluid chosen for this experiment was Freon 11 because of its desirable vapor pressure/boiling point relationship which is such that it will be in liquid form when stored at the environmental temperature of Spacelab and can therefore be readily vaporized with modest heat addition in the test section. This provides convenient control of the liquid/vapor phase of the fluid without undue complexity in control or excessive component design pressure differentials. Use of the single fluid then will provide the desired two-phase flow relationship over the quality range of interest.

4.2.2 METHOD OF OPERATION. After the Flow Pattern Experiments are completed, the water tank is isolated from the system, the test loop is vented to the Spacelab vent assembly and all water and air from the test section is removed. Freon-11 is then introduced from the reservoir. This fluid uses the same recirculating loop as the previous experiment. Two quality meters (X<sub>1</sub> and X<sub>2</sub>) are used to monitor the quality of the Freon-11 upstream and downstream of the test section. The flow through the test section is set by regulators R<sub>1</sub> and R<sub>2</sub>. Make-up F-11 is supplied through regulator R<sub>3</sub> which holds a set pressure value at the inlet to the recirculation pump. As F-11 is vaporized and vented during several experiments, the regulator will allow make-up F-11 to enter the test loop. The amount of F-11 lost during testing at the maximum heat input of 679 watts (Ref. 1) for 40 seconds amounts to 0.148 kg (0.326 lb) or about 100 cc (6.1 cu in) of liquid. This corresponds to a liquid level drop in the separator of approximately 0.58 cm (0.23 in). Thus, over a number of runs, liquid will have to be made up by the F-11 supply reservoir.

The design layout for Experiment 2 is shown in Figure 4-3. Although most of the system uses the same components as Experiment 1, the layout is presented separately for clarity as to where the additional components are located and to show dimensional compatibility with the rack.

### 4.3 INSTRUMENTATION

Instrumentation requirements for Experiments 1 and 2 are shown in Table 4-2. The common test section is made from clear plastic for flow pattern observation. It contains an integral heater with power monitored by  $W_1$ . Measurement of five fluid temperatures ( $T_3 - T_7$ ), six wall temperatures ( $T_8 - T_{13}$ ), and other loop temperatures are required. Thermistors are recommended for these measurements because of their high sensitivity. The CDMS will be programmed to scan the thermistors and then acquire the required temperature data.

Test section pressure differentials, as tabulated in Table 4-1, are extremely low during low mass velocity experiments and will be difficult to measure. Selectable differential pressure measurement transducers which cover vastly different ranges are indicated for these measurements ( $\Delta P_1$  through  $\Delta P_4$ ) to achieve maximum sensitivity. A differential pressure transducer is also used to measure the liquid-to-gas differential at the separator. Other flow system pressures are monitored as indicated in the flow schematic by standard pressure transducers.

Flowmeters  $F_1$  and  $F_2$  measure the water and air flow during Experiment 1. To minimize the air line pressure drop, a hot wire anemometer type of flow meter has been used. This type of meter has been fabricated at Convair from standard thermistors for use in earlier testing and was very successful. The liquid flow measurements are made with turbine type flowmeters. Data from the  $F_1$  and  $F_2$  sensors are sampled at 2 times/second by the CDMS. These measurements should be displayed in real time in the vicinity of the experiment package to facilitate setting the quality of the flow through the test section. Drag type flowmeters have been used with good results by NASA/LeRC and are worthy of more consideration for both gas and liquid measurement for the next phase of this program.

Quality meters  $X_1$  and  $X_2$  are used during the flow boiling experiments with F-11. The quality meter consists of a turbine flowmeter to measure mass flow rate and a capacitance sensor to measure fluid density. Available meters are 5.1 cm (2 in) in diameter, thus requiring an enlargement in the approximately 1.9 cm (0.75 in) diameter tubing leading to and from the test section.

The accelerometer package senses g-levels in the x, y, and z directions down to  $10^{-4}$  g. These g-levels are displayed, for camera recording, by three voltmeters.

A survey was made to determine sensor availability to meet these experiment requirements. A selective list of currently available instruments offered commercially is included in Appendix A. These items represent the type, accuracy, size, and weight of candidate hardware. The instrumentation list of Table 4-2 reflects this information but does not attempt to define or recommend a vendor.



Table 4-2. Instrumentation/Component Requirements for Experiments 1 and 2, Flow Patterns and Flow Boiling

I. D.	Measurement Description	Sensor Type	Range	Resolution (Accuracy)	Test Runs		Data Sampling Rate	Notes
					No.	Dura- tion		
T <sub>1</sub>	F-11 or H <sub>2</sub> O Temperature	Thermistor	-3.3 - 30C (26-86F)	0.28 (±0.28C) (0.5F (±0.5F))	138	3520 sec total	1/2 sec	Quality meter temp. meas.
T <sub>2</sub>	Air Blower Outlet Temperature	Thermistor	21-38C (70-100F)	0.28 (±0.28C) (0.5F (±0.2F))	"	"	1/2 sec	37C (99F) for isent. comp.
T <sub>3</sub> -T <sub>7</sub>	Test Section Fluid Temperature	Thermistor	-3.3 - 30C (26-86F)	0.11 (±0.11C) (0.2F (±0.2F))	"	"	1/2 sec	
T <sub>8</sub> -T <sub>13</sub>	Test Section Wall Temperature	Thermistor	-3.3 - 30C (26-86F)	0.11 (±0.11C) (0.2F (±0.2F))	"	"	1/2 sec	
T <sub>14</sub>	Ambient Temperature	Thermistor	21-38C (70-100F)	0.11 (±0.11C) (0.2F (±0.2F))	"	"	1/10 sec	
P <sub>1</sub>	F-11 or H <sub>2</sub> O Inlet Press.	Xducer	34.5-207.0 kN/m <sup>2</sup> (5-30 psia)	1.4 (±1.4 kN/m <sup>2</sup> ) (0.2 (±0.2 psia))	"	"	2 sec	Quality meter press. meas.
P <sub>2</sub>	Blower Outlet Air Pressure	Xducer	0-27.6 kN/m <sup>2</sup> (0 - 4 psia)	1.4 (±1.4 kN/m <sup>2</sup> ) (0.2 (±0.2 psia))	"	"	1/2 sec	
P <sub>3</sub>	Test Section Absolute Press. (Inlet)	Xducer	34.5-138 kN/m <sup>2</sup> (5-20 psia)	1.4 (±1.4 kN/m <sup>2</sup> ) (0.2 (±0.2 psia))	"	"	1 sec	Display required near package to set regulators.
P <sub>4</sub>	Cabin Pressure	Xducer	0-138 kN/m <sup>2</sup> (0-20 psia)	1.4 (±1.4 kN/m <sup>2</sup> ) (0.2 (±0.2 psia))	"	"	1/5 sec	
ΔP <sub>1</sub> -ΔP <sub>4</sub>	Test Section Diff. Pressure	Xducer	0.0014-300 kN/m <sup>2</sup> (0.0002-4.35 psia)	TBD	"	"	2 sec	0.0002 psi = 0.0055 in W.G.
ΔP <sub>5</sub>	G/L Separator Liquid Outlet Pressure	Xducer	0-34.5 kN/m <sup>2</sup> (0-5 psig)	TBD	"	"	1 sec	
F <sub>1</sub>	Flowmeter, Blower Air Outlet, Into Test Section	Calibrated Thermistor	0.85-453 lpm (0.03-16 cfm)	0.057 lpm (0.002 cfm) for Lo Flow (±0.002 cfm)	"	"	2 sec	Range may require two meters. Real time display required.
F <sub>2</sub>	Flowmeter, F-11 or H <sub>2</sub> O Into Test Section		0.038-6.8 lpm (0.01-1.8 gpm)	0.0038 (±0.0019) lpm (0.001 ± 0.0005 GPM)	"	"	2 sec	Range may require two meters. Real time display required.
X <sub>1</sub> & X <sub>2</sub>	F-11 Quality Meas. in and out of Test Section	Dielectric ρ meas. plus turbine flowmeter	6.4-407 kg/hr (14-898 lb/hr) 0.02-0.61 gm/cc (1.33-38.3 lb/ft <sup>3</sup> )	2% of nominal flow qual (±1%)	"	"	5 sec	Instrument to perform this measurement can be provided by Quantum Dynamics by special order.

Table 4-2. Instrumentation/Component Requirements for Experiments 1 and 2, Flow Patterns and Flow Boiling (Continued)

Measurement		Sensor Type	Range	Resolution (Accuracy)	Test Runs		Data Sampling Rate	Notes
I. D.	Description				Number	Duration		
$g_{x,y,z}$	Test Section Acceleration Level	Accelerometer	(1-50) × 10 <sup>-4</sup> g	.00001 (±.00001) g	138	3520 sec. Total	10/sec.	Display for $g_x$ , $g_y$ , & $g_z$ reqd.
$W_1$	Power to Heater <u>COMPONENTS</u>	TBD	10.6-679 w.	0.1 watt ±.05 w.	"	"	1/sec.	
Camera	B&W, 16 mm, Hi Speed							200 frames/sec
Tank, Freon	Liquid Freon-11 (1 reqd)	Positive expulsion or capillary acquisition	Freon capacity: 14.0 kg 26.6 litre					Capacity obtained from Ref. 1 NAS CR-135327.
Pump	Recirculating H <sub>2</sub> O or F-11 Pump - Variable Speed Drive Motor	Small centrifugal or gear pump	2.3-403 kg/hr 5.7-406 kg/hr $\Delta P \approx 103$ kN/m <sup>2</sup>					Use same pump for H <sub>2</sub> O & Freon-11.
Blower	Air Supply Blower for Air/Water Flow Pattern Exp. Variable Speed	High speed, multistage centrifugal or positive displacement such as sliding vane type, etc.	0.85-453 lpm @ 30°C 27.6 kN/m <sup>2</sup> diff					28 volt DC or 400 Hz 115/200 volt variable speed motor reqd. IIP $\approx$ .75 (50% eff.) ; PWR = 0.56 kw
Separator	G/L Separator for Air/Water or F-11	Dynamic Separator	<u>FLOW RANGE:</u> <u>AIR/WATER</u> Total Flow Range: 6.35 - 407 kg/hr Air Flow Range: 0.063 - 32.6 kg/hr (0.88 - 445 lpm) Water Flow Range: 2.27 - 403 kg/hr (0.037 - 6.80 lpm) <u>FREON-11</u> Total Flow Range: 6.35 - 407 kg/hr Gas Flow Range: 0.033 - 44.4 kg/hr (0.108 - 343 lpm) Liquid Flow Range: 5.67 - 405 kg/hr (0.062 - 4.53 lpm)					
Tank, Water	Makoup Water, 1 Reqd.	Diaphragm Type	3.28 litre capacity					
BPR <sub>1</sub>	Back Pressure Regulator		27.6-103 kN/m <sup>2</sup>	±0.34 kN/m <sup>2</sup>				

#### 4.4 COMPONENTS

The major components in these experiments are the pump, the blower, the separator, and the tanks.

4.4.1 PUMP. The pump requirements are those of a low capacity, low head unit, for which the maximum specific speed is about 500 rpm for a pump rotational speed of 5000 rpm. Specific speed is a term used to describe performance of a type centrifugal pump. This speed is a constant for all geometrically similar pumps and defines the RPM necessary to provide one gpm at one foot of head. The equation used is

$$N_s = N \sqrt{Q} / (\Delta h)^{0.75}$$

where

$N_s$  = specific speed, rpm  
 $N$  = actual speed, rpm

$Q$  = quantity flow, gpm  
 $\Delta h$  = pump head, ft of fluid

This is quite low for a centrifugal pump and suggests the use of a positive displacement type of pump such as a gear pump. Such a pump is self-priming and is the type used in the package. The same pump can be used for both Experiments 1 and 2 as long as seals are compatible with Freon-11.

4.4.2 BLOWER. The blower required is also of low capacity but has a relatively high head requirement for a centrifugal type of machine. Thus, a positive displacement type blower is needed and a sliding vane type is used. It will produce the required 27.6 kN/m<sup>2</sup> (4 psid) at 7550 cc/sec (16 cfm).

4.4.3 SEPARATOR. The gas/liquid separator proposed is of the dynamic type and collects liquid around its perimeter. The pressure of the liquid will depend on separator size, liquid level and rotational velocity.

This pressure (P) consists of the two components, the static pressure resulting from the centrifugal force field within the drum, and the dynamic head of the rotating liquid impacting the end of the collection tube. These two terms are

$$P = P_{\text{static}} + P_{\text{dynamic}}$$

$$P = \frac{\rho \omega^2 r}{g} d + \frac{\rho V^2}{2g}$$

where

$\rho$  = density

$\omega$  = angular drum velocity

$r$  = effective radius of the liquid rotating within the drum

$d$  = liquid depth in drum

$g$  = gravitational constant

$V$  = velocity of liquid impacting the end of the collection tube (assumed to be equal to  $\omega r'$  where  $r'$  is the drum radius at the pick-up tube)

A pressure of approximately  $1.3 \text{ kN/m}^2$  would correspond to the performance of the separator used in previous testing and described in Reference 1. This assumes a liquid depth of 2.5 cm (1 in) above the pick-up tube which is located at a radius of 14 cm (5.5 in) and the drum rotating at 300 rpm. A similar separator, but smaller, is recommended for use herein. This unit would have linear dimensions of half those of the previous unit, and would reduce the envelope volume from  $0.0504 \text{ m}^3$  to  $0.0062 \text{ m}^3$ . The rotational velocity corresponding to  $1.3 \text{ kN/m}^2$  would have to be increased to approximately 615 rpm.

#### 4.4.4 TANKS

The tanks can be of the bladder positive expulsion type or capillary acquisition type. The latter was selected in our previous study (Ref. 1) for the Freon-11 and is used herein.

A 29.2 cm (11.5 in) diameter spherical tank will provide the required volume for the 18.2 kg (40 lb<sub>m</sub>) of F-11 (Ref. 1). A small, high pressure nitrogen bottle will be used for pressurizing the capillary Freon-11 tanks.

For the water, a spring loaded bladder type positive expulsion tank was selected. Its capacity is 3277 cc (200 cu in) or 3.3 kg<sub>m</sub> (7.2 lb<sub>m</sub>) of water. A cylindrical tank would be about 20.3 cm (8 in) in diameter by 15.2 cm (6 in) long.

#### 4.5 ANALYSIS

Pressure drops were calculated for both the constant quality, air/water two-phase flow and the Freon-11 flow boiling experiments. Compressibility of the gas phase was included in the calculations. In the cases for both experiments, two models were used to calculate pressure drop: a homogeneous and a separated two-phase flow model. The homogeneous model is a straight-forward theoretical approach, whereas the separated flow model requires experimental correlations for the void fraction  $\alpha$  and the two-phase friction multiplier  $\phi_f^2$ . The relationships of Baker and Lockhart-Martinelli were used for these parameters. For given experimental conditions, the calculated pressure drops were found to span a range of four orders of magnitude. It is expected that the actual pressure drop will follow the results of the homogenous model for lower mass qualities and follow the results of the separated flow model for higher mass qualities. The pressure drops calculated using the relationships of Baroczy seem to verify this transition between models.

##### 4.5.1 PRESSURE DROP FOR AIR/WATER EXPERIMENT 1

###### Homogeneous Model

Fluids for the constant quality two-phase pressure drop experiment are air and water. The system temperature and pressure are assumed to be at standard conditions. The

pressure drop across a test section of length L and diameter D can be calculated using a homogeneous two-phase flow model. The equation governing pressure drop for this model, neglecting the contribution of gravity and liquid compressibility, is the following

$$-\frac{dP}{dz} = \frac{(2f_{TP} G^2 v_f/D) [1 + x(v_{fg}/v_f)] + G^2 v_{fg} (dx/dz)}{1 + G^2 x (dv_g/dP)} \quad (1)$$

where

- G           ≡ mass flux, (kg/m<sup>2</sup>-sec)
- x           ≡ mass quality
- v<sub>f</sub>         ≡ specific volume of liquid, (m<sup>3</sup>/kg)
- v<sub>g</sub>         ≡ specific volume of gas, (m<sup>3</sup>/kg)
- v<sub>fg</sub>        ≡ v<sub>g</sub> - v<sub>f</sub>
- f<sub>TP</sub>        ≡ two phase friction factor
- dv<sub>g</sub>/dP    ≡ gas compressibility, (sec<sup>2</sup> - m<sup>4</sup>/kg<sup>2</sup>)

The two phase friction factor is given by the Blasius expression

$$f_{TP} = 0.079 (GD/\bar{\mu})^{-1/4} \quad (1a)$$

where

$$1/\bar{\mu} \quad \equiv (x/\mu_g) + [(1-x)/\mu_f] \quad (1b)$$

μ<sub>f</sub>         ≡ absolute viscosity of the liquid

μ<sub>g</sub>         ≡ absolute viscosity of the gas

When constant quality is considered, the term G<sup>2</sup> v<sub>fg</sub> (dx/dz) is identically zero and since no other parameters are functions of the longitudinal position, z, equation 1 can be readily integrated to give the pressure drop of a test section of length, L. The resulting equation is as follows

$$-\Delta P = \frac{2f_{TP} G^2 v_f L}{D} \frac{[1 + x(v_{fg}/v_f)]}{1 + G^2 x(dv_g/dP)} \quad (2)$$

### Separated Flow Model

The separated flow approach to calculate pressure drops differs from the homogeneous model in that the phases are assumed to travel at unequal mean velocities. Again neglecting the contributions of gravity and liquid compressibility, the equation governing pressure drop for the separated flow model is the following

$$-\frac{dP}{dz} = \frac{\frac{2f_{fo} G^2 v_f}{D} \phi_{fo}^2 + G^2 \frac{dx}{dz} \left[ \frac{2xv_g}{\alpha} - \frac{2(1-x)v_f}{(1-\alpha)} + \frac{d\alpha}{dx} \left( \frac{(1-x)^2 v_f}{(1-\alpha)^2} - \frac{x^2 v_g}{\alpha^2} \right) \right]}{1 + G^2 \left[ \frac{x^2}{\alpha} \frac{dv_g}{dP} + \frac{d\alpha}{dP} \left( \frac{(1-x)^2}{(1-\alpha)^2} v_f - \frac{x^2 v_g}{\alpha^2} \right) \right]} \quad (3)$$

where

$G, x, v_f, v_g, dv_g/dP$  are as before and

$\alpha \equiv$  void fraction

$f_{fo} \equiv$  friction factor when total flow is considered as a liquid

$\phi_{fo}^2 \equiv$  two-phase frictional multiplier

Baker's formula (Reference 2) can be used to calculate  $\alpha$  as a function of  $x$  when the criteria  $7.5 \leq y \leq 300$  and  $G < 950 \text{ kg/m}^2\text{-sec}$ .

$$x = \frac{\alpha^2 (y^{1/3} - 1) + \alpha}{y - \alpha (y - y^{1/3})} \quad (4)$$

or

$$\alpha = \frac{\sqrt{(1 + cm)^2 + 4 abx} - (1 + cx)}{2a} \quad (5)$$

where

$a \equiv (y^{1/3} - 1)$

$b \equiv y$

$c \equiv (y - y^{1/3})$

$$y \equiv 0.021 (v_g/v_f)G^{0.686}$$

The derivative of  $\alpha$  with  $x$  may also be found from the above equations.

$$\frac{d\alpha}{dx} = \frac{-(1+cx)(c/2a) + b}{[(1+cx)^2 + 4abx]^{1/2}} - \frac{c}{2a} \quad (6)$$

For those flow rates which are high enough to give  $y > 300$ , Lockhart-Martinelli relationships (Reference 2) are used to find  $\alpha$ ,  $d\alpha/dz$ . These equations are the following

$$\alpha = - [1 + (20/X) + (1/X^2)]^{-1/2} + 1 \quad (7)$$

$$\frac{d\alpha}{dx} = \frac{[(10/X^2) + (1/X^3)](v_f/v_g)^{1/2} (\mu_f/\mu_g)^{1/8} [x/(1-x)]^{1/8} (7/9x^2)}{[1 + (20/X) + (1/X^2)]^{3/2}} \quad (8)$$

where  $X$  is defined below.

The two phase friction multiplier  $\phi_{fo}^2$ , is also calculated from an equation based on the work of Lockhart-Martinelli which assumes both the liquid and the gas phases are turbulent (Reference 2).

$$\phi_{fo}^2 \equiv \phi_f^2 (1-x)^{1.75} \quad (9)$$

where

$$\phi_f^2 \equiv 1 + (20/X) + (1/X^2)$$

$$X \equiv [(1-x)/x]^{7/8} (v_f/v_g)^{1/2} (\mu_f/\mu_g)^{1/8}$$

As a check of the Lockhart-Martinelli equation for two-phase friction multiplier  $\phi_{fo}^2$ , Baroczy's method given in Reference 2 was also used to calculate  $\phi_{fo}^2$ , for flow rates of  $G = 320$  and  $640 \text{ kg/m}^2\text{-sec}$ . At mass qualities below 0.04, Baroczy's method gave higher values of  $\phi_{fo}^2$ . Above  $X = 0.04$ , the results were nearly identical.

Equation 3 was integrated to give pressure drop. As noted earlier,  $dx/dz$  is identically zero for constant quality flow. To make the integration tractable the term  $(d\alpha/dP)\{\cdot\}$  is ignored. The resulting equation is the following:

$$-\Delta P = \frac{2f_{fo} G^2 v_f L}{D} \phi_{fo}^2 \left[ \frac{dv_g}{dP} \right] \quad (10)$$

#### 4.5.2 PRESSURE DROP FOR FLOW BOILING, EXPERIMENT 2

4.5.2.1 Homogeneous Model. The homogeneous model for flow boiling pressure drop is again based on Equation 1. As flow boiling occurs with a constant and uniform wall heat flux, a linear change in mass quality is assumed to occur; i.e.,  $dx/dz = \text{constant}$ . Integrating Equation 1 gives the following equation.

$$-\Delta P = \frac{\eta L}{\psi} \left[ \lambda + \frac{1-\lambda\psi}{(x_0-x_1)} \ln \frac{(1+\psi x_0)}{(1+\psi x_1)} \right] + \frac{\kappa}{\psi} \ln \frac{(1+\psi x_0)}{(1+\psi x_1)} \quad (11)$$

where

$$\eta = 2\bar{f}_{TP} G^2 v_f/D$$

$$\lambda = v_{fg}/v_f$$

$$\kappa = G^2 v_{fg}$$

$$\psi = G^2 (dv_g/dP)$$

$\bar{f}_{TP} \equiv$  average friction factor over the test section

The expression for  $\bar{f}_{TP}$  is obtained by evaluating the integral

$$\left[ \int_{x_1}^{x_0} f_{TP}(x) dx \right] / (x_0 - x_1)$$

where  $f_{TP}$  is given by Equations 1a and 1b.

$$\bar{f}_{TP} = \frac{0.10533}{\left(\frac{GD}{\mu_f}\right)^{1/4} (x_o - x_i)} \frac{\left[1 + \left(\frac{\mu_f}{\mu_g} - 1\right)x_o\right]^{3/4} - \left[1 + \left(\frac{\mu_f}{\mu_g} - 1\right)x_i\right]^{3/4}}{\frac{\mu_f}{\mu_g} - 1} \quad (12)$$

### Separated Flow Model

Using the separated flow model of Equation 3 to calculate pressure drop is a more complex problem. The integral is given by the following

$$-\Delta P = \int_{x_i}^{x_o} \left[ \frac{2f_{fo} G^2 v_f L}{D(x_o - x_i)} \phi_{fo}^2 + G^2 \left[ \left( \frac{2x v_g}{\alpha} - \frac{2(1-x)v_f}{(1-\alpha)} \right) + \frac{d\alpha}{dx} \left( \frac{(1-x)^2 v_f}{(1-\alpha)^2} - \frac{x^2 v_g}{\alpha^2} \right) \right] \right] \frac{dx}{1 + G^2 \left( \frac{x^2}{\alpha} \right) \left( \frac{dv_g}{dP} \right)} \quad (13)$$

In the above integral,  $\alpha$  and  $d\alpha/dx$  are complex functions of  $x$  whose form may change depending on the mass flow rate  $G$ . The numerical integration procedure used was a composite trapezoidal approach.

4.5.3 PRESENTATION AND DISCUSSION OF CALCULATIONS. For both experiments 1 and 2 the values of mass flow rate  $G$  were chosen to be  $G = 10, 20, 40, 80, 160, 320$  and  $640 \text{ kg/m}^2\text{-sec}$ . Qualities used in calculating  $\Delta P$  for the air/water system (Exp. 1) were  $x = 0.01, 0.02, 0.04, 0.08, 0.16, 0.32$  and  $0.64$ . A summary of inlet and outlet qualities  $x_i, x_o$  for the flow boiling system (Exp. 2) is given in the following table.

Table 4-3. Inlet and Outlet Qualities - Flow Boiling System.

TSAT	20C (68F)		12C (54F)		4C (40F)		-3C (26F)	
	$x_i$	$x_o$	$x_i$	$x_o$	$x_i$	$x_o$	$x_i$	$x_o$
$G = 10 \text{ kg}/(\text{m}^2\text{-sec})$	0.0052	0.037	0.041	0.072	0.075	0.106	0.109	0.598
20	↓	↓	↓	↓	↓	↓	↓	↓
40	↓	↓	↓	↓	↓	↓	↓	↓
80	↓	↓	↓	↓	↓	↓	↓	0.354
160	↓	↓	↓	↓	↓	↓	↓	0.231
320	↓	↓	↓	↓	↓	↓	↓	0.170
640	↓	↓	↓	↓	↓	↓	↓	0.140

Calculated pressure drops are presented in Figures 4-4 and 4-5. The most striking feature of these results is that the range of expected pressure drops span four orders of magnitude. Instrumentation to measure pressure drop over such a range is accomplished by using selectable differential pressure transducers (see Figure 4-1).

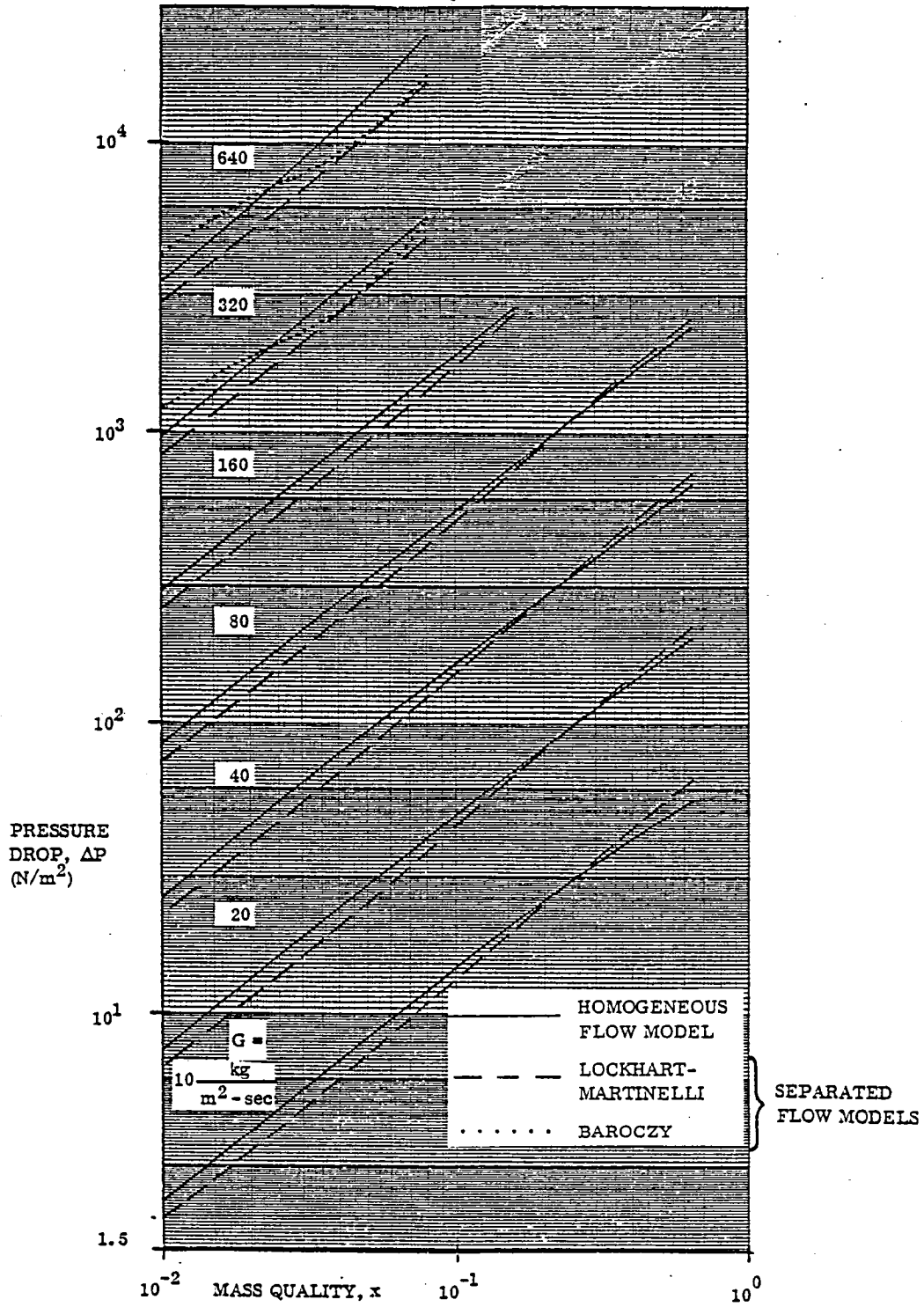


Figure 4-4. Pressure Loss as a Function of Quality for Isothermal Air Water System

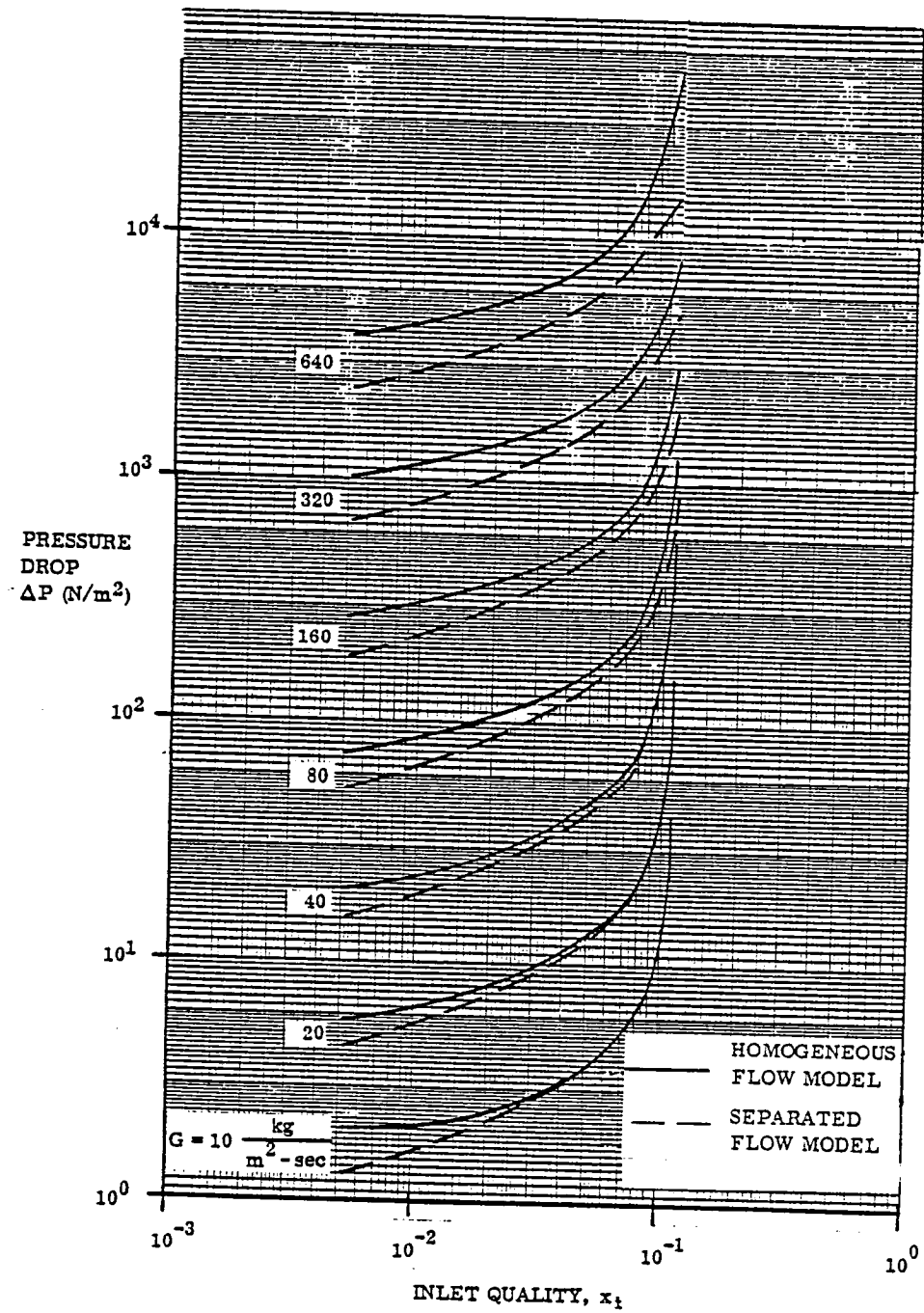


Figure 4-5. Pressure Loss as a Function of Inlet Quality for Flow Boiling System

The results also indicate that the homogeneous model almost always predicts a larger pressure drop than the predictions resulting from the separated flow model when the Lockhart-Martinelli equations are used to calculate  $\phi_{fo}^2$ . The use of the Baroczy relationships\* in the calculation of  $\phi_{fo}^2$ , (done for  $G = 320, 640 \text{ kg/m}^2\text{-sec}$  in the air-water system), accounts for the effect that  $G$  may have on the two phase frictional multiplier  $\phi_{fo}^2$ . Therefore the pressure drops resulting from the use of Baroczy's equations may be more realistic than those resulting from either the homogeneous or Lockhart-Martinelli approach. It may be hypothesized that as mass quality increases from one test case to another, the "true" pressure drop curve may initially follow the results of the homogeneous model, undergo a transition, and subsequently follow the results of the separated flow model. The results of the Baroczy method would seem to indicate this.

4.5.4 WALL TEMPERATURE CALCULATIONS FOR FLOW BOILING EXPERIMENT. In the flow boiling experiment, wall temperatures as well as fluid temperatures will be measured. Calculations were therefore performed to predict wall temperature for various experimental conditions.

Figure 4-6 indicates the flow patterns and heat transfer mechanisms expected when a subcooled fluid passes through a heated test section. In the experiments to be conducted however, the fluid enters in a saturated state and the heat flux and flow rates are such that liquid dryout does not occur. Therefore saturated nucleate boiling and forced convection are the only heat transfer mechanisms that need to be considered. It remains to assess the contribution of both heat transfer mechanisms to the total heat transfer coefficient. The relative importance of one heat transfer mechanism to the other, for any given position in the tube, is a function of mass flux, fluid properties and the gravity level.

The effect of mass flux and fluid properties on both heat transfer mechanisms are included in the approach of Chen (Reference 3). The effect of gravity is not considered. His equations are presented and subsequently will be used in solving for the wall temperatures. It may be hypothesized that the reduced gravity will allow for larger bubbles to form at the nucleation sites and will reduce the frequency of bubble departure. The magnitude of the nucleate boiling heat transfer coefficient should therefore decrease. It is expected that given identical test conditions, the wall temperatures initially will be larger in the reduced gravity case and will approach the one-g values as one traverses downstream. This gravitational effect on wall temperature should be more pronounced for lower mass fluxes.

---

\*The actual mass fluxes used by Baroczy are 678 and 339  $\text{kg/m}^2\text{-sec}$ . Therefore the pressure drops calculated from this method are a little larger, (by 12%), than the pressure drops that would have resulted if  $G$  was equal to the values 640 and 320  $\text{kg/m}^2\text{-sec}$ .

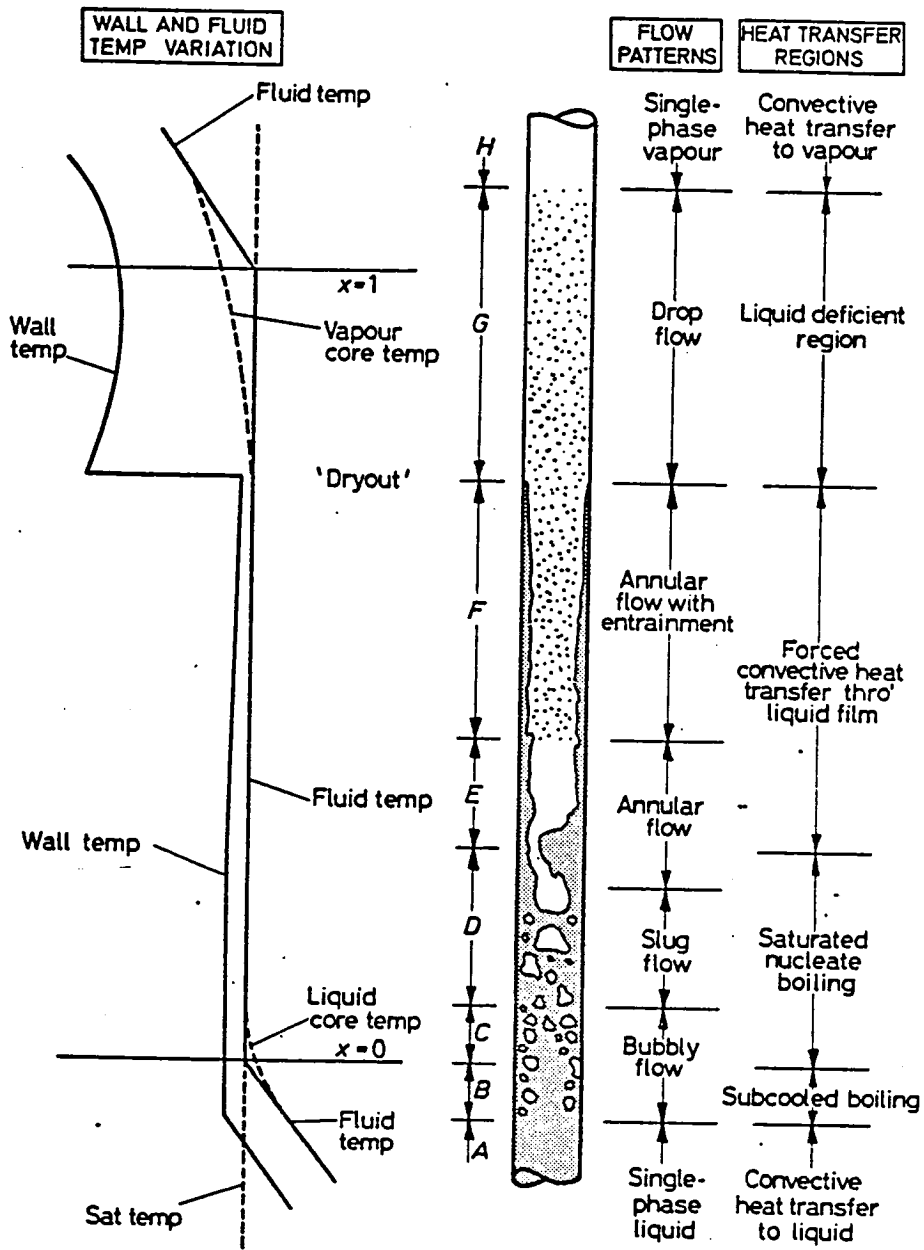


Figure 4-6. Regions of Heat Transfer in Convective Boiling

The equation that Chen has derived to calculate the nucleate boiling and forced convective heat transfer coefficients are given below. The factors which determine the relative contributions of each mechanism, F and S, can be found in Figure 4-7.

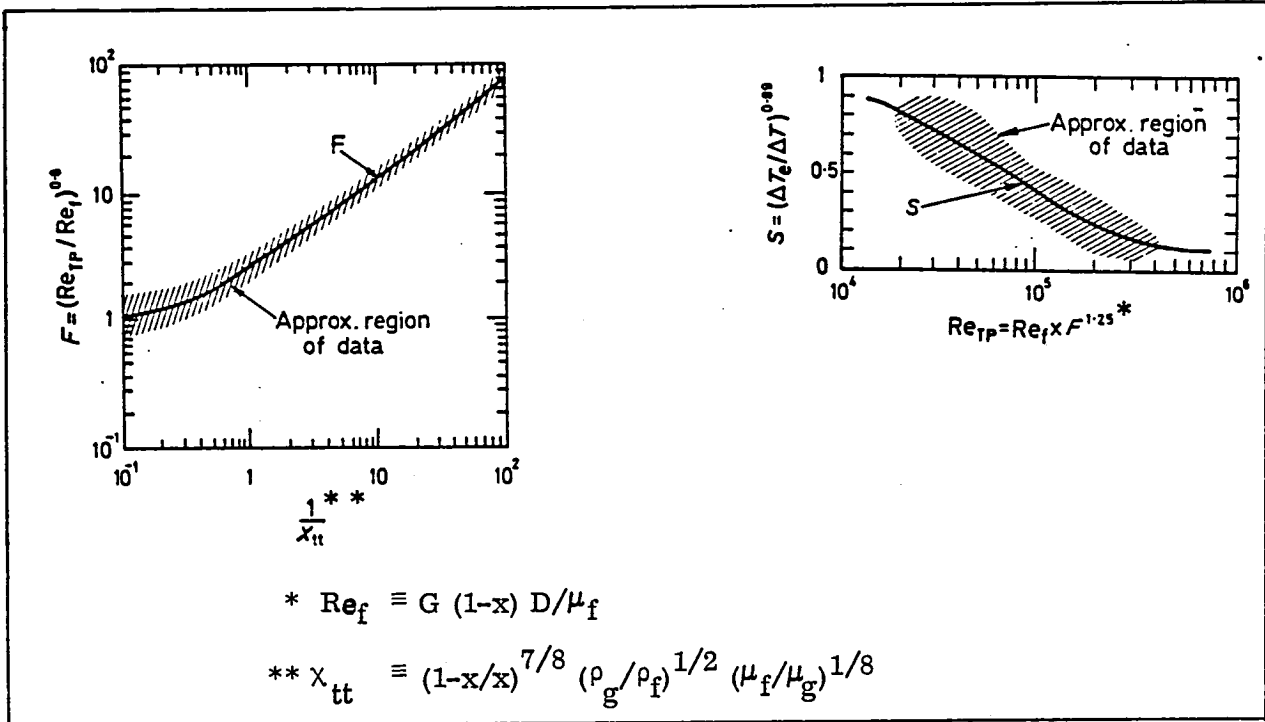


Figure 4-7. Values of F and S as Used in Equations 14 and 15

$$h_c = 0.023(G(1-x)D/\mu_f)^{0.8} (\mu c_p/k)_f^{0.4} (k_f/D)(F) \quad (14)$$

$$h_{NCB} = 0.00122 \frac{k_f^{0.79} C_{pf}^{0.45} \rho_f^{0.49}}{\sigma^{0.5} \mu_f^{0.29} i_{fg}^{0.24} \rho_g^{0.24}} \Delta T_{SAT}^{0.24} \Delta P_{SAT}^{0.75} (S) \quad (15)$$

where

$C_{pf}$  = constant pressure specific heat of liquid phase, (Btu/lb<sub>m</sub>-F)

D = diameter of tube,(ft)

F = defined in Figure 4-7, (φ)

G = mass flux, (lbm/ft<sup>2</sup>-sec)

$h_c$  = convective heat transfer coefficient, (Btu/ft<sup>2</sup>-sec-F)

$h_{NCB}$  = nucleate boiling heat transfer coefficient, (Btu/ft<sup>2</sup>-sec-F)

- $i_{fg}$  = heat of vaporization, (Btu/lbm)  
 $k_f$  = thermal conductivity of liquid phase, (Btu/ft-sec-F)  
 $S$  = defined in Figure 4-7 ( $\phi$ )  
 $x$  = mass quality, ( $\phi$ )  
 $\Delta P_{SAT}$  = difference in saturation pressure corresponding to  $\Delta T_{SAT}$ , (lbf/ft<sup>2</sup>)  
 $\Delta T_{SAT}$  = difference between wall and saturation temperatures (F)  
 $\mu_f$  = dynamic viscosity of liquid phase, (lbm/ft-sec)  
 $\rho_f$  = density of liquid phase, (lbm/ft<sup>3</sup>)  
 $\rho_g$  = density of gas phase, (lbm/ft<sup>3</sup>)  
 $\sigma$  = surface tension, (lbf/ft)

- The method of calculation employed to find the wall temperatures can be summarized as follows. Given  $G$ ,  $x$ ,  $T_{SAT}$ ,  $q$  and fluid properties, find  $T_w$  such that when  $h_c$  and  $h_{NCB}$  are evaluated, the following equation is satisfied as well.

$$q = (h_c + h_{NCB})(T_w - T_{SAT})$$

The values of the experimental parameters that were used in calculating the results are summarized in Table 4-3 below.

The resulting wall temperature values were calculated at 25, 60 and 75 percent of the test section's length and curves were fit through these points. The results are shown in Figure 4-8. It can be seen that the decline of the influence of  $h_{NCB}$  and the subsequent increase in  $h_c$  as one moves downstream, result in wall temperature that remain approximately constant along the test section. Since Chen's equations are based on experimental data generated in one-g, the wall temperatures calculated here are applicable for one-g as well. The effect of a reduced gravity field on the wall temperature distribution were earlier postulated to increase the wall temperatures in the region of the test section where nucleate boiling is significant. In the region where forced convection heat transfer is dominant, there should be no effect of the gravity level on the wall temperature.

Table 4-3. Heat Fluxes For Wall Temperature Calculations.  
 $q$  ( $\text{j}/\text{m}^2 - \text{sec}$ )

	$x_i = 0.0052$ $x_o = 0.037$ $T_{SAT} = 20C$	$x_i = 0.041$ $x_o = 0.072$ $T_{SAT} = 12.2C$	$x_i = 0.075$ $x_o = 0.106$ $T_{SAT} = 4.4C$	$x_i = 0.709$ $T_{SAT} = 3.3C$
$G$ ( $\text{kg}/\text{m}^2 - \text{sec}$ ) =				
10	240.8	238.4	242.0	3873.0 ( $x_o = 0.598$ )
20	481.6	476.8	483.9	7746.0 ( $x_o = 0.598$ )
40	963.1	953.5	967.9	15492.0 ( $x_o = 0.598$ )
80	1926.0	1907.0	1936.0	15500.0 ( $x_o = 0.354$ )
160	3852.0	3814.0	3871.0	15500.0 ( $x_o = 0.231$ )
320	7705.0	7628.0	7743.0	15500.0 ( $x_o = 0.170$ )
640	15410.0	15256.0	15486.0	15500.0 ( $x_o = 0.140$ )

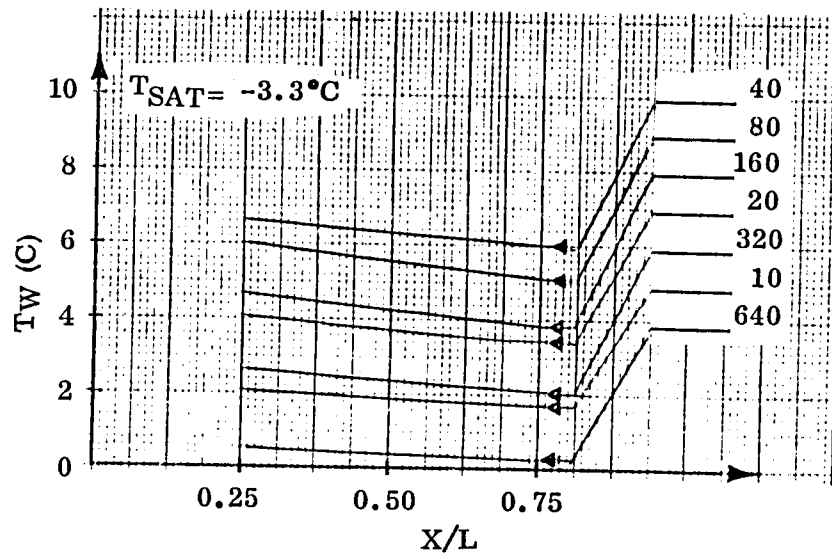
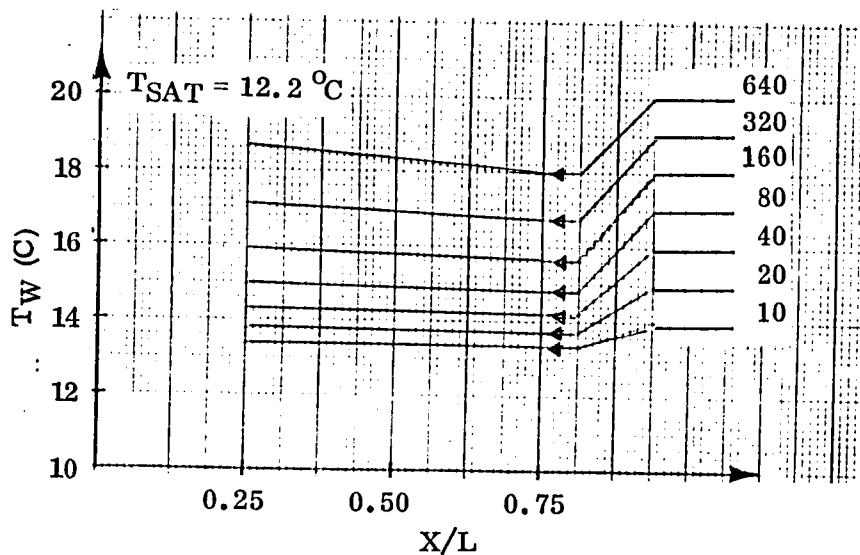
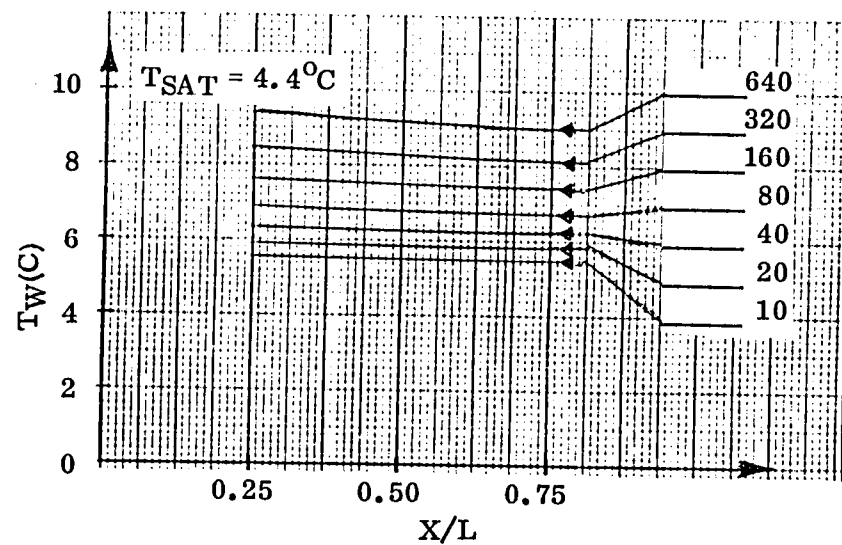
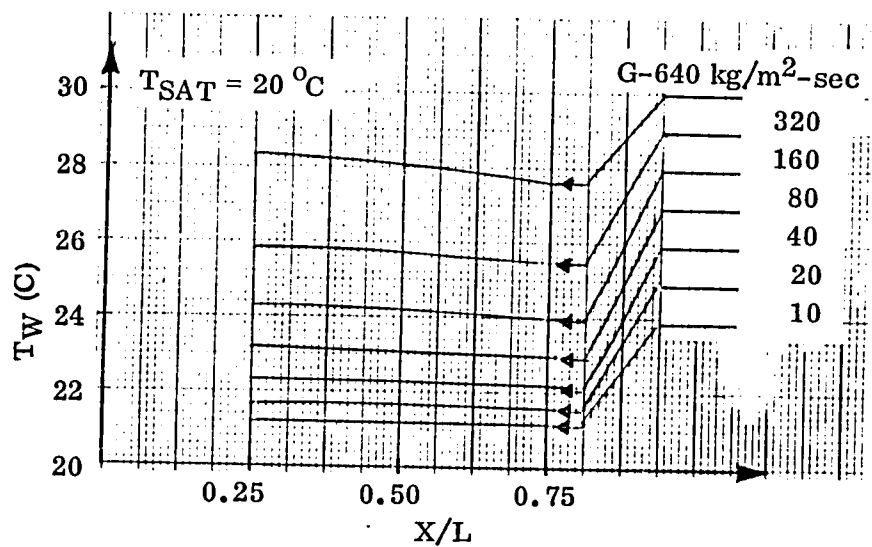


Figure 4-8. Wall Temperature as a Function of Position Along Tube for Various Experimental Conditions

# 5

## POOL BOILING, EXPERIMENT 3

### 5.1 DESCRIPTION

The pool boiling experiment consists of 12 sealed cells (four large size and eight small size) each containing a single wire electric heating element immersed in a liquid. The cells are stored in a preconditioning chamber which preheats and maintains the fluids close to the saturation temperature desired for the test. A typical cell consists of a closed box with flat ends and sides. The top is a formed section with compound curvature leading to a standpipe in the top center of the box. An isolation valve in the standpipe affords a means to connect to a line containing an adjustable backpressure regulator which is in turn connected to the Spacelab vent assembly. The top curvature is such as to prevent vapor entrapment during vapor evolution in the course of the test. This avoids square corners where capillary action could cause liquid encirclement of a vapor bubble preventing vapor venting, and resulting in pressure increase in the cell which would in turn change the fluid saturation temperature. The cell is equipped with opposed optical windows to permit photography of the boiling within the cell and a means to provide back-lighting for best photographic results. An internal heating wire, pressure ports, thermocouples and electrical connectors are integral with each cell. The cells are constructed of high quality copper to minimize cell temperature gradients. Sufficient ullage is allowed in the fill procedure to provide for fluid volume change for the maximum expected temperature excursion during shipment, handling, and transport to orbit conditions. The vapor-phase thermocouple will be used as a filling hole.

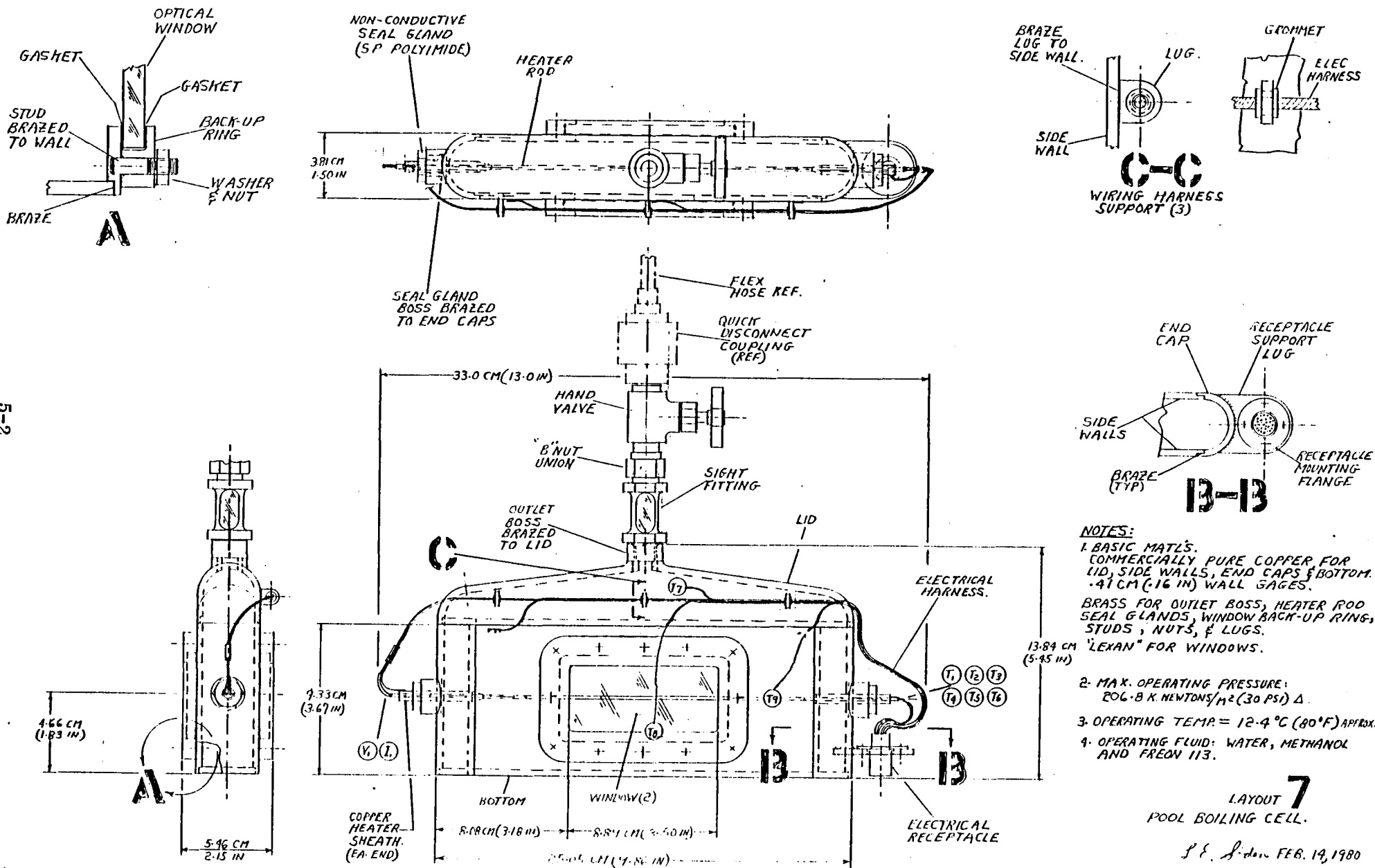
The box will be heated to the normal boiling temperature of the liquid it is to contain. A tube will be inserted through the open port (with a little clearance) and directed into the bottom of the box. Saturated vapor will then be blown through the tube. Most of it will scavenge air from the box and some will condense. The liquid level in the box will be adjusted to that desired by controlling the inlet temperature of the vapor. The scavenging process will be permitted to proceed for an hour or so to remove almost all of the air. Then the top thermocouple will be inserted and the box will be permanently sealed.

The preheating chamber is sized to hold the 12 cells. A chamber closure is optional but not considered necessary at this time. Each cell bottom rests firmly on a strip heater which provides the proper heat input to maintain the fluid at or near to the saturation temperature desired during the test.

The cell configuration is shown in Figure 5-1 for the large cell. Both large and small cells are geometrically similar.

### 5.2 METHOD OF OPERATION

The pool boiling experiment is located in the central portion of the rack. This is shown in Figure 5-2. The packaging arrangement proposed dictates that this experiment be run first. All experiments are initially mounted in the rack with the bubble dynamics in a



- NOTES:**
1. BASIC MATLS.  
COMMERCIALLY PURE COPPER FOR LID, SIDE WALLS, END CAPS & BOTTOM.  
.41 CM (.16 IN) WALL GAGES.  
BRASS FOR OUTLET BOSS, HEATER ROD SEAL GLANDS, WINDOW BACK-UP RING, STUDS, NUTS, & LUGS.  
"LEXAN" FOR WINDOWS.
  2. MAX. OPERATING PRESSURE:  
206.8 K. NEWTONS/M<sup>2</sup> (30 PSI) Δ.
  3. OPERATING TEMP. = 12.4 °C (80 °F) APPROX.
  4. OPERATING FLUID: WATER, METHANOL AND FREON 113.

LAYOUT **7**  
POOL BOILING CELL.  
J. E. Lidon FEB. 14, 1980

Figure 5-1. Pool Boiling Test Cell, Large Box Illustrated

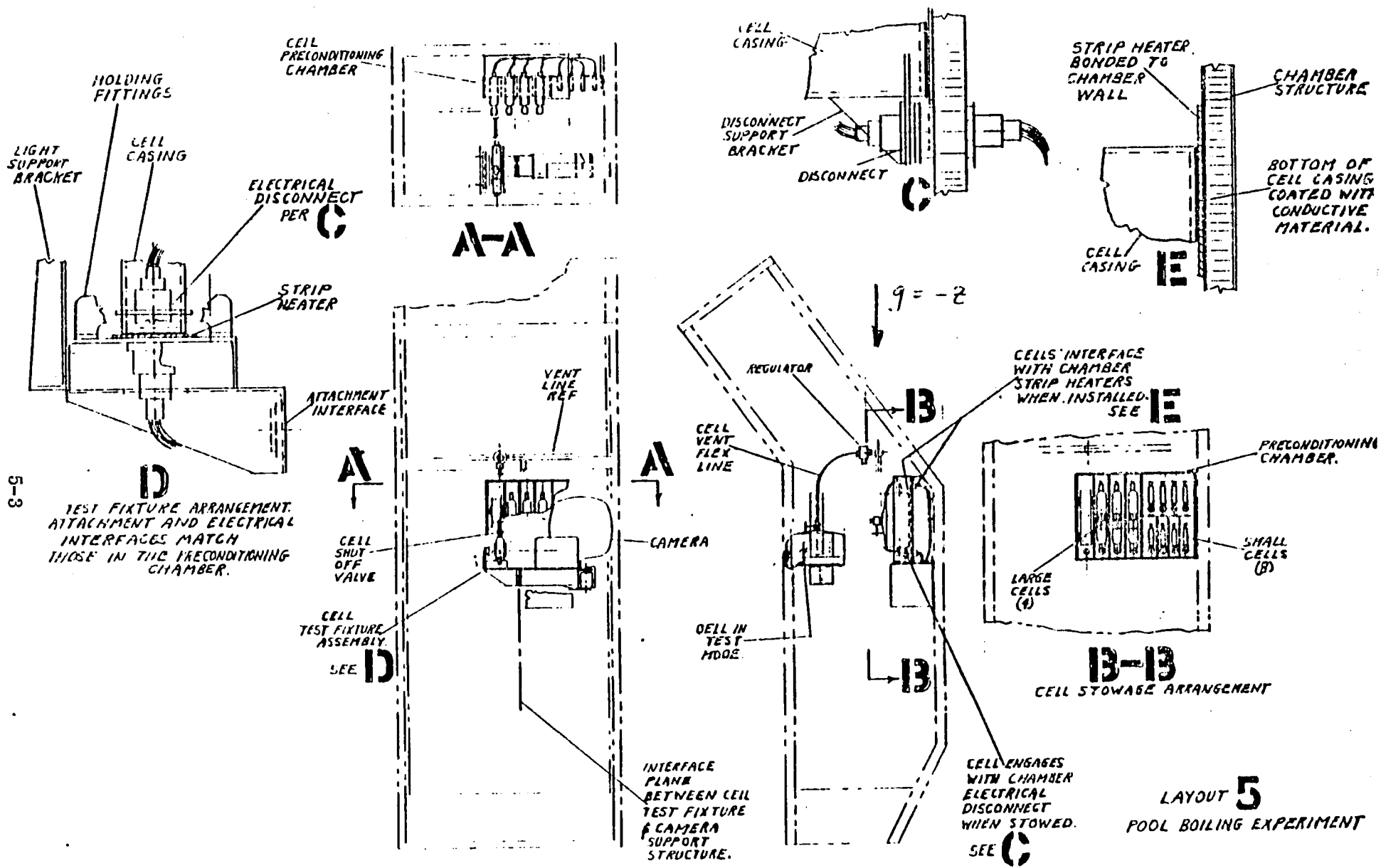


Figure 5-2. Pool Boiling Layout

L E Jan. July 26, 1979

stored position remote from the position in which it will finally be tested. The pool boiling experiment is equipped with a single test section. Each cell is taken in turn from the preconditioning chamber and placed in the test position in the test section, and test connections are made for venting, power, and instrumentation. Cameras are adjusted and testing of the cell configuration is accomplished. The tested cell is returned to the preconditioning chamber and another cell is selected for test. The process is repeated until all testing is completed. The pool boiling apparatus is then removed from the rack and stored in one of the available Spacelab storage compartments.

While in the preconditioning chamber, each cell is individually heated and maintained at essentially constant temperature by individual temperature sensing in the cell and switching heater power on and off by use of the sensor output signal. Because of high thermal inertia of the fluid/cell combination, the control need not be fast acting although accuracy to maintain a narrow control band is desired. This same high thermal inertia is felt to be adequate to allow a reasonable time lapse between removal of a cell from the preconditioning chamber and initiation of the test without undue drift of temperature or establishment of significant fluid temperature gradients.

The testing to be accomplished for this experiment is summarized in Table 5-1.

### 5.3 INSTRUMENTATION

Instrumentation consists of one pressure transducer to set the backpressure regulator and monitor cell pressure, thermocouples to record internal temperatures, heater voltage and current, an accelerometer, and camera coverage. The instrumentation location within the experiment is shown in Figure 5-1. An instrumentation list showing required sensor characteristics and also detailing the significant experiment components is shown in Table 5-2.

Table 5-1. Test Parameters for Pool Boiling Experiment

TEST NO.	FLUID	TEMP C (F)	PRESS. kN/m <sup>2</sup> (PSIA)	CELL SIZE	VOLTS	AMPS	g LEVEL
1	H <sub>2</sub> O	57(134.6)	17.2 (2.5)	Small	.843	15.5	1.0 × 10 <sup>-4</sup>
2	↓	↓	↓	↓	1.04	19.1	3.3 × 10 <sup>-3</sup>
3	↓	↓	↓	↓	1.57	4.0	1.0 × 10 <sup>-4</sup>
4	↓	↓	↓	↓	1.87	4.76	3.3 × 10 <sup>-3</sup>
5	CH <sub>3</sub> OH	39(102.2)	33.4 (4.85)	Large	3.33	35.4	3.3 × 10 <sup>-3</sup>
6	↓	↓	↓	Large	2.74	29.1	1.0 × 10 <sup>-4</sup>
7	↓	↓	↓	Small	.87	17.8	1.0 × 10 <sup>-4</sup>
8	↓	↓	↓	Small	1.1	12.9	3.3 × 10 <sup>-3</sup>
9	F-113	36(96.8)	67.9 (9.85)	Small	.687	4.8	1.0 × 10 <sup>-4</sup>
10	↓	↓	↓	Small	.837	5.35	3.3 × 10 <sup>-3</sup>
11	↓	↓	↓	Large	1.774	18.1	1.0 × 10 <sup>-4</sup>
12	↓	↓	↓	Large	2.155	22.0	3.3 × 10 <sup>-3</sup>

Table 5-2. Instrumentation/Component Requirements - Experiment 3, Pool Boiling

Measurement		Sensor Type	Range	Resolution (Accuracy)	Test Runs		Data Sampling Rate	Notes
I. D.	Description				Number	Duration Each, Sec.		
T <sub>1</sub> to T <sub>6</sub>	Heater Temperature	TC specified by P.I. Chromel-Al.	15.6-538C (60-1000F)	1.1C(±1.1C) (2F(±2F))	12-24	45	1/sec.	T sensors are incorporated in each test cell.
T <sub>7</sub> to T <sub>9</sub>	Fluid Temp.	TC spec. by P.I. Chrom.-Al.	15.6-65.6C (60-150F)	0.56C(±0.56C) (1F(±1F))	12-24	45	1/sec.	Display of T <sub>8</sub> during standby is required.
P <sub>1</sub>	Vent Pressure	Xducer	17.2-67.9 kN/m <sup>2</sup> (2.5-9.85 psia)	±0.69 kN/m <sup>2</sup> ±0.1 psia	12-24	45	1/sec.	Display on experiment package required for pressure control adjustment.
V <sub>1</sub>	Htr. Voltage	None Req'd.	0.69-3.3 v (0-50 nom.)	±0.007 v	12-24	45	1/sec.	This voltage can be directly sampled by the CDMS RAU.
I <sub>1</sub>	Htr. Current	Ammeter	4-35.4 amp (0-50 nom.)	0.04 amps	12-24	45	1/sec.	
g <sub>x, y, z</sub>	g-level	Accelerom-	10 <sup>-4</sup> - 10 <sup>-2</sup>	10 <sup>-5</sup> ±10 <sup>-5</sup> g	12-24	45	10/sec.	Display to be monit. by Cam.
<b>COMPONENTS</b>								
BPR <sub>1</sub>	Back Press. Reg.		6.9-103 kN/m <sup>2</sup> (1-15 psia)	±0.69 kN/m <sup>2</sup> ±0.1 psia				Monitor thru P.
Camera	B&Q 16 mm, HI Spd.							200 frames/sec
C <sub>1</sub>	Controller for Strip Htrs., 12 req'd., On-Off TC Input							
S <sub>1</sub>	Relay, dc, 24 v.							For heater power control.

#### 5.4 ANALYSIS TO PREDICT FLUID TEMPERATURE GRADIENTS

Fluid in the pool boiling containers must be heated to near saturation conditions before actual experimentation takes place. A convenient method of preheating the fluid is to heat the container bottom at a sufficiently low flux that thermal gradients remain very small. The containers are constructed of copper material (with glass viewing ports) which helps to minimize temperature gradients. A thermal analysis was performed to determine fluid temperature gradients occurring with the above preheating method.

Two sizes of test cell containers are used with three different fluids. Container dimensions are defined in Reference 4 and are shown in Figure 5-3. Two thermal model approaches were considered in setting up a nodal network for computer analysis. The first was a two-dimensional approach for both the large and small-sized boxes. This approach disregards the presence of the window and end effects but provides adequate results which simplify preliminary analysis. To check the accuracy of the 2-D model a 3-dimensional model was developed. Because this approach is more complex, albeit more realistic, and as the thermal gradients are expected to be greater for the large box, the 3-D approach was done for the large box only.

Heat transfer from container wall to the fluid was assumed to occur solely by conduction. Forced conduction of ambient air surrounding the test cell was conservatively assumed

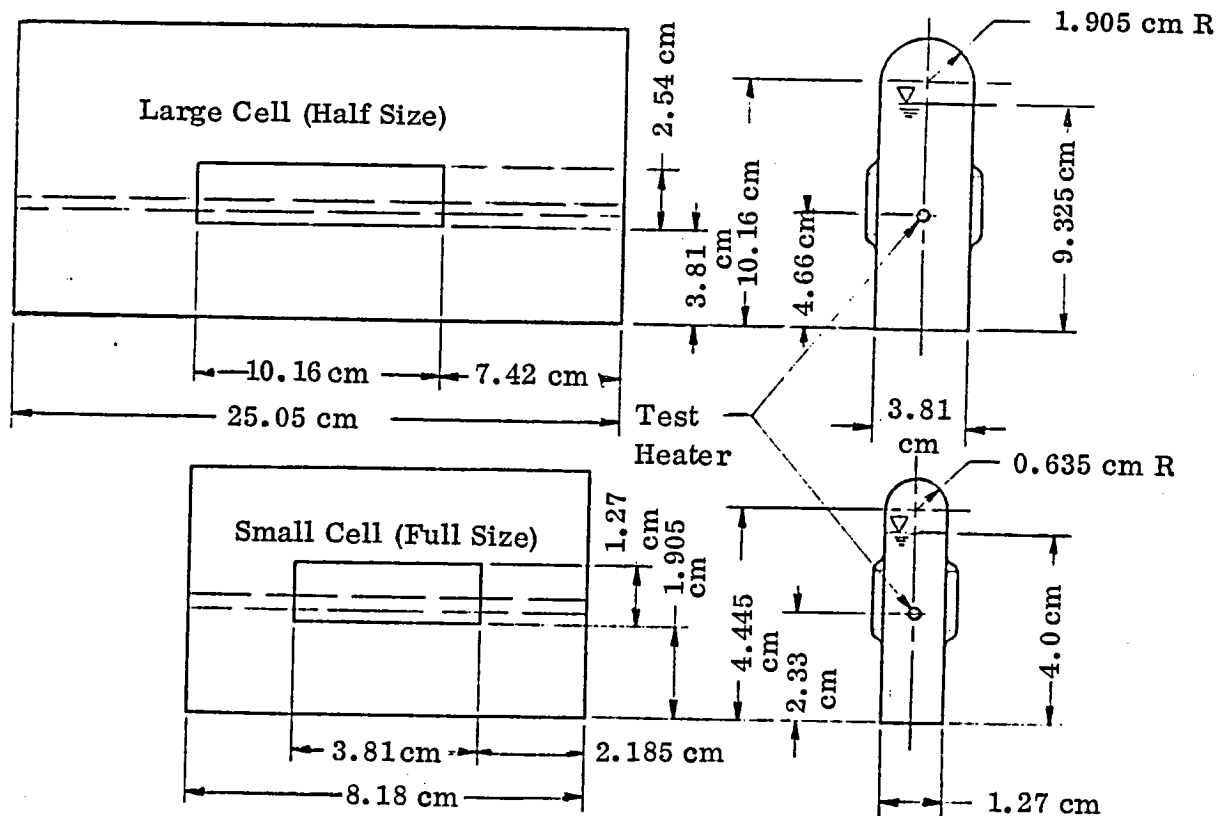


Figure 5-3. Test Cell Configuration

to give a convective heat transfer coefficient of approximately  $2.3 \text{ watt/cm}^2\text{-K}$  ( $4 \text{ Btu/hr-ft}^2\text{-F}$ ). Each analysis simulated an amount of heat addition to the container bottom which brings the fluid from 293K to saturation temperature in eight hours.

Temperature distributions at the end of the eight hour preheating period were calculated for each fluid/box size combination using the 2-D and 3-D approaches. The fluid temperature distributions as well as the heat rate necessary to achieve such distributions are presented in Figure 5-4. It can be seen that the application of relatively low power results in nearly uniform temperature distributions for all cases considered. The largest deviation (2.4 percent) occurs when the fluid considered is Freon-113 and the 3-D model is used. The vertical thermal gradients in the smaller boxes, as expected, are smaller than those in the larger boxes. The 3-D models show a requirement for slightly greater heat addition indicating the additional heat loss from the container ends not accounted for in the 2-D model.

A summary of heating requirements is shown in Table 5-3.

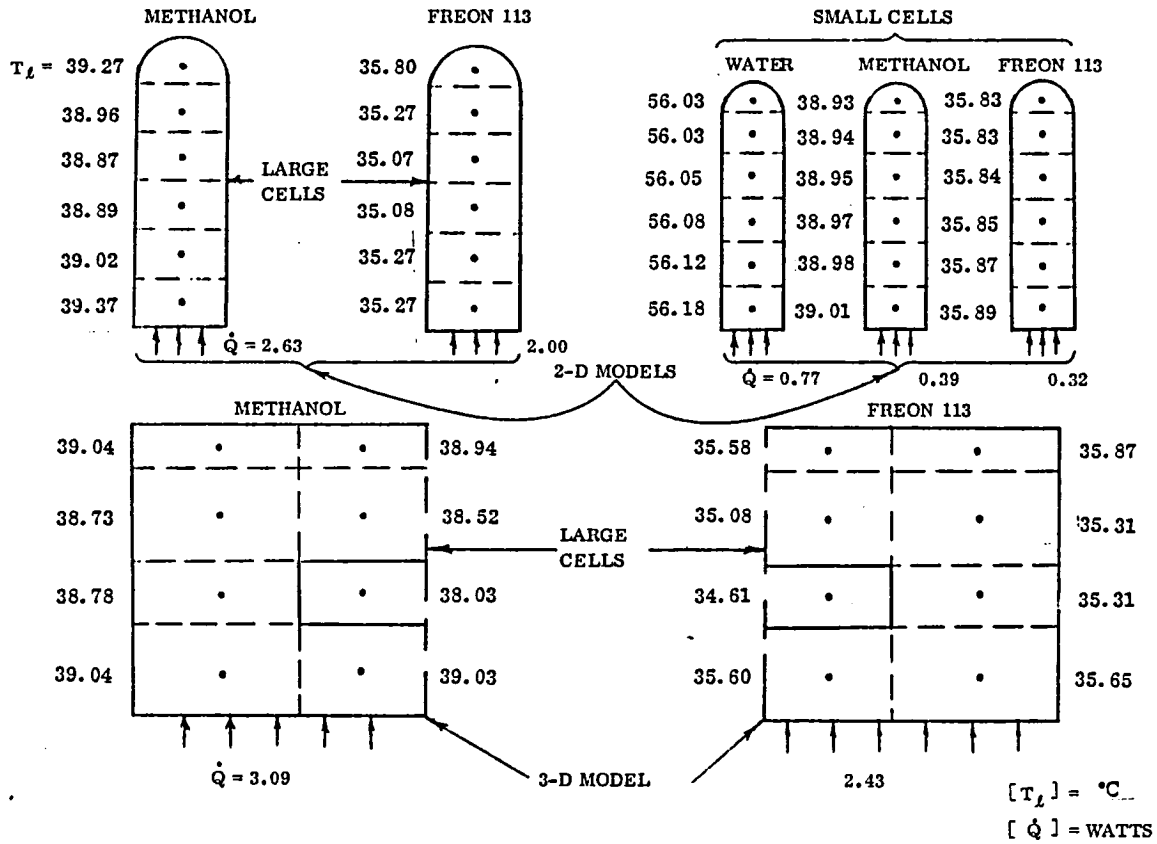


Figure 5-4. Fluid Temperature Distribution After Eight Hours of Heating

Table 5-3. Thermal Analysis Results

Preheating Power (Maximum, W)		
Fluid	Large Cells	Small Cells
Methanol	3.15	1.45
Freon 113	2.40	1.21
Water	-	2.89
Total Power Supplied to Warming Box (W)		
Methanol Cells	2 (3.15) + 2 (1.45) =	9.20
Freon 113 Cells	2 (2.40) + 2 (1.21) =	7.22
Water Cells	4 (2.89) =	<u>11.56</u>
	Total	27.98



# 6

## LIQUID REORIENTATION, EXPERIMENT 4

### 6.1 DESCRIPTION

The objective of this test is to obtain experimental data on the liquid reorientation process when caused by either constant acceleration or by a short duration impulse. To evaluate the effect of geometry, two tank sizes were selected; one with L/D = 2, and the other with L/D = 4. To allow commonality of fluids as far as possible, Freon 113 was chosen for the experiment. The tanks are made of clear Lexan so that photographic data of liquid movement and liquid front reorientation can be analyzed. The schedule of tests to be performed is given in Table 6-1 with respect to fill levels, g-levels, and test times.

Table 6-1. Test Parameters for Liquid Reorientation, Experiment 4

Tank #	No. of Runs	Duration each Run	Liquid Levels	g-Levels	Comment
1	5	80 sec.	20-70% ↓	$1.8 - 2.6 \times 10^{-4}$	Steady G
2	5	80 sec.		$5.5 - 7.8 \times 10^{-4}$	Steady G
1	5	.3 sec impulse ~ 20 sec. data		0.01	G Impulse
2	5	1.2 sec. Imp. ~ 20 sec. data		0.005	G Impulse

The test setup is shown in Figure 6-1 and the design layout showing its position and installation within the rack is shown in Figure 6-2. The reservoir shown is a capillary acquisition tank and is sized to contain all the liquid necessary to fill both tanks to the required level, the plumbing, plus a 10% reserve capacity.

### 6.2 METHOD OF OPERATION

Each tank is equipped with dual purpose isolation and fill and vent valves. The tanks are connected in parallel so that each may vent to a gas/liquid separator. The gas side of the separator connects through a back pressure regulator to the Spacelab vent assembly. The liquid side returns liquid to the reservoir by pumping action of the separator. The tanks as initially installed are filled with dry GN<sub>2</sub> with a slightly positive pressure with respect to sea level pressure and isolation valves closed to maintain the sealed integrity of the tank interior. When it is desired to begin testing,

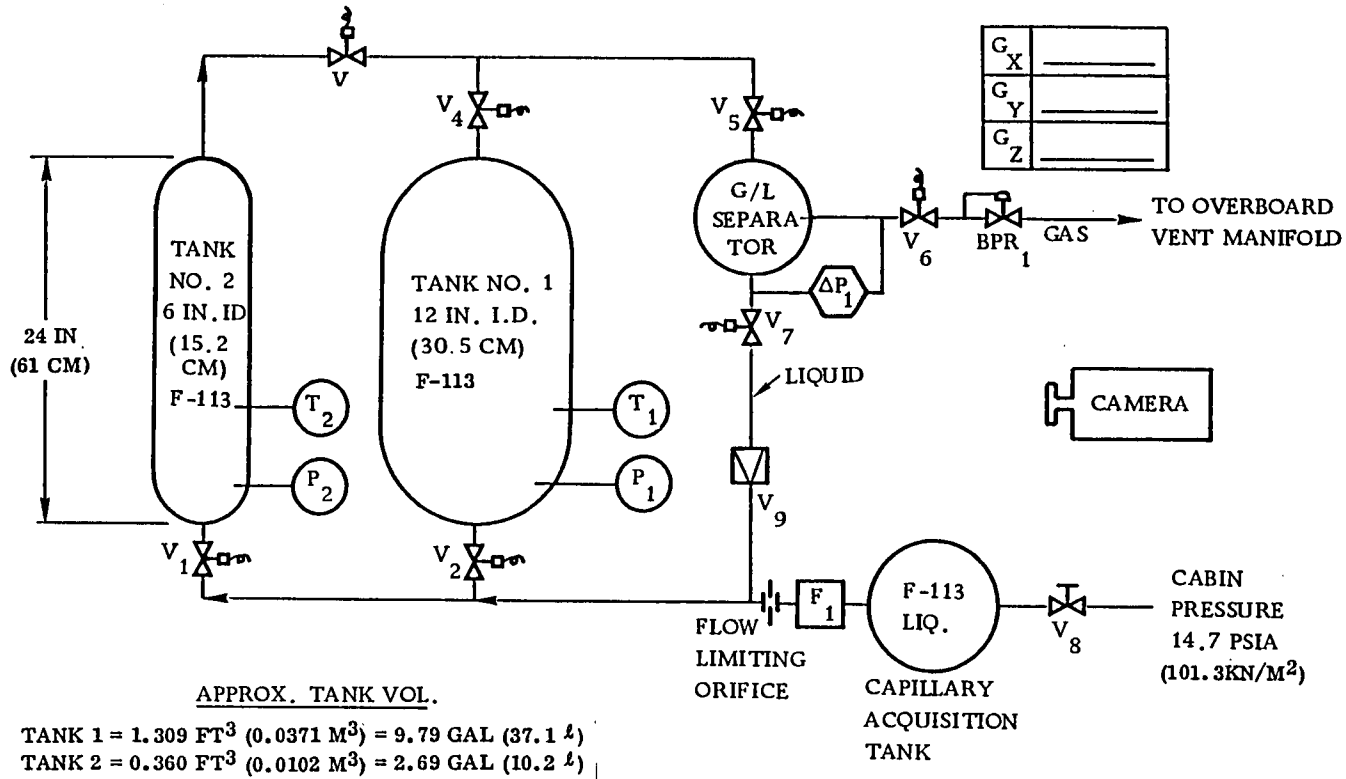
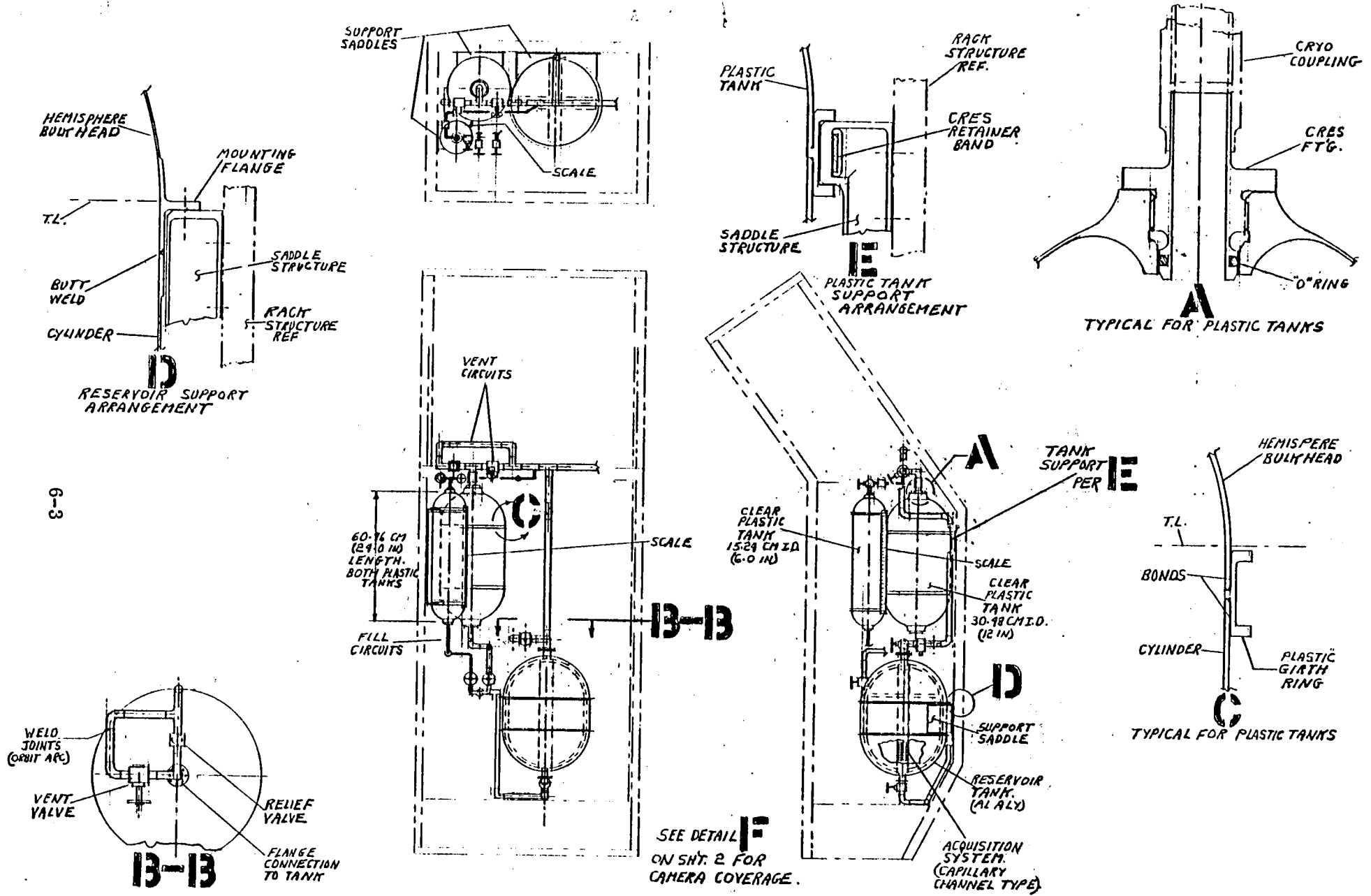
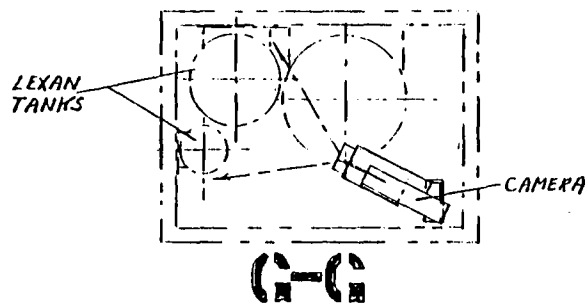


Figure 6-1. Liquid Reorientation Schematic, Experiment 4

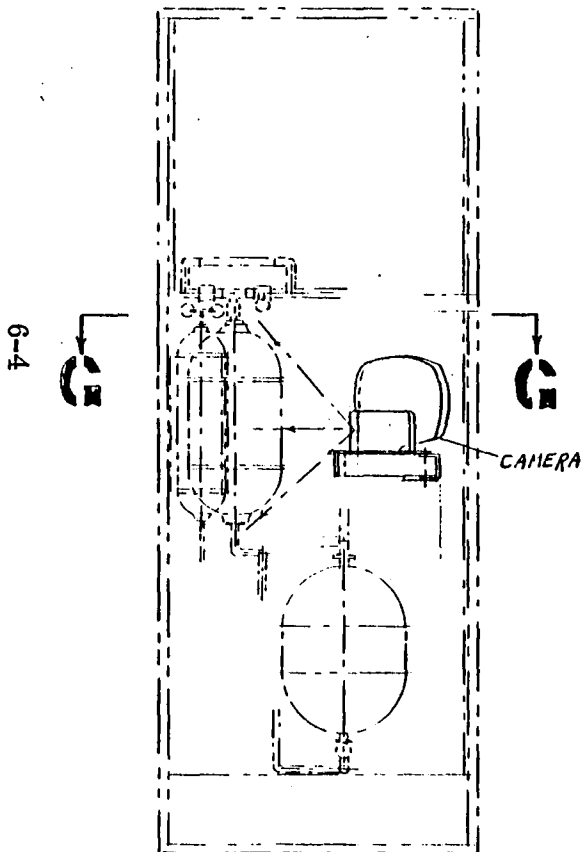


6-3

Figure 6-2. Liquid Reorientation Experiment Layout



6-3



FROM SH. 1

ITEM	NO	WT.
	SCALE	KG
		(LBS)
		1.36
RESERVOIR ACQUISITION SYSTEM		(3.0)
		3.18
PLUMBING		(7.0)
		1.81
INSTRUMENTATION & ELECTRICAL		(4.0)
		1.36
MSC. BOLT, NUTS, CLIPS & FITTINGS.		(3.0)
10% CONTINGENCIES		2.72
		(6.0)
TOTAL		29.7
		(65.5)

ITEM	NO	WT.
	SCALE	KG
		(LBS)
		2.09
30.5 CM PLASTIC BULKHEADS		(4.6)
		2.50
30.5 CM DIA. CYLINDER & GIRTH RINGS		(5.5)
		1.36
END FITTINGS FOR PLASTIC TANKS		(3.0)
		1.18
15.2 CM DIA. PLASTIC BULKHEADS		(2.6)
		1.36
15.2 CM DIA. CYLINDER & GIRTH RINGS		(3.0)
		0.14
SCALE	INCL. ALLOW. FOR SUPPORTS	(.3)
		2.27
SUPPORT SADDLES	AL ALY	(5.0)
		3.40
RESERVOIR BULKHEADS	AL ALY	(7.5)
		0.91
RESERVOIR CYLINDER	AL ALY	(2.0)
		4.08
RELIEF & SHUT OFF VALVES		(9.0)

Figure 6-2. Liquid Reorientation Experiment Layout (Continued)

and recognizing that the procedure will be the same for either tank, the procedure using Tank #1 is as follows:

With the back pressure regulator set to a predetermined value of the probable saturation pressure corresponding to the Freon temperature in the reservoir, Valve  $V_6$ ,  $V_5$ , and  $V_4$  are opened and Tank #1 evacuated to this regulated pressure. Valve  $V_8$  is then opened to pressurize the Freon reservoir and  $V_2$  then opened to admit Freon to Tank #1. Valve  $V_7$  is opened and the separator started at the same time. As Freon flows into the tank, the pressure in the tank will increase, the backpressure regulator will open to maintain the control pressure and gas will be vented from the system. Ideally this gas would be  $GN_2$  but there is the possibility of some Freon vapor formation during the fill process and also, because of the velocity imparted to the liquid entering the tank, some liquid may also attempt to leave through valve  $V_4$ . If this occurs the liquid will be separated in the separator and returned to the inlet to the tank. The flowmeter  $F_1$  monitors and integrates the flow leaving the reservoir. When the required amount has been transferred to satisfy the fill level required, valves  $V_2$  and  $V_4$  are sequentially closed. Valves  $V_5$ ,  $V_6$ ,  $V_7$ , and  $V_8$  are then closed and the separator turned off. After a short period during which the liquid in the tank will assume a representative condition obtained in a vehicle coast phase, testing is initiated and data are collected. Preparation for the next test is initiated in the same manner as described above.

### 6.3 INSTRUMENTATION

Minimum instrumentation will be required for this experiment as most of the data obtained will be visual and recorded by camera. Liquid movement, front relocation and speed of travel, and geysering, if it occurs, will be the main items of interest. To assist in analytical correlation, the fill level will be obtained by measuring total flow with the integrating flow meter  $F_1$ . The acceleration during the experiment is measured by the experiment common, triaxial accelerometer. Pressure and temperature within each tank will be obtained and, when operating, the  $\Delta P$  across the gas/liquid separator will be obtained for indication that liquid is recirculating. The instrumentation locations are shown in Figure 6-1. A list of instrumentation and instrumentation characteristics is given in Table 6-2.

### 6.4 COMPONENTS

Major components are also shown in Table 6-2. Although a capillary acquisition tank is shown in Figure 6-1, this tank could be either this type or a positive expulsion bladder type. The size and weight of either would be acceptable and would be compatible with the design layout shown in Figure 6-2. The Lexan tanks will be designed to withstand collapsing loads resulting from inadvertent venting to vacuum in the event of failure of the back pressure regulator. Pressure relief is not considered to be necessary because of the low vapor pressure versus temperature relationship of

Table 6-2. Instrumentation/Component Requirements - Experiment 4, Liquid Reorientation

Measurement		Sensor Type	Range	Resolution (Accuracy)	Test Runs		Data Sampling Rate	Notes
I. D.	Description				Number			
T <sub>1</sub>	Tank 1 Liq. Temp.	Thermistor	10-32.2C (50-90F)	0.28C (0.5F)	5 St. G 5 Imp.	80 20	1/5 sec. 1/5 sec.	
T <sub>2</sub>	Tank 2 Liq. Temp.	Thermistor	10-32.2C (50-90F)	0.28C (0.5F)	5 St. G 5 Imp.	80 20	1/5 sec. 1/5 sec.	
P <sub>1</sub>	Tank 1 Press.	Xducer	34.5-138 kN/m <sup>2</sup> (5-20 psia)	0.69 kN/m <sup>2</sup> (0.1 psia)	5 St. G 5 Imp.	80 20	1/sec. 1/sec.	
P <sub>2</sub>	Tank 2 Press.	Xducer	34.5-138 kN/m <sup>2</sup> (5-20 psia)	0.69 kN/m <sup>2</sup> (0.1 psia)	5 St. G 5 Imp.	80 20	1/sec. 1/sec.	
ΔP <sub>1</sub>	Separator Liq/Gas Differential Pressure	Xducer	0-34.5 kN/m <sup>2</sup> (0-5 psid)	0.69 kN/m <sup>2</sup> (0.1 psia)	5 St. G 5 Imp.	80 20	1/sec. 1/sec.	
F <sub>1</sub>	Tank Fill Rate		0-7.6 lpm (0-2 gpm)	0.076 lpm (0.02 gpm)	8 Oper.	~1 min.	5/sec.	For Freon 113 integrate signal.
E <sub>x,y,z</sub>	g-Level	Accel.	1.8-200 ×10 <sup>-4</sup> g	5×10 <sup>-6</sup> g	10 10	80 20	10/sec.	Monitor display with camera.
<u>COMPONENTS</u>								
BPR <sub>1</sub>	Venting Back Press. Regulator		6.9-103 kN/m <sup>2</sup> (1-15 psia)	±0.69 kN/m <sup>2</sup> (±0.1 psia)				video
	Camera, B&W, 16 mm, III Speed, 1 Reqd.							
Tank	Liquid Freon-113, 1 Reqd.	Positive ex- pulsion or capillary ac- quisition type	Liquid Capacity: 23.8 litre (0.84 ft <sup>3</sup> ) 37.6 kg (82.8 lb)					
G/L Sep.	Separator to provide gas venting							This separator is identical to that used in Exp. I & II.

Freon 113 and the maximum expected temperature ranges to which the tanks might be exposed when partially filled with Freon.

### 6.5 ANALYSES, LIQUID REORIENTATION TIME

The liquid reorientation experiment, whose basic geometry is given in Figure 6-3 below, is to be conducted on Spacelab in two modes of operation: in one, a constant acceleration of approximately one minute duration is applied to the system, and in the other an "impulsive acceleration" (constant acceleration of very short duration; typically less than one sec), is applied to the system. The objective of the experiment is to quantitatively study the motion of the leading liquid edge and collection characteristics under both the constant and impulsive acceleration modes for a variety of fill levels and tank geometries. The purpose of the analysis is to predict the times required for fluid collection to aid selection of accelerations and duration of application for the experiments.

A parallel effort in support of this analysis was accomplished by Lead Scientist Professor T. E. Bowman of the Florida Institute of Technology. This effort resulted in a closed-form method of solution for liquid propellant reorientation velocity increments. This development and resulting parametric curves have been provided as an adjunct to this report and are included in Appendix B.

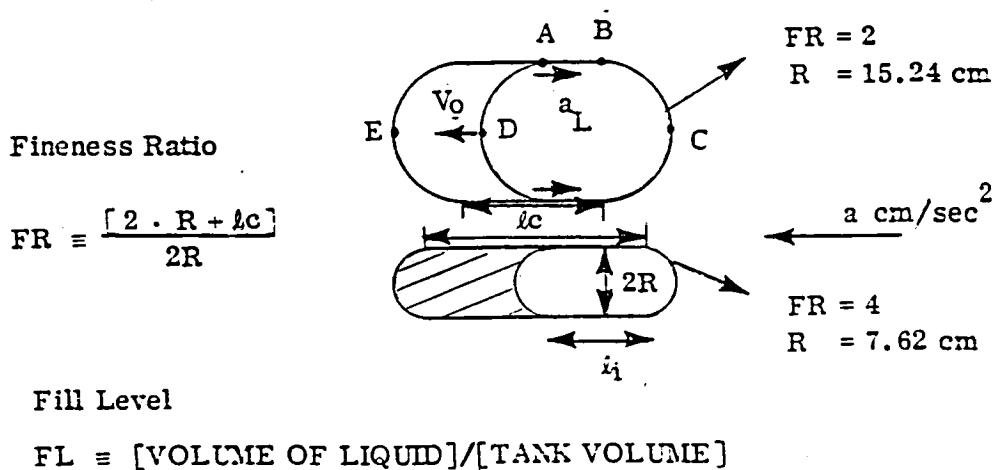


Figure 6-3. Tank Geometries for Liquid Reorientation Analysis

The test fluid is Freon 113. The relevant properties of this refrigerant are the following.

$$@ 20^\circ\text{C} \left\{ \begin{array}{l} \rho = 1.579 \text{ gm/cm}^3 \\ \sigma = 18.6 \text{ dynes/cm} \\ \mu = 0.7 \text{ CP (0.007 gm/cm-sec)} \end{array} \right. \left\{ \begin{array}{l} \beta \equiv \frac{\sigma}{\rho} = 11.78 \text{ cm}^3/\text{sec}^2 \end{array} \right.$$

6.5.1 CONSTANT ACCELERATION — Different acceleration ranges are planned for experimentation with each tank. For the large tank the acceleration is to range between 0.18 and 0.25 cm/sec<sup>2</sup>. For the smaller tank the range is 0.54 to 0.76 cm/sec<sup>2</sup>. The percentage of liquid in the tanks is to vary between twenty and seventy percent. Having specified the fluid properties, the acceleration ranges, the tank sizes and the fraction of tankage volume occupied by liquid, it is now possible to calculate estimates of the time required to reorient the liquid, using the method outlined in References 5 and 9.

Prior to the application of the reorientation thrust, the liquid configuration is assumed to have reached its zero-g state. For freons this state is defined as having a constant radius of curvature equal to the radius of the tank and as having a contact angle of zero degrees. Equations will be given which will lead to the calculation of various time intervals defined as the following.

- $t_1$    ≡ time necessary for the liquid leading edge to progress from point A to point B (Figure 6-3).
- $t_2$    ≡ time necessary for the liquid leading edge to progress from point B to point C
- $t_3$    ≡ time necessary to settle remaining liquid (questionable accuracy)
- $t_4$    ≡ time necessary for vertex of ullage bubble, point D, to progress to point E
- $t_5$    ≡ time necessary for the dispersal of liquid film on the walls (questionable accuracy)

Because the drop tower test data used to generate the methods for calculating the above times was limited to a maximum of three seconds, sufficient time was not allowed to accurately formulate expressions for  $t_3$  and  $t_5$ . It is hoped that the Spacelab experiments will alleviate this problem. The equations used to find  $t_1$  are now given in sequential order.

Given  $a$ ,  $FR$ ,  $FL$ ,  $R$ ,

$$B_o \equiv a R^2 / \epsilon \quad (\text{Bond number})$$

$$V_o = 0.4S (aR)^{1/2} [ 1 - (0.84/B_o)^{B_o/4.7} ]$$

$$a_L = 3.8 V_o^2 / R$$

$$l_1 \equiv [ (1 - FL) (FR - 1/3) - 2/3 ] 2R$$

$V'_L \equiv$  Velocity of leading edge @ point C

$$= [2 a_L (\ell_1 + R)]^{1/2}$$

$W_e = V'_L{}^2 R/\epsilon$  (Weber number)

$$t_1 = 2 (\ell_1)^{1/2} (\ell_1 + R)^{1/2} / V'_L$$

$$t_2 = 2 (\ell_1 + R) [1 - (\ell_1 / (\ell_1 + R))^{1/2}] / V'_L \quad (18)$$

$$t_3 = 0.0516 B_o W_e (R^3/\epsilon)^{1/2} \quad (19)$$

$$t_4 = (\ell_c - \ell_i) / V_o \quad (20)$$

$$\ell_j \equiv [ (FR - 1) - FL (FR - 1/3) + 1/3 ] 2R$$

$$t_5 = 2 (\ell_j + R) / V'_L \quad (21)$$

For the case where the fill level is sufficiently large that  $\ell_1$  of Figure 6-3 would be negative, the ullage actually takes on a spherical shape with a radius less than R and the assumption of zero contact angle cannot hold. In this case  $t_5$  is zero, the total time is given by  $t_4$  which is calculated as shown below and calculations for  $t_1$ ,  $t_2$  and  $t_3$  are disregarded.

$$V_T = (FR - 1/3) 2 \pi R^3$$

$$R_o = (3 V_T (1 - FL) / (4 \pi))^{1/3}$$

$$\ell_o = 2 (R FR - R_o)$$

$$t_4 = \ell_o / V_o$$

The time necessary to totally reorient the liquid is given by either of the two sums:

$$t_T \equiv t_1 + t_2 + t_3 \quad \text{or}$$

$$t_T \equiv t_4 + t_5, \text{ whichever one is larger}$$

The change in velocity of the accelerating system, (the Orbiter in this case), is given by the following equation.

$$\Delta V = a t_T$$

A minimization of this quantity over the given range of accelerations will minimize the amount of propellant required by the thrusting mechanism of the Orbiter. The acceleration that accomplishes this minimization will be termed the optimal acceleration for that given FL and FR.

An example of this method will now be demonstrated. Assume that FL = 0.20, FR = 4, a = 0.61 cm/sec<sup>2</sup> and R = 7.62 cm.

$$\begin{aligned} B_o &= (0.61 \text{ cm/sec}^2) (7.62 \text{ cm})^2 / (11.78 \text{ cm}^3/\text{sec}^2) \\ &= 3.01 \end{aligned}$$

$$\begin{aligned} V_o &= 0.48 ((0.67 \text{ cm/sec}^2) (7.62 \text{ cm}))^{1/2} [1 - (0.84/3.01)^{3.01/4.7}] \\ &= 0.577 \text{ cm/sec} \end{aligned}$$

$$\begin{aligned} a_L &= (3.8) (0.577 \text{ cm/sec})^2 / (7.62 \text{ cm}) \\ &= 0.1661 \text{ cm/sec}^2 \end{aligned}$$

$$\begin{aligned} l_i &= [(1 - 0.20) (4 - 1/3) - 2/3] 2 (7.62 \text{ cm}) \\ &= 34.54 \text{ cm} \end{aligned}$$

$$\begin{aligned} V'_L &= [2 (0.1661 \text{ cm/sec}^2) (34.54 \text{ cm} + 7.62 \text{ cm})]^{1/2} \\ &= 3.74 \text{ cm/sec} \end{aligned}$$

$$\begin{aligned} W_e &= (3.74 \text{ cm/sec})^2 (7.62 \text{ cm}) / (11.78 \text{ cm}^3/\text{sec}^2) \\ &= 9.06 \end{aligned}$$

$$\begin{aligned} t_1 &= 2 (34.54 \text{ cm})^{1/2} (34.54 \text{ cm} + 7.62 \text{ cm})^{1/2} / (3.74 \text{ cm/sec}) \\ &= 20.39 \text{ sec} \end{aligned}$$

$$\begin{aligned} t_2 &= 2 (34.54 \text{ cm} + 7.62 \text{ cm}) [1 - (34.54 \text{ cm} / (34.54 \text{ cm} + 7.62 \text{ cm}))^{1/2}] / (3.74 \text{ cm/sec}) \\ &= 2.14 \text{ sec} \end{aligned}$$

$$\begin{aligned} t_3 &= 0.0516 (3.01) (9.06) ((7.62 \text{ cm})^3 / (11.78 \text{ cm}^3/\text{sec}^2))^{1/2} \\ &= 8.62 \text{ sec} \end{aligned}$$

$$\begin{aligned} t_4 &= (45.72 \text{ cm} - 34.54 \text{ cm}) / (0.577 \text{ cm/sec}) \\ &= 19.36 \text{ sec} \end{aligned}$$

$$l_j = [(4-1) - 0.20 (4 - 1/3) + 1/3 ] 2 (7.62 \text{ cm})$$

$$= 39.62 \text{ cm}$$

$$t_5 = 2 (39.62 \text{ cm} + 7.62 \text{ cm}) / (3.74 \text{ cm/sec})$$

$$= 25.26 \text{ sec}$$

$$\left. \begin{array}{l} t_1 + t_2 + t_3 = 31.15 \text{ sec} \\ t_4 + t_5 = 44.62 \text{ sec} \end{array} \right\} \therefore t_T = 44.62 \text{ sec and } \Delta V = 27.22 \text{ cm/sec}$$

The  $\Delta V$  values for three other discrete accelerations were found to be the following:

$\Delta V$ (cm/sec)	29.85	25.57	28.17
$a$ (cm/sec <sup>2</sup> )	0.54	0.68	0.76

A complete table following the calculations in the above example was generated for four accelerations for each of the four chosen fill levels. Once the  $\Delta V_s$  are found for a range of accelerations, the acceleration that minimizes the magnitude of  $\Delta V$  is chosen as the optimal one for that fill level and tank geometry. For the above example, a parabola is fitted through the points associated with the accelerations 0.61, 0.68 and 0.76 cm/sec<sup>2</sup>.

The minimum of this parabola is calculated and the corresponding acceleration and duration time is found. The optimal accelerations and their duration times are summarized in the following table.

FILL LEVEL	FINENESS RATIO	$a_{\text{OPTIMAL}}$	$t_{\text{TOTAL}}$
0.2	2	0.18 cm/sec <sup>2</sup>	60.47 sec
0.3		0.196	60.85
0.4		0.213	61.11
0.5		0.25	56.30
0.7		0.25	60.70
0.2	4	0.676	37.90
0.3		0.76	37.96
0.4		0.76	43.86
0.5		0.76	49.76
0.7		0.76	61.34

NOTE: This table was developed under the constraints of 0.18-0.25 cm/sec<sup>2</sup> acceleration limits for the large tank and 0.54 to 0.76 cm/sec<sup>2</sup> limits for the small tank. This range could be extended to define an optimal which minimizes Orbiter propellant usage.

Weber number was also plotted as a function of Bond number for the two tanks and five fill levels of the experiments and is shown in Figure 6-4. Minimum values for Weber number, and thus the points for minimum propellant consumption, are thus identified.

6.5.2 IMPULSIVE SETTling. The previous discussion concerned the case where an acceleration was applied for the entire time that liquid settling was taking place. Impulsive settling is defined as the reorientation process which takes place when an acceleration is applied for a small fraction of the total resettling time. This process is now considered for the same tank geometry, test fluid and range of fill levels as before. The accelerations required, however, will be between the values 4.9 and 9.8 cm/sec<sup>2</sup>. The acceleration imparted to the tank will cause liquid leading edge acceleration for as long as the artificial g-field is imposed. Once the acceleration is stopped, the leading edge will still propagate; but now (it is assumed) at a constant velocity. This can be represented by a Weber number relationship.

$$\begin{aligned} We &\equiv v_T^2 R/\beta \\ &= a_L^2 \Delta t^2 R/\beta \end{aligned}$$

The acceleration of the leading edge is denoted at  $a_L$ , as before, and the burn time is denoted by  $\Delta t$ . For Bond numbers greater than twelve, which is the case here,  $a_L$  is directly proportional to the imposed acceleration:  $a_L = (0.8755)a$ . It remains to choose a Weber number criterion so that  $\Delta t$ 's can be found for the given range of accelerations. Using the criterion of minimizing propellants used by the thrusters, then for a given acceleration, the burn time should be kept as small as possible. It is noted in Reference 5 that a geyser will form when the leading edge Weber numbers are greater than four at the point of impingement. Therefore, the burn time,  $\Delta t$ , should be minimized for both propellant savings and prevention of undesirable geyser formation. The consequence of making burn-times smaller is to increase the amount of time necessary to collect the liquid. A prediction of these collection times was not done, so a minimum allowable We based on maximum allowable collection time was not made. For the maximum We criterion, the value of four should be an absolute limit.

Rearranging the above Weber number equation results in the following:

$$\begin{aligned} We &= a_L^2 \Delta t^2 R/\beta \\ &= (0.8755)^2 a^2 \Delta t^2 R/\beta \\ a\Delta t &= \sqrt{We \beta/R} \quad (1.1422) \end{aligned} \tag{22}$$

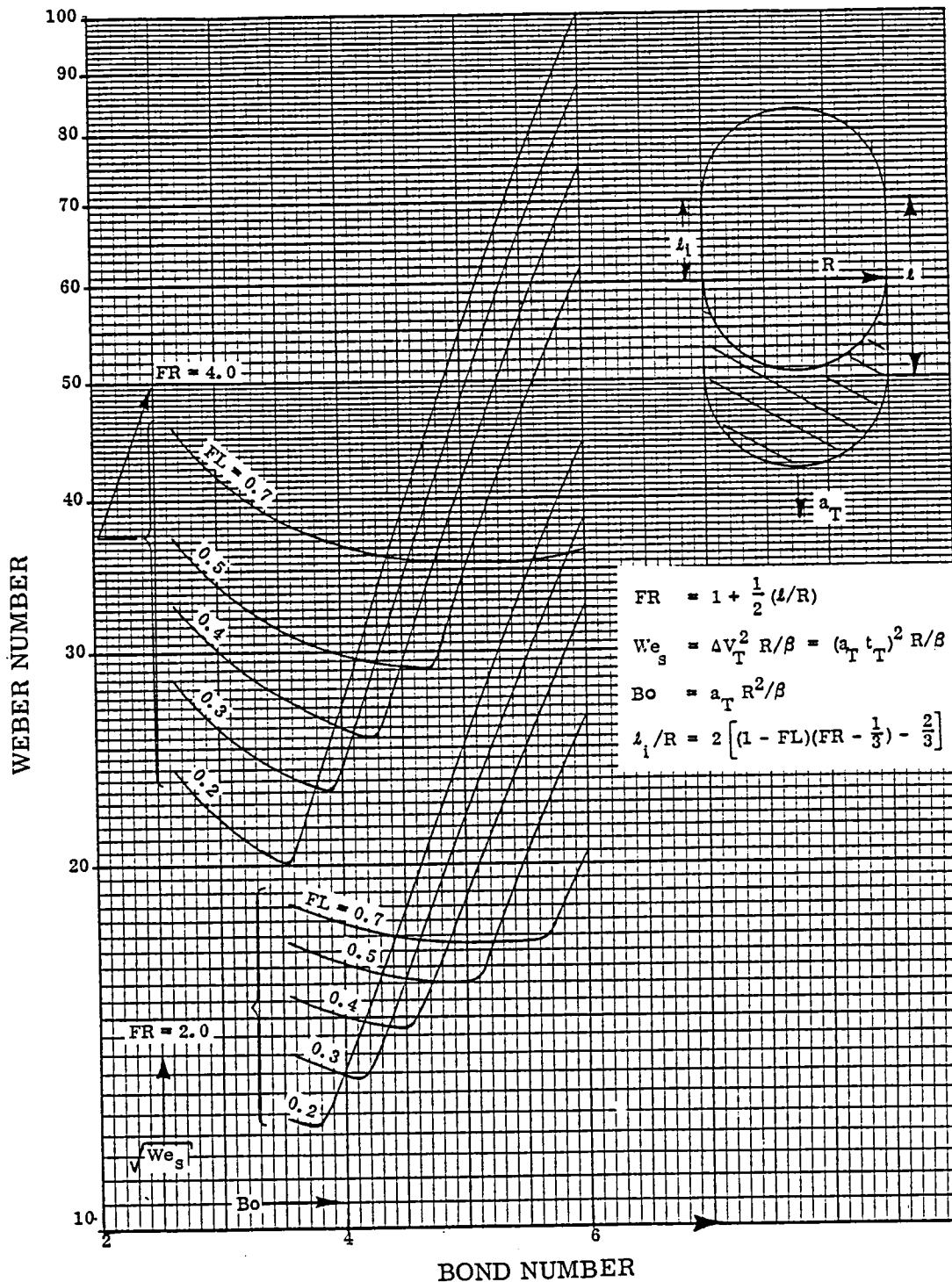


Figure 6-4. Settling Weber Number Versus Bond Number for Various Fill Levels and Fineness Ratios

This relationship is plotted in Figure 6-5 for the given range of accelerations, 4.9 to 9.8 cm/sec<sup>2</sup>, for both tanks, (R = 7.62 and 15.24 cm), and for We equal to 2, 3 and 4. A Weber number of near to, but less than four is recommended to promote efficient collection of liquid and to prevent excessive total collection time.

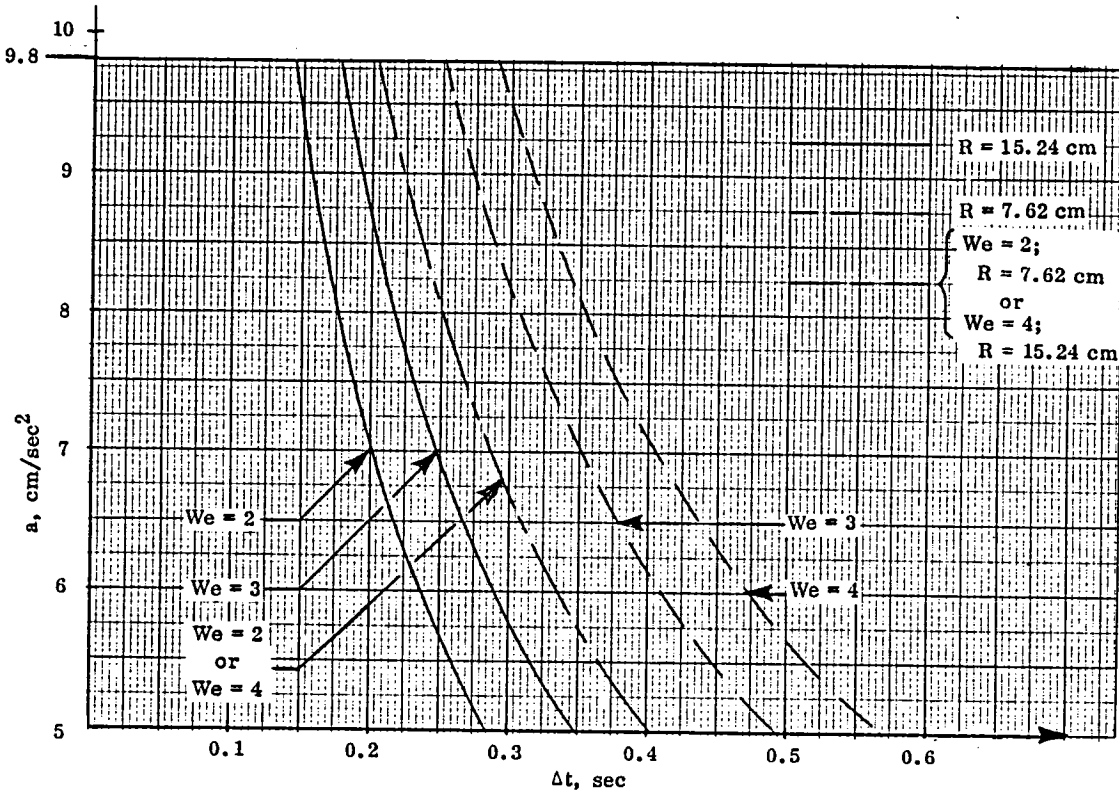


Figure 6-5. Acceleration and Burn Times for Impulsive Settling

An extension of this analysis was provided by Professor Bowman who developed closed-form solutions to equations (A1) through (A22) of TM-78969 to give total velocity increments directly in terms of settling Bond number. This work defining these solutions is included in Appendix B.



## BUBBLE DYNAMICS, EXPERIMENT 5

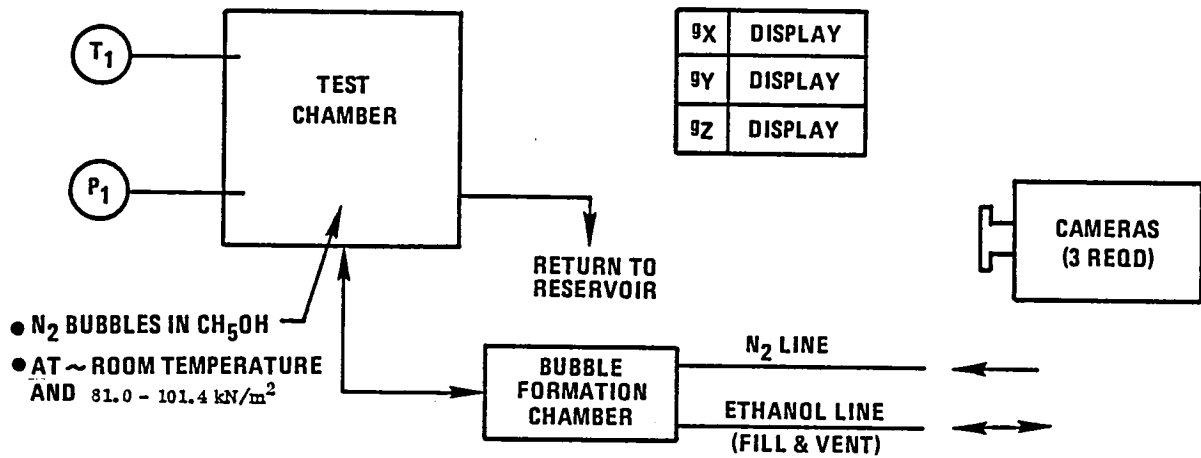
### 7.1 DESCRIPTION

The objective of the bubble dynamics experiment is to investigate the interaction of a single non-condensable isothermal bubble with a liquid-vapor interface in a low-gravity environment. In this experiment, the behavior of nitrogen bubbles in ethanol and Fluorcarbon FC-78 was investigated. A schematic and a layout of the experiment are shown in Figures 7-1 and 7-2. A test container with an open top is used, which provides a free liquid surface. The container is enclosed in a housing to prevent any possible contamination of the cabin. Bubbles of various sizes are introduced into the liquids in the test containers and their behavior is monitored by three 16 mm high speed cameras.

### 7.2 METHOD OF OPERATION

This experiment is stored in the overhead portion of the rack and will be the last of the five experiments to be performed. It will be moved to the center position as shown in Figure 7-2 and the three cameras necessary for this experiment positioned in their respective, predetermined locations on the camera support rack. The test container is initially dry and will be hand filled by the pump syringe used to transfer liquid from the reservoir to the test container.

The test container is filled to exactly the upper lip of the container so that there is no meniscus effect at the edges of the container and the liquid/gas interface is flat.  $\text{GN}_2$  is introduced into the bubble generator until a bubble of the desired size is formed at the end of the capillary tube extending from the  $\text{GN}_2$  syringe into the bubble generator. A 3-way valve connecting the bubble generator to either the main liquid reservoir or to a smaller auxiliary reservoir is positioned to allow liquid from the auxiliary reservoir to be transferred to the bubble generator. The liquid motion will drag the gas bubble from the end of the  $\text{GN}_2$  capillary to the opening in the generator communicating with the bottom of the test container. The bubble will then rise through the liquid because of the small acceleration applied during this experiment. Bubble motion during ascent will be recorded in two planes to define the 3-dimensional motion of the bubble. Two cameras are used for this purpose. The third camera (with higher frame rate than the other two) will record the action at the liquid/chamber gas interface when the bubble reaches the interface and breaks through. A small line is connected between the test chamber and the back side of the syringe used to transfer liquid to move the bubble in the bubble generator. This will provide a closed circuit for liquid transfer without overfilling the test chamber which should remain exactly filled.



**TESTS TO BE RUN  
(WITH WATER & FC 78)**

NO. OF RUNS	DURATION (SEC)	g-LEVEL (g)	BUBBLE DIA. (cm)
3	60	10 <sup>-3</sup>	0.05 TO 5
6	60	5 × 10 <sup>-4</sup>	0.05 TO 5

**ETHANOL VAPOR PRESSURE**

T C	P kN/m <sup>2</sup>
18.9	5.3
35.0	13.3
63.3	53.4
78.3	101.4

**F.C. 78 VAPOR PRESSURE**

T <sub>1</sub> C	P <sub>1</sub> kN/m <sup>2</sup>
-5.0	6.9
22.2	22.6
34.4	48.3
42.2	69.0
50.6	101.4

Figure 7-1. Instrumentation Schematic - Experiment 5 Bubble Dynamics

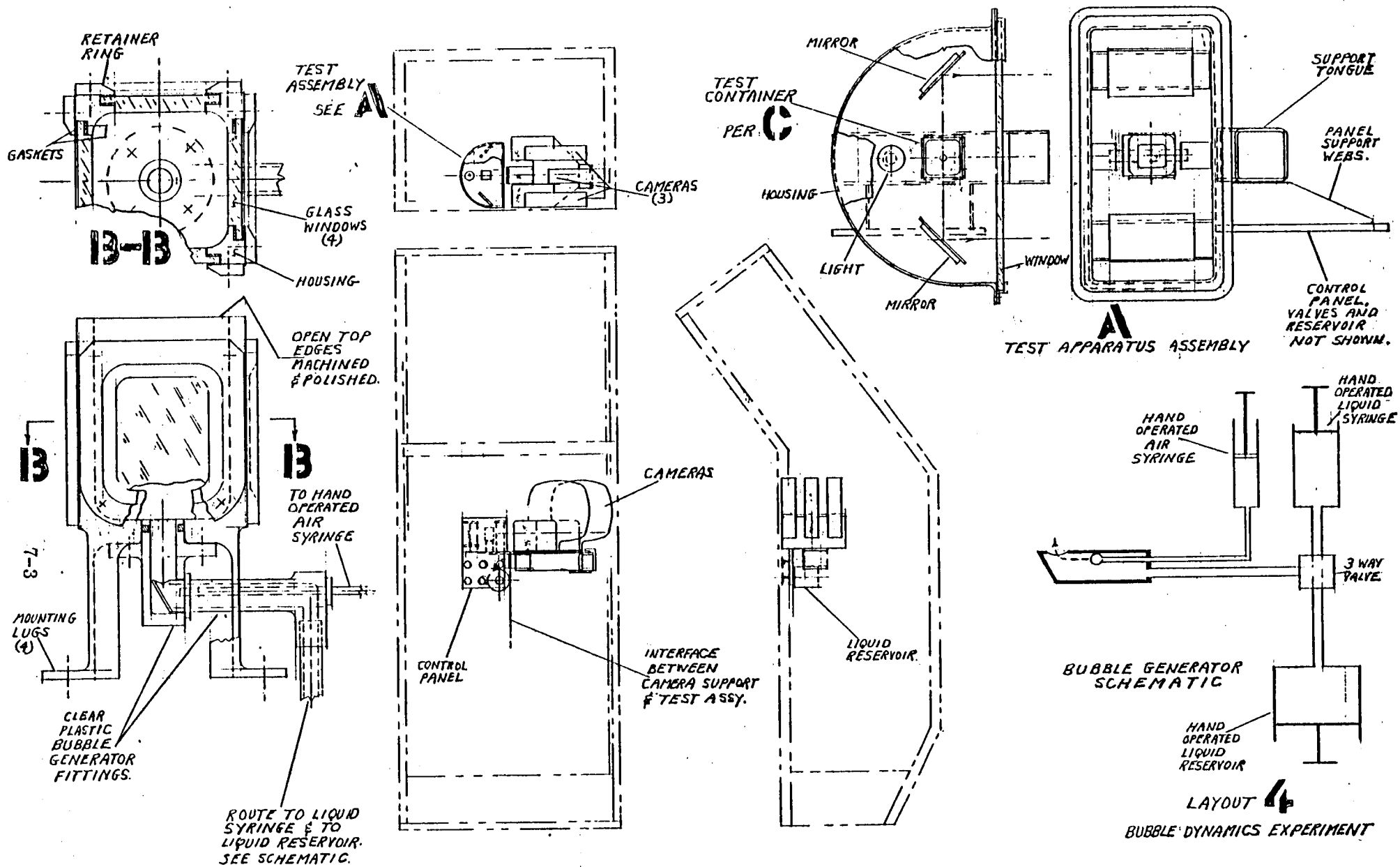


Figure 7-2. Bubble Dynamics Experiment Layout

L. E. Liden July 29, 1979

At present, the experiment is designed to test one fluid, either ethanol or FC-78. No provision has been made to run one fluid and then flush and clean the system to run a new series of tests with a second fluid on the same flight.

### 7.3 INSTRUMENTATION AND COMPONENTS

Instrumentation and components are listed in Table 7-1. The temperature and pressure of the liquid within the test container is monitored by a thermistor and a pressure transducer. The same accelerometer which is used in all the other experiments will also be used here. The three cameras which are needed for this experiment can be shared with the other experiments.

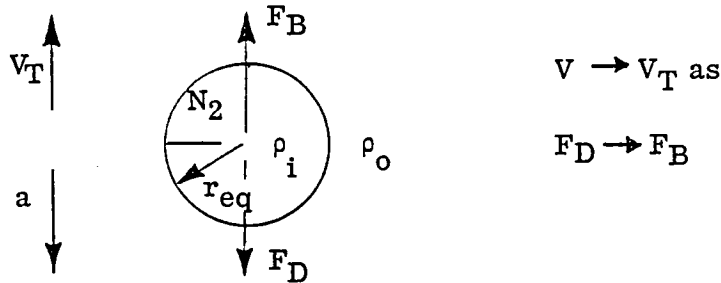
### 7.4 ANALYSIS OF BUBBLE TERMINAL VELOCITY

The ultimate aim of the bubble dynamic experiment is to study the motion of the bubble as the free surface is approached and to quantify a criterion for bubble breakthrough into the surrounding vapor phase. The fluid behavior that results is critically dependent upon the bubble approach velocity. A knowledge of the approximate magnitude of these terminal velocities will be useful in the choice of camera speeds, vessel geometry and the design of the experimental package as a whole. The purpose of this analysis is to estimate terminal velocities for various bubble sizes and acceleration fields.

7.4.1 FORCE BALANCE WITH A SUBMERGED GAS BUBBLE. With reference to the figure below, the terminal velocity condition is reached when the buoyant force equals the drag force on the bubble.

Table 7-1. Instrument/Component Requirements - Experiment Versus Bubble Dynamics

Measurement		Sensor Type	Range	Resolution (Accuracy)	Test Runs		Data Sampling Rate
I. D.	Description				No.	Duration	
T <sub>1</sub>	Ethanol or F.C. 78	Thermistor	10-32 C	0.56C (±0.28C)	9	60	1/5 sec.
P <sub>1</sub>	Ethanol or F.C. 78 Press.	Transducer	0-103 kN/m <sup>2</sup>	1.38 kN/m <sup>2</sup> (±1.38 kN/m <sup>2</sup> )	9	60	1/5 sec.
g <sub>x,y,z</sub>	G-Level  <u>Component</u>	Accelerometer	0.5-1 × 10 <sup>-4</sup> G	5 × 10 <sup>-6</sup> (10 <sup>-4</sup> - 10 <sup>-2</sup> nom.)	9	60	10 sec. Monitor displays with camera.
	Camera, B&W, 16 mm, High Speed, Three Required						{ 400 frames/sec



The terminal velocity condition,  $F_B = F_D$ , can be stated in terms of a drag coefficient, the terminal velocity, the g-level and fluid properties

$$F_B = 4 \pi r_{eq}^3 (\rho_o - \rho_i) a/3$$

$$F_D = C_D (1/2 \rho_o V^2) \pi r_{eq}^2$$

$$\begin{aligned} \therefore F_B = F_D \Rightarrow C_D &= 8 r_{eq} (1 - \rho_i/\rho_o) a/3 V_T^2 \\ &\cong 8 r_{eq} a/3 V_T^2 \text{ for } \rho_i \ll \rho_o \end{aligned} \quad (23)$$

Using the equation defining the Reynolds number and the equation given above, the following relationship can be derived.

$$Re = 2 r_{eq} V_T / \nu_o \Rightarrow$$

$$V_T = \left[ \frac{4}{3} \frac{\nu_o a Re}{C_D} \right]^{1/3} \quad (24)$$

$$r_{eq} = \left[ \frac{3}{32} \frac{\nu_o^2}{a} C_D Re^2 \right]^{1/3} \quad (25)$$

Hence knowledge of drag coefficient dependency on Reynolds number can be used to determine terminal velocity and equivalent radius. Under 1-g conditions, experiments have been conducted which resulted in  $C_D$  (Re) relationships for the case of the rising gas bubble immersed in a liquid. Peebles and Garber, Reference 6, conducted such experiments and successfully generated drag coefficient expressions for a wide variety of liquids. Haggard and Masica, Reference 7, performed drop tower tests and generated drag/Reynolds number data for reduced gravity. They compared their data to the theoretical approach of Moore, Reference 8, and found fair agreement. The balance of this analysis will address (1) 1-g predictions of terminal velocities for various bubble sizes using the correlations of Peebles and Garber, and checking these

values with Moore's theoretical predictions, and (2) using Moore's approach to predict bubble velocities in reduced gravity and comparing these values with the data of Haggard and Masica.

7.4.2 NORMAL GRAVITY CALCULATIONS. The equations used in Reference 6 to predict terminal velocities for normal gravity, are repeated below for convenience.

Region

(i) [ Stokes flow; infinite boundary layer regime; spherical bubbles ]

$$V_T = 2 r_{eq}^2 (\rho_l - \rho_g) a / (9 \mu_l) \quad (26)$$

$$C_D = 24 / Re \text{ for } Re \leq 2$$

(ii) [ finite boundary layer spherical bubbles ]

$$V_T = 0.33 a^{0.76} (\rho_l / \mu_l)^{0.52} r_{eq}^{1.28} \quad (27)$$

$$C_D = 18.7 Re^{-0.68} \text{ for } 2 \leq Re \leq 4.02 G_1^{-0.214}$$

(iii) [ deformed bubbles of ellipsoidal cross-section ]

$$V_T = 1.35 [\sigma / (\rho_l r_{eq})]^{0.50} \quad (28)$$

$$C_D = 0.0275 G_1 Re^4$$

$$\text{for } 4.02 G_1^{-0.214} \leq Re \leq 3.10 G_1^{-0.250}$$

(iv) [ deformed bubbles of mushroom shape ]

$$V_T = 1.18 (\sigma a / \rho_l)^{0.25} \quad (29)$$

$$C_D = 0.82 G_1^{0.25} Re \text{ for } Re \geq 3.10 G_1^{-0.250}$$

where  $G_1 \equiv (a \mu_l^4) / (\rho_l \sigma^3)$

As noted earlier, proposed experiment fluids are nitrogen gas and anhydrous ethanol as the liquid. The relevant liquid properties are summarized below

$$\rho_l = 0.789 \text{ gm/cm}^3$$

$$\sigma = 22.3 \text{ dynes/cm (gm/sec}^2)$$

$$\mu = 1.2 \text{ CP}$$

$$= 0.012 \text{ gm/cm-sec}$$

Calculations were made using the above equations for bubble radius ranging from 0.04 to 0.20 cm. The results are summarized below.

$$a = 980.7 \text{ cm/sec}^2$$

$$4.02 G_1^{-0.214} = 293.0$$

$$G_1 = 2.3242 \cdot 10^{-9}$$

$$3.10 G_1^{-0.25} = 446.5$$

$r_{eq}$ (cm)	0.04	0.06	0.08	0.10	0.12	0.14	0.16	0.18	0.20
$V_T$ (cm/sec)	8.87	14.91	21.54	22.70	20.72	19.18	17.94	16.92	16.05
$C_D$	1.370	0.731	0.468	0.507	0.730	0.994	1.298	1.643	2.029
Re	46.7	117.6	226.7	298.5	326.9	353.1	377.5	400.4	422.1

Region (ii)

Region (iii)

These results are contained in the ( $V_T$  vs  $r_{eq}$ ) and ( $C_D$  vs Re) graphs in Figures 7-3 and 7-4, respectively.

Although ethanol was not among the fluids used by Peebles and Garber in their experiments, an examination of the parameter,  $G_1$ , (which delineates between regions (ii), (iii) and (iv)) indicates that the correlations developed can be used for ethanol.

It can be seen from Figures 7-3 and 7-4 that the comparison between the predictions of Peebles and Garber and Moore's theory for the drag coefficient and the terminal velocity is fairly good. In both approaches, the parameter  $\mu_l^4 \alpha / \rho_l \sigma^3$  was proposed as the parameter through which the effects of a variable gravity field will influence the results. Since the correlations of Peebles and Garber were developed from one-g data, it remains to compare the results of Moore's theory as outlined in Reference 8, to the reduced gravity test data of Haggard and Masica.

**7.4.3 REDUCED GRAVITY CALCULATIONS.** Moore's theory for predicting bubble drag and terminal Reynolds number is summarized by the equations below. The distortion parameter,  $x$ , is confined to be between the values of one and four and the Reynolds number must be greater than fifty.

$$C_D = 48G(x) [1 + H(x)/(Re)^{1/2}] / Re \quad (30)$$

$$G(x) = \frac{1}{3} x^{4/3} (x^2 - 1)^{3/2} \frac{(x^2 - 1)^{1/2} - (2 - x^2) \sec^{-1}(x)}{[x^2 \sec^{-1}(x) - (x^2 - 1)^{1/2}]^2} \quad (31)$$

$$C_D = \frac{4}{3} Re^4 M/We^3(x) \quad (32)$$

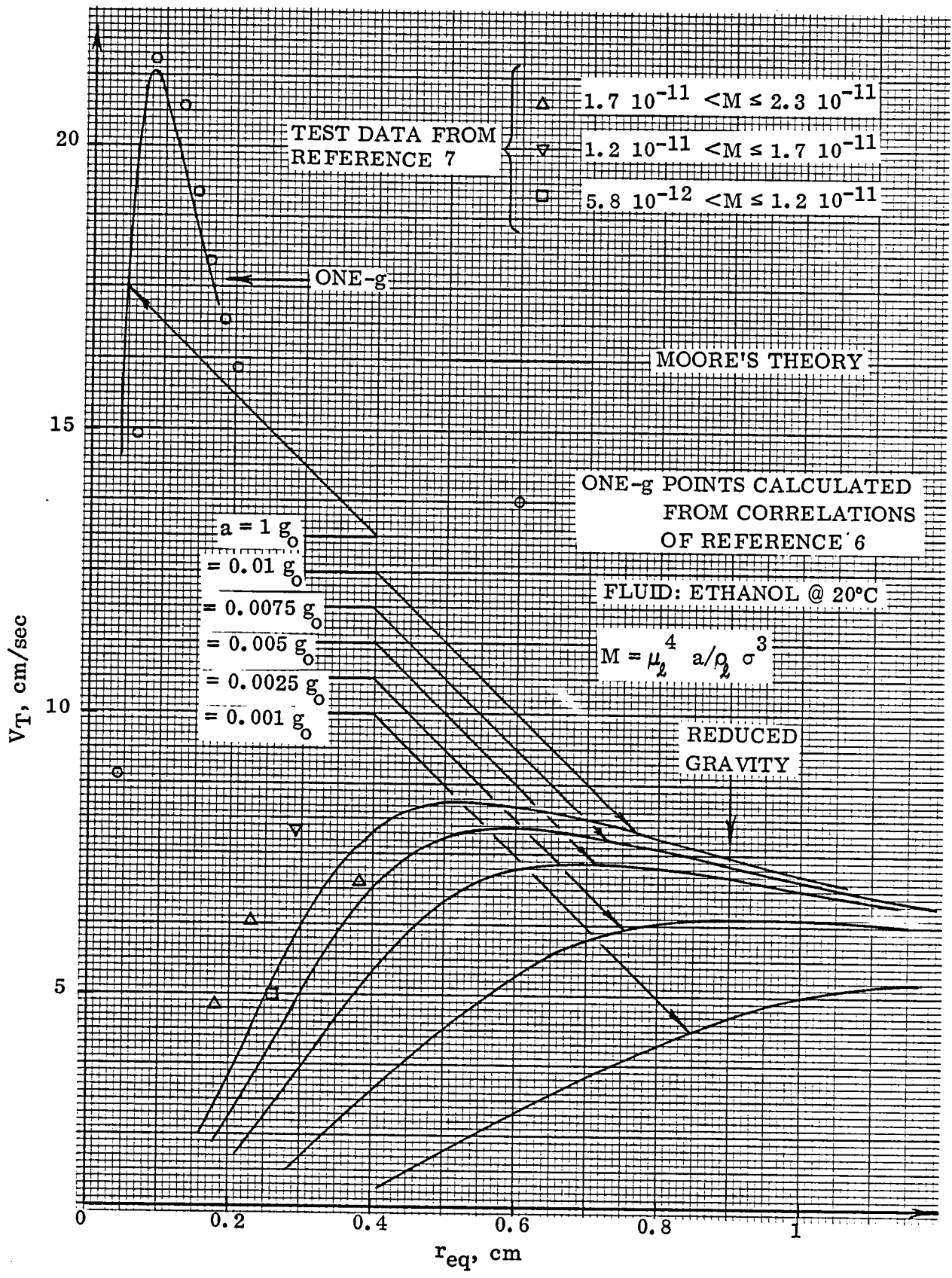


Figure 7-3. Terminal Velocities For Various Acceleration Levels

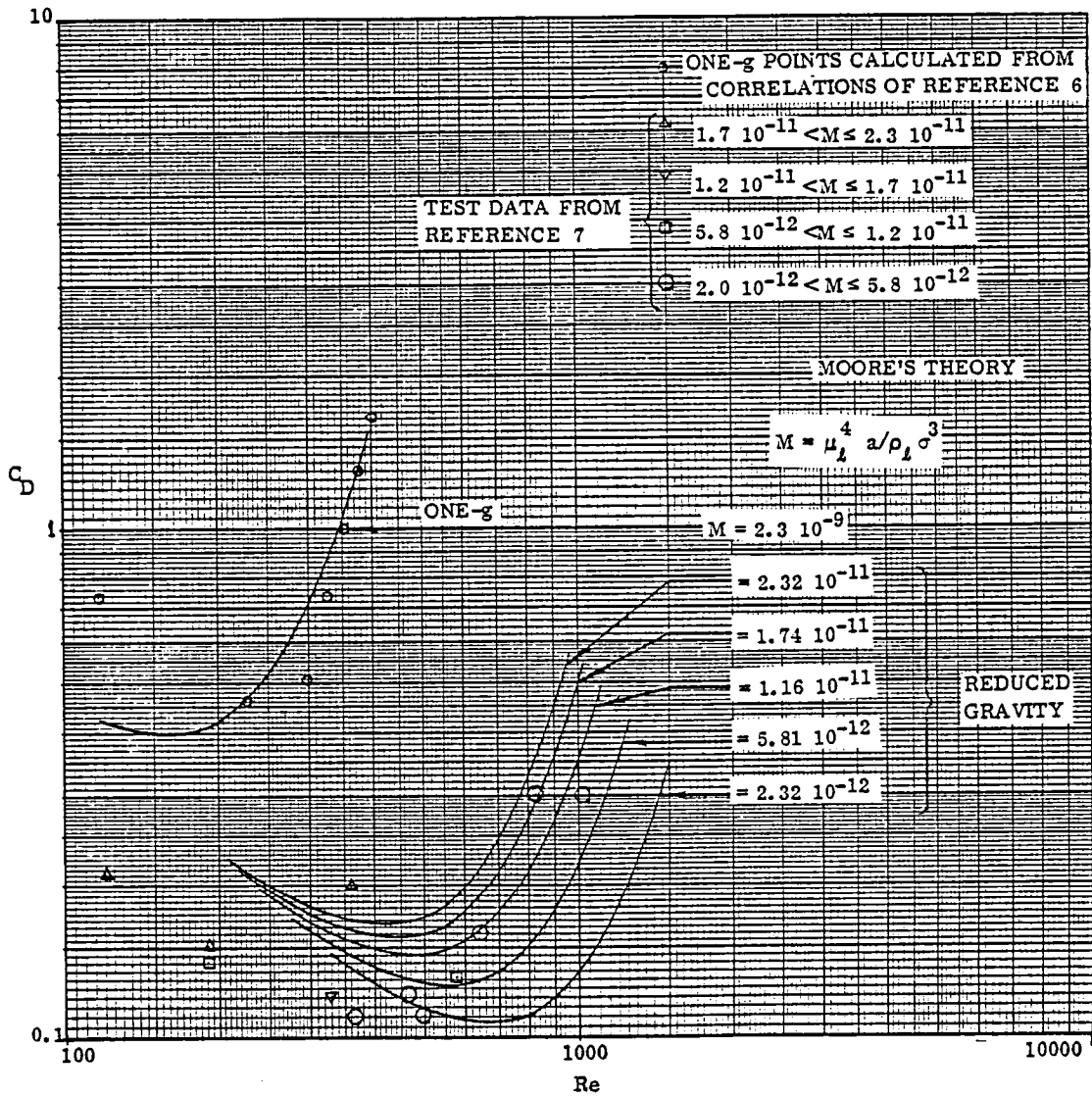


Figure 7-4. Drag Coefficients for Various Acceleration Levels

$$We(x) = 4x^{-4/3} (x^3 + x - 2) \frac{[x^2 \sec^{-1}(x) - (x^2 - 1)^{1/2}]^2}{(x^2 - 1)^3} \quad (33)$$

where

$$M \equiv \mu_L^4 a / \rho_L \sigma^3 \text{ and } H(x) \text{ is a tabulated function}$$

The method of solution is not straightforward. Given  $M$  and  $x$ , the Reynolds number is varied until the equations for the drag coefficient yield the same value. As  $x$  is varied between 1 and 4, a relationship for  $C_D$  as a function of  $Re$  is generated. The reduced gravity fields considered in the calculations were 0.01, 0.0075, 0.005, 0.0025 and 0.001 times earth normal gravity. As Figure 7-4 shows, the  $C_D$  vs.  $Re$  curves are shifted downward as the applied acceleration field is reduced. A similar downward shift is observed in Figure 7-3. Measured reduced gravity data from Reference 7 having  $M$  values in the range used for Moore's theoretical curves are presented in Figures 7-3 and 7-4 for comparison.

7.4.4 DISCUSSION OF RESULTS. The theoretical method of Moore was found to give good agreement with the 1-g correlations of Peebles and Garber. In reduced gravity, the theoretical approach gave fair agreement with the measured data of Haggard and Masica. Moore's solution tended to over predict the drag coefficient for the lower  $Re$  portion of the curves and to under predict the drag coefficient for higher  $Re$  (Figure 7-4). Conversely, Moore's solution under predicted terminal velocity at lower  $Re$  values and over predicted terminal velocity at higher  $Re$  (Figure 7-3). On the whole, however, Moore's solution gives a useful approximate estimate of terminal velocities.

# 8

## PHOTOGRAPHIC DATA RECORDING

### 8.1 CAMERA REQUIREMENTS

Photographic coverage is planned for all experiments. The design of the integration and installation of the five experiments has allowed room for both the cameras and film cartridges and the lighting necessary to provide the picture quality necessary to provide engineering data. It is believed that one camera will provide adequate coverage of all experiments except the bubble dynamics experiment. Provisions are made for installation of three cameras for this experiment to photograph, not only the bubble/liquid interface phenomena, but also bubble motion in orthogonal planes from bubble generation to surface contact. The cameras will be hard mounted in prelocated positions with different locations as dictated by the experiment in test.

The pressure drop and flow boiling experiments may prove difficult as the length of the flow section may be excessive for a wide angle lens especially if the camera location is kept within the confines of the rack. Two options are available to resolve this potential problem. One is the use of two cameras. This leads to a time correlation problem which, although not insurmountable, is not desirable. Space is available however, to do this. The second is the use of mirrors to split and overlay the top and bottom half of the experiment section. This would probably provide clear pictures without requiring a field of depth necessitating the location of the camera external to the rack. This is a system which would require development of the proper technique through testing.

For proper focusing of each experiment it is considered to be necessary to use different lenses for the experiments. The lenses would be tagged and stored in a separate compartment and selected and installed as required for each experiment. A second choice, but one leading to possible experimenter error, would be the use of a zoom lens which could cover all experiments. This is probably undesirable because it increases the installation volumetric requirement and also increases the criticality of the payload specialist's alertness in establishing the proper setting for each experiment.

The camera recommended for this application which is readily available is the Photo-Sonics Model 16 mm - 1 PL. A photo of this camera is shown in Figure 8-1 which also shows two of the three magazines which can be used with the camera. An outline drawing of the camera with magazines is shown in Figure 8-2. The camera, by itself, fit an envelope approximately 14.0×11.4×20.3 cm (5.5×4.5×8 in). The additional envelope dimensions to accommodate the magazines are shown in Figure 8-2. It is seen that

MAGAZINE CONCEPT

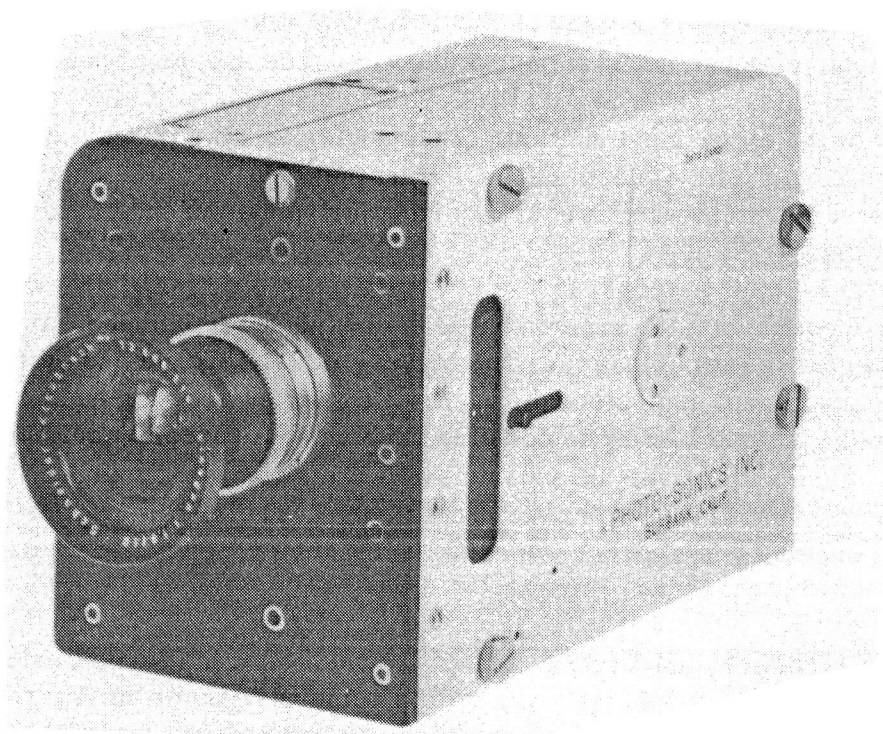
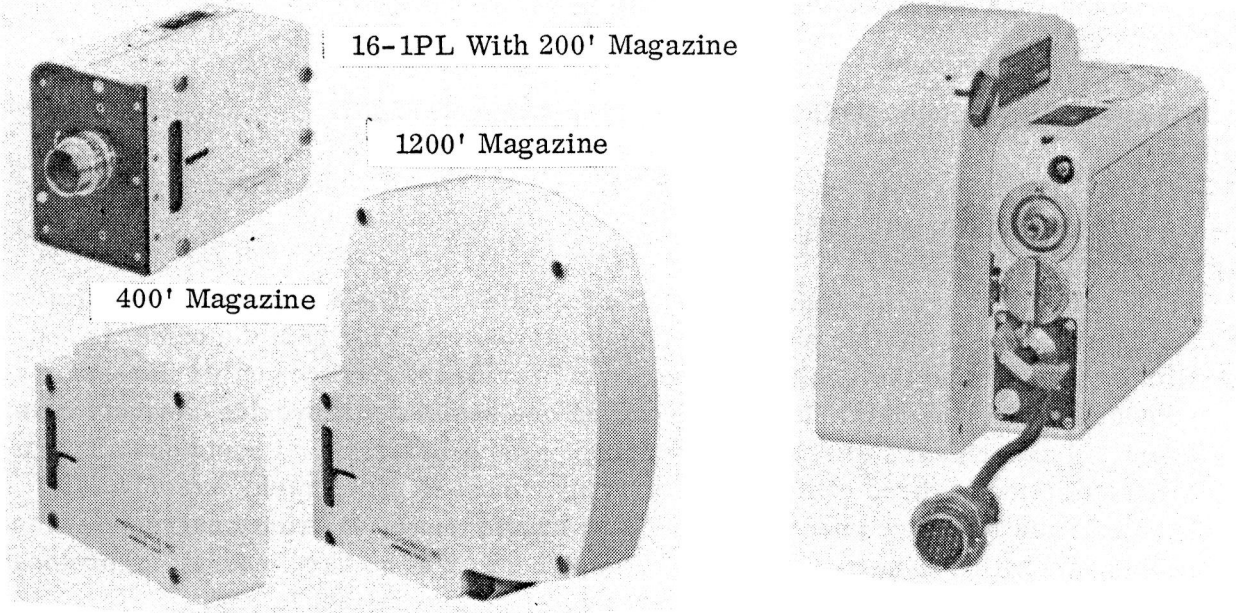
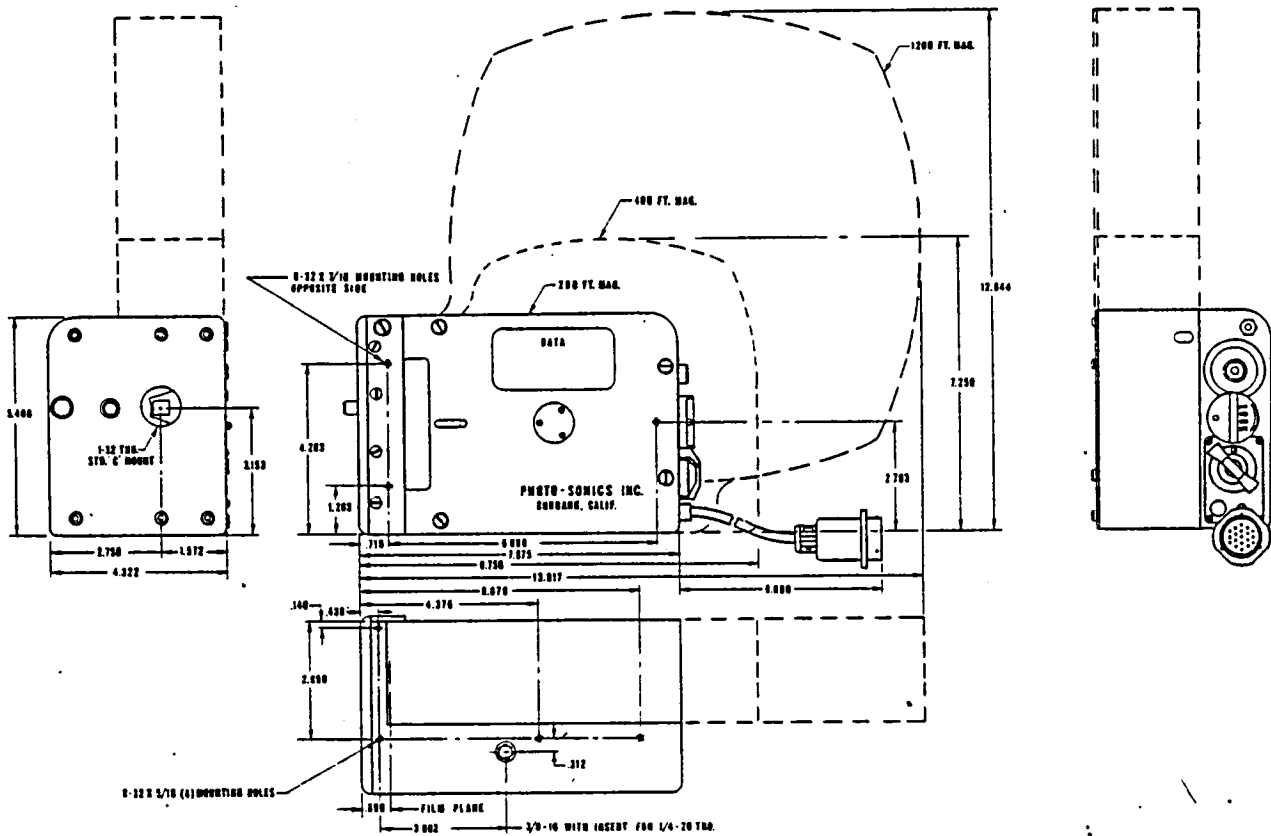


Figure 8-1. Candidate Photographic Equipment

Outline drawing —



Manufactured by Photo-Sonics, Inc., Burbank, CA

Figure 8-2. Photographic Data Recording

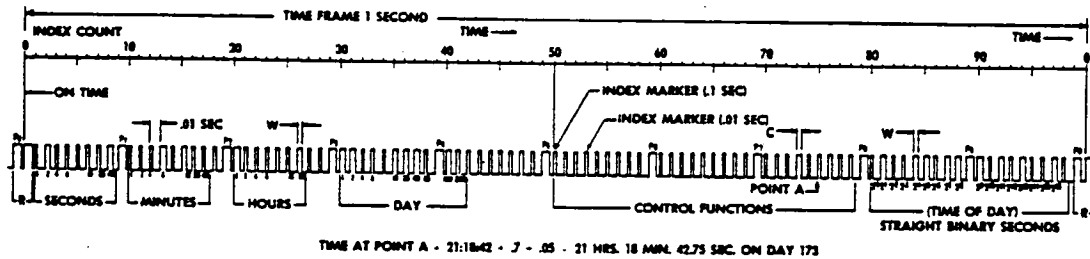
this is a highly compact camera installation with framing rate capability from 10 to 500 frames per second (FPS). The framing rate is easily accomplished by adjustment of the frame rate control on the camera (see Figure 8-1). The magazines can be quickly loaded and unloaded and fresh and used ones can be stored separately from the rack. For simplification of testing and to minimize the work load on the payload specialist, it is recommended that the film/magazine be handled as an integral unit rather than attempt to load film into the magazine and camera for each new roll of film required.

The camera events can be synchronized to physical data acquisition and recording signals with event timing through a time code generator and imposing IRIG standard format time codes on the film. The suggested format and sample of the format is shown in Figure 8-3.

The camera has a variable shutter angle of 7.5° to 160°. The exposure time is related by shutter angle and framing rate by:

$$t = \text{shutter angle} / (360 \times \text{framing rate})$$

Performance characteristics of the 16-1P camera and specifications are shown in Table 8-1.



**FORMAT B: 100-PPS, 30-BIT BCD TIME-OF-YEAR/17-BIT BINARY TIME-OF-DAY CODE**

Figure 8-3. IRIG Standard Format Time Codes

Table 8-1. Photosonics Camera Model 16 mm - 1 PL

**Performance Characteristics, 16-1PL —**

The camera was designed and developed to obtain high-speed, high-quality motion pictures at frame rates from 10 to 500 frames per second, and in various vibration and acceleration load conditions.

It is designed to withstand acceleration from 10 to 25 Gs, vibration of 5 to 7 Hz at 0.7" d.a. and 17 to 4000 cps at 10 Gs (not applicable to the 1200' magazine).

The camera system is similar in design and construction to the KB-21C Camera system furnished to the Air Force.

The KB-21C was tested in temperature conditions ranging from -65°F to +160°F. The KB-21C was operated and performed to design requirements during these tests. With the 16mm-1PL having a larger heater installed, operation in the lower temperature range should present no problems provided a warm-up period of 3 minutes is allowed prior to camera operation.

**Standard specifications, 16-1PL —**

**Frame rate:** 10 to 500 fps by transistorized speed control.  
Accuracy  $\pm 1\%$  or  $\pm 1$  frame, whichever is greater.

**Aperture size:** .296" x .410" (USA PH 22.7-1964).

**Film specification:** Uses both .3000" pitch (USA PH 22.5-1953) and .2994" pitch (USA PH 22.110-1965), both 4- and 6-mil with no adjustments.

**Film capacity:** 200', 400' and 1200' daylight loading magazines.

**Film transport:** Intermittent, two registration pins and two pull-down pins with film held captive in aperture gate at all times.

**Shutter:** Fixed 90°, substitution of one fixed 7.5° to 160° available at no additional cost.

**Timing lights:** Two, one each side of film outside picture area; uses NE2J lamps. LEDs may be substituted at time of purchase at no additional cost.

**Motor:** 28V DC, 8 amps maximum at 500 fps; 115V AC 50/400 Hz motor available upon request at no additional cost.

**Weight:** 6 lbs.

**Mounting:** 3/8-16 with 1/4-20 insert for tripod; top, bottom and side mounting provisions.

**Lens mount:** "C" (USA PH 22.76), threaded so that focusing and iris index always appear on the left side of the camera.

**Heater:** 115V AC or VDC, 300 watts, thermostatically controlled.

Specifications subject to change without notice.

## 8.2 LIGHTING

Space and weight provision for lighting has been made but definite arrangements, and wattage required can only be determined by real or prototype mockup. The heat generated by the lighting will be a function of both the lighting arrangement and the radiated energy or wattage dissipated. Since this is indefinite at this time, no thermal analysis was done. Because the duration of a single test point is short, it is not believed that the thermal effects of the lighting on the experiment will be significant. This, however, must be a subject of consideration as the program moves into the hardware phase.

## 8.3 DATA RECORDING

A summary of photographic data recording requirements is shown in Table 8-2. For some experiments video tape recording will be adequate and is therefore stipulated rather than film. This reduces cost and storage requirements. The frame speed shown is believed to be adequate to record the experimental phenomena and leads to the estimate of film footage required and thus the number of film magazines required for the total experiment package.

Table 8-2. Photographic Data Recording

Experiment	No. of Cameras	Total Filming Time-Sec	Film Speed Frames/Sec	Feet of Film
1. Pool Boiling	1	540	200	2,700
2. Pressure Drop	1	1,800	Video	Video Tape
3. Film Boiling	1	1,520	200	7,600
4. Liquid Reorientation	1	1,300	Video	Video Tape
5. Bubble Dynamics	3	540	400	<u>16,200</u>
				26,500



# 9

## DISCUSSION AND CONCLUSIONS

The five experiments considered in this study have been extensively analyzed to determine the major characteristics of each experiment. The experiments were then designed with instrumentation necessary to collect test data to analyze fluid behavior and heat transfer in a low gravity field. These experiments were packaged, along with the associated instrumentation and data recording elements, to be installed collectively in a double experiment rack in the Space Shuttle Spacelab payload module. This packaging arrangement is shown in Figure 9-1 to illustrate that the five experiments are physically compatible with the rack dimensional constraints. This installation was found to be practical and has been accomplished in such a manner that each of the five experiments can be performed using the integrated double rack design installation. The experimental procedure proposed requires that the pool boiling experiment be run first. The pool boiling experiment elements are removed from the rack subsequent to experiment completion and stowed in external Spacelab compartments.

The bubble dynamics experiment is initially installed in a stowed condition in the upper portion of the rack. It must be relocated within the rack for testing. Since it must be placed in a test position which would obstruct camera view of the other experiments, it is preferable to run this experiment last. Either the liquid reorientation experiment or the flow pattern/pressure drop experiment may be run second. The order of test preparation and making of test connections would make it desirable to run the flow boiling experiment following the pressure drop test. This is because it is planned to evacuate the water from the experiment section by connecting to the Spacelab vacuum vent and holding a vacuum on the system until dry. The vacuum vent would be left connected for venting of the halon from the flow boiling experiment.

Installation, testing, data collection and recording of the pertinent data appears to present no more than normal development problems. There are two major problems associated with the actual conduct of the experiment. The first is merely one of limited expendables with respect to the amount of RCS thruster fuel available. As shown previously, under the most optimistic assumptions the amount of fuel required to complete the test program is nearly equal to the total available for the full complement of experiments used for the selected shuttle mission. This is perhaps permissible if the Fluid Mechanics and Heat Transfer facility was the only user of RCS fuel but, even so, the amount of fuel available is considered to be marginal. As a supplement to the RCS fuel, there is approximately 909 kilograms of fuel available from the orbital maneuvering system (OMS). This is not an online capability however, as special provisions must be made to provide interconnection and transfer capability between the RCS and OMS tankage. At present, this is not incorporated in the shuttle design.

# TWO-PHASE FLUID MECHANICS AND HEAT TRANSFER FACILITY FOR SPACELAB (NAS3-21750)

FLOW PATTERN, PRESSURE DROP, AND  
FLOW BOILING EXPERIMENTS.

9-2

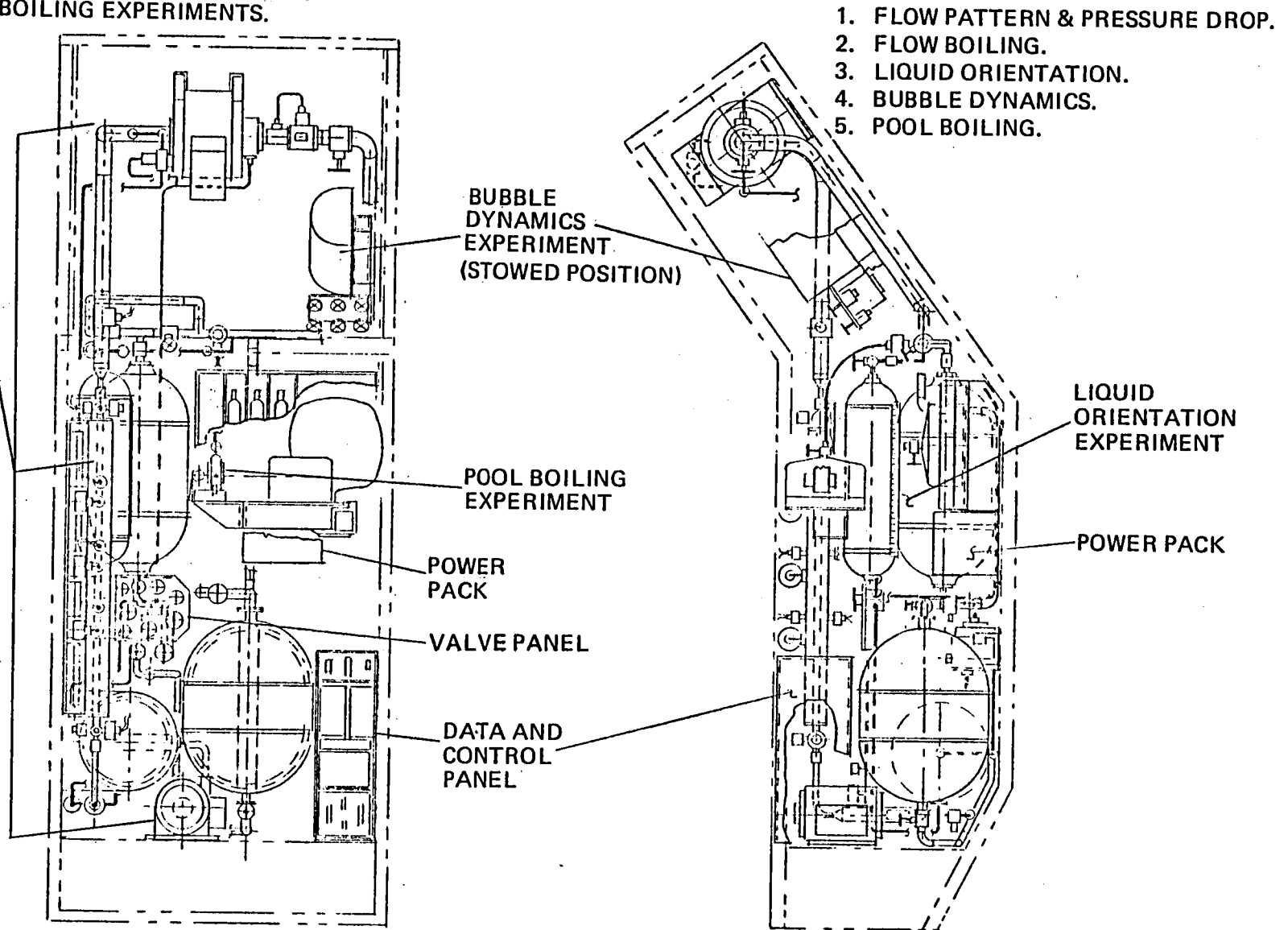


Figure 9-1. General Installation of Five Experiments in Spacelab Double Rack

A second, more serious problem, is the attainment of the proper thrust level with the RCS. This system can provide approximately true translational motion only by firing several thrusters simultaneously to counteract the rotary motion caused by the line-of-thrust not being directed through the vehicle center of gravity. The primary thrusters have a thrust of 870 lbs each. The vernier thrusters provide 24 lbs thrust each but are not suitable for attaining translation in the desired axis. From Table 2-2, translation in the z-axis results in the most efficient use of the thruster fuel and the experiments have been packaged to take advantage of this fact. Because of the fixed thrust level of the thrusters, only one discrete level of acceleration can be obtained by firing the RCS in a sustained mode. It is possible that intermittent firing might produce a satisfactory quasi-acceleration if the pulse duty cycle could be programmed adequately. There are problems associated with this concept also. The first is the physical limitation of 48 ms for the primary thruster valve to respond. If this is overcome, the system becomes software limited to 40 ms by the autopilot computer limit. An adverse effect acting in conjunction with either of the above time limitations is the thrust build-up and tail-off effect of the thruster itself. This is illustrated in the following Figure 9-2.

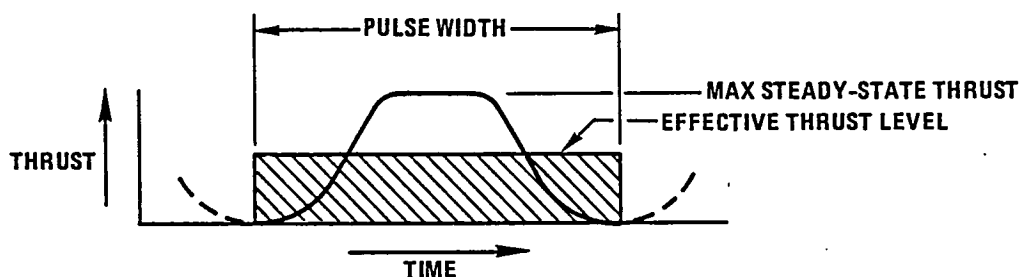


Figure 9-2. Primary Thruster ON-OFF Pulse

From the sketch it is seen that both the pulse-width and the start and stop transients influence the effective thrust level. Theoretically, it should be possible to set a duty cycle in such a manner as to provide an average thrust level which would be very close to the desired steady-state level. This condition is illustrated in Figure 9-3.

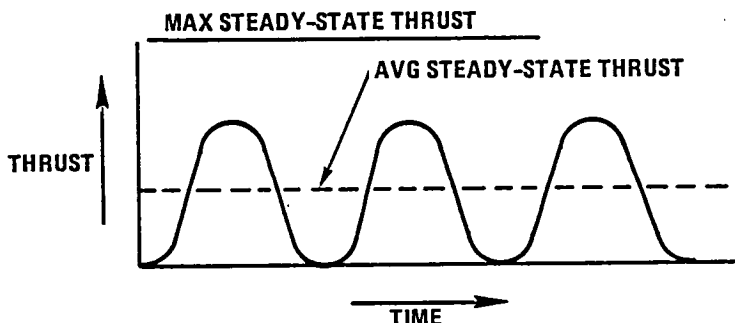


Figure 9-3. Primary Thruster ON-OFF Pulse

If it were not for the valve characteristics or the computer load sharing time limitations, the average steady-state thrust can be made to very closely approximate a continuous thrust level. This short cycle pulsing does not appear to be possible, however, in the present shuttle configuration. Some pulsing is possible but only in a manual mode and subject to the time limitations stated above. This would result in a poor approximation of a steady-state acceleration environment for levels below about  $3 \times 10^{-3}$  g and, in the opinion of the lead scientist advisors on this contract, would not be satisfactory for the conduct of their tests. The RCS thrusters do provide a satisfactory controlled acceleration at a g-level of about  $3 \times 10^{-3}$  g and therefore a part of the desired test spectrum can be covered with the existing shuttle RCS design and experiment definition presented herein.

Professor Bowman indicated that redesign of the reorientation experiment tankage could be accomplished and testing redefined within the present system constraints to allow collection of suitable data. This redefinition was not incorporated because neither the remaining study time nor the scope of the contract was sufficient to do so. There exists the possibility to include an experiment peculiar thrusting system which could be pallet mounted and chargeable to the experiment. With pre-mission planning to define the probable location and excursion limits of the vehicle center of gravity, a system could be designed and optimized to provide vehicle acceleration independent of the RCS or as a supplement to the RCS capability. With such a system, located to provide thrust in the proper direction through the center-of-gravity, any desired acceleration could be achieved as long as the requirement is greater than the inherent acceleration caused by vehicle atmospheric drag.

A secondary problem exists in the effects of g-jitter as defined by Table 2-1 of this report. The only experiment which appears to be significantly sensitive to this perturbation is the pool boiling experiment. Professor Lienhard has expressed concern over this effect disrupting and invalidating results of this heat transfer phenomenon at the low gravity levels required for his experiment. He suggests, as an alternate to a separate thrusting system, a centrifuge concept. His initial estimate of a probable satisfactory centrifuge would have an approximate radius of one meter and would have to be extremely well shock-isolated to prevent g-jitter effects. Further definition of this concept was not pursued. Based on the results of this study it is concluded that:

1. The five experiments defined herein can be packaged and installed together within one double experiment rack.
2. The experiment system components necessary to run meaningful tests are available within the framework of existing manufactured components.
3. The instrumentation with necessary accuracy and sensitivity can be readily obtained with the possible exception of a suitable fluid quality meter.

4. Photographic techniques must be evaluated based on mockup to identify proper lighting, camera field depth, focus, film and framing rates.
5. A completely adequate range of g-level testing is not possible using the existing shuttle RCS alone but a major portion of the experiment testing can be accomplished.
6. Solutions exist and should be further defined for more precise attainment of experiment acceleration control.
7. Sufficient analysis and design has been accomplished to allow proceeding to a hardware procurement and development phase.



# 10

## EXPERIMENT FACILITY COSTS

Preliminary cost estimates for the two-phase Fluid Mechanics and Heat Transfer facility for Spacelab were generated to provide an aid to budget planning and to identify high cost areas where potential cost reductions may be made.

These data represent preliminary top level estimates that can only reflect the program definition work performed to date and, therefore, cannot be considered complete or final. They do, however, represent a reasonable estimate based on information available at this time and are usable for concept comparisons and planning purposes. As the program proceeds and more detailed definition of specific hardware becomes available, increased accuracy of individual cost element estimates can be attained.

### 10.1 ESTIMATING METHODOLOGY

Initially a cost work breakdown structure was developed that includes all elements, chargeable to the Experiment Facility Project for each of the program phases, i.e., development, production, and operations. This cost WBS then sets the format for the estimating model, the individual cost estimating relationships (CERs), cost factors or specific point estimate requirements, and, finally, the cost estimate output itself. Cost estimates are then made for each element, either at the WBS breakdown level shown or one level below in certain cases. These estimates are then accumulated according to the WBS to provide the required development, flight article production, and first flight operations costs.

The estimating methodology varies with the cost element and with the availability of historical data or vendor quotes. For new non-off-the-shelf hardware, parametric CERs are used. These CERs were developed during past cost analysis activities performed by Convair on space experiment systems and were used during the Space Transportation Systems Payloads and Data Analysis (SPDA) study (Contract NAS8-29462). These CERs have been derived for various categories of hardware and many subcategories representing differing levels of complexity or technology families. These CERs are derived from available historical cost data or detailed estimating information and relate cost to a specific driving parameter such as weight, area, power output, etc. For example, the various facility structural mechanical items, mechanisms, control systems, etc., were estimated using such CERs. In some cases relating to existing aerospace type non-flight qualified an estimating procedure was used that was developed from the Rockwell International study "Analysis of Commercial Equipment and Instrumentation for Spacelab Payloads (NAS8-30541).

Point estimates were used for specific pieces of equipment where the definition data was sufficiently detailed or the hardware item was existing equipment and cost data was available. Certain electronic equipment and instrumentation were estimated in this manner. In another example of point estimates, several task areas in ground and mission operations consist of all labor and, therefore, manloading estimates were made and converted to cost.

The remaining "floating item" cost elements such as system engineering and integration, program management, etc., are estimated using simple cost factors consisting of appropriate percentages of the applicable related program effort.

## 10.2 GROUND RULES AND ASSUMPTIONS

The following general ground rules and assumptions were used in estimating the Experiment Facility project costs presented herein.

- a. Costs are estimated in current/constant FY 1980 dollars.
- b. No prime contractor fee is included.
- c. Costs are estimated for nonrecurring, recurring production, and recurring operation phases. The costs include all facility payload-related costs incurred from the start of Phase C/D (development phase) through a single (first) Spacelab launch of the facility including experiment orbital monitoring and data acquisition.
- d. All facility level development and qualification testing is conducted using the flight article.
- e. All purchased components are assumed close to or aerospace flight qualified and only minor modifications or testing are required. Fabricated components require normal design, analysis testing and qualification.
- f. A multipurpose high fidelity Spacelab rack mockup will be required as a dimensional tooling aid, integration mockup, test stand, and experiment shipping structure. It is assumed that no flight rack will be provided prior to Level IV integration. Cost estimates also include the cost of one dedicated Spacelab flight double rack.
- g. It was assumed that only standard and available test equipment and servicing equipment (water and Freon) was available and the only experiment chargeable GSE may be some special tools and shipping related items.
- h. No heat exchanger interface with Spacelab is required.
- i. NASA IMS and Program Office costs are excluded.
- j. This cost data is for planning purposes only.

### 10.3 COST ESTIMATE

The resulting nominal cost estimates for the experiment facility is detailed in Table 10-1 through 10-4 for the experiment hardware complement and summarized for the complete facility in Table 10-5. The costs are constant FY 1980 thousands of dollars and exclude prime contractor fee. The experiment hardware estimates identify costs for both component development (design, modification, test article procurement, and component test and qualification) as well as experiment level design analysis and test for each major component or group of components. In addition, the procurement and/or fabrication cost of the hardware items for the flight article is included under the production column. All plumbing (lines and fittings), secondary structure mounting provisions, etc., cabling and harnesses, data management (signal conditioning), and software are accumulated and estimated at the facility level. The experiment total including the basic direct costs of the experiment hardware components but more of the overall costs of integrating it into the facility, which are estimated at the total facility level in Table 10-5.

The costs for the combined Experiment I and II are shown in Table 10-1. It will be noted that the subsequent cost tables for Experiment III, IV, and V (Table 10-2, 3, and 4) include certain items with asterisks. This indicates that the basic development, modifications, qualifications for that particular component has already been accounted for in the Experiment I and II estimate. The total cost of these latter experiments (III, IV and V) does not reflect the total cost of that experiment if its development was conducted independently because of the common use components. These hardware costs will, however, sum correctly for the total facility estimate.

This total facility estimate is shown in Table 10-5. This facility level includes all secondary structure, fluid lines and fittings, wiring harnesses, data management and signal conditioning, and software as noted above. Also at this level is flight support equipment FSE and Ground Support Equipment (GSE), and initial spares. Other Wraparounds include facility level design and analysis, system engineering and integration, facility level testing, and project management. The operations costs include support operations and logistics, ground operations (Spacelab Level IV, III, II, I) and post-mission operations, and Mission Operating (mission control data handling/processing and mission support) post flight maintenance and refurbishment have been excluded in this estimate.

No required facilities were identified chargeable to this experiment.

As may be seen, the nominal nonrecurring development cost is \$2.53M and the flight unit about \$1.24M including a dedicated double rack costing \$0.68M. Operations cost for a single flight is about \$4.2M including \$3.9M for STS user charges. (In this case user charges were calculated as a simple pro rated share of a double rack in a full long module Spacelab.) The resulting nominal cost of this facility project including one flight is \$8.0M.

Table 10-1. Preliminary Experiment Hardware Cost Estimate  
Experiment 1 and 2

Experiment I Flow Pattern and Pressure Drop and Experiment II Flow Boiling		(Cost in 1980 K\$)				
<u>ASSEMBLY/COMPONENT</u>	<u>WT, KG (LB)</u>	<u>DEVELOPMENT</u>	<u>QTY</u>	<u>UNIT</u>	<u>PRODUCTION</u>	
Test Section Assy	9.1 (20.1)	75.1	1	19.5	19.5	
Separator/Motor Assy	6.0 (13.2)	52.2	1	6.3	6.3	
Blower/Motor Assy	6.5 (14.3)	20.0	1	4.0	4.0	
Pump Assy	2.0 (4.4)	10.0	1	2.0	2.0	
Freon Tank	3.6 (8.0)	45.1	1	4.0	4.0	
Water Tank	0.9 (2.0)	8.4	1	1.7	1.7	
Valves & Controls		10.0	-	-	10.0	
Transducers		99.4	-	-	42.2	
Quality Meter		10.0	2	25.0	50.0	
Accelerometer		20.0	1	50.0	50.0	
Displays		5.0	1	3.0	3.0	
Photo System		5.0	-	-	15.1	
	Hardware Subtotal	360.2			207.8	
Experiment Level						
	Development	108.2				
	Test Article	103.0				
	Test	72.2				
	Experiment Total	644.5			207.8	

Table 10-2. Preliminary Experiment Hardware Cost Estimate  
Experiment 3

Experiment III Pool Boiling		(Cost in 1980 K\$)				
<u>ASSEMBLY/COMPONENT</u>	<u>WT, KG (LB)</u>	<u>DEVELOPMENT</u>	<u>QTY</u>	<u>UNIT</u>	<u>PRODUCTION</u>	
Preconditioning Chamber		5.0	1	2.0	2.0	
Test Chamber/Light		5.0	1	1.0	1.0	
Test Cell (Large)		14.0	4	2.5	10.0	
Test Cell (Small)		9.0	8	2.0	16.0	
Controls		19.0	-	-	9.0	
Transducers		19.5	-	-	6.1	
Photo System		(*) -	-	-	(*) -	
	Hardware subtotal	71.5			44.1	
Experiment Level						
	Development	28.3				
	Test Article	22.1				
	Test	18.9				
	Experiment Total	140.8			44.1	

(\*) From Exp. I & II

Table 10-3. Preliminary Experiment Hardware Cost Estimate  
Experiment 4

EXPERIMENT IV. LIQUID ORIENTATION (COST IN 1980 \$K)					
<u>ASSEMBLY/COMPONENT</u>	<u>WEIGHT KG (LB)</u>	<u>DEVELOPMENT</u>	<u>QTY</u>	<u>UNIT</u>	<u>PRODUCTION</u>
Tank (Large)	5.3 (11.6)	20.4	1	4.2	4.2
Tank (Small)	3.2 (7.1)	15.9	1	3.1	3.1
Freon Tank	5.7 (12.6)	28.2	1	5.9	(*)5.9
Gas/Liquid Separator		(*) -	-	-	(*) -
Controls		(*) -	-	1.0	1.0
Transducers		(*) -	-	-	8.5
Photo System		(*) 5.0	-	-	(*) 2.0
	Hardware Subtotal	69.5			24.7
Experiment Level					
	Development	66.9			
	Test Articles	12.4			
	Test	44.6			
	Experiment Total	193.4			24.7

(\*) From Exp. I & II

Table 10-4. Preliminary Experiment Hardware Cost Estimate  
Experiment 5

EXPERIMENT V. BUBBLE DYNAMICS (COST IN 1980 K \$)					
<u>ASSEMBLY/COMPONENT</u>	<u>WEIGHT KG (LB)</u>	<u>DEVELOPMENT</u>	<u>QTY</u>	<u>UNIT</u>	<u>PRODUCTION</u>
Test Chamber and Bubble Generator	13.6 (30)	45.9	1	19.1	19.1
Transducers		(*) -		(*) 1.7	(*) 1.7
Controls		(*) -		(*) -	(*) -
Photo System		-			(*)22.1
	Hardware Subtotal	45.9			42.9
Experiment Level					
	Development	28.9			
	Test Article	21.5			
	Test	19.2			
	Experiment Total	115.5			42.9

(\*) From Exp. I & II

Table 10-5. Preliminary Two-Phase Fluid Mechanics and Heat Transfer Facility Project Cost

	Cost 1980 K\$		
	<u>Development</u>	<u>Flight Unit</u>	<u>Operations</u>
Experiment I & II	644.5	207.8	-
Experiment III	140.8	44.1	-
Experiment IV	193.5	24.7	-
Experiment V	115.4	42.9	-
Secondary Structure	32.1	16.1	-
Fluid Lines/fittings	43.4	23.7	-
Wiring Harness	29.5	9.2	-
Data Mgmt./Sig Conditioning	42.6	18.4	-
Project Level Eng & Support	404.8	52.8	-
System Eng/Integration	353.3	-	-
FSE/GSE	140.0	10.0	-
Installation & Assy.	-	44.0	-
Software	40.0	-	-
System Test	157.2	44.0	-
Support Ops /Logistics	-	-	57.0
Initial Spares	72.5	-	-
Ground Ops	-	-	64.0
Mission Ops	-	-	175.0
Facilities	-	-	-
Dedicated Double Rack	0	680.0	-
Shuttle Transportation	-	-	3900.0
Project Management	<u>120.5</u>	<u>26.9</u>	<u>14.8</u>
Project Total	2530.1	1244.6	4210.8
Grand Total		7985.5	

This experiment facility is necessarily at a very early state of definition and it was not possible to look in detail at off-the-shelf component usability and detail designs of unavailable components. For this reason, it was desired to examine the estimate from the viewpoint of assumptions as to task difficulty and magnitude. Accordingly, the estimates were re-run for a minimum program with optimistic projection and a highly conservative estimate in addition to the nominal estimate presented above, the results are shown in Table 10-6 for the range of uncertainty examined.

Table 10-6. Cost Estimate Range

	Cost (FY 1980 M\$)		
	<u>Development</u>	<u>Flight Unit</u>	<u>Total</u>
Minimum	1.28	1.16	2.44
Nominal	2.53	1.25	3.77
High	3.92	1.30	5.22

In the minimum case, it is assumed that this project is austere and success oriented (i. e., little or no development problems), the hardware is as currently defined, and maximum use is made of existing components (i. e., little or no modification or testing). System level ground testing is conducted using the flight article.

The nominal case includes provisions for more extensive modification and tests for existing components and more conservative estimates for new components. Also some latitude was allowed for unidentified components in the facility definition. The concept of a single facility for both ground and flight test was retained.

In the high estimate component costs were retained from the nominal estimate but an even more conservative approach regarding definition data and facility level requirements. In addition in this case an all up ground test unit was added.



# 11

## REFERENCES

1. Bradshaw, R. D. and King, C. D. "Conceptual Design for Spacelab Two-Phase Flow Experiments," CASD-NAS-77-025, NASA CR-135327, Contract NAS3-20389, December 1977.
2. Collier, J. G., Convective Boiling and Condensation, McGraw-Hill Book Co., (UK) Limited, London, 1972, pp. 33-54.
3. *ibid*, pp. 208-13.
4. Lienhard, J. H. and Peck, R. E., "Conceptual Design for Spacelab for Boiling Experiment," NASA CR-135378/UKY TR106-78 ME15, March, 1978.
5. Sumner, I. E., "Liquid Propellant Reorientation in a Low-Gravity Environment," NASA TM-78969, LeRC, July 1978.
6. Peebles, F. N. and Garber, H. J., "Studies on the Motion of Gas Bubbles in Liquids," Chem. Eng. Prog., Vol 49, February 1953.
7. Haggard, J. B. and Masica, W. J., "Motion of Single Bubbles under Low-Gravitational Conditions," NASA TN D-5462, LeRC, Oct. 1969.
8. Moore, D. W., "The Velocity Rise of Distorted Gas Bubbles in a Liquid of Small Viscosity," J. of Fluid Mech., Vol 23, Pt. 4, December 1965, pp. 749-66.
9. Hill, M., "Reorientation Analysis for Spacelab Experiment," TM696-0-T-79-458, 25 January 1979.
10. Hill, M., "Terminal Velocity Calculations for Spacelab Bubble Dynamic Experiment," TM696-0-T-79-471, 14 March 1979.
11. Hill, M., "Pressure Drop Calculations for Two-Phase Flow and Flow Boiling Experiments," TM696-0-T-79-520, 31 May 1979.
12. Hill, M., "Thermal Analysis of Spacelab Pool Boiling Experiment, Fluids and Containers," TM696-0-T-79-535, 7 August 1979.
13. Hill, M., "Wall Temperature Calculations for Flow Boiling Spacelab Experiment," TM696-0-T-79-623, 26 November 1979.

14. Frichtl, George, Personal Communication on Data for G-Jitter, ES 82, NASA/MSFC, 1979.

APPENDIX A  
INSTRUMENTATION/COMPONENT  
HARDWARE DESCRIPTIONS



## APPENDIX A

### INSTRUMENTATION/COMPONENT HARDWARE DESCRIPTIONS

A survey was conducted to determine availability, size, cost, and performance of instrumentation and component hardware suitable for the experiment facility items identified in the study. A preliminary specification was then prepared for each item giving the information shown below:

#### Preliminary Specification Sheet Format

1. Item Name
2. Purpose & Requirements
3. Hardware Status — Gives status of items such as off-the-shelf, specially fabricated, etc.
4. Description — Gives general description of equipment, model number, weight, size, power and cost.
5. Applicable Experiments

This Appendix presents the preliminary specification for each item followed by vendor supplied catalog information. The facility hardware items covered are listed alphabetically in Table A-1.

Table A-1. List of Instrumentation/Component Items Surveyed

Accelerometer	A-4
Ammeter	A-14
Back Pressure Regulator	A-15
Blower (Air)	A-18
Controller, Heater	A-25
Differential Pressure Transducer	A-33
Flowmeter, Air	A-37
Flowmeter, Liquid	A-43
Gas/Liquid Separator	A-49
Pressure Transducer	A-52
Pump	A-58
Quality Meter	A-61
Tank, Freon	A-66
Tank, Water	A-67
Thermistors	A-68
Thermocouple Reference Junction	A-74

## ACCELEROMETER

### PURPOSE & REQUIREMENTS

To monitor g-levels at the experiment package during testing. Measurements in three orthogonal directions and a display compatible with the 16 mm camera are required.

Sensitivity  $\pm$  .0001 g  
Freq. Response  $\cong$  0-100 Hz

### HARDWARE STATUS

No off-the-shelf accelerometer is available with the required sensitivity (Ref. Endevco Corp., 714/831-9200). A special unit is available from Sundstrand Data Control, Inc., Redman, Washington, 206/885-3711. Displays compatible with the dc voltage output of this unit are readily available. Bell Aerospace Textron has developed a unit with high sensitivity for use in future Spacelab experiments.

### TECHNICAL DESCRIPTION

Attached sheets from both firms describe the Sundstrand triaxial accelerometer and the Bell Aerospace triaxial accelerometer packages.

#### Sundstrand Accelerometer

Size:	7.62 $\times$ 8.89 $\times$ 6.35 cm (3 $\times$ 3.5 $\times$ 2.5 inches)
Weight:	0.45 kg (1 lb) (est.)
Power:	5 watts (est.)
Cost:	\$50K (est. by Sundstrand)

#### Sundstrand Display, Digital

Size:	327.7 cm <sup>3</sup> (20 in <sup>3</sup> )
Weight:	0.45 kg (1 lb)
Power:	5 watts (est.)

### APPLICABLE EXPERIMENTS

All.

# Sundstrand Data Control, Inc.

unit of Sundstrand Corporation



## TECHNICAL DESCRIPTION

The proposed design for the MBB Space Laboratory Experiment package will consist of three QA-1200 Q-Flex accelerometers mounted on a common triad structure, as shown in Figure A-1.

The structure will be an enclosed cube with flanges on two sides and the common power and signal connector mounted on the bottom to simplify build and calibration.

The top of the support structure will hold a printed wiring board where the sensor load resistors and the additional output amplifiers required for all three output channels are located. A separate printed wiring board will be used to contain the necessary input power filtering and conditioning for + 15 VDC and - 15 VDC power

The power filtering and conditioning will consist of passive components sized to meet the EMC requirements for the package.

The 3-channel output amplifier PWB will contain components for the following functions (all three channels) :

- Sensor load/read-out resistors
- Scale-factor trim selects
- Null bias trim selects
- Precision output amplifier with associated compensation, filtering and gain setting
- Resistors for voltage output of the sensor temperature monitors

### Electrical Description

The main electrical design trade-off will be the voltage scale factor and voltage gain established at the sensor load resistor versus the output amplifier gain.

The QA-1200 with current output allows for stable operation over a wide range of resistor values (voltage scale factors). This factor will reduce the output amplifier gain requirements and associated amplifier caused errors.

# Sundstrand Data Control, Inc.

unit of Sundstrand Corporation 

Page -2-

As an example, with a 15 Kohm sensor load (read-out) resistor, the sensor voltage scale factor would nominally be approximately 20 mV/mg (@ 1.33 micro-amps/milli-g).

To achieve an output scale factor of 1 volt/mg, the output amplifier gain required would be 50, which is reasonable for a precision operational amplifier. A full scale of 10 volts for 10 mg will be easily achieved with the + 15 VDC and - 15 VDC supply voltages.

Because of the high signal gain required at 1 volt/mg output, additional filtering may be required outside the QA-1200 electronics. The filtering would be established during the development testing of the output amplifier.

During calibration and acceptance test procedure testing, the output voltage scale factor will be increased (reducing read-out resistor value from 10 volts/10 milli-g to 10 volts/lg to allow testing per normal methods on a dividing head in a lg field. The 10 volts/10 milli-g scaling will be operationally (not performance) checked at 10 mr or 0.57 degrees from vertical to verify the +/- 10 volt output signal range. This approach will reduce testing time and actually improve the calibrated accuracy of the unit.

A basic Error Budget is presented for the sensor and electronics in Table A-2.

## Mechanical Description

The support structure will consist of a triad mounting block that is attached to the separate flanged base. This design approach will allow for mechanical alignment, if required, through the use of shims.

The cover will be secured to the base with four corner screws. A Cannon 26 pin miniature connector (MS 27499E16A26P) will be mounted in the base for ease of manufacturing.

The dimensions of Figure A-1 may be reduced, as determined during the mechanical design and lay-out of the package.

\* \* \* \* \*

DAA:bp  
12/16/77

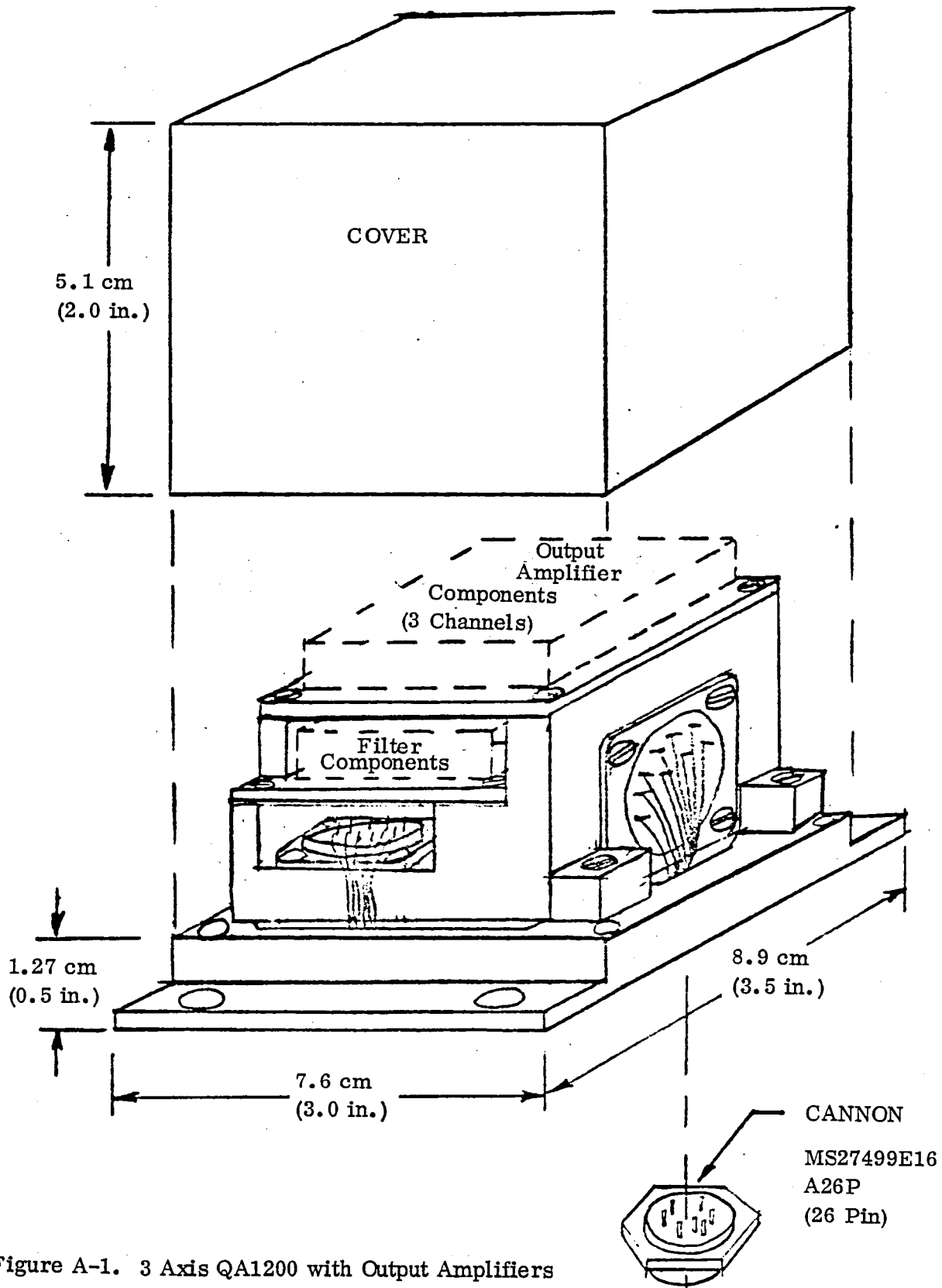


Figure A-1. 3 Axis QA1200 with Output Amplifiers and Power Filters (for MBB Program)

TABLE A-2

ERROR BUDGET

Standard QA1200-AA08 performance characteristics are assumed, unless otherwise stated.

<u>Characteristic</u>	<u>Sensor (Untrimmed)</u>	<u>External Electronics</u>	<u>Total Trimmed Sensor with External Electronics</u>
Scale Factor Accuracy:			
Linearity 100ug-10mg)	-	-	.1% Full Scale
Temperature Coefficient	180 ppm/°C	100 ppm/°C	< 200 ppm/°C
Bias: (Initial)	+ 3 milli-g (Typ)	-	
	+10 milli-g (Max)	-	200 ug
Temperature Coefficient	10 ug/°C	< 10 ug/°C	15 ug/°C
Thermal Hysteresis	-	-	100 ug
Acceleration Hysteresis	-	-	10 ug
Resolution	1 ug	1 ug	1 ug
Threshold	1 ug	1 ug	1 ug
Alignment (in Support Structure)	0.001 g/g	-	0.01 g/g
Output Resistance	-	100 ohm	100 ohm
Frequency Response (+10%)	> 800 Hz	TBD	TBD (To be Determined)
Excitation/Power Supply Voltages	-	-	+ 15 VDC ± 5% and - 15 VDC ± 5%
Power Supply Quiescent Current	15 ma Per Supply Per Channel	< 5 ma Per Supply Per Channel	< 20 ma Per Supply Per Channel
External Temperature Monitor:	-	-	
Repeatability			< 1%

September 1979



BELL AEROSPACE TEXTRON INERTIAL MEASUREMENTS GROUP  
ACCELERATION MEASUREMENTS  
(IN THE RANGE OF  $10^{-2}$  TO  $10^{-9}$  G)

## INTRODUCTION

This document describes the Bell Miniature ElectroStatic Accelerometer (MESA), designed to measure acceleration in the range of  $10^{-2}$  to  $10^{-9}$  g. This instrument represents the results of over 20 years of continuous development and thousands of hours of on-orbit use. The primary application is in spacecraft and space research and technology. The MESA may be configured for either single or three axis measurement.

## ACCELERATION MEASUREMENT

Conventionally, high precision acceleration measurements are made by determining the force required to constrain a proofmass against an unknown input acceleration applied to the enclosing case. Instruments of this type are force rebalance accelerometers and are an application of Newton's second law of motion.  $F = Ma$ , where  $M$  = mass of the proofmass,  $a$  = acceleration, and  $F$  = force required to accelerate the proofmass. Force rebalance can be accomplished by a number of methods. Typical examples are a spring, a string under tension, or a force which continuously nulls the motion or deflection of the proofmass with respect to its case through a feedback amplifier. This force can be generated electromagnetically, electrostatically, or some other way. Conventional force rebalance accelerometers are electromechanical devices with their scaling and environmental capabilities fixed at the time of fabrication. They must be capable of surviving without performance degradation, the extreme environmental conditions of spacecraft launch, and staging. Typically, this could include steady-state accelerations of 10 g's and up to 10,000 g's peak during stage separation using pyrotechniques. Within seconds after experiencing these extreme accelerations they may be called upon to measure inputs as small as  $10^{-6}$  g's. In addition to surviving the very large in-flight dynamic range, the accelerometer must be capable of being tested and calibrated in the normal steady-state 1-g environment of the laboratory. The Bell MESA meets all these requirements by the use of a unique mechanical design combined with electrostatic forcing.

## ELECTROSTATIC FORCING

Electrostatic forcing has a property which makes it ideal for proofmass rebalance. It always attracts regardless of polarity or frequency. This means the force due to a potential difference may be developed by the use of unipolarity pulses, bi-polarity pulses, d-c or either polarity, sine waves of any frequency and a-c signals of any wave shape. This characteristic allows the forcing and position sensing signals to be applied simultaneously to a single electrode without coupling by using different frequencies for each function.

## PROOFMASS

The proofmass is a flanged cylinder made of beryllium. Its inside diameter is a nominal 0.5 inch and weighs 1 gram. The proofmass cylinder is suspended radially by a slightly smaller diameter electrode carrier which fits inside the cylinder. The electrode carrier is ceramic with a pattern of eight deposited electrodes that act against the inside wall of the cylinder and form the X and Y axes. Facing both sides of the flange are two ceramic discs which have a three ring electrode pattern that acts against the flange and forms the Z axis. The gap between the flange and ring electrodes is a nominal 0.0037 inch, and is maintained by a ceramic ring shaped spacer centered over the edge of the flange. The gap in the X and Y axes is a nominal 0.0013 inch, and is established by the difference between the inside radius of the proofmass cylinder and the outside radius of the carrier.

### MESA SPECIFICATIONS

<u>Type:</u>	Three Axis	<u>Ranges Available:</u>	3 from $10^{-2}$ to $10^{-4}$ in X & Y 3 from $10^{-2}$ to $10^{-5}$ in Z
<u>Size:</u>	3.5"×5"×8.5"	<u>Environment:</u>	
<u>Weight:</u>	5.5 Lb	(Nonoperating)	
<u>Power:</u>	8 Watts	<u>Temperature:</u>	-25F to 185F
<u>Sensitivity:</u>	Z Axis $10^{-9}$ g X & Y Axis $10^{-7}$ g	<u>Shock:</u>	50 g, 8 msec, 3 axes
<u>± Full Scale:</u> (Lowest Range)	Z Axis $10^{-5}$ X & Y Axis $10^{-4}$ g	<u>Vibration:</u>	Sine: 20 to 2000 Hz, 10 g's peak Random: 20 to 2000 Hz, 20 g's rms
<u>± Full Scale:</u> (Highest Range)	All Axes $10^{-2}$ g	<u>Pyro:</u>	6000 g's
<u>Accuracy:</u> (Worst Case)	1% of Full Scale	<u>Acceleration:</u>	15g, 3 axes
<u>Output:</u>	±8 Vdc = ± Full Scale, All Ranges	<u>Altitude:</u>	Space
		(Operating)	
		<u>Temperature:</u>	-10F to +160F
		<u>Altitude:</u>	Space
		<u>Cost:</u>	Approximately \$100K

## APPLICATION ENGINEERING

Potential users of low-g accelerometers always face the obvious problem of matching requirements against available instruments. This task is usually complicated by two factors: (1) lack of precise knowledge of all the environmental and acceleration inputs which the instrument is expected to experience throughout its life, and (2) lack of precise definition by the accelerometer manufacturer of all its characteristics and performances in terms that match each user requirement.

The questions which the user should ask himself in attempting to select an accelerometer generally fall into the following categories: (1) Maximum available power, weight and size? (2) Single axis or 3 axis sensing? (3) Range of input acceleration expected? (4) Maximum frequency of input acceleration to be measured? (5) Accuracy required? (6) Command and data interface requirements? (7) Environmental conditions such as temperature range, launch acceleration, pyro shock, electromagnetic interference levels, etc. (8) Delivery schedule and rates? (9) Dollar budget? The accelerometer manufacturer, on the other hand, must characterize the instrument in these terms plus present

possible options to each requirement which may be considered to accomplish the measurement in the most efficient manner. The instrument characteristics and some available options are described for each accelerometer type in the appropriate section. Some of these can only be described in general terms. Precise electrical interface circuits involving data rates, voltage levels, impedances, etc., must be customized for each application. Typical applications in which these instruments have been used or could be used are: ion engine thrust measurement, air density, solar pressure, navigation & guidance, fuel venting accelerations, mass attraction, gravity gradient, attitude control, vehicle acceleration monitoring, and vehicle angular acceleration. A single package containing the mechanical instrument assembly and its associated electrostatic force rebalance constraint loops represents the minimum hardware which can be purchased. Various accessories are available which may be added to this basic hardware to perform a variety of functions. These generally fall into the six major categories. They can be added to either single or three axis configuration. (1) Power input conditioning. (2) Signal output conditioning. (3) Multiple ranges. (4) Temperature control. (5) In-flight calibration. (6) Special packaging.

1. Power Input Conditioning - This converts any available input voltage to the voltages required to operate the constraint loops. Total conditioning would normally include an EMI filter on the input line, a regulator, and a transformer coupled DC to DC converter followed by the normal power supply filter for each of the five d-c voltages required.

2. Signal Output Conditioning - This converts the normal  $\pm 8$  Vdc voltages which represent  $\pm$  full scale to the desired output voltage and impedance level. It can also convert the d-c output to a serial digital data stream and filter and average the output either in analog or digital form.

3. Multiple Ranges - The constraint loops may be switched to set full scale input limits at three different levels or ranges. Range selection may be by external command or by an internal autorange circuit. The later will automatically adjust each axis to the appropriate scale required to accommodate the input acceleration level experienced at that particular time.

4. Temperature Control - This maintains the accelerometer case within  $\pm 1F$  or a pre-set temperature. It is normally used if the environment temperature range is large and scale factor temperature coefficients established during calibration cannot be used to correct the output data.

5. In-flight Calibration - This is used in special applications where the full scales selected are lower than permitted by ground calibration. An alternative is to use higher scales to permit ground calibration and utilize a longer averaging time per data point to obtain the required resolution and sensitivity.

6. Special Packaging - The accelerometer may be packaged in various form factors. The instrument and its attached preamplifiers, if packaged separately, would occupy a box-shaped volume with dimensions of 3.5" x 5" x 4". The instrument loop electronics, if

packaged separately, is 3.5" x 5" x 5". If combined in a single package the total volume is slightly less as shown on the specification sheets. If packaged separately the constraint loop electronics should not be more than 10 inches from the instrument package. The accessory circuits described in 1. through 6. may be located up to 48 inches from the constraint loop electronics. A single package configuration is always the most efficient from the standpoint of cost, volume, and performance.

### MESA - CUBE PROOFMASS

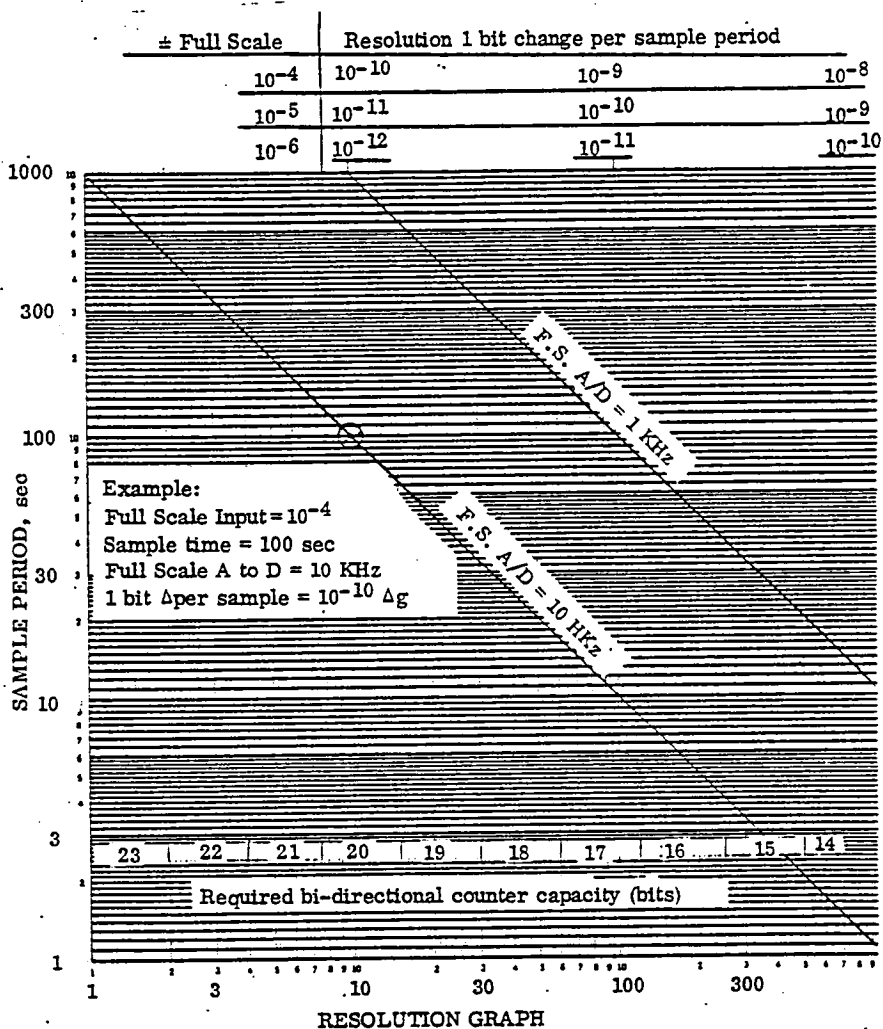
The proofmass is a cube made of beryllium. Its outside dimensions are a nominal 0.5 inch, and its weight is 1 gram. Facing each of the six sides is a dual electrode assembly. The individual electrodes together with the one on the opposite face form one of the six constraint loops. The electrodes are oriented to provide constraint against six degrees of freedom and are insulated from each other and the metal base by a ceramic insulator. The gap between electrodes and proofmass is a nominal 0.002 inch and is maintained by the cylindrical shaped cage into which all six electrode assemblies are mounted. The cage assembly fits inside the hermetically sealed hexagon shaped housing, with the 12 electrode terminals exiting radially through both ends. The six preamplifiers are attached to the external housing flats to provide short direct connections to the internal electrode. The output of the preamplifiers is at a low impedance, high signal level for connection to the rest of the constraint loop electronics. The instrument case has three mounting pads which are used to attach it to the vehicle structure at which the input acceleration is to be measured. The instrument case is hermetically sealed and filled with a mixture of 90% dry nitrogen and 10% helium. The pressure is a nominal one atmosphere (15 psi in vacuum). This gas provides the viscous damping required for stable loop operation as well as protecting the proofmass during the unpowered high-g launch environment. The materials used have been selected for easy machining, matching temperature coefficients, and require no special plating or finishes. A small amount of radioactive material is located within the gap cavity to provide a means for removing any charge which might accumulate on the proofmass during the unpowered and initial phase at power turn-on.

### MESA SPECIFICATION

<u>Type:</u>	Three Axis - Cube Proofmass	<u>Ranges Available:</u>	3 from $10^{-2}$ to $10^{-6}$
<u>Size:</u>	3.5" x 5" x 9.5"	<u>Environment:</u>	
<u>Weight:</u>	6 lb	(Nonoperating)	
<u>Power:</u>	9 Watts	Temperature:	-25F to 185F
<u>Sensitivity:</u>	$10^{-10}$ g	Shock:	50 g, 8 msec, 3 axes
<u>± Full Scale:</u>	$10^{-6}$ g	Vibration:	Sine: 20 to 2000 cps 10 g's
(Lowest Range)			Random: 20 to 2000 cps 20 g's rms
<u>± Full Scale:</u>	$10^{-2}$ g	Acceleration:	Pyro: 6000 g's
(Highest Range)		Altitude:	15g, 3 axes
<u>Accuracy:</u>	0.5% of Full Scale	(Operating)	Space
(Worst Case)		Temperature:	-10F to +160F
<u>Output:</u>	± 8 Vdc = ± Full Scale	Altitude:	Space
	All Ranges	<u>Cost:</u>	Approx. \$100K

# DATA OUTPUT

The acceleration signal originates as a bipolar analog voltage at a point in the constraint loop just prior to amplification before being applied to the forcing electrodes. The levels at this point are normalized to  $\pm 8V$  dc representing  $\pm$  full scale output on all ranges. The resolution is determined by sample time, full scale A/D conversion frequency, and full scale constraint loop capability. The relationship between these variables is shown in the resolution graph on the next page. The example shown illustrates typical values which could be used. Example: Full scale constraint capability =  $\pm 10^{-4}$  g, Full scale A/D conversion =  $\pm 10$  kHz, Sample time = 100 sec. For these values the signal resolution in terms of 1 bit change per sample period would be  $10^{-10}$  g. The equation for resolution is:  $\Delta g = \{ [\text{full scale (g's)}] / [\text{full scale A/D (kHz)}] \} \times \{ 1 / [\text{sample time (sec)}] \}$ . The bidirectional counter capacity is also shown. The example would require 20 bits storage per sample period.



## AMMETER

### PURPOSE & REQUIREMENTS

To measure dc current to the heaters of the cells of the Pool Boiling Experiment, No. III.

Range:	0-35.4 amps
Interface:	CDMS

### HARDWARE STATUS

Simple electronic elements can be assembled to provide a voltage signal to the CDMS which is proportional to current.

### TECHNICAL DESCRIPTION

Weight:	0.05 kg (0.1 lb) (est.)
Size:	160 cm <sup>3</sup> (10 in <sup>3</sup> ) (est.)
Power:	0

### APPLICABLE EXPERIMENTS

Experiment No. III, Measurement I.

## BACK PRESSURE REGULATOR

### PURPOSE & REQUIREMENTS

To provide controlled pressure venting of gas from various experiments.

Pressure Range: 6.9 - 103.4 kN/m<sup>2</sup> (1-15 psia) (nominal)  
Accuracy: ( $\pm 0.35$  kN/m<sup>2</sup>) kN/m<sup>2</sup> ( $\pm 0.05$  psia)

### HARDWARE STATUS

Off-the-shelf hardware is available.

### TECHNICAL DESCRIPTION

Model: Kendal Model 10132 BP, Precision Back  
Pressure Regulator  
Weight: 0.68 kg (1.5 lb)  
Size: 7.6  $\times$  7.6  $\times$  15.2 cm (3  $\times$  3  $\times$  6 in.)  
Cost: \$50

### APPLICABLE EXPERIMENTS

<u>Experiment No.</u>	<u>Component No.</u>	<u>No. Req'd.</u>
II	BPR <sub>1</sub>	1
III	BPR <sub>1</sub>	1
IV	BPR <sub>1</sub>	1



MODEL 10BP



MODEL 10BP

## BACK PRESSURE REGULATION

### HIGH FLOW - HIGH SENSITIVITY

- **SENSITIVE BACK PRESSURE REGULATION.** The Kendall Model 10 BP can be set to  $\frac{1}{8}$  inch of water. Fast response to controlled system pressure changes results from high ratio of diaphragm area to valve seat area.
- **HIGH FLOW CAPACITY.** Flow of 40 scfm can be attained (depending on setpoint pressure and port size).
- **LARGE EXHAUST PORT.** Excessive system pressure is exhausted through the main control valve port, not a small, low capacity, relief port.
- **STANDARD COMPONENTS.** Service proven basic components from Kendall Model 10 pressure regulator are used in this instrument.
- **FLOW COMPENSATION.** Back pressure control is assisted by the compensating action of the venturi type velocity-pressure tube which adjusts valve opening in accordance with velocity — pressure variations of the flow from the controlled system.
- **SIMPLIFIED MAINTENANCE.** Unit construction eases servicing. Regulator can be serviced and maintained without removing it from the line. There are no fine restrictions to be kept clean.

FOR TOTAL CONTROL...  
WHEN THE PRESSURE'S ON



**FAIRCHILD**  
INDUSTRIAL PRODUCTS DIVISION

1501 FAIRCHILD DRIVE, WINSTON-SALEM, N. C. 27105  
Tel. 919-757-6010 Telex-90-6429



## BLOWER, AIR

### PURPOSE AND REQUIREMENTS

To provide air flow for Experiment I, Flow Patterns and Pressure Drop

Pressure Output:	27.6 kN/m <sup>2</sup>
Flow:	0.85-453 lpm (0.03-16 cfm) at 1 atm & 30C (86F)
Power Input:	28 watt dc or 115/200 volt 400 Hz

### HARDWARE STATUS

Off-the-shelf hardware with minor modifications can be used.

### TECHNICAL DESCRIPTION

<u>Blower:</u> Model:	Airborne Mfg. Co. Model 441CC
Type:	Sliding Carbon Vane
Weight:	14. kg (3.1 lb)
Size:	10.5 cm dia × 16.1 cm long (4.12 in. dia × 6.35 in. long)

Blower Motor/Controller: The variable speed motor which was used by Convair during the aircraft flight testing of fluids in zero-g, Ref. 2-2, was a Minarik permanent magnet motor. This motor was easily modified to operate on 400 Hz power. Such a motor should be suitable for driving the blower. The motor below has a maximum speed of 2400 rpm which is marginal for the high flow, high quality test run of Experiment I. If higher speed blower operation is required, a slight increase could be provided with a small gear box.

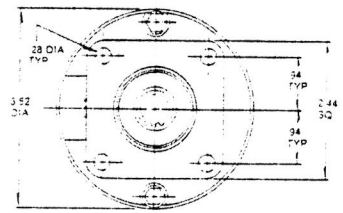
Motor P/N :	504-36-140
Speed Range:	30-2400 rpm
Power:	746 watts
Weight:	15.4 kg (34 lb)
Size:	38.7 × 17.8 × 17.8 cm (15 × 7 × 7 in.)
Cost:	\$230

Speed Controller No.:	N 280
Weight:	2.15 kg (4.75 lb)
Size:	7.6 × 11.4 × 25.4 cm (3 × 4.5 × 10 in)
Power:	230 volt input, 0-180 volt output, 9 amp output
Cost:	\$184

### EXPERIMENT APPLICATION

Experiment I

# dry air pumps vacuum/pressure positive displacement, engine driven



The complete Airborne line of light-weight dry air pumps originally was developed for gyro instrument, deice, and cabin pressurization systems of today's light aircraft industry. This quality line of pumps is now the standard of the entire light aircraft industry, supplying some 95 per cent of its needs.

Airborne dry air pumps utilize the inherent dry lubrication of their carbon rotors and vanes. They require no messy lubrication nor oil separation systems, ever. Constructed of tough, lightweight aluminum, all are of aircraft quality, but are price-competitive in the industrial market.

The innovation, experience, and technical excellence reflected in Airborne dry air pumps is now recognized and approved in broad industrial classifications.

#### Four basic sizes are available:

Low capacity pumps weighing as little as 1.8 pounds deliver 10 CFM at 6 in. Hg. vacuum or pressure at 3500 RPM. Maximum load is 5.5 PSI or 11" Hg. vacuum.

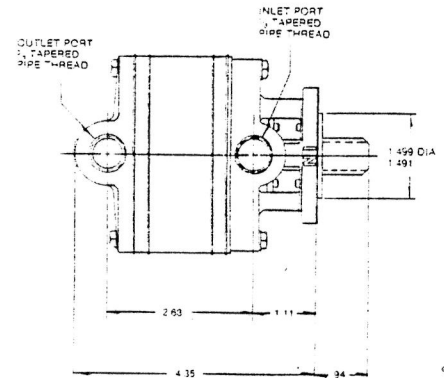
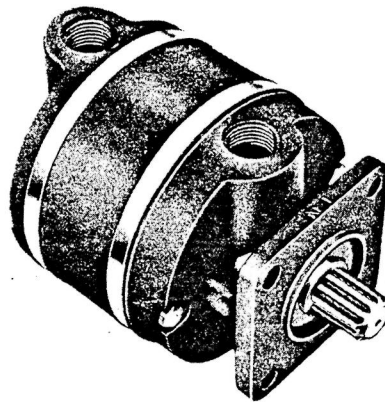
Low capacity, higher pressure units, weighing 2.3 pounds, contain cooling fins and deliver 12 CFM at 11 PSIG and 3750 RPM.

Medium capacity units, weighing 3.1 pounds, deliver 21 CFM at 11 PSIG and 3750 RPM.

High capacity pumps, weighing 6.5 pounds, deliver 47 CFM at 11 PSIG and 3500 RPM.

Maximum continuous pressure for any pump with cooling fins is 12.5 PSIG while intermittent pressures up to 22 PSIG are acceptable. Maximum allowable discharge air temperature is 375°F. Maximum continuous speed 4,000 RPM. Maximum intermittent speed is 5,000 RPM.

Whatever your problem, your need, your application, you can rely upon Airborne technical development know-how. To assist you, Airborne maintains a professional design staff, thoroughly knowledgeable in the needs of industry. Our creative staff is supported by modern, fully equipped development laboratories to conceive, design, develop, test and manufacture more reliable and less expensive products.



## Models 211CC/211CC-9/212CW/212CW-6

Ideal for gyros-only applications on normally-aspirated and turbocharged aircraft. Ultra-light, rugged construction assures excellent performance and service life.

#### Pressure Systems -

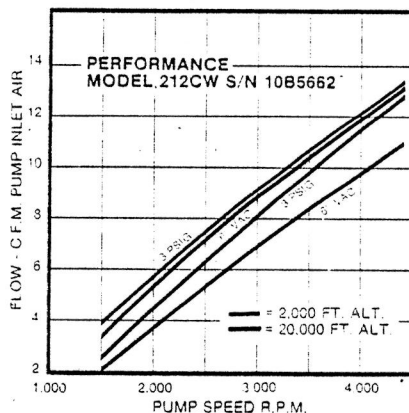
Two gyros and optional low pressure pneumatic autopilot normally operating at 2.5-5.0 PSI (5"-10" Hg.) at gage. (Pressure systems are especially recommended for turbo-charged aircraft.)

#### Vacuum Systems -

Two gyros and optional low pressure vacuum autopilot operating at 5"-8" Hg.

#### Maximum Recommended Operating Cruise Altitude

Model	Vacuum Pressure
211CC/211CC-9	15,000 ft. 24,000 ft.
212CW/212CW-6	15,000 ft. 24,000 ft.



**Model 211CC** — Counterclockwise rotation as viewed looking at the engine pad.

**Model 212CW** — Clockwise rotation as viewed looking at the engine pad.

**Model 211CC-9** — Vertical mount-counter-clockwise rotation as viewed looking up the engine pad.

- Weight ..... 1.8 lbs
- Overhang Moment ..... 3.7 lb.-in.
- Mounting Pad ..... AND 20000
- Typical Pump Torque
- 3000 RPM and 5" Hg. Suction Load ..... 9 lb.-in.
- 4000 RPM and 10" Hg. Suction Load ..... 12 lb.-in.
- Maximum Continuous Suction Pressure (to 15,000 ft.) ..... 11 in. Hg.V
- Maximum Continuous Discharge Pressure (to 24,000 ft.) ..... 5.5 psig
- Maximum Continuous Total Pressure ..... 5.5 psi
- Maximum Static Shear Torque of Coupling ..... 250 lb.-in.
- Maximum Continuous Allowable Exhaust Air Temperature ..... 300 Degrees F.
- Maximum Ambient Air Temperature ..... 200 Degrees F
- Dew Point Limit Based on 80% Allowable Wear at 1,000 Hrs. 8" Hg. 10,000 Feet ..... -70 Degrees F
- Maximum Speed — Continuous 4,000 RPM.
- Maximum Speed — Intermittent 5,000 RPM.

Typical Speed at which 4" Hg vacuum or pressure is obtained with 2 gyros (4 SCFM) ..... 1500 RPM



# Application Chart

For Best System Performance and Extended Pump Life . . . Follow These Recommendations  
 Select the Airborne pump compatible with your aircraft system's performance requirements.  
 Consult Airborne for specific applications.

PUMP MODEL NO.	CONSTRUCTION	CRUISE RPM	MAXIMUM CONTINUOUS ΔP AT PUMP (PSI)	NORMAL CRUISING ALTITUDE UP TO (Vacuum—Pressure)	SYSTEM FLOW LIMIT (INLET CFM)	SPECIAL CONSIDERATIONS
211 & 212 211CC-9	Fixed End Plate No Fins	3,000-3,500	5.5	18,000 24,000	7	Gyros only
241 & 242	Finned Floating End Plate	3,000-3,500	11.0	22,000 30,000	7	Gyros high pressure auto-pilots. Door seals
441 & 442	Finned Floating End Plate	3,000-3,500	11.0	22,000 30,000	14	Gyros high pressure autopilots Deice boots. Door seals.
841 & 842	Finned Floating End Plate	2,600-2,800	8.0	22,000 30,000	33	For cabin pressurization deice boots, pressure auto-pilots, gyros, door seals

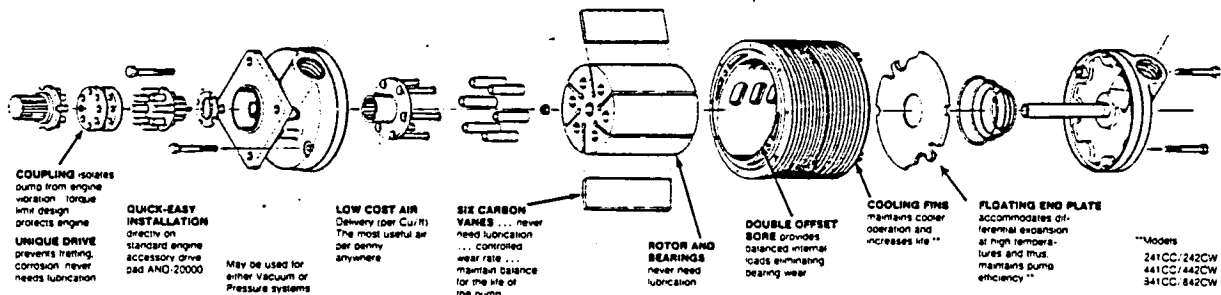
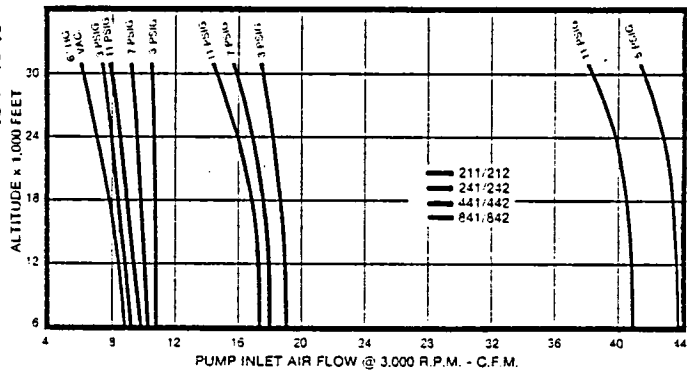
## Designing the system

1. Determine pneumatic load in CFM.
2. Determine maximum continuous differential pressure required at the pump.
3. Determine altitude requirements.
4. Determine pad speed and pump RPM.
5. Use Application Chart to select pump which meets all requirements.
6. Select system components and line sizes for low pressure drop and flat regulation.
7. Provide protection from foreign materials for pumps, gyros and servo mechanisms.
8. Provide blast cooling for pumps operating above 6 psi ΔP across the pump.
9. "Breadboard" the system to determine that performance pressure demands are within design goals or ask Airborne to do it for you.
10. Call Airborne . . . benefit from our experience.

## Comparative operating characteristics of

Mod.

211/212  
241/242  
441/442  
841/842



Dry air pumps are a product of Airborne innovation: a continuous, independently-motivated program dedicated to anticipating and solving the problems of aircraft functional systems as operational demands increase.

Relying heavily upon original technical development, Airborne maintains a large design staff, thoroughly knowledgeable in the needs of general aviation. They are supported by one of the industry's finest development laboratories to conceive, design, develop, test and manufacture more reliable and less expensive pneumatic and fuel system components for general aviation.

Airborne's ability to comprehend industry problems and conceive practical solutions is confirmed by all leading airframe manufacturers who are using Airborne components as original equipment.

Airborne has established a world-wide network of authorized distributors capable of providing technical information and product support.

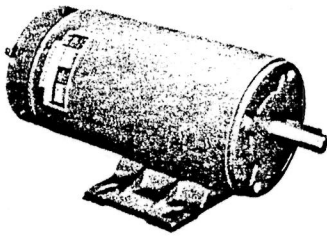
In North America, exchange programs provide rapid, low-cost service. Factory-approved overhaul facilities have been established in other parts of the world.

M  
 Fc  
 of  
 up  
 alt  
 eit  
 ar  
 pr  
 Th  
 hc  
 pt  
 in  
 A.  
 wt  
 to  
 mi  
 Sa  
 C:  
 24  
 M  
 Ci  
 pe

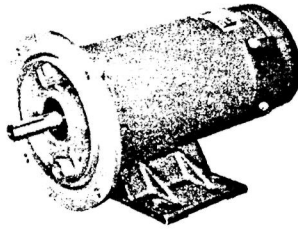
FLOW CFM PUMP INLET AIR

## BLUE CHIP II MOTORS

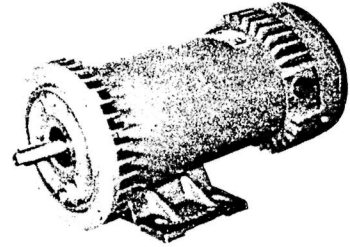
Blue Chip II Motors recognized under the Component Program  
of Underwriters' Laboratories, Inc., File Number E64416.



48X TENV



56CB TENV  
56CB24 TENV



56CB TENV  
56CB24 TENV

### BLUE CHIP II MOTORS <sup>PM TYPE</sup> 90 VDC for use with BLUE CHIP II CONTROLS 115 VAC, 50/60 HERTZ INPUT

SPEED RANGE RPM	TORQUE IN POUND INCHES	HP	MINARIK MOTOR TYPE/FRAME NUMBER <sup>1</sup>	TYPE OF ENCLOSURE	DIM DRWG. <sup>2</sup>	MINARIK STOCK NUMBER	CONTROL MODEL NUMBERS
30-1800	8.75	1/4	1/4 48X	TENV	A3	504-06-006	
30-1800	8.75		1/4 56CB	TENV	B3	504-06-027	
30-1800	8.75		1/4 56CB(XP)	EXPLOSION PROOF	C3	504-06-032	
30-2400	6.56		1/4 56CB24	TENV	B3	504-06-036	
30-1800	11.69	1/3	1/3 48X	TENV	A3	504-06-010	
30-1800	11.69		1/3 56CB	TENV	B3	504-06-028	BC90
30-2400	8.75		1/3 56CB24	TENV	B3	504-06-037	BC90UD4
30-1800	17.5	1/2	1/2 48X	TENV	A3	504-06-014	BCR90
30-1800	17.5		1/2 56CB	TENV	B3	504-06-029	N80
30-1800	17.5		1/2 56CB(XP)	EXPLOSION PROOF	C3	504-06-033	NR80
30-2400	13.13		1/2 56CB24	TENV	B3	504-06-038	
30-1800	26.25		3/4	3/4 56CB	TEFC	F3	504-06-030
30-1800	26.25	3/4 56CB		ODP	D3	504-06-018	
30-2400	19.69	3/4 56CB24		TEFC	F3	504-06-039	

### BLUE CHIP II MOTORS <sup>PM TYPE</sup> 180 VDC for use with BLUE CHIP II CONTROLS 230 VAC, 50/60 HERTZ INPUT

30-1800	17.5	1/2	1/2 56CB	TENV	B3	504-36-029	
30-2400	13.13		1/2 56CB24	TENV	B3	504-36-038	BC290
30-1800	26.25	3/4	3/4 56CB	TENV	E3	504-36-035	BC290UD4
30-2400	19.69		3/4 56CB24	TEFC	F3	504-36-039	BCR290
30-1800	35.0	1	1 56CB	TEFC	G3	504-36-131	N280
30-2400	26.25		1 56CB24	TEFC	G3	504-36-140	NR280
30-1800	52.0	1 1/2	1 1/2 56CBPM	TEFC	G3	504-36-041	

<sup>1</sup> All 56CB and 56CB24 motors are NEMA-56 C-faced with removable bases. If 56CB(XP) motors are NEMA C-faced with welded bases, Class 1, Groups C and D. All 48X motors are NEMA 48 base dimensions but have 5/8" diameter shafts.

<sup>2</sup> Motor dimensions and weights are pages 34 and 35.

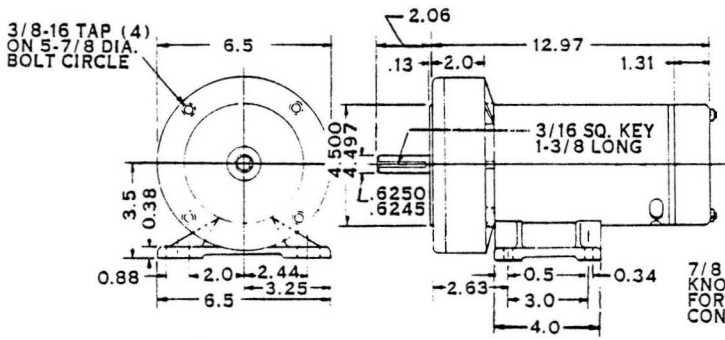
NOTE:— For extra cool running motors use the "SLF" Series of filtered controls shown on page 63.

300

# Blue Chip II

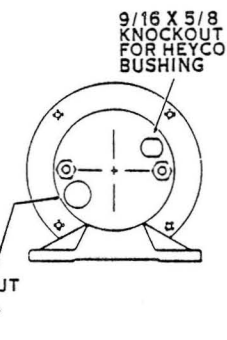
## MOTOR DIMENSIONS

3/4 through 1 1/2 HP

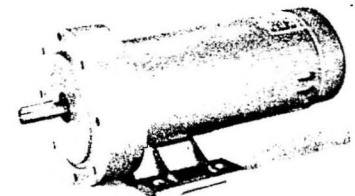


DRAWING "DS"

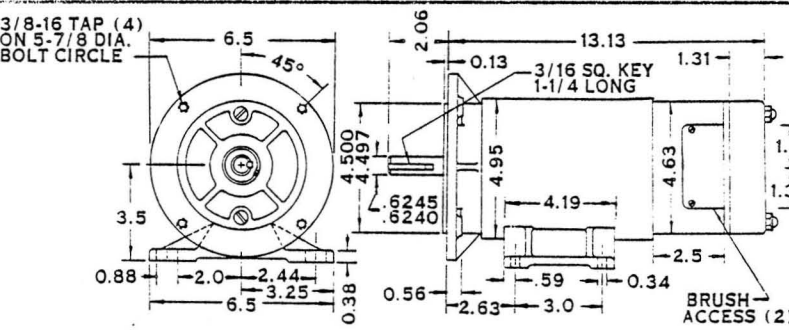
ALL DIMENSIONS IN INCHES



530B FRAME  
1 1/2 HP OPEN DRIP PROOF  
Permanent Magnet

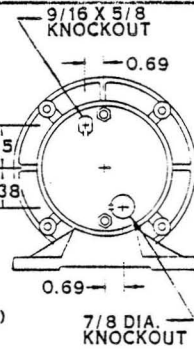


Approximate Shipping Weight = 24 pounds

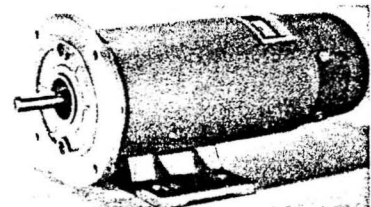


DRAWING "EM"

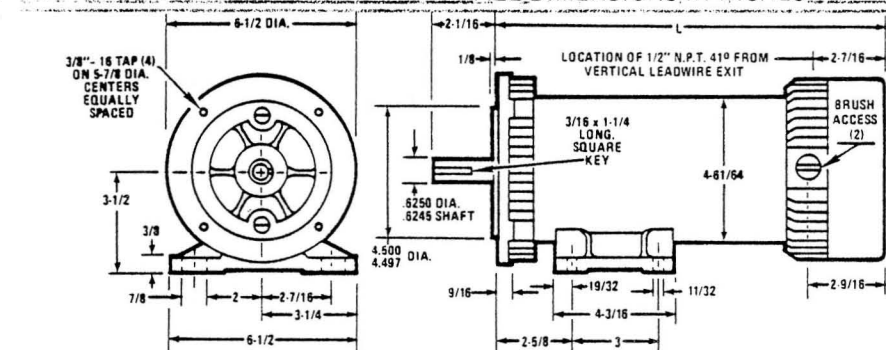
ALL DIMENSIONS IN INCHES



530B FRAME  
1 HP TENV  
Permanent Magnet



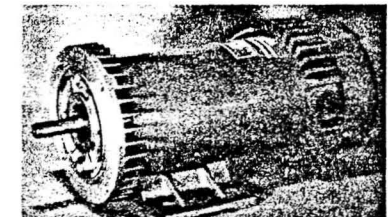
Approximate Shipping Weight = 30 pounds



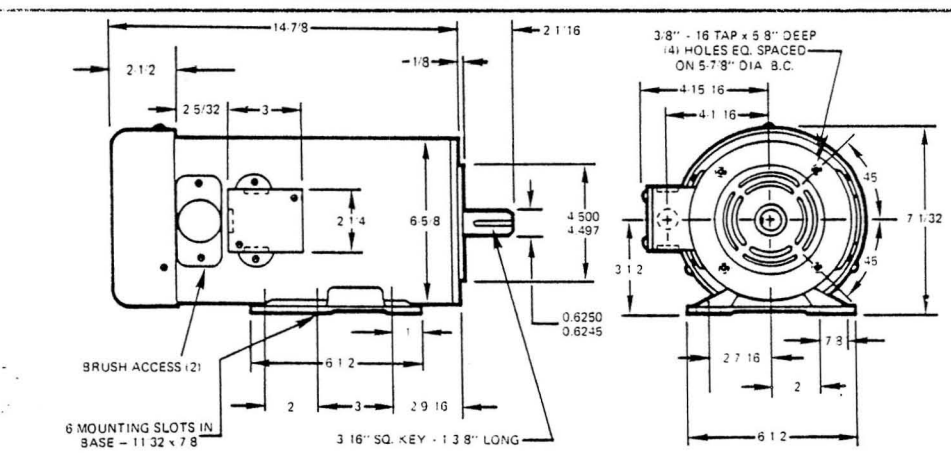
DRAWING "FS"

ALL DIMENSIONS IN INCHES

530B FRAME  
1 HP TENV  
Permanent Magnet



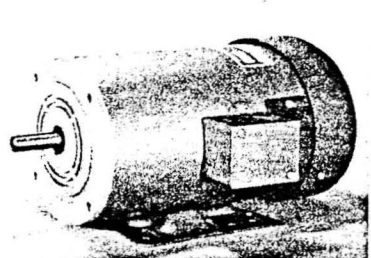
Approximate Shipping Weight = 30 pounds



DRAWING "GS"

ALL DIMENSIONS IN INCHES

530B FRAME  
1 and 1 1/2 HP TEFC  
Permanent Magnet



HP	L	APPROX. SHIP WT.
1	11.88	34 lbs
1 1/2	14.88	61 lbs

300

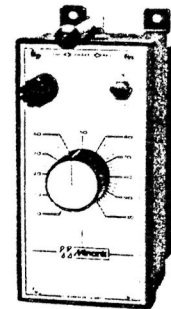
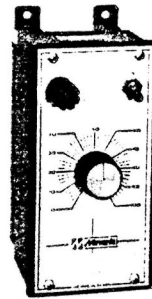
**"N" and "NR" CASED MODEL "SEALED" ADJUSTABLE SPEED CONTROLS for PM MOTORS**

**FEATURES**

- › TEMPERATURE COMPENSATION
- › LINE VOLTAGE COMPENSATION
- › LINE STARTING and STOPPING
- › ADJUSTABLE MAXIMUM SPEED
- › ADJUSTABLE MINIMUM SPEED
- › ADJUSTABLE IR COMPENSATION
- › ADJUSTABLE CURRENT LIMITING
  - › 2% REGULATION TYPICAL
- › SMOOTH MOTOR ACCELERATION
- › FULL WAVE ARMATURE SUPPLY

**SPECIFICATIONS**

Controls include speed knob, Off-On power switch and external fuse post with fuse. Reversible models also have Forward/Dynamic Brake/Reverse lever actuated switch. Case is 16 gauge steel, totally enclosed, constructed and gasketed similar to NEMA 4 and 12 to seal out dust, moisture and oil.



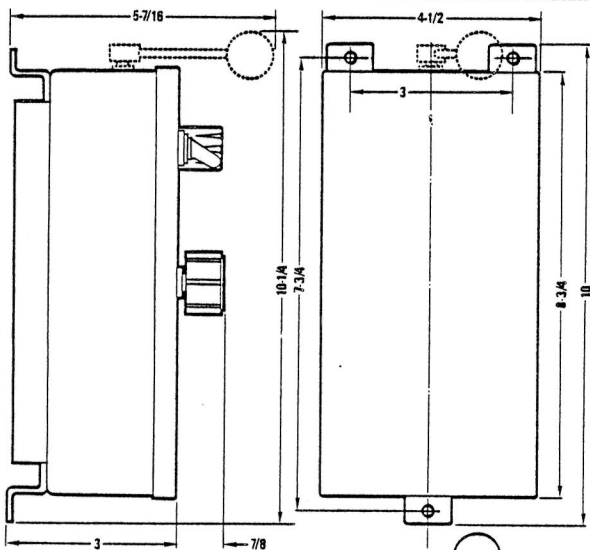
**UNIDIRECTIONAL MODELS**  
N80 and N280  
Approximate Shipping Weight . 4.75 pounds

**REVERSIBLE MODELS**  
NR80 and NR280  
Approximate Shipping Weight .. 5.0 pounds

MODEL NUMBER	UNI-DIRECTIONAL	REVER-SIBLE	MOTOR HP	INPUT 50/60 HERTZ	OUTPUT ARMATURE
N80		NR80	¼ thru ¾	115 VAC	0-90 VDC @ 9 amps max
N280		NR280	½ thru 1½	230 VAC	0-180 VDC @ 9 amps max

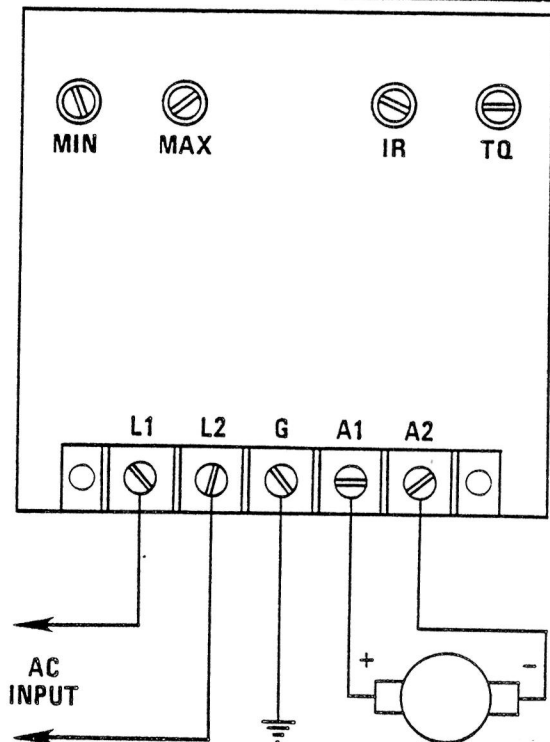
Motors for these controls are listed on page 29.

**"N" and "NR" CASED MODEL DIMENSIONS and CONNECTION DIAGRAM**



NOTE: DOTTED LINE SHOWING FWD-BRK-REV HANDLE ON NR80 and NR280 MODELS ONLY

2 each 7/8" CONDUIT KNOCKOUTS ON BOTTOM OF CASE



## CONTROLLER, HEATER

### PURPOSE & REQUIREMENTS

To control the temperatures of the test cells of the Pool Boiling Experiment, No. III, while they are in the standby mode. One of the fluid thermocouples of each cell was assumed to be used for the signal to the heater controller.

Control Mode:	On/Off
Accuracy:	$\pm 1.1\text{C}$ ( $\pm 2\text{F}$ )

### HARDWARE STATUS

A number of off-the-shelf T.C. controllers exist but these units would generally require modification to minimize weight and size requirements. A typical controller is shown in the attached catalog sheet and includes cold junction compensation, a set point adjustment control, and a read-out. Since the Pool Boiling experiment set point temperatures will be predetermined, the set point adjustment would not be required. Also, although 12 controllers are required, simultaneous temperature read-out is not. For the above reasons, specially built controllers are recommended. They would take thermocouple readings as corrected by a reference cold junction and provide on-off power control to the standby heaters.

### TECHNICAL DESCRIPTION

#### Reference Junction

Model:	Omega OM 101 Reference Junction modified for 12 rather than 10 T.C. channels
Weight:	0.45 kg (1 lb)
Size:	15.5×8.1×3.0 cm (6.1×3.2×1.2 in.)
Power:	0.5 watts, 28 volt dc ( $\pm 14$ volt dc)
Cost:	\$500

#### Solid State Controllers (specially built)

Weight:	0.23 kg (0.5 lb) (est.)
Volume:	164 cm <sup>3</sup> (10 in <sup>3</sup> ) (est.)
Power:	1 watt (est.)
Cost:	\$200 ea. (est.)

CONTROLLER, HEATER (Cont'd)

APPLICABLE EXPERIMENT

One reference junction and 12 controllers required for Pool Boiling Experiment,  
No. III:



# **NEW!** Digital Controllers

**\$215 and up**

## **Features:**

- J or K Thermocouples
- Accuracy:  $\pm 0.4\%$  Full Scale
- 1° Resolution
- Adjustable Proportional Band or On-Off
- Single and Dual Set Point Models
- Relay, Triac or 4-20 ma Output
- 1/4 DIN Metal Case
- Full Plug-In Construction

Sensor Type	Material Type	Range	Resolution	Number of Set Points	Model	Price
J	Iron/Constantan (Iron vs Copper-Nickel)	0 to 999° F 0 to 500° C	1°F 1°C	Single	4001JF 4001JC	\$215
		0 to 999° F 0 to 500° C	1°F 1°C	Dual	4002JF 4002JC	\$260
K	Chromel/Alumel (Nickel/Chromium vs Nickel/Aluminum)	0 to 1990° F 0 to 999° C	1°F 1°C	Single	4001KF 4001KC	\$215
		0 to 1999° F 0 to 999° C	1°F 1°C	Dual	4002KF 4002KC	\$260

### RTD

Platinum RTD  
 $\alpha = .00385 \text{ ohms/ohm/}^\circ\text{C}$

To be available early 1979, please consult factory for price and delivery.

#### General:

The Omega 4000 series digital controller distinguishes itself by features, construction and operation one would expect to find only in controller costing much, much more. Bright, easy to read, LED digits yield an unambiguous temperature indication which is not achievable with an analog controller. The standard unit includes adjustable proportional band, manual reset, plus a metal case with full plug-in construction allowing front removal of the entire control unit without disturbing the case and its rear wiring. Series 4000 Controllers are available in single and dual set-point models with relay outputs as a standard. Triac or 4-20 ma optional outputs are offered on the first point at no additional cost. Models 4001 and 4002 lend themselves to a broad spectrum of control applications: single point control, dual set-point control, and single point control with either high or low limit alarm. Truly a quality built controller at a remarkably low price.

#### Model 4001 Single Set-Point Proportional and On-Off Controller **\$215**

This versatile digital controller can be operated both as a proportional or on-off controller. Set the adjustable band width at up to 5% of full scale and it's a proportional controller. With the band width adjustment set fully counter clockwise, it's a "on-off" controller. The set-point temperature is always available. Simply push the spring loaded set-point switch to the right and the set-point is digitally displayed. To change the set point, with the switch deflected to the right, adjust the knob to the right of the switch until you get the desired reading. The standard Model 4001 has an internal SPDT relay (7 amp resistive at 120 VAC). This model is also available with optional Triac or 4-20 ma output in place of the relay. These options are covered in the Option and Specification sections.

#### Model 4002 Dual Set-Point Controller **\$260**

The first set-point of the Model 4002 incorporates the same features as the Model 4001 and also can be ordered with the optional Triac or 4-20 ma output. The second set-point may be set at any value within the full span of the controller. It energizes the SPDT internal relay (3 amp resistive 120 VAC) which can be used as either an on-off control, a high limit alarm, or a low limit alarm. For an alarm with latching features an external latching relay and push button to reset are suggested. The second set-point is set and displayed using the same procedure as for the Model 4001 except the switch is deflected to the left and the left adjustment knob is used.

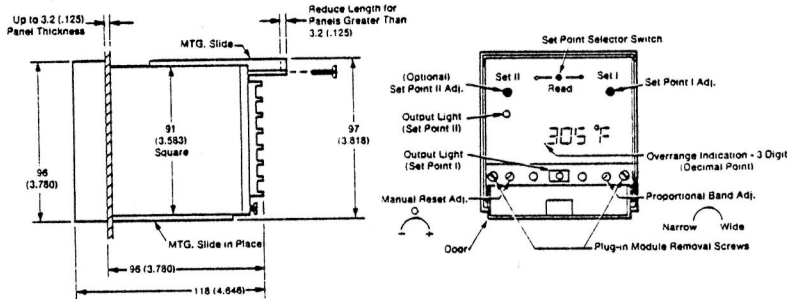
#### Option "T" Triac Output No Additional Charge.

Option "T" replaces the relay output on the first set point with a solid state plug-in Triac which yields time proportional, or on-off switching. The Triac is rated at 2 amps continuous and 10 amps in rush for both 120/240 VAC service. For higher amperage loads the Triac may be used to drive higher rating solid state relays or mechanical contractors. Specify "Option T" after the model number when ordering.

#### Option "F" (4-20 ma Output) No Additional Charge.

This option is applicable to the first set point only and is used to drive proportioning devices such as SCR power controller, motor positioners or electropneumatic actuators. The 4-20 ma DC output signal can be connected to a maximum of 1000 ohm resistance load. This signal is 20 ma at the low temperature end of the proportional band and is decreased linearly thru the band to 4 ma at the high temperature end. If the driven device is not isolated (ungrounded) an ungrounded thermocouple must be used with the Series 4000 which is designed for only one ground in the system. When ordering call out "Option F" after the model number.

# Specifications



Thermocouples .....	Type "J" & "K"
Max. T/C lead resistance .....	100 ohm for rated accuracy
Cold junction compensation .....	Automatic — electric
T/C Break protection .....	Built in, upscale on open sensor
Calibration Accuracy .....	±0.4% of span over 10 to 90% of range
Common mode rejection .....	Max error ± 1°C with 240V, 60Hz applied as common mode signal between sensor input and chassis ground.
Series mode rejection .....	Max error ± 1° with series mode signal of 100 MV PK-to-PK at 60 Hz

### 1st. Set-Point (Adjustable time proportional or on-off)

Relay (Standard Model) .....	SPDT relay 7 amps resistive at 120 VAC, 5 amps resistive at 240 VAC
Option "T" (Triac) .....	Solid state plug-in triac rated 2 amp holding and 10 amps in-rush
Option "F" (Current Proportional) .....	4-20 ma (DC) into 1000 ohm max

### 2nd. set point

Relay (on-off only) .....	SPDT, rated 3 amps at 120 VAC
---------------------------	-------------------------------

Proportional Band (gain) .....	0-5% of span
Manual Reset (off-set) .....	Adjustable
Cycle time .....	Automatically adjusts with band adjustment to give least wear with minimum ripple (10 sec. minimum total time).

Temperature .....	Filtered LED, 3 or 3½ digits, 2 reading per second update. Readability is 1°F or 1°C.
Set-Point .....	By spring loaded switch, 1st or 2nd set-point is displayed in place of temperature. Set-Point adjusted by 25 turn pot. .1°F or 1°C Setability
Outputs .....	LED indication for both 1st and 2nd set-points. LED are "on" when output drive signal present. "On-off" indication on relay and triac model. Proportional intensity for option "F".
Temperature overrange .....	Red LED indication.

Resolution .....	1°F or 1°C
Repeatability .....	±0.1% to ±0.2% of span
Adjustment .....	By 25 turn pot. See "Set Point" under "Display and Indication" section.
Power .....	120/240 VAC (+10%, -15%), 50/60 Hz. Power consumption less than 5 watts.

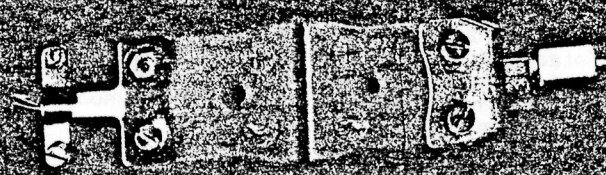
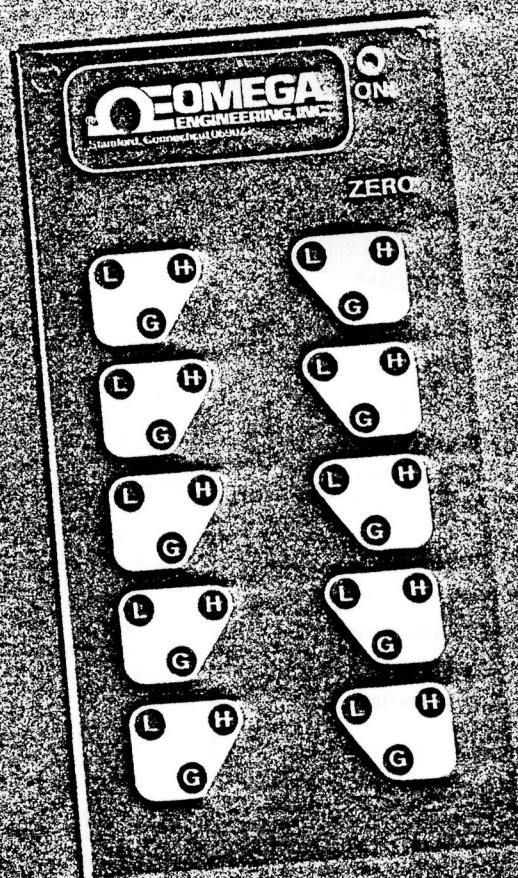
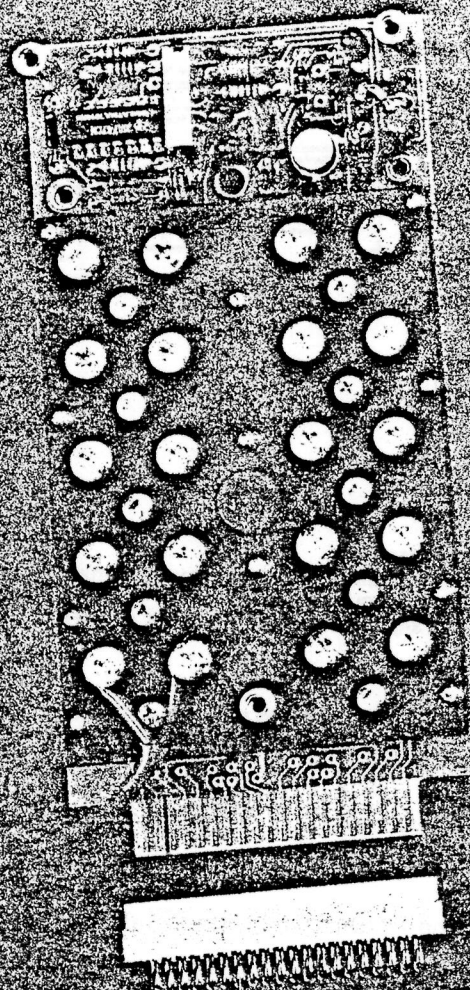
Operating temperature .....	30-130°F
Weight .....	2 lb.
¼ DIN Case .....	Metal, full plug in, with screw terminal on rear. Adjustable brackets for panel mounting. Panel cut out is 3.622" vertical and horizontal dimensions.

### Discount Schedule:

1 to 4 units .....	Net	11 to 24 units ..	10%	50 plus units ...	15%
5 to 10 units .....	5%	25 to 49 units ..	12%		

# A modular software solution to thermocouple termination

**\$395**

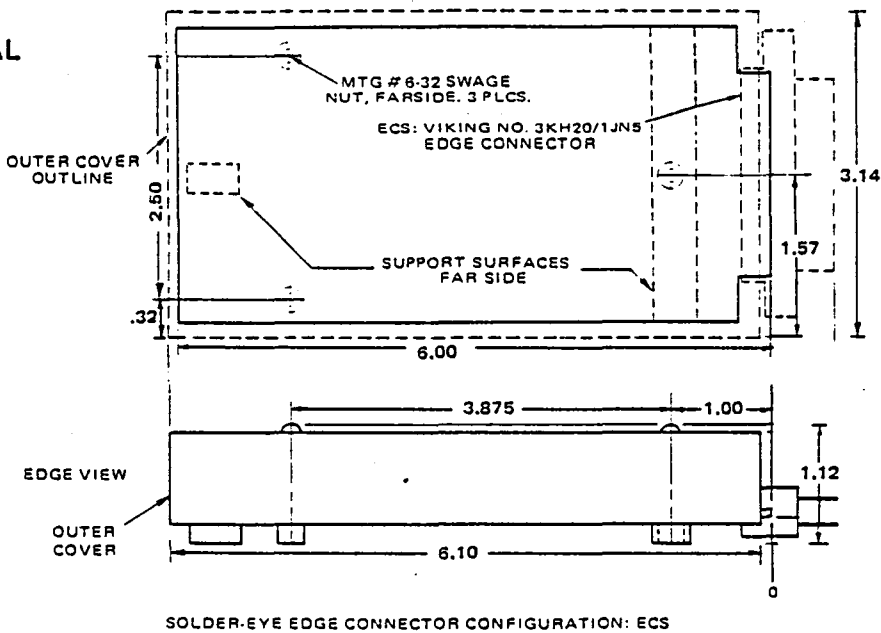


## The OM101 Ten-Channel Modular Reference Junction

- Ideal for use with microprocessor and data acquisition modules
- Any wire type with any tolerance coefficients
- Normalization built-in
- Thermocouple terminals with fused terminals
- Precision electronic parameter assembly, never needs calibration

**NEW!**

## OM101 MECHANICAL OUTLINES



## PERFORMANCE SPECIFICATION

### 1. FUNCTIONAL

- 1.1 **Compensation Method:** Entirely self-contained precision electronic thermometer measures temperature of an isothermal ambient tracking terminal assembly and provides the temperature at 1 mV per Celsius.
- 1.2 **Channels:** 10, numbered "0" through "9" in "HI" "LO" pairs, with separate guard terminals for each pair.
- 1.3 **Wire Types Available:** Software coefficients furnished for compensation for any standard wire type.
- 1.4 **Calibration and Adjustments:** Thermometer sensitivity is calibrated by OMEGA and sealed for life. Zero adjustment through cover provided for customer convenience.
- 1.5 **Options:** Choice of output connections (Item 3.4).
- 1.6 **Reliability:** Rated at 200,000 hours (23 years) MTBF based on MIL-HDBK 217B and GIDER tables. Burn-in at 50C for 50 hours cycle aging for stability.

### 2. MECHANICAL

- 2.1 **Protection:** Heavy duty cover stagnates air and provides mechanical protection.
- 2.2 **Overall Dimensions:** (±.02") With cover and edge connector: 3.0" W x 6.00" L x 1.00" H.
- 2.3 **Thermocouple Wire Attachment:** Heavy duty terminal posts and thermoelectrically matched No. 6-32 trusshead screws accommodate up to No. 14 AWG thermocouple wire.
- 2.4 **Mechanical Mounting:** Three No. 6-32 screws engage matching swage nuts which are integral to the module body.

2.5 **Weight:** Approximately 1 lb. with cover.

### 3. ELECTRICAL/THERMAL

- 3.1 **Output Sensitivity:** 1 millivolt change per 1 Celsius change in temperature of the isothermal transition to copper.
- 3.2 **Compensation Error:** Within or equal to  $\pm 0.1C/C$   $\pm 1C$  about a midpoint of  $25C \pm 20C$ .
- 3.3 **Compensation Stability:** Aged, premium-grade silicon sensor produces long-term stability within  $0.01C/C$  per year.
- 3.4 **Zero Adjustment:** 60 millivolts overall;  $\pm 20$  turns. Factory set to  $2C$  or better; customer adjustable.
- 3.5 **System Connections:** Options: solder-eye edge connector for wires or ribbon edge connector for ribbon cable.
- 3.6 **Output Impedance:** Less than 900 ohms. Short circuit and overvoltage protected.
- 3.7 **Line Regulation:** Within  $0.3C/volt$  relative to D.C. supply voltages.
- 3.8 **Power Requirements:**  $+14$  to  $+16$  volts, 19 mA max;  $-14$  to  $-16$  volts, 20 mA max.
- 3.9 **Indication of Operation:** Red light-emitting diode (LED) integral with thermometer circuit.
- 3.10 **Isothermal Uniformity:** With cover installed,  $1C$  channel-to-channel,  $2C$  any channel to sensor.
- 3.11 **Dielectric Isolation:** 1000 Megohms at 310 volts peak channel-to-channel or channel-to-compensator.
- 3.12 **Ambient Ranges:** Operating:  $0C$  to  $70C$ ; storage:  $-65C$  to  $+155C$ . Relative humidity to 95%.

Each unit is tested across a wide ambient range from  $5C$  to  $45C$  and the thermometer is adjusted and permanently sealed to the above specification. A calibration certificate traceable to NBS is furnished with each unit.

#### NOTE:

When ordering your OM101, do not wish to select certain connector options, i.e. solder-eye edge connector, ribbon edge connector, or ribbon cable. Consult factory for correct connector selection before ordering.

**NEW!**

## WHAT IT DOES

The OM101 Reference Junction is a precision isothermal thermometer which provides temperature information on 10 thermocouple wire termination pairs. Using this information, your computer can universally compensate any thermocouple wire type or mixture of types.

All experienced system designers have painfully learned software techniques for the compensation of thermocouple leads require much more than a 100 ppm temperature sensor located in the general vicinity of a plastic barrier block. Shielding the terminations in a chamber not susceptible to conduction, convection, or direct heat fluxes flowing in the wires, and entrance or exit of the bare instrument can easily produce 2 to 3 Celsius temperature differences at the lead termination.

Super thermocouple thermometry requires an accurate, highly linear, fine scale thermometer bonded to a carefully designed thermal shield capable of virtually eliminating these temperature differences.

The OM101 isothermal assembly and electronic thermometry

are combined in a single package and the factory adjustments are sealed for life. Only a zero adjustment is provided as a convenience. Compensation for different wire types is achieved by software coefficients stored in computer memory. OMEGA provides all coefficients and the unit comes ready to bolt directly to your data logger rear panel, or rack. You have a choice of edge connectors ( solder eye or ribbon cable).

Thermocouple connection is easy. Attach your wires (diameters up to No. 14 AWG) to the large binding posts using the provided brass head screws. You'll also find an extra terminal at each channel for shields or guards. They include the entire assembly within the rugged guard cover, and you're ready to operate.

The OM301 is a compact module (EIA 314) and it means you can fit 60 channels (i.e. 15 modules) laterally across a standard 19" rack slot, with an inch or more remaining. The OM101 requires less than 500 milliwatts of roughly regulated power. Compare this to the notorious and inefficient compensation at around 100 watts!

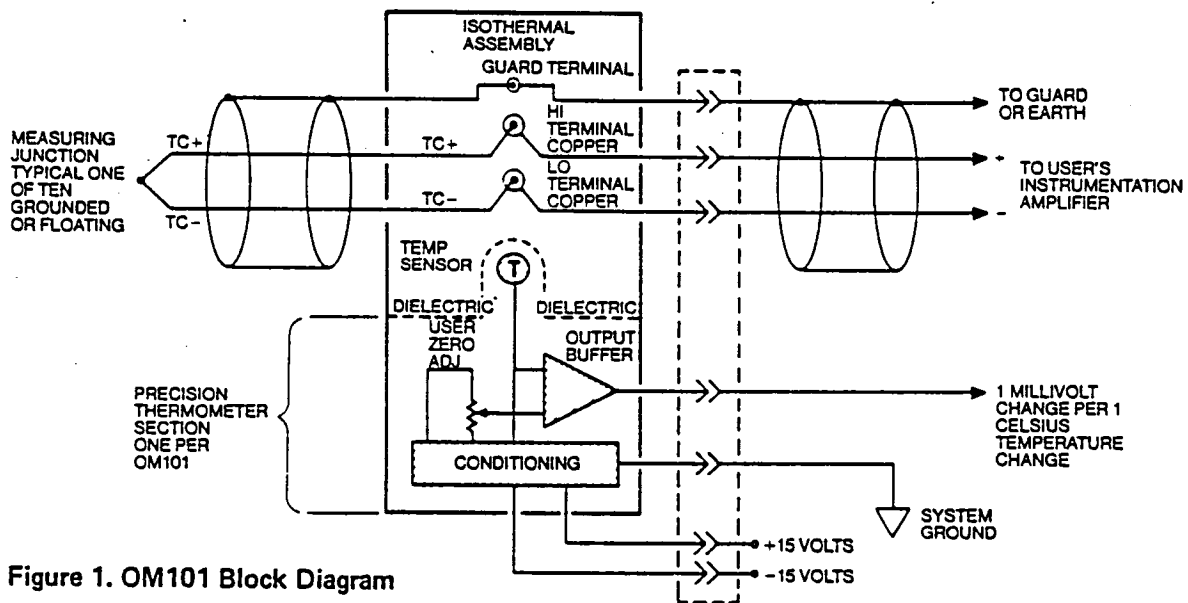


Figure 1. OM101 Block Diagram

## HOW IT DOES IT ...

Every OMEGA reference junction is an electronic design combined with a thermal one (Fig. 1). An aged silicon temperature sensor which is electrically isolated from all thermocouple terminals, but thermally coupled to them, senses the instantaneous temperature of a carefully configured isothermal assembly and

through a signal conditioner produces a precision 1mV/C output signal. The silicon sensor has a long-term stability which rivals platinum and a linearity exceeding that of platinum. A user zero adjustment is provided as a convenience.



DIFFERENTIAL PRESSURE TRANSDUCER (Cont'd)

APPLICABLE EXPERIMENTS

<u>Experi- ment No.</u>	<u>Measurement No.</u>	<u>Number Required</u>	
		<u>Xducer</u>	<u>Power Supply</u>
I & II	$\Delta P_{1A} - \Delta P_{4A}$ 0-0.34 kN/m <sup>2</sup> diff (0-0.05 psid)	4	4
I & II	$\Delta P_{1B} - \Delta P_{4B}$ 0.34-1.72 kN/m <sup>2</sup> diff (0.05-0.25 psid)	4	use above
I & II	$\Delta P_{1C} - \Delta P_{4C}$ 1.72-6.9 kN/m <sup>2</sup> diff (0.25-1 psid)	4	use above
I & II	$\Delta P_{1D} - \Delta P_{4D}$ 6.9-34.5 kN/m <sup>2</sup> diff (1-5 psid)	4	use above
I & II	$\Delta P_5$ 0-34.5 kN/m <sup>2</sup> diff (0-5 psid)	<u>1</u>	<u>1</u>
	$\Sigma$	17	5

# P109D DIFFERENTIAL PRESSURE TRANSDUCER

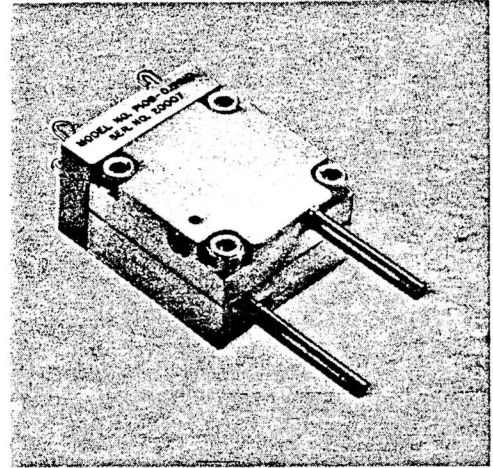
# VARIABLE RELUCTANCE

## FEATURES

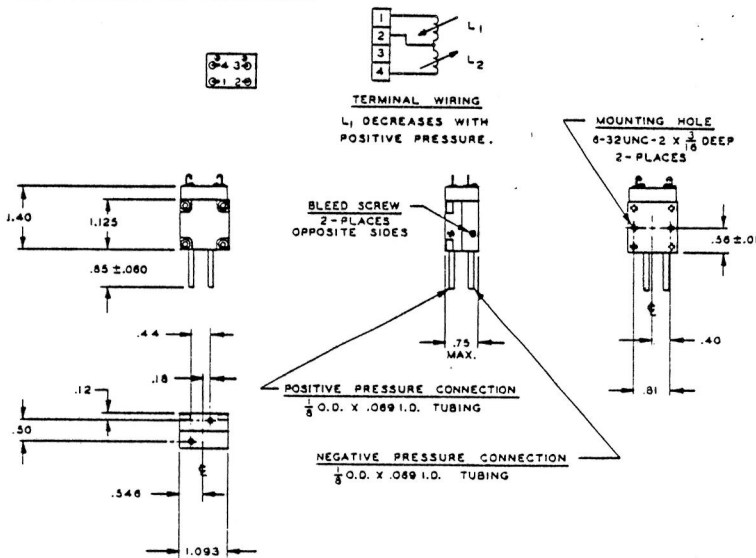
- MINIATURE — WEIGHS 3.5 OUNCES.
- RANGES OF  $\pm 0.05$  TO  $\pm 15$  PSID.
- HIGH SENSITIVITY.
- WIDE DYNAMIC RESPONSE RANGE.
- WITHSTANDS EXTREME SHOCK AND VIBRATION.

## DESCRIPTION

Model P109D Miniature Sensitive Differential Pressure Transducers operate on the variable reluctance principle and are intended for installations involving minimum space and weight. Liquids as well as gases may be admitted to either port at pressure levels from vacuum to 15 psi. Pressure difference is applied across the magnetic stainless diaphragm resulting in proportional deflection and consequent change in inductance ratio between two pickoff coils imbedded in the case on either side. The embedded coils are sealed off with a non-magnetic stainless cover so that both pressure cavities present a stainless exposure to the working medium. Full scale pressure results in an inductance change of 5% in each coil, equivalent to a full scale output of 25 mv per volt of excitation in bridge circuit operation. The Model P109D may be used in most carrier systems. When operated with the Model CD32 Miniature Carrier-Demodulator, a DC output of 0-5 volts is delivered to the associated recording or telemetry system. Vent valves facilitate complete liquid filling for dynamic measurement.



## INSTALLATION DRAWING



A-35



**Celesco Transducer Products, Inc.**  
division of Transducer Controls Corporation

7800 Deering Ave • Canoga Park • California 91304 • (213) 894-6860 • Telex: 67-3382 • TWX: 910-494-1951

# P109D DIFFERENTIAL PRESSURE TRANSDUCER

# VARIABLE RELUCTANCE

## SPECIFICATIONS

**Ranges:**  $\pm 0.05$  to  $\pm 15$  psi differential.  
**Linearity:**  $\pm 1/2\%$  F.S. best straight line.  
**Hysteresis:**  $1/2\%$  F.S. pressure excursion.  
**Overpressure:** 200% of range in either direction with less than  $1/2\%$  zero shift.†  
**Line Pressure:** 100 psi, maximum.  
**Output:** 25mv/v full scale nominal.  
**Inductance:** 20 mh nominal, each coil, zero balance within 10% full scale.  
**Excitation:** 1,000-20,000 Hz, 15 volts max. at 3,000 Hz. Coils available for 400 Hz and other frequency requirements.  
**Working Fluids:** Liquids, materials and gases, both sides. Compatible with 400 series Stainless standard models.  
**Temperature:** Operational —  $65^\circ$  to  $+250^\circ\text{F}$   
Compensated —  $15^\circ$  to  $+165^\circ\text{F}$

Maximum error (from room temperature) above compensated range: 1 psi and above  $<3\%$  F.S.  
Below 1 psi  $<5\%$  F.S.

**"O" Rings:** Buna N — other materials on special order.  
**Pressure Cavity Volume:**  $3 \times 10^{-3}$  cubic inch.  
**Volumetric Displacement:**  $3 \times 10^{-4}$  cubic inch, full scale.  
**Acceleration Response:** Most sensitive axis (across diaphragm).\*

Range	Static	Vibratory	Nat. Freq.
$\pm 0.05$ psid	1%/g	1%/g	3K Hz
$\pm 1$ psid	0.2%/g	0.2%/g	5K Hz
$\pm 15$ psid	0.03%/g	0.05%/g	8K Hz

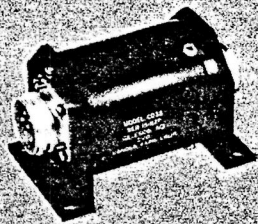
**Installation Details:** See drawing on front.

**Weight:**  $3\frac{1}{2}$  ounces.

\*Acceleration response any axis in diaphragm plane 1% of value listed in table.

†Factory preconditioning for higher overpressures on special order.

**MODEL CD32  
CARRIER-DEMODULATOR**



The Model CD32 Miniature Carrier-Demodulator operates on unregulated 22-32 VDC at 20 ma with Transducers to provide a 0-5 or  $\pm 5$  VDC full scale output for voltage controlled telemetry and other DC systems. Transducer excitation is 5 Volts at 5 K Hz. Frequency response is flat  $\pm 5\%$ , 0-1,000 Hz. Encapsulation in a small, light-weight aluminum case assures reliable performance under extreme shock and vibration. Static acceleration is 100 g. Ambient temperature range is  $-65^\circ\text{F}$  to  $+250^\circ\text{F}$ . Weight is 7 ounces and Size is  $1\frac{1}{2}$ " dia. x  $3\frac{3}{8}$ " overall length.

**MODEL CD10 DC OUTPUT  
CARRIER-DEMODULATOR**



A small Carrier-Demodulator, designed for operation on 95-125 Volts, 60-400 Hz at 5 watts, the Model CD10 operates with Variable Reluctance Pressure Transducers in DC systems. Transistorized for reliability, it is compact (may be mounted inside many recorders) and provides an output of 0-10 VDC (0-2.5 ma maximum current) or  $\pm 10$  VDC full scale. Transducer excitation is 5 Volts at 5 K Hz. Frequency response is flat  $\pm 5\%$ , 0-1,000 Hz. Regulated against input voltage variation, it operates reliably over an ambient temperature range of  $40^\circ\text{F}$  to  $120^\circ\text{F}$ . Long term stability is  $\pm 1/2\%$ . Weight is 34 ounces and Size is  $3\frac{1}{4}$ " wide x 3" deep x  $5\frac{1}{4}$ " long.

REPRESENTED BY

A-36



**Celesco Transducer Products, inc.**

division of Transducer Controls Corporation

7800 Deering Ave • Canoga Park • California 91304 • (213) 884-6860 • Telex: 67-3382 • TWX: 910-494-1951

## FLOWMETER, AIR

### PURPOSE/REQUIREMENTS

This flowmeter is needed to measure air flow in the Flow Patterns/Pressure Drop Experiment, No. I.

Flow Range:	0.85-453 lpm (0.03 to 16 cfm)
Accuracy:	±0.056 lpm (±0.002 cfm)

### HARDWARE STATUS

A standard thermistor will be used to fabricate a hot wire type of flowmeter for this application. This type of meter was used successfully during Convair's previous aircraft flight test program, Ref. 2-2. It has a very low pressure drop compared to the turbine type of flowmeter.

### TECHNICAL DESCRIPTION

For information on the thermistor sensor, see the Thermistor specification sheet. Estimated proportion of the flowmeter, including a low voltage power supply and electronic circuitry, is:

Weight:	0.91 kg (2 lb)
Size:	1.42 litre (0.05 ft <sup>3</sup> )
Power:	115 volt, 400 Hz, 5 watts
Cost:	\$2,000

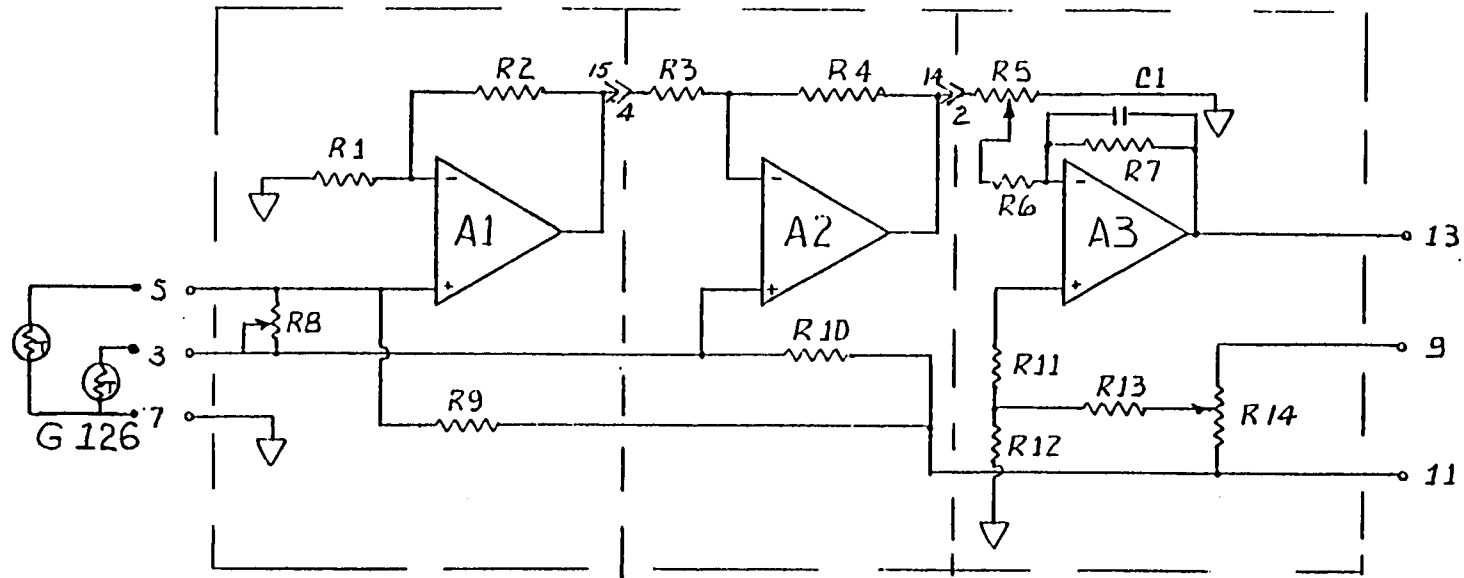
### APPLICABLE EXPERIMENTS

Exp. I.

## CONVAIR AIR FLOW METER DESIGN

An air flowmeter was designed, developed and fabricated at Convair for aircraft flight testing of fluids in zero gravity. The finalized air flow sensor circuit design is given in Figure A-2 and includes zero balance and adjustable gain functions. The two sensing thermistors are Fenwal GC32L1. They are purchased as a matched pair and are mounted in the Fenwal G126 probes shown in Table A-3. For insertion into the air stream, the probes were assembled into metal housings. Except for the thermistors, all of the electronic components shown in Figure A-2 are mounted on printed circuit cards.

The gain and zero balance of the air flow sensor amplifier was adjusted to give 5 volts output for  $56.64 \text{ dm}^3/\text{sec}$  (120 cfm) and zero volts for no flow. The sensor was calibrated at the GDC Gas Dynamics Lab with the sensor located at its normal site in the air duct. The calibration data are shown in Figure A-3. The output, as noted above, is non-linear with a greater sensitivity to the lower air flows. The air flow meter display has a non-linear display face. Normally, for data reduction, the sensor output voltage was recorded and flow obtained by using Table A-4. The overall accuracy of the sensor was estimated to be within 5 percent.



A1, A2, A3	FRCHLD 7741393	R8	5.23K
R1	20.5K	R9	1.6K, WW 1%
R2	10.2K	R10	1.6K, WW 1%
R3	10.3K	R11	10.2K
R4	20.5K	R12	10.2K
R5	5K	R13	49.9K
R6	20.5K	R14	5K
R7	102K	G126	Fenwal GC32L1

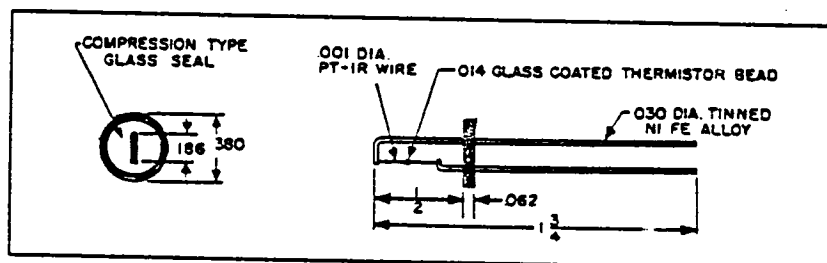
Figure A-2. Air Flow Sensor Electronics

TABLE A-3

MATCHED THERMISTOR CHARACTERISTICS

Specifically designed for use in Gas Chromatographic Equipment and other Thermal Conductivity Gas Analysis Instruments.

The G-112, G-126 and G-128 are matched pairs of thermistors with each bead mounted on a special hermetically sealed stem. The higher resistance units should be used at higher ambient temperatures for maximum sensitivity.



CHARACTERISTICS	G126	G112	G128
$R_0$ at 25°C	2000 $\Omega$ $\pm$ 25%	8000 $\Omega$ $\pm$ 20%	100,000 $\Omega$ $\pm$ 20%
$R_0$ at 0°C (approx)	4900 $\Omega$	23,200 $\Omega$	355,000 $\Omega$
$R_0$ at 50°C (approx)	890 $\Omega$	3,200 $\Omega$	34,000 $\Omega$
Ratio of $R_0$ 0°/50°C	4.95 to 6.95	6.56 to 7.99	9.45 to 11.20
Beta Nominal at 25°C	3000°K	3495°K	4115°K
Temp. Coeff. at 25°C	-3.4%/°C	-3.9%/°C	-4.6%/°C
T.C. Still Air	1 Second	1 Second	1 Second
D.C. Still Air	0.16 MW/°C	0.16 MW/°C	0.16 MW/°C
D.C. Helium	0.5 MW/°C	0.5 MW/°C	0.5 MW/°C
Power Rating, Air	15 Milliwatts	45 Milliwatts	45 Milliwatts
Power Rating, Helium	60 Milliwatts	140 Milliwatts	140 Milliwatts
Max. Temp. Ambient	100°C	250°C	250°C
Max. Temp. Operating (incl. self-heat)	150°C	300°C	300°C
$R_0$ at Max. Temp. Operating	88 $\Omega$	25 $\Omega$	110 $\Omega$
Pair Matched $R_0$ at 25°C	5%	2%	5%
EI Pair Matching	Still Air at 25°C to 15 Millivolts at 5.10 and 15 Milliamps	Helium at 25°C to 35, 25, 20 and 20 Millivolts at 2, 5, 10 and 15 Milliampers	Helium at 25°C to 100 Millivolts at 0.8, 1.5, 2.5 and 4 Milli- amperes

**TIME-CONSTANT:** (T.C.) equals time required by a thermistor to change 63% of the difference between its initial and final temperature measured with thermistor suspended by its leads in specified environment.

**DISSIPATION CONSTANT:** (D.C.) equals power in milliwatts required to raise thermistor temperature 1°C measured with thermistor suspended with leads in specified environment.

A-41

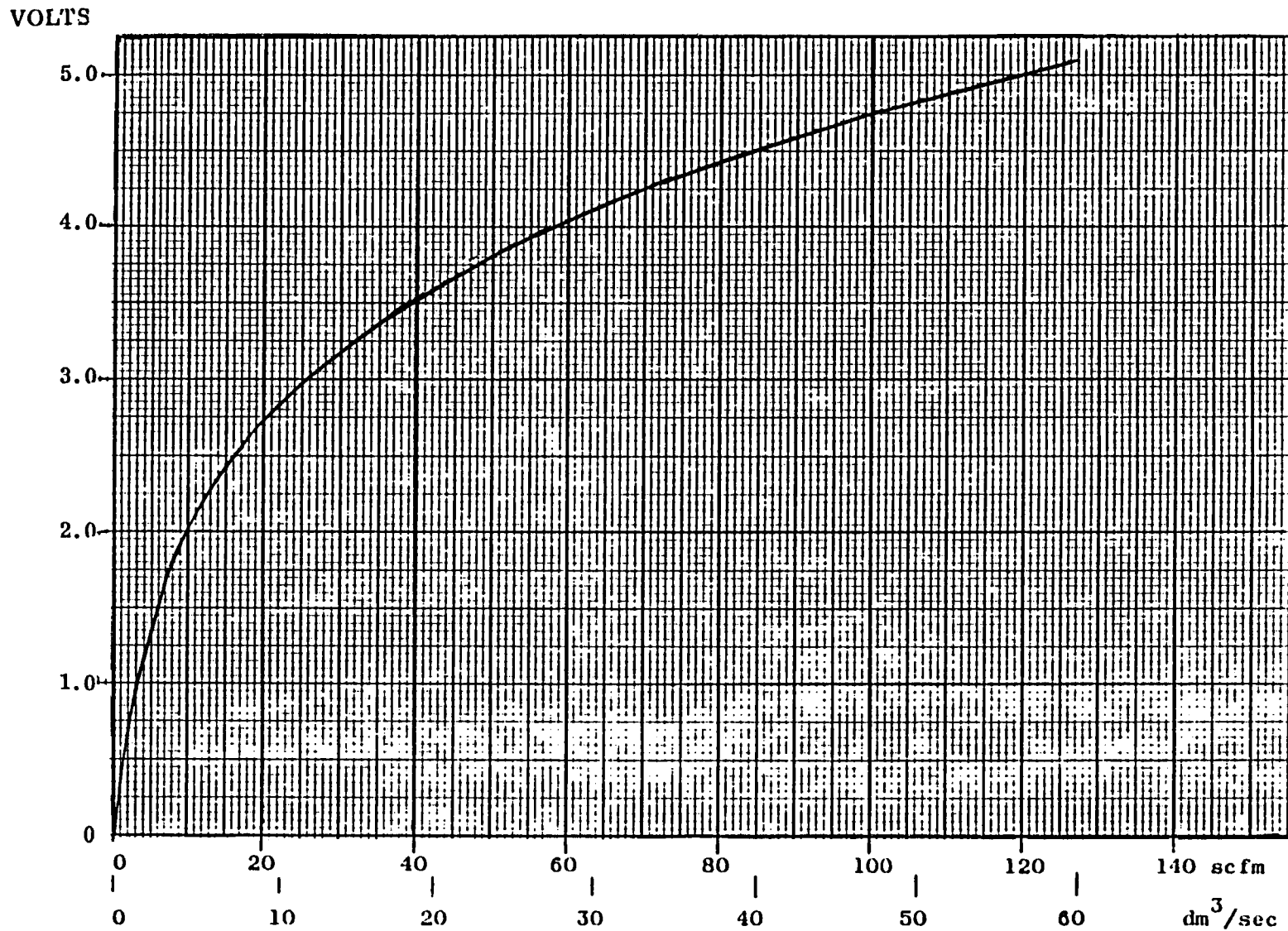


Figure A-3. Air Flow Sensor Calibration Performed at Gas Dynamics Laboratory,  
General Dynamics/Convair. Date: 8 August 1973.

TABLE A-4

## AIR FLOW SENSOR CONVERSION CHART

<u>Voltage</u>	<u>Flow</u>		<u>Voltage</u>	<u>Flow</u>		<u>Voltage</u>	<u>Flow</u>	
	<u>lpm</u>	<u>cfm</u>		<u>lpm</u>	<u>cfm</u>		<u>lpm</u>	<u>cfm</u>
0	0	0	3.14	821	29	3.99	1642	58
0.45	28.3	1	3.18	850	30	4.01	1671	59
0.75	56.6	2	3.22	878	31	4.03	1699	60
1.0	85.0	3	3.26	906	32	4.08	1756	62
1.25	113	4	3.30	935	33	4.12	1812	64
1.40	142	5	3.34	963	34	4.15	1869	66
1.63	170	6	3.37	991	35	4.19	1926	68
1.73	198	7	3.40	1019	36	4.22	1982	70
1.82	226	8	3.43	1048	37	4.26	2039	72
1.95	255	9	3.47	1076	38	4.30	2095	74
2.03	283	10	3.50	1104	39	4.33	2152	76
2.14	312	11	3.53	1133	40	4.36	2209	78
2.23	340	12	3.56	1161	41	4.39	2265	80
2.32	368	13	3.59	1189	42	4.43	2322	82
2.39	396	14	3.62	1218	43	4.46	2379	84
2.45	425	15	3.65	1246	44	4.50	2435	86
2.51	453	16	3.67	1274	45	4.53	2492	88
2.58	481	17	3.70	1303	46	4.57	2549	90
2.63	510	18	3.72	1331	47	4.60	2605	92
2.69	538	19	3.75	1359	48	4.63	2662	94
2.75	566	20	3.78	1388	49	4.66	2718	96
2.79	595	21	3.81	1416	50	4.69	2775	98
2.84	623	22	3.84	1444	51	4.73	2832	100
2.89	651	23	3.86	1472	52	4.75	2888	102
2.94	680	24	3.88	1501	53	4.78	2945	104
2.99	708	25	3.90	1529	54	4.81	3002	106
3.03	736	26	3.92	1557	55	4.84	3058	108
3.07	765	27	3.94	1586	56	4.867	3115	110
3.10	793	28	3.97	1614	57	4.89	3172	112
						4.92	3228	114
						4.94	3285	116
						4.97	3341	118
						5.0	3398	120

## FLOWMETER, LIQUID

### PURPOSE/REQUIREMENTS

To measure the water flow rate during the Flow Pattern/Pressure Drop Experiment, No. I, and the Freon-113 flow from the storage tank in the Liquid Orientation Experiment, No. IV.

Range:	0.038-6.8 lpm (0.01-1.8 gpm (180/1)(Exp. I & II) 1.9 lpm ( ~0.5 gpm) (Exp. IV)
Accuracy:	0.0038 lpm (0.001 gpm) (Exp. I & II) 0.038 lpm (0.01 gpm) (Exp. IV)

### HARDWARE STATUS

Off-the-shelf hardware is available. Two turbine type flowmeters were successfully used in the zero-g aircraft flight experiments for liquid flow measurements. Two were required in order to cover the flow range. The same type of turbine flowmeter is used here. An Omniflo meter available from Flow Technology is described below. Two meters have been assumed for Exp. I & II in order to cover the required flow range without excessive pressure drop. They will be plumbed in parallel with appropriate isolation valves.

### TECHNICAL DESCRIPTION

#### Transducer

Model:	Omniflo Turbine Flow Transducer
Total Range:	0.0038-18.9 lpm (0.001 - 5.0 gpm)
Weight:	0.45 kg (1 lb) (est.)
Cost:	\$630

#### Pulse Rate Converter

Model:	PRC-101
Weight:	0.23 kg (1/2 lb) (est.)
Size:	7.6 × 7.6 × 1.9 cm (3 × 3 × 0.75 in)
Power:	1 watt, 28 volt dc
Cost:	\$290

FLOWMETER, LIQUID (CONT'D)

APPLICABLE EXPERIMENTS

<u>Experiment No.</u>	<u>Measurement No.</u>	<u>No. Required</u>	
		<u>Xducer</u>	<u>Converter</u>
I & II	F <sub>2</sub>	2	2
III	F <sub>1</sub>	1	1

# PRODUCT DATA from FLOW TECHNOLOGY, INC.



4250 EAST BROADWAY ROAD ■ P.O. BOX 21346 ■ PHOENIX, ARIZONA 85036 ■ PHONE (602) 268-8776 ■ TELEX 668-344

## OMNIFLO® TURBINE FLOW TRANSDUCERS

**FLUID FLOW RATES AS LOW AS 0.001 GPM**

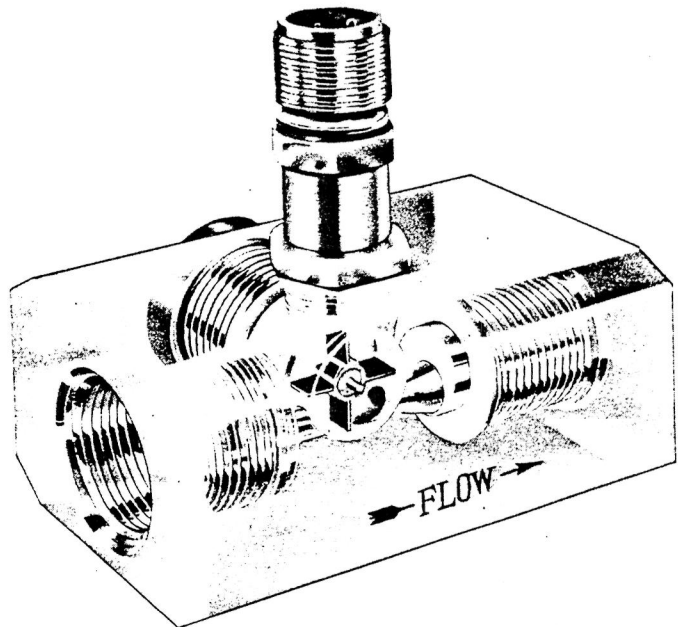
**MEASURES EITHER GASES OR LIQUIDS**

**PULSE SIGNAL OUTPUT**

**AVAILABLE IN A WIDE VARIETY OF MATERIALS**

**EXTREME TEMPERATURE RANGE  
OF -430°F to +350°F**

**HIGH PRESSURE CAPABILITY TO 5000 PSI**



## PRINCIPLE OF OPERATION

Flow Technology's "Omniflo" represents an outstanding achievement in the realm of ultra-low-level fluid flow measurement. The "Omniflo" turbine flow transducer is an in-line metering device utilizing a bladed rotor to generate digital flow information. There is an obvious similarity between the "Omniflo" and conventional turbine flow transducers; however, the "Omniflo" differs in several important aspects in its mode of operation.

Within the "Omniflo" meter a precision orifice directs all of the measured fluid tangentially past the underside of a paddle bladed rotor. The rotor responds by rotating in a plane in line with the fluid's motion in much the manner of an undershot water wheel. The "Omniflo's" turbine rotor, being freely suspended and of low mass, has effectively no ability to either absorb energy from, nor inject it into the moving fluid, so it must rotate at

a speed which perfectly characterizes the velocity of the flowing fluid. A magnetic pick-off coil, located externally but adjacent to the rotor, has generated within it an electric current whose frequency is directly proportional to the rotation of the rotor and in turn proportional to fluid flow. The frequency of the generated pulses is proportional to the flow rate, and the sum of the pulses corresponds to the total fluid volume measured. These pulses can be fed directly into digital totalizers, frequency-to-DC converters, and, in fact, into any one of many frequency indicating, recording and control devices available within the field.

The unique character of the "Omniflo" is its ability to measure very low liquid and gas flow under high temperature and pressure conditions and to do this with accuracy and reliability.

# GENERAL SPECIFICATIONS

## FREQUENCY OUTPUT

The output of the "Omniflo" is a series of electrical pulses generated within its pick-off coil. The frequency range of these pulses will normally be within 2 to 1,000 Hz., supplied at a minimum level of at least 15 millivolts peak-to-peak.

## CONNECTIONS

Standard fluid end fittings of the "Omniflo" are 1/2" AN-10050-8 or 1/2" female NPT. The electrical pick-off connector mates with an MS3106-10SL-4S two pin connector. The mating connector is furnished. Special connectors for either the fluid or electrical connections can be furnished upon request.

## TEMPERATURE

Standard "Omniflo" transducers may be operated over a temperature range of -430°F to +350°F. Temperature rating to +750°F available with reduced performance.

## MATERIALS

Standard "Omniflo" housings are fabricated of 316 stainless steel. Transducers to meet special requirements have been fabricated of aluminum, 316 and 347 stainless steels, Hastalloy, K-Monel, and PVC. An extensive selection of bearing materials and types are available — graphitic or carbide journals, ball bearings, or vee-jewel pivot bearings, for example.

## PRESSURE

Fluid end connections are the governing factors in determining the "Omniflo's" pressure limitation. The standard transducer can operate with a fluid pressure of 5,000 psi at 100°F with the AN-10050-8 fitting option.

## LOW FLOW — SPECIAL REQUIREMENTS

In order to sense and measure flow rates below 0.01 GPM liquid or 0.05 ACFM gas, the "Omniflo" must utilize an LFA (Low Flow Amplifier.) The LFA is normally supplied within its own enclosure and is used as a pre-amplifier between the "Omniflo" pick-off and the readout. See bulletin REA for details.

# MEASUREMENT CHARACTERISTICS

## LIQUID

### REPEATABILITY

Within a normal 10 to 1 liquid flow range, the "Omniflo" will operate with a repeatability to within  $\pm 0.1\%$  of reading.

### LINEARITY

The performance of an "Omniflo" turbine meter is inherently non-linear. The degree of non-linearity is dependent upon the range of the particular meter selected and upon the viscosity of the fluid in which it will operate. Linearity characteristics for low viscosity fluids, (approximately 1 centistoke are shown on bulletin TD-023.

Optional premium linearities are available for ball bearing "Omniflos" with flow rates above 0.1 GPM and ranges no greater than 10 to 1 operating in fluids with viscosities less than 3 centistokes.

### FLOW RATE RANGE

The overall measurement capability of the "Omniflo" series covers the entire flow range of 0.001 to 5.0 gpm. Individual transducers are normally supplied to measure any specified 10 to 1 segment within the 0.001 to 5.0 gpm flow range.

### VISCOSITY

"Omniflo" transducers are calibrated with MIL-C-7024B calibration fluid and furnished with calibration data. Calibration at other viscosities and fluids can be furnished upon request. Maximum viscosity varies from 5 to 50 centistokes depending upon flow range.

### PRESSURE DROP

The pressure drop, based on water, will not exceed 10 psi for the maximum normal flow rate of any given "Omniflo" transducer, but will vary as a function of density and viscosity. Pressure drop requirements can be met by proper sizing of the transducer. See TD-024.

## GAS

### REPEATABILITY

The basic repeatability of the "Omniflo" transducer in gas service is  $\pm 0.2\%$  at all points within a normal 10 to 1 actual-volume flow range; however, when referring this measured volume to standard conditions, it must be remembered that the repeatability experienced becomes a function of the precision of the temperature and pressure measurements, in addition to the actual volume of flow.

### LINEARITY

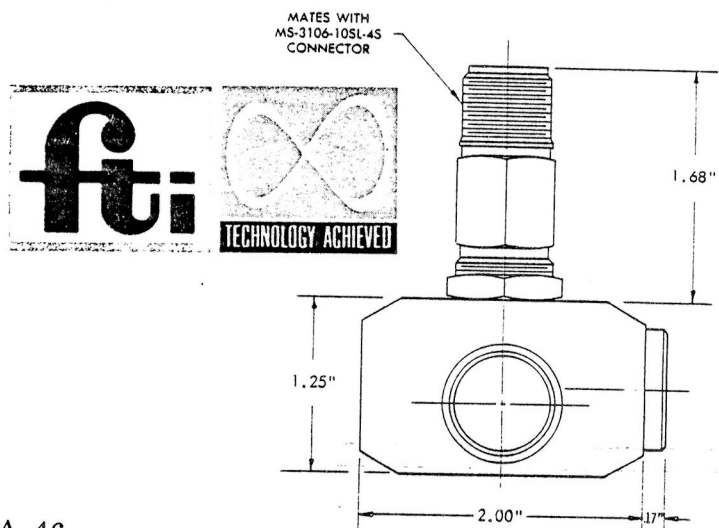
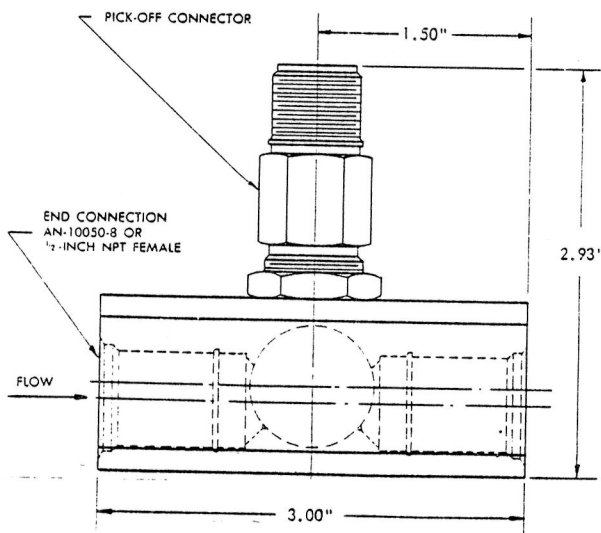
While "Omniflos" are basically non-linear, the linearity characteristics of "Omniflo" meters in gas are dependent upon the density of the gas as well as the flow range of the individual meter. Typical linearity characteristics for air at standard conditions are shown in bulletin TD-025. **NO EXTENDED RANGES ARE AVAILABLE EXCEPT AS SHOWN ON TD-025.**

### FLOW RATE RANGE

The "Omniflo" transducer being a volumetric measuring device senses only the actual-volume of the measured gas at the measurement point (at the turbine rotor). The overall actual-volumetric-flow rate range for gas is from 0.0015 to 1.0 ACFM, with individual transducers being supplied to cover any specified 10 to 1 segment of this range. When calculating the relationship between the actual and standard condition volumetric flow range, normal temperature and pressure corrections must be used. Temperatures and pressures for the "Omniflo" should be taken immediately down-stream.

### PRESSURE DROP

The gas density and viscosity largely determines the maximum pressure drop, however, under average conditions this should not exceed 1/2 psi. See TD-024.

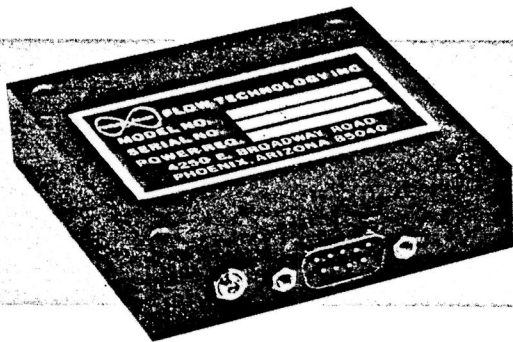


# PRODUCT DATA from FLOW TECHNOLOGY, INC.



4250 EAST BROADWAY ROAD ■ P.O. BOX 21346 ■ PHOENIX, ARIZONA 85036 ■ PHONE (602) 268-8776 ■ TELEX 668-344

## PULSE RATE CONVERTERS ALL SOLID-STATE FREQUENCY CONVERTERS



MODEL PRC-101



MODEL PRC-104

- ACCEPT ALL TURBINE FLOWMETER INPUT PULSES
- ANALOG VOLTAGE (PRC-101) OR CURRENT (PRC-104) OUTPUTS
- 10 V PULSE OUTPUT
- $\pm 0.2\%$  LINEARITY
- SOLID-STATE RELIABILITY
- COMPACT DESIGN AND FORM FACTOR

### DESCRIPTION

The Pulse Rate Converters Model PRC-101 and Model PRC-104 are all solid-state, miniaturized frequency converters designed for use with FTI turbine flowmeters.

Featuring the compact reliability of modern integrated circuits and solid-state design, they are potted into enclosures measuring only 3" x 3" x 3/4".

The Model PRC-101 is a frequency-to-voltage converter producing a 0-to-5 VDC output whose voltage level is a function of the input pulse frequency from the flowmeter.

The Model PRC-104 is a frequency-to-current converter that provides an analog output current proportional to the input pulse frequency from the

flowmeter. Two variations of the PRC-104 are available: (a) the PRC-104B produces an output current of 4 to 20 ma, while (b) PRC-104C output is 10 to 50 ma.

All models also provide a pulse output of 10 volts peak-to-peak with the same frequency as the input. A 1 to 5 VDC signal is also present.

Power required for all units is normally 28 VDC at 20 ma, plus load current.

The outputs of these units can be used to drive indicators, meters, totalizers, or process control equipment. Their primary application is to interface FTI turbine flowmeters with existing read-out and control equipment.

# GENERAL SPECIFICATIONS

## OUTPUTS:

	PRC-101	PRC-104B	PRC-104C
Analog Voltage:	0-5 VDC	1-5 VDC	1-5 VDC
Output Current:	10 ma max.	4-20 ma	10-50 ma
Output Pulse:	10 v gnd. base	10 v gnd. base	10 v gnd. base
Linearity:	±0.2%	±0.2%	±0.2%
Load Impedance:	n.a.	1000 ohms @ 28 vdc	400 ohms @ 28 vdc
Adjustments:	Span	Span & zero	Span & zero
Span Adjustment:	2 to 1	2 to 1	2 to 1
Zero Offset Adjustment:	optional	standard	standard

## SIGNAL INPUT:

Frequency Range:	5-10,000 Hz (full-scale selected at factory to order)
Input Level:	10 mv to 10 v peak-to-peak

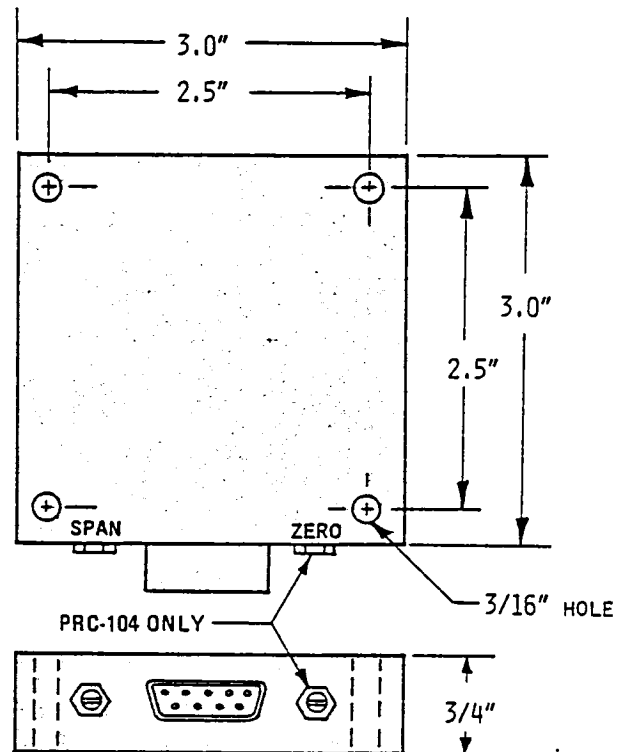
## POWER REQUIREMENTS:

Voltage:	22 to 32 vdc
Current:	20 ma + load current
Options:	115 VAC, 60 Hz 220 VAC, 50 Hz

**CONNECTOR:** Cinch-Jones DEM-9P  
(mating connector supplied)

**CASE SIZE:** 3" x 3" x 3/4",  
+28 VDC unit only

**Options:** JIC Box 3" x 4" x 6",  
115, 220 VAC unit.  
Explosion-proof enclosure,  
all units.



FOR ADDITIONAL INFORMATION  
CONTACT FTI OR YOUR FTI REPRESENTATIVE:



## GAS/LIQUID SEPARATOR

### PURPOSE/REQUIREMENTS

This item is used to separate gas/liquid mixtures in the zero-g environment. Mixtures of water and air of varying qualities, and of gaseous and liquid Freon 11 of varying qualities, will be handled.

Flow Range:

#### Air/Water

Total Flow Range: 6.35 - 407 kg/hr  
Air Flow Range: 0.063-32.6 kg/hr (0.88-445 lpm)  
Water Flow Range: 2.27 - 403 kg/hr (0.037 - 6.8 lpm)

#### Freon-11

Total Flow Range: 6.35 - 407 kg/hr  
Gas Flow Range: 0.033 - 44.4 kg/hr (0.108 - 343 lpm)  
Liquid Flow Range: 5.67 - 405 kg/hr (0.062 - 4.53 lpm)

Pressure: 34.5-101.3 kN/m<sup>2</sup> (5-14.7 psia)(-9.7 to 0 psig)

Temperature: 26-70°F

### HARDWARE STATUS

This item will require special design and fabrication and two companies were contacted to inquire into applicable designs and hardware. These companies were AiResearch Division of Garrett Corp., and Hamilton Standard Division of United Aircraft Corp. In the past, gas liquid separators were made by those two companies for various spacecraft applications. It was found that AiResearch is not doing any work in this area, and are not making any separators. Hamilton Standard, however, is making two separators for the Space Shuttle, and also can specially build a model of their old separator which was used on Skylark. However, these units are smaller than required for the fluid experiment package application and would require redesign.

The following technical description is based upon Convair's separator design which was used successfully in the Aircraft Flight Testing of Fluids in Zero-Gravity Experiments, Ref. 2-2. The unit has been reduced in size, however.

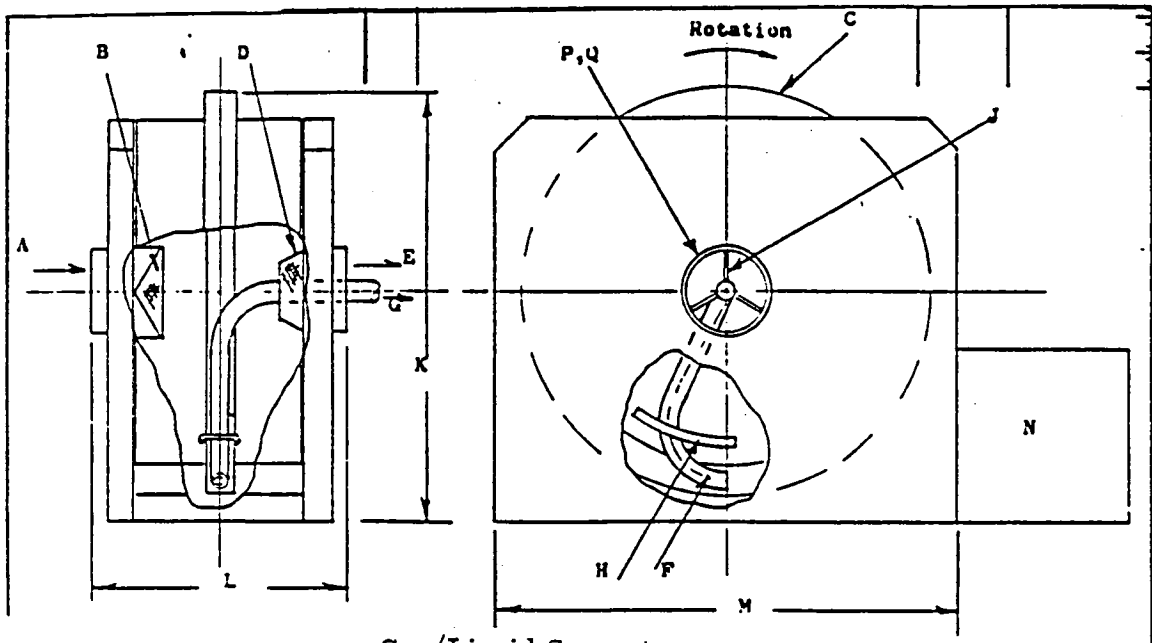
GAS/LIQUID SEPARATOR (CONT'D)

TECHNICAL DESCRIPTION

Weight:	13.6 kg (30 lb)(est.)
Volume:	11.3 litre (0.4 ft <sup>3</sup> (est.))
Power:	150 watts (est.)

APPLICABLE EXPERIMENTS

The separator will be used for Experiments I & II.



Gas/Liquid Separator

PART IDENTIFICATION AND NOMINAL DIMENSIONS:

- A - Mixture inlet 3.8 cm diameter
- B - Inlet baffle rotating with drum
- C - Rotating drum
- D - Outlet air baffle rotating with drum
- E - Air outlet 3.8 cm diameter
- F - Liquid pick-up tube
- G - Liquid outlet 0.97 cm diameter tubing
- H - Pick-up tube splash baffle
- J - Pick-up tube support
- K - Unit height 20.3 cm max.
- L - Unit width 15.2 cm max.
- M - Unit depth 20.3 cm max.
- N - Drive motor
- P - Drum bearing supports
- Q - Drum rotating part liquid seal

REQUIREMENTS:

- Design rotational speed of drum 725 rpm maximum.
- Nominal static liquid volume approximately 819 cm<sup>3</sup> (storage volume).
- Design fluids: water or Freon 10

## PRESSURE TRANSDUCER

### PURPOSE/REQUIREMENTS

Various liquid and gas pressure measurements. Several different pressure range transducers will be required, see below under APPLICABLE EXPERIMENTS.

### HARDWARE STATUS

Off-the-shelf hardware is available.

### TECHNICAL DESCRIPTION

A typical transducer for this application is

#### Pressure Transducer

Model: Celesco Model PLC  
Weight: 0.086 kg (0.19 lb)  
Volume: 32.8 cm<sup>3</sup> (2 in<sup>3</sup>)  
Pressure Port: 0.64 cm (1/4 in.) NPT, MALE  
Cost: \$165 ea.

#### Power Supply

(Celesco Carrier-Demodulator dc Output, Single Channel)

Model No. CD10  
Weight: 0.97 kg (2.13 lb)  
Volume: 836 cm<sup>3</sup> (51 in<sup>3</sup>)  
Cost: \$325 ea.

### APPLICABLE EXPERIMENTS

Experiment Number	Measurement Number	<u>Hardware Required</u>	
		Xducer	Power Supply
I & II	P <sub>1</sub>	1 required, 0-206.8 kN/m <sup>2</sup> (0-30 psia)	1
I	P <sub>2</sub>	1 required, 0-103.4 kN/m <sup>2</sup> gauge (0-15 psig)	1
I & II	P <sub>3</sub>	1 required, 0-137.9 kN/m <sup>2</sup> (0-20 psia)	1

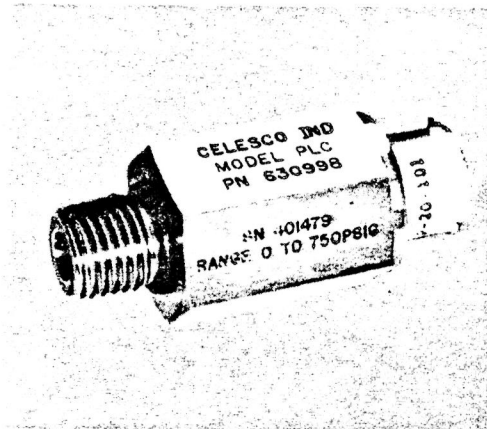
PRESSURE TRANSDUCER (CONT'D)

Experiment No.	Measurement No.	<u>Hardware Required</u>	
		Xducer	Power Supply
I & II	P <sub>4</sub>	1 reqd, 0-137.9 kN/m <sup>2</sup> (0-20 psia)	1
III	P <sub>1</sub>	1 reqd, 0-103.4 kN/m <sup>2</sup> (0-15 psia)	1
IV	P <sub>1</sub> & P <sub>2</sub>	2 reqd, 0-137.9 kN/m <sup>2</sup> (0-20 psia)	2
V	P <sub>1</sub>	1 reqd, 0-103.4 kN/m <sup>2</sup> (0-15 psia)	1

# MODEL PLC PRESSURE TRANSDUCER

## FEATURES

- **LOW COST** – Priced with the lowest for industrial and commercial use. Large discounts for OEM users.
- **ACCURATE** – Low non-linearity and hysteresis. No moving parts assures infinite resolution and long term calibration stability.
- **INTERCHANGEABLE WITHOUT RECALIBRATION** – All units permanently calibrated and adjusted to give the same output signal.
- **RUGGED CONSTRUCTION** – Withstands high vibration and rough field handling.
- **SMALL SIZE** – Fits in tight places. Allows direct mounting to pressure port.
- **TEMPERATURE COMPENSATED** – Each unit compensated within close limits over a wide temperature range.
- **WEATHERPROOF** – Designed for outdoor installations in any climate.



## APPLICATIONS

- **Aircraft** – Air, hydraulic, oil pressure measurements.
- **OEM Equipment** – Air conditioning equipment, pumps, engines, compressors, machine tools.
- **Laboratory** – General purpose pressure measurements.
- **Automotive** – Intake manifolds, diagnostic systems, fuel systems.
- **Hydraulic and Pneumatic Systems** – To replace pressure gauges, switches, or other transducers for upgrading or automation.
- **Process Industries** – Steel, oil, petrochemical, chemical, food, and many others.

## DESCRIPTION

The Model PLC Pressure Transducer sets new standards for the industry in terms of performance, low cost, and rugged dependability. It is a small high-accuracy transducer that uses semiconductor strain gauges bonded to a flat diaphragm to form a Wheatstone bridge. Conservatively designed, it will provide millions of cycles of service in either laboratory or field applications and Celesco advanced manufacturing techniques permit the lowest possible prices, especially for large quantity users.

The PLC transducer is temperature compensated and matched for output sensitivity, so all units are completely interchangeable without recalibration. Also, for most applications, no calibration or maintenance is ever needed for the life of the unit. This rugged transducer is completely rain and weather-proof, dustproof, resistant to most corrosive atmospheres, and insensitive to mounting torque. With no moving or sliding parts to wear out, it will deliver the same high accuracy for many years of continuous service.

The PLC meets a wide variety of general purpose and industrial needs and is available in nine standard ranges from 0-15 to 0-5000 psi gauge or absolute. With an unusually high resonant frequency and large output signal, this transducer is well suited to high vibration environments such as direct mounting to engines or other vibrating equipment.

For many volume applications, the Model PLC can be offered at a price low enough to replace dial pressure gauges, conventional pressure switches, potentiometer pressure transducers, etc. By incorporating a regulator, amplifier, or other appropriate circuitry inside the transducer, it can be operated directly from a battery or other voltage source and drive a meter or recorder without additional signal conditioning.

Special pressure ranges, materials, signal conditioning, and other modifications to meet individual requirements can also be provided at customer request.

A-54



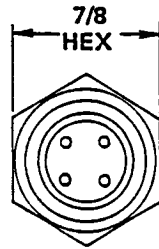
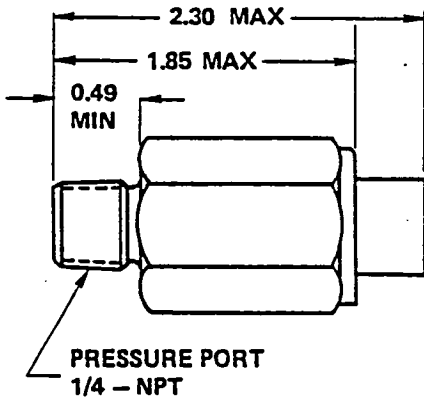
**Celesco Transducer Products, inc.**

division of Transducer Controls Corporation

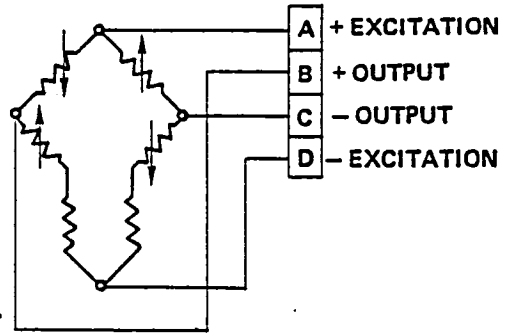
7800 Deering Ave • Canoga Park • California 91304 • (213) 884-6860 • Telex 67-3382 • TWX: 910-494-1951

# MODEL PLC PRESSURE TRANSDUCER

## INSTALLATION DRAWINGS



STANDARD  
4 PIN CONNECTOR BENDIX  
#PT1H-8-4P OR EQUIV.



## TYPICAL CHARACTERISTICS

### Mechanical:

Standard Pressure Ranges: 0 to 15, 20, 50, 100, 200, 500, 1000, 2000, and 5000 psi gauge or absolute.

Overpressure: 2 X full scale.

Burst Pressure: 10 X full scale or 10,000 psi whichever is less.

Pressure Cavity Volume: 0.037 in<sup>3</sup>

Weight: 3 oz.

Construction Materials: Stainless steel.

### Electrical:

Excitation: 10 to 20 V, d-c or a-c.

Input Impedance: 500 Ω min.

Output Impedance: approx. 500Ω

Output/Input: non-isolated, floating, 4 wire.

### Environmental:

Maximum Temperature Range: -65° F to +300° F

### Performance:

Output: 10mV/V ±1%

Accuracy (linearity, hysteresis, and repeatability): ±0.5% of full scale

Zero Balance: ±1.0% of full scale

Temperature Range: 0 - 130° F

Thermal Zero Shift ±0.01%/° F

Thermal Sensitivity Shift ±0.01%/° F

Temperature Range: -20° F to 250° F

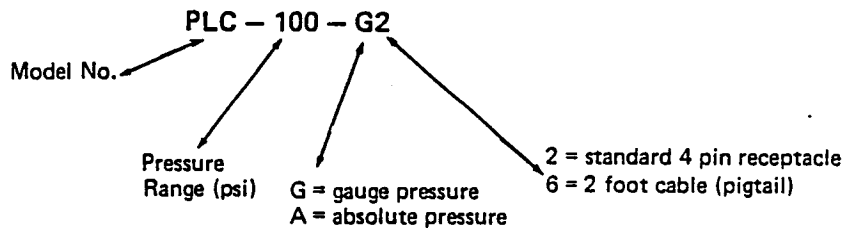
Thermal Zero Shift ±0.02%/° F

Thermal Sensitivity Shift ±0.02%/° F

Resolution: Infinite

Life: Millions of cycles

## HOW TO ORDER



Specifications subject to change without notice.

A-55



**Celesco Transducer Products, inc.**

division of Transducer Controls Corporation

7800 Deering Ave - Canoga Park - California 91304 - (213) 884-6860 - Telex 67-3382 - TWX 910-494-1951

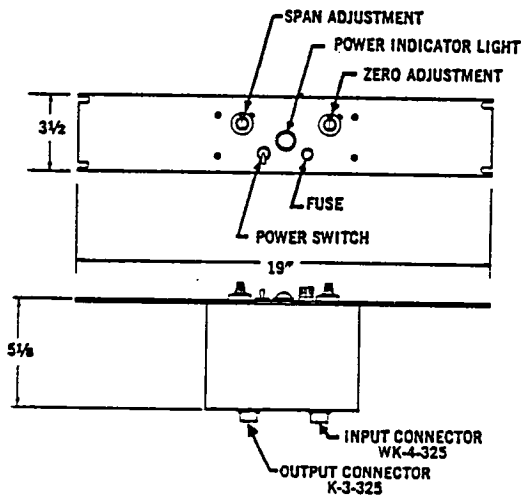
## SPECIFICATIONS

**Power Requirements:** 95-125 Volts, 60-400 Hz at 5 watts.  
**Output:** 0-10 VDC (0-2.5 ma short circuit current) or  $\pm 10$  VDC full scale. Regulated against input voltage variation.  
**Output Impedance:** 2,000 ohms, nominal.  
**Carrier Frequency:** 5 K Hz.  
**Frequency Response:** Flat 0-1,000 Hz, within  $\pm 5\%$ .

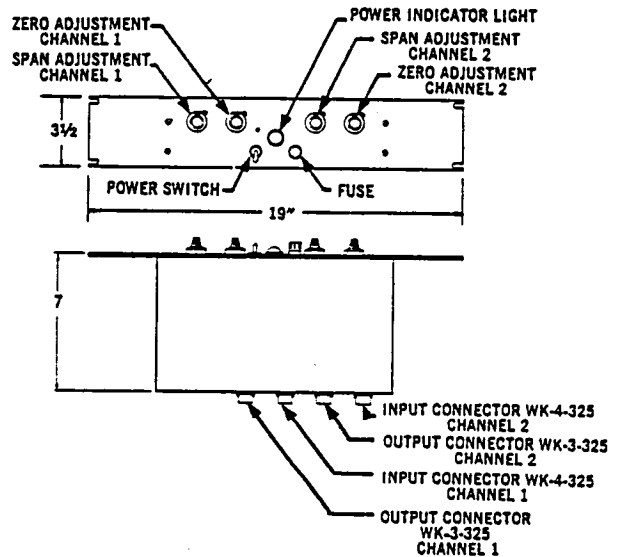
**Stability:**  $\pm 1/2\%$ , long term.  
**Ripple:** 10 mv max. rms.  
**Temperature Range:** 40°F to 120°F.  
**Ambient Thermal Effect:** Zero, .01% / °F.  
**Gain:** .02% / °F.  
**Installation Details:** See drawing on front.  
**Weight:** 34 ounces.

## RACK MOUNTED VERSIONS OF CD10

Single Channel — CD11



Dual Channel — CD12



REPRESENTED BY

A-56

**celesco**  
 Transducer Products, inc.

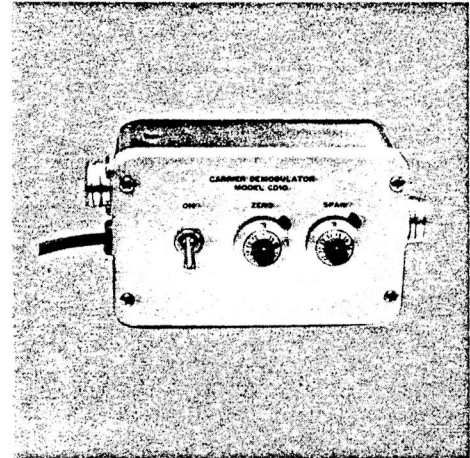
7800 Deering Ave. • P.O. Box 1457 • Canoga Park • California • 91304  
 (213) 884-6860 • Telex: 67-3382 • TWX: 910-494-1951

## FEATURES

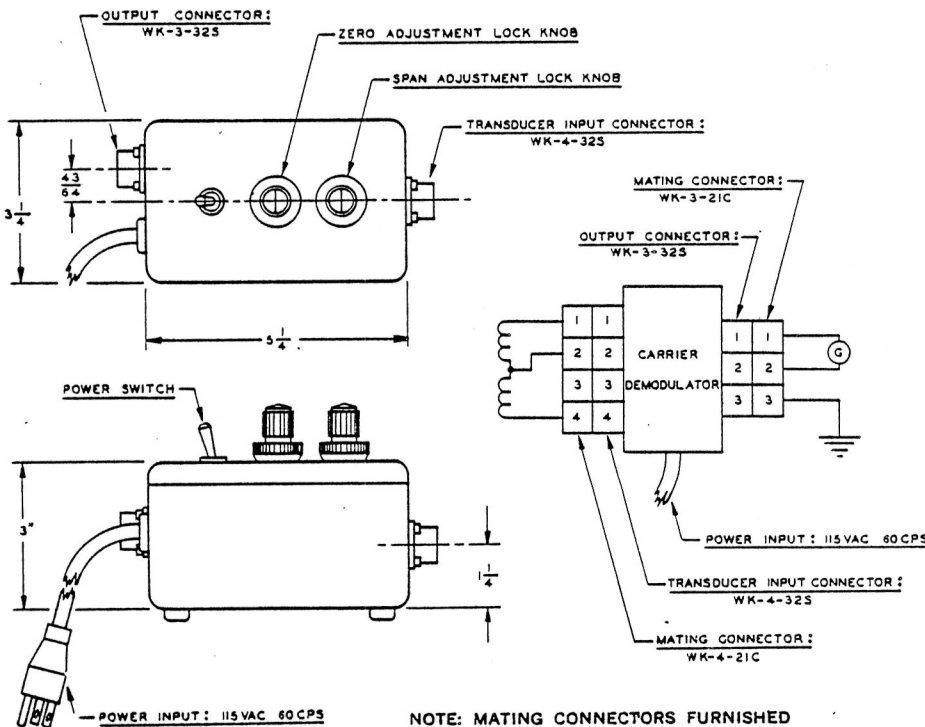
- OUTPUT  $\pm 10$  V DC
- COMPACT — MOUNTS INSIDE RECORDER.
- REGULATED AGAINST LINE VOLTAGE VARIATION.
- TRANSISTORIZED FOR RELIABILITY.

## DESCRIPTION

The Model CD10 Miniature Carrier-Demodulator, designed for operation on 95-125 volts, 60-400 Hz at 5 watts, operates with Variable Reluctance Transducers in DC systems for dynamic as well as steady state measurement. Excitation of 5K Hz is applied to a bridge including the two inductance ratio arms of the transducer. A solid-state amplifier and demodulator converts the bridge output to DC. Response is uniform from steady state to 1,000 Hz. Small enough to be included in the case of most receiving and recording instruments, the Model CD10 is regulated against input voltage variation and will operate reliably over an ambient range of 40°F to 120°F.



## INSTALLATION DRAWING



A-57

## PUMP

### PURPOSE & REQUIREMENTS

To circulate water and Freon-11 around the test section loop of the Flow Patterns and Flow Boiling Experiments, Nos. I & II.

Flow:            0.038 - 6.74 lpm (0.01 - 1.78 gpm) water  
                  0.061 - 4.39 lpm (0.016 - 1.16 gpm) Freon-11  
 $\Delta P$ :             $\cong 103.4 \text{ kN/m}^2$  diff (15 psid)

### HARDWARE STATUS

Off-the-shelf components are available.

### TECHNICAL DESCRIPTION

A Lear Siegler, Romec Division pump can be used for this application.

Weight:           1.27 kg (2.8 lb)  
Power:            115/200 VAC, 3 phase, 400 Hz power required. Power  
                  input is approximately 300 watts at  $103.4 \text{ kN/m}^2$  gauge  
                  (15 psig) discharge pressure.  
Size:               $15.2 \times 6.35 \times 10.2 \text{ cm}$  ( $6 \times 2.5 \times 4 \text{ in.}$ )

### APPLICABLE EXPERIMENTS

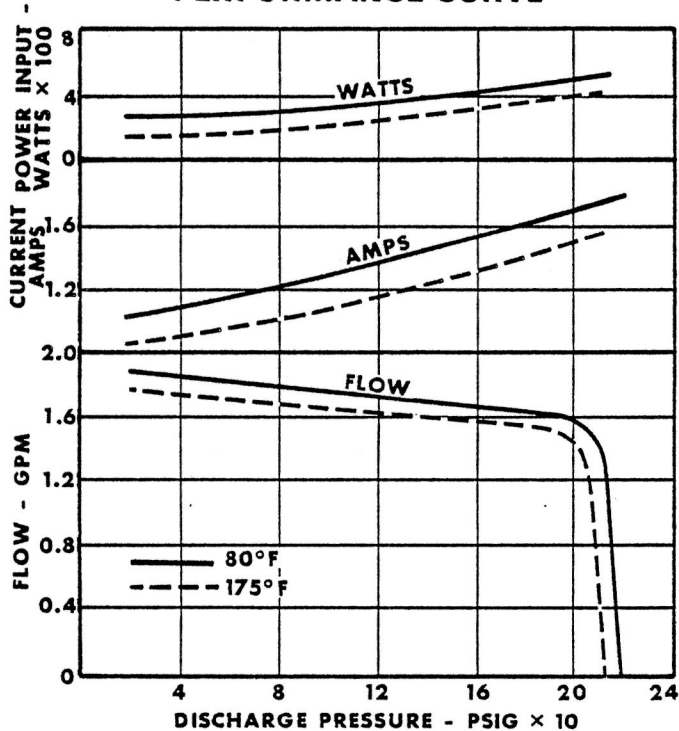
Experiment I & II can use the same pump.

# COOLANT PUMP

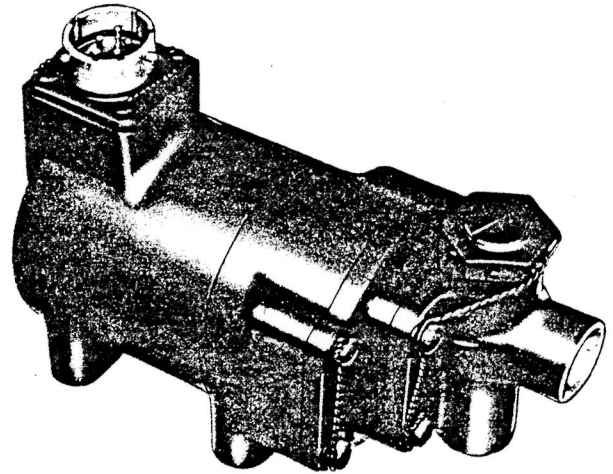
GEAR TYPE • BASE MOUNTED • 1.75 GPM

**ROMECC**  
**PRODUCT DATA**

## PERFORMANCE CURVE



## MODEL RG17400B



## ENGINEERING DATA

### TYPE

Fixed clearance, spur gear type positive displacement, electric motor driven coolant pump. Provided with integral relief valve for pressure regulation. Designed for pumping coolant fluids, but capable of pumping other fluids.

**DISPLACEMENT** . . . . . 0.0385 cu in/rev

### PERFORMANCE

(Pumping Monsanto "Coolanol -45" Dielectric Coolant Fluid at 175° F.)  
 Rating . . . . . 1.75 gpm minimum at 50 psig  
 Fluid temperature range . . . . . -65°F to +175°F  
 Ambient temperature range . . . . . -65°F to +200°F  
 Duty cycle . . . . . Continuous

### MOTOR DATA

Type . . . . . Direct drive  
 Rating (continuous) . . . . . 0.18 hp at 11,300 rpm  
 115/200 VAC, 3 phase, 400 cps

Rotation . . . . . CW viewing drive end  
 Duty cycle . . . . . Continuous  
 Electrical connection . . . . . PT02 P14-5P receptacle

### PORT SIZES

Inlet and Discharge . . . . . 9/16-18UNF-3B  
 per AND10050-6

### PRESSURE REGULATION

Integral relief valve adjustable for full by-pass pressure of 170 to 225 psig. Preset for customer specification and lockwired.

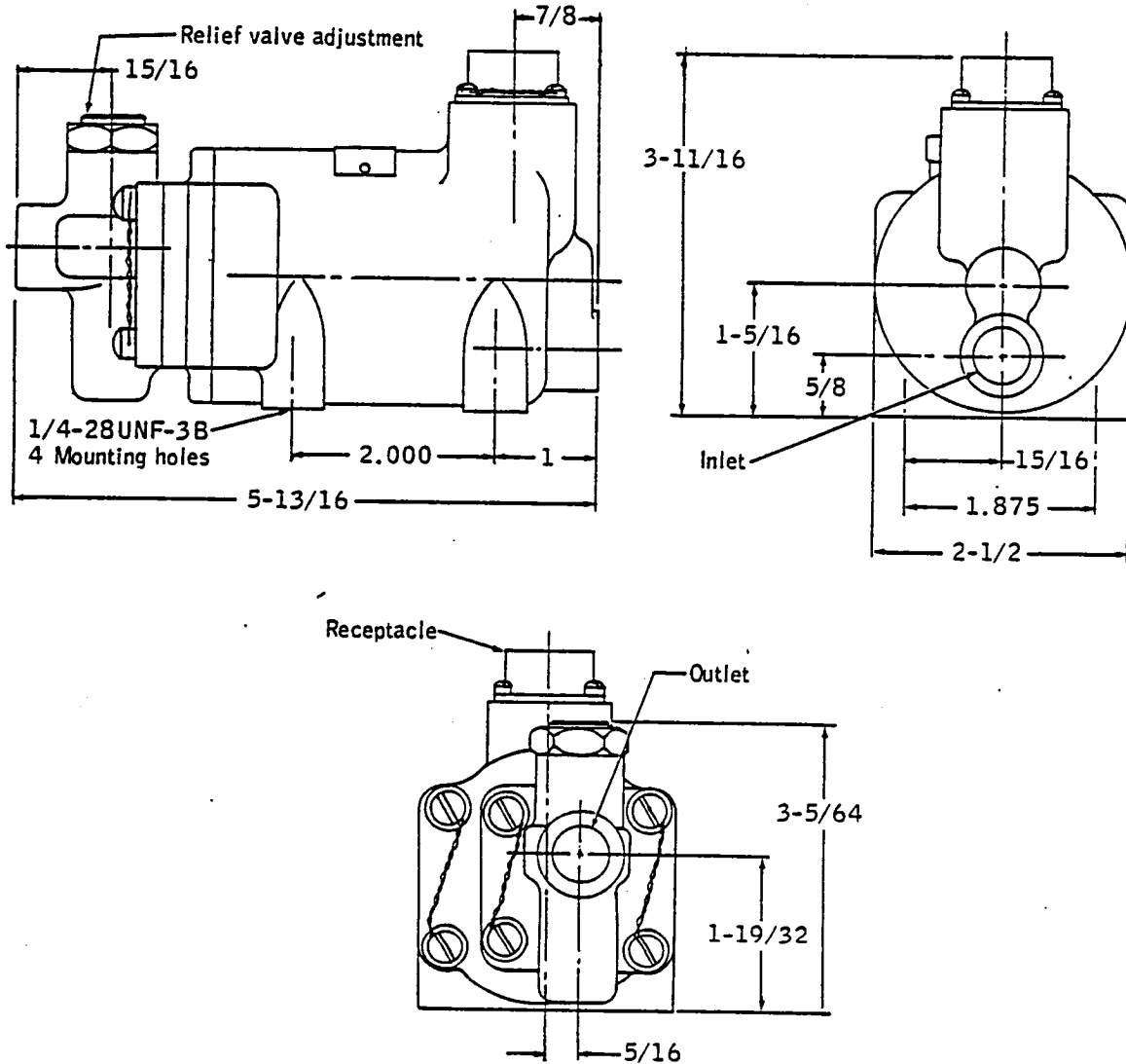
**MOUNTING** . . . . . See sketch, reverse side

**UNIT WEIGHT** . . . . . 2.8 lb

### TYPICAL APPLICATION

Cooling system, ground support equipment

**MODEL RG17400B ILLUSTRATED**



**LEAR SIEGLER, INC.**



**ROME C DIVISION**

241 SOUTH ABBE ROAD  
 ELYRIA, OHIO 44035  
 216-323-3211

**DOMESTIC AREA OFFICES**

● LOS ANGELES, CALIFORNIA

● ELYRIA, OHIO

● DAYTON, OHIO

● WALTHAM, MASSACHUSETTS

**EXPORT REPRESENTATIVE**  
**AMERICAN AVITRON, INC.**  
 RYE, NEW YORK

## QUALITY METER

### PURPOSE & REQUIREMENTS

To measure the quality of the Freon 11 fluid upstream and downstream of the test section in the Flow Boiling Experiment, No. II.

### HARDWARE STATUS

Available on special order from Quantum Dynamics.

### TECHNICAL DESCRIPTION

The following estimates are based on information from Dr. Frederick F. Liu of Quantum Dynamics. Their quality measurement unit consists of three parts: (1) a turbine type flowmeter, (2) a dielectric (density) measurement device, and (3) an electronics package to process the signal from these instruments and read out quality and flow rate.

#### Flowmeter

Weight: 0.91 kg (2 lb) (est.)  
Size: 7.6 × 7.6 × 5.1 cm (3 × 3 × 2 in.)

#### Density Meter

Weight: 4.5 kg (10 lb) (est.)  
Size: 5.1 cm dia × 50.8 cm long (2 in. dia × 20 in. long)

#### Signal Processor

Weight: 4.5 kg (10 lb) (est.)  
Size: 35.6 cm wide × 12.7 cm high × 30.5 cm deep  
(14 in. wide × 5 in. high × 12 in. deep)  
Power: TBD

The cost of the total three part package, as provided by Quantum Dynamics, was estimated at \$16K by Dr. F. Liu of Quantum Dynamics.

### APPLICABLE EXPERIMENTS

Experiment No. II, 2 reqd.

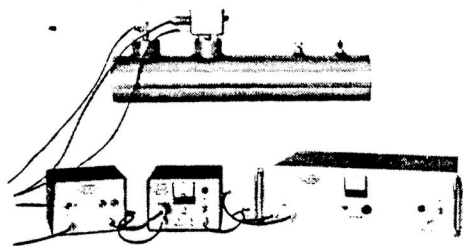


Figure 1. Liquid/supercritical Hydrogen Mass Flowmeter with Vacuum Jacket

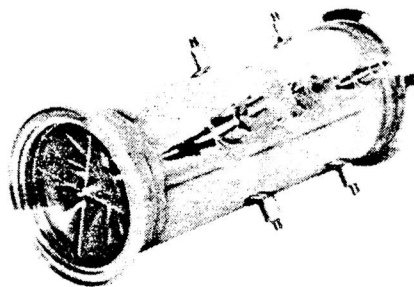


Figure 2. 3 In. Liquid Hydrogen Flowmeter

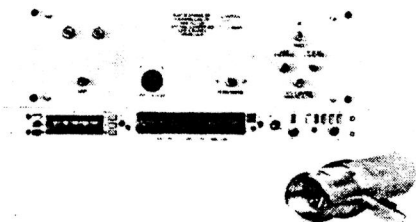


Figure 3. Liquid Fluorine Mass Flow System

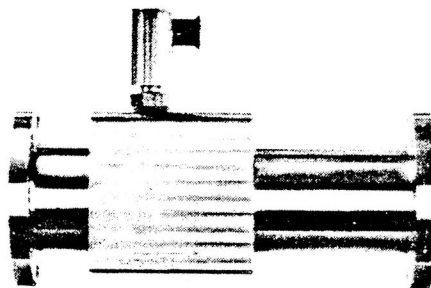


Figure 4. 2 In. Liquid Oxygen Flowmeter

## INTRODUCTION

Modern cryogenic technology poses many new problems in measurement techniques. Not only should instruments be usable under a variety of extreme environmental conditions, but also they must be designed with a high degree of theoretical rigor commensurable with reliability and system engineering considerations. Without these, accuracy and usefulness under extremely low temperatures and cryogenic fluid-dynamic condition become improbable. Moreover, in the face of the high cost and laborious processes involved in cryogenic calibration, many measurement instruments — based on conventional concepts of "brute-force" calibration — are of dubious cost effectiveness.

Cognizant of such considerations, Quantum Dynamics has developed new cryogenic instrumentation for the high-resolution measurement of flow (mass, volumetric, and transient flowrates), density (steady and transient), and temperature (steady and transient) of liquid and super-critical gases at high accuracy and signal levels. Original and theoretically sound approaches are applied to the instrument design. Compared with conventional general-purpose measurement devices, Quantum Dynamics' cryogenic instrumentation represents a line of products that is conceptually rigor-

ous yet meticulously engineered for efficient field applications with liquid and super-critical hydrogen, helium, nitrogen, fluorine, oxygen, and other gases.

## VOLUMETRIC FLOWMETERS

(For Measuring Mass Flowrate, Volume Flowrate, Transient Flowrate, and Totalized Flow of Liquid and Super-Critical Gaseous Flows)

### DESCRIPTION

THE QUANTOMICS-LIU (QL) series of cryogenic flowmeters is specifically designed for measuring the flow of liquid and super-critical gases. New concepts and rigorous theories are used in these flowmeters, taking into account the characteristics and complex phase (liquid, vapor, and solid not excluded) structure of the cryogenic fluids and including knowledge of both normal and abnormal cryogenic flow phenomena (Fig. 5). Designed with an awareness of the related problems and verified through prolonged experimental testing, the QL cryogenic flowmeters have been confirmed for their conceptual and performance superiorities.

A minimum of constriction is preferred in the QL flowmeters to anticipate and accommodate the often unstable characteristics of cryogenic fluids and to insure a smooth and stable flow-through

process. The least amount of perturbation in the fluids' thermodynamic properties is realized through the maintenance of favorable flow impedance,<sup>2</sup> whereupon the pressure drop is also reduced to a minimum. Designed for use with even the most corrosive fluids, such as liquid fluorine, these features are responsible for the durability and accuracy of the QL flowmeters, which have the corrosive-cavitational effects greatly minimized.

These deliberate design efforts, while noteworthy, are of particular importance to modern propulsion and industrial applications where cumulative line-drop and system instabilities are to be minimized. Whereas, in conventional general-purpose flowmeters, it has been the practice to achieve low-range performance through "brute-force" constriction of the entrance or rotor section for favorable Reynolds number effects, such methods can be detrimental to cryogenic applications. In the QL flowmeters, accuracy over a wide flow range is achieved through use of novel design features — features based on knowledge of cryogenic fluid dynamics which, due to the different characteristics of liquid gases, cannot always be dealt with in the same manner as in ordinary liquid flow.

<sup>2</sup>Flow impedance is defined as the ratio of pressure variation to flowrate variation.

**EL**  
ELASTRONICS  
LABORATORIES



**QUANTOMICS, INC.**

**QUANTUM  
DYNAMICS**

19458 Ventura Blvd., Tarzana, California 91356  
Phone: 213-345-6828  
Mailing Address: P.O. Box 865, Tarzana, California 91356

## NEW CONCEPTUAL FEATURES OF QUANTOMICS-LIU SYSTEMS

1. Highly responsive, near-frictionless, "piggy-back" bearing principle of long operating life.
2. Concept of matching flow impedances.
3. Feedback effects due to positive and negative blade concept.
4. Least-constriction configuration with fluid dynamic control device.
5. High-resolution, linear density sensing without moving parts or springs.
6. Nonretarding and dragless cryotronic pickup.
7. Anti-seizure mechanical design.
8. Exact electronic computing of density and mass flow.

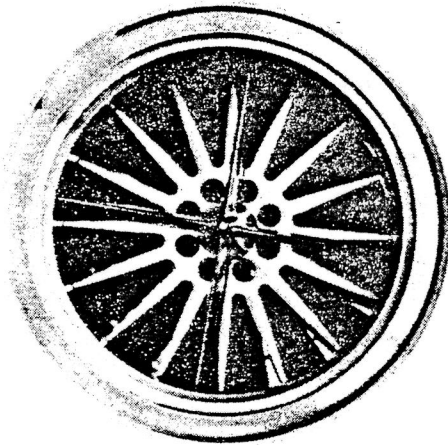
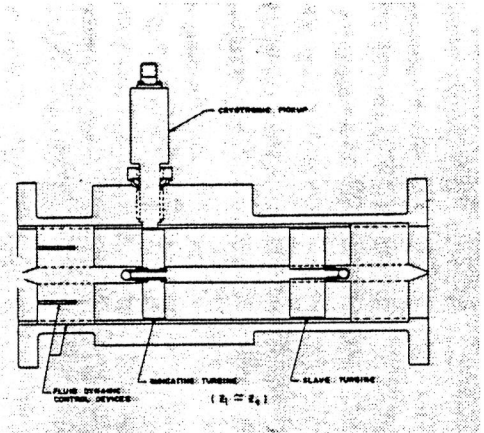


Figure 5.



In terms of general physical features (Fig. 5), the QL flowmeter consists of an "indicating" turbine which rides "piggy-back" on the rotating shaft of a slave turbine. Both turbines respond to the same flow at approximately the same speed, so the relative motion between the indicating turbine and its bearing shaft is maintained at near zero level. In totality, this arrangement then represents a radically new bearing principle which, according to Petroff-Sommerfeld theories, reduces the dynamic friction (or retarding force) to a constant minimum level over an extremely wide range of flowrate. This new concept, in combination with the flowmeter's dragless, cryotronic pickup, accounts for the flowmeter's exceptional response sensitivity. The co-rotational feature also creates two, well matched, impedance zones in the flow field — a feature which is highly beneficial from the fluid-dynamic standpoint. At the same time, an overall feedback effect is also created, which contributes to the enhanced accuracy and stability of metering response. In some larger flowmeters, such as for liquid hydrogen applications, a local feedback effect is also added, utilizing Liu's "negative blade" concept. In terms of fluid-dynamic features, the angle, contour and moment of inertia, etc., of the turbine blades as well as the stream straightening, coupling and profile-control devices are designed to effect the best possible compromise between the theoretical correctness, responsiveness, and adequate strength over a wide range of flow conditions.

To insure reliable and fail-safe operation at low temperature, QL flowmeters use only selected special alloys, metals, and nonmetallic materials. Because the flowmeter does not rely on the magnetic method of sensing, magnetic metal is not permitted in the instrument: the ferritic content of the vital sensing element is kept well below 1 percent. This prevents damage due to "twist" changes or other brittle failures in the crystal structure. The trouble free and long life operation of QL flowmeters is further implemented by an anti-seizure design of the moving element assembly, which automatically adjusts for the thermal contraction and expansion factor, even under the most sudden temperature change.

QL flowmeters use a "cryotronic" sensing

method which differs drastically from the conventional magnetic frequency pickups. The greatly increased magnetic coupling of conventional pickups adversely affects the accuracy of cryogenic flow measurement because the field increases by tens or hundreds of times at very low temperatures. Recent literature also indicates that near the critical points, radiating magnetic fields can be generated by the collapse and formation of vapor pockets; such spurious fields are known to have caused erroneous outputs in many conventional magnetic and FM pickups, resulting in signals which are irrelevant to the flow quantities. In contrast, the self-adjusting cryotronic pickups of QL flowmeters are dragless sensors, designed to be completely immune to any such detrimental effects at low temperatures (see Bulletin 5.1). These flowmeters give unhindered freedom of response, high resolution, and high sensitivity of the turbine in metering cryogenic flow, and provide a strong flowrate-proportional signal over a wide range of temperature without the necessity for any manual adjustments.

### LARGE FLOWMETERS

Aside from material and other engineering factors, the reliability and fail-safe features of a cryogenic flowmeter are intimately related to the fluid dynamics of the effluent and the dynamic response of the sensing elements. For large-diameter cryogenic flowmeters and or high flow rates, where the reliability considerations are of particular importance, the large sensing element must be made responsive. For, a large mass of "struggling" sensing element is incapable of performing reliable, accurate flow-measurement functions, as is evident by the following simplified differential equation in which the dynamic terms of flowmeter response occupy an important role:

$$\tau \dot{\omega} + \omega = K\dot{Q}$$

where

$$\tau = C K\dot{Q}$$

is the time constant of the sensing element.

$\dot{Q}$  is the flowrate.

\*Liu, F. F., *Archiv. F. Tech. Messen*, 174R, 145 (Nov. 1958); Liu, F. F. and Berwin, T. W., *Rev. Sci. Instr.*, 29, 14 (1958); Liu, F. F. et al, *NBS Monograph* 67 (1964); Ower, E., *Phil. Mag.*, Ser.7, 23, 992 (1937).

$\omega = K\dot{Q}(1 - e^{-t/\tau})$  is the output frequency of the flowmeter.

K and C are constants.

QL flowmeters of all sizes, in consideration of accuracy and reliability, have always emphasized transient response. Large QL cryogenic flowmeters are often custom designed for specific operations. Such designs are arrived at through methodical analysis and solution of a number of simultaneous equations, so that reliability, measurement accuracy, and resolution are optimized for the particular application. But the basic superiority of these large QL flowmeters is due to the numerous original design features; as a result, these QL flowmeters represent a radical departure from conventional flowmeters, not only with greatly improved reliability and life span but also with considerably higher measurement resolution and accuracy.

### ADJUSTABLE-MANIFOLD FLOWMETERS

The QL Adjustable-Manifold Multirange Flowmeter System was developed to fill a need for highly precise and unusually wide-range flow measurement, calibration, control, and automatic fluid

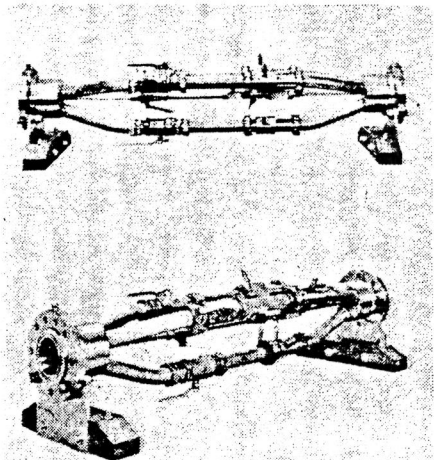


Figure 6. Adjustable-Manifold Flowmeter System

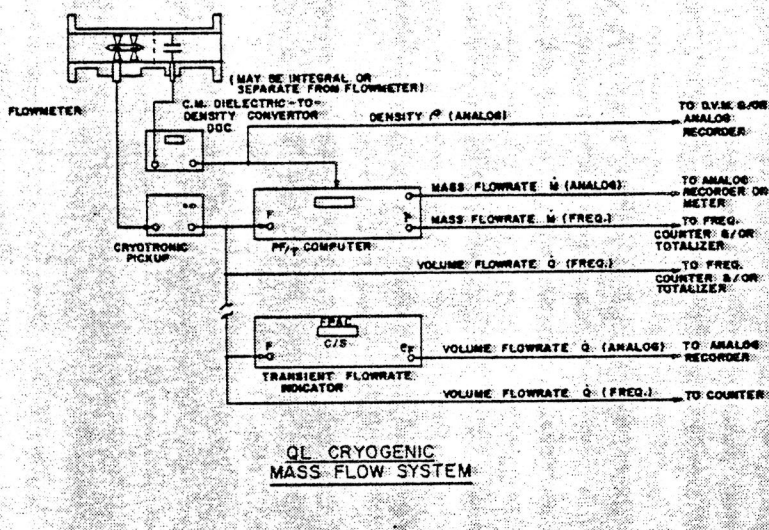


Figure 7. QL Cryogenic Mass Flow System

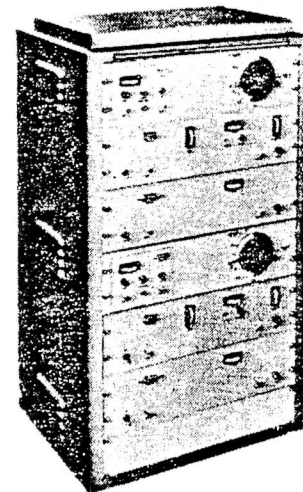
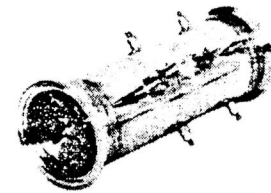


Figure 8. Early Model of Dual-Channel LH<sub>2</sub> Mass/Transient Flow Measurement System

transfer in aerospace and industrial applications. This system makes possible very high resolution and accurate measurement at exceptionally high flowrates by summing the multichannel frequency outputs; yet the same system also enables the metering of low flowrates with each individual flowmeter. Implementing the smooth-transition manifold design with the use of adjustable Foettinger-Frey vanes, the QL manifold flowmeter system has the following notable features:

- Insures proper distribution of the fluid flow between the individual flow channels under various pressure-head, flowrate, and fluid characteristics.
- Provides means for the precise adjustment of flow distribution with a minimum of detrimental fluid-dynamic phenomena, such as serious cavitation, cross-over transient, vortex, swirling, and other undesirable hydrodynamic and acoustic phenomena.
- Facilitates the use of a number of high-resolution, smaller-sized flowmeters for the precise measurement of large amounts of flow, while at the same time insures that the properties of the effluent (e.g., density) are maintained essentially the same in all flow channels. This can only be done if the distribution of the flow can be adjusted and divided smoothly and evenly.
- Drastically reduces the pressure drop and flow impedance at high flowrates.

With a passive type of manifold, it would be virtually impossible to satisfy the above features while achieving the proper distribution of flow among a multiplicity of channels; as such, the passive manifold is incapable of highly accurate measurement, calibration, and control functions

of many channels. Such disadvantages are eliminated in Quantum Dynamics' adjustable-manifold flowmeters.

Existing standard QL adjustable-manifold systems (Fig. 6) are of 3-, 4-, or 5-channel design and of stainless-steel construction. A typical system has flanged inlet and outlet sections of 4.81-in. ID. The individual channels are of 2-inch tubing, designed for operating pressures of up to 3500 psi. As a gaseous-flow calibration system, a 5-channel unit of existing design that uses 2-in. QL flowmeters has a flow range of from 1.5 to 5000 scfm, achieving a count-rate output of 5000 cps at maximum flowrate. For cryogenic flow, the same system has an operating flow range of from 2.5 to 5000 gpm.

#### SPECIFICATIONS, QUANTOMICS-LIU FLOWMETERS

**Effluent:** cryogenic hydrogen, helium, nitrogen, oxygen, fluorine, argon, and other gases in liquid and/or vapor-gaseous phases, including mixed-phase fluids and cryogenic fluids in supercritical and superheated states.

**Sizes:** standard, ½, ¾, 1, 1¼, 1½, 2, 3 inches; special, ¼, 4, 5, 8, 16 inches.

**Temperature range:** 5°K to 370°K.

**Flowrate range:** consult Quantum Dynamics' engineering and sales staff on size and flow range for your particular application, in view of the consideration that mass-flow range determination involves the state and density of the fluid, pressure drop, measurement resolution, etc.

**Accuracy:** 0.2% or within.

**Linear response range:** 50-to-1 or higher; special units have achieved 500-to-1 or higher.

**Materials used:** special cryogenic-grade stainless steel, alloyed for low-temperature operation.

**Coupling effect of sensing element:** none.

**Associated equipment:** vacuum jacket; CM dielectric-to-density converter; PF/T computer; FPAC transient-flowrate indicator. Flowrate (limit-setting) warning devices can be supplied with the basic volumetric flowmeters as additional units for a variety of flow measurement and control functions.

**Outputs available:** (for general arrangement, see Fig. 7)

Output signal	Basic form	Available form
mass flowrate	frequency	analog
totalized mass flow	totalized pulse number	
volume flowrate	frequency	analog
totalized volume flow	totalized pulse number	
density	analog voltage	frequency
transient (time-varying) flowrate	analog voltage	

#### MASS FLOW SYSTEMS

Quantum Dynamics' QL flowmeters — when teamed with its CDDC density-measurement unit and compact Model PF/T-500 Mass Flow Computer (Bulletin 4.1) — provide, in one single compact system, accurate readings of mass flowrate, volume flowrate, totalized mass and or volume flow, and density (Fig. 7). The flowmeter represents an advanced, cryogenic flow-measurement unit that covers flow ranges from very minute to extremely large flowrate (with a QL adjustable-manifold flowmeter system) and provides accurate data from the lowest temperature down through the liquid-solid phase to supercritical temperature regimes.

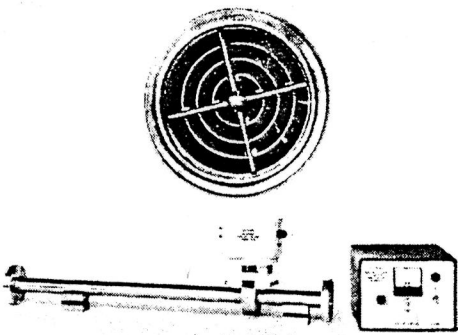


Figure 9. Dielectric and Level Sensing Section.

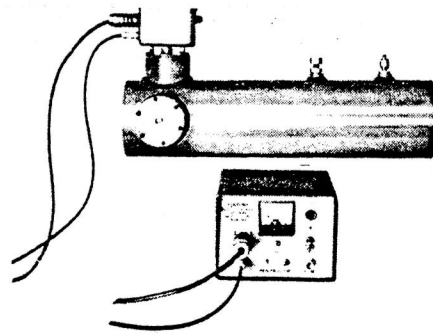


Figure 10. Vacuum Jacketed LH<sub>2</sub> Dielectric-to-Density Converter

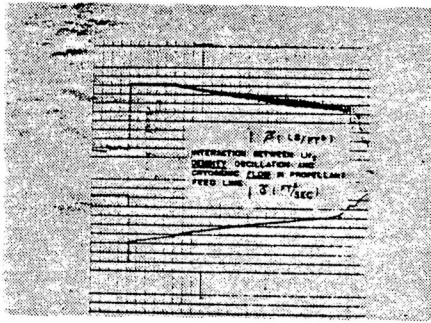


Figure 11. Simultaneous Recording of LH<sub>2</sub> Density and Flowrate

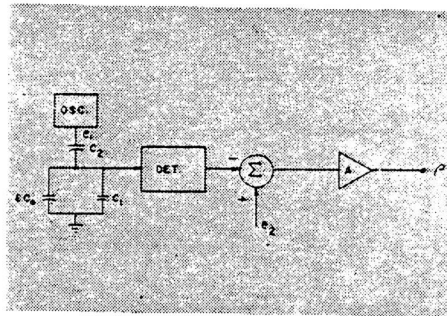
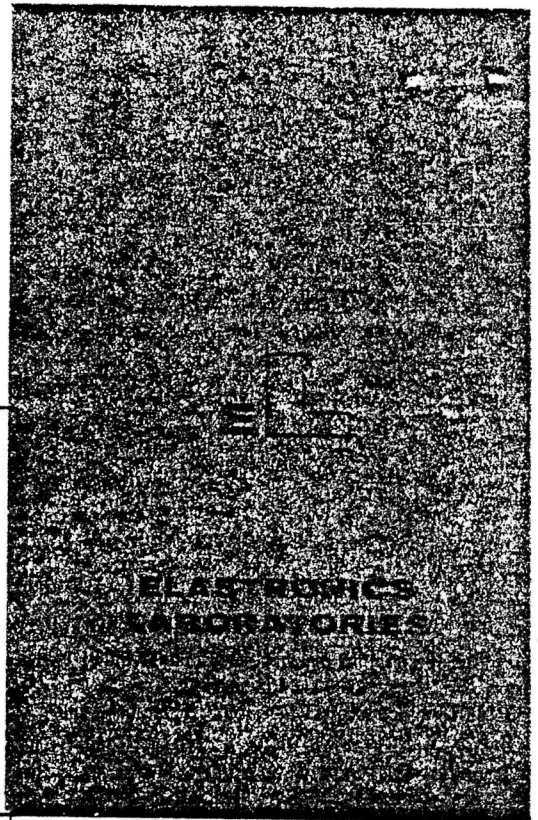


Figure 12. Block Diagram of CDDC Electronic Indicator



## CRYOGENIC DENSITY MEASUREMENT DEVICES

### (Quantum Dynamics/Elastronics CDDC Type Cryogenic Dielectric-to-Density Converter)

From the lowest temperature limit of liquid gases, through the supercritical, to the gaseous regimes, there is encompassed many hundreds of degrees of temperature difference. The equations of the state for each regime differ from one another. Only one density-measurement method is known to be valid throughout the liquid and supercritical regimes;<sup>1</sup> this is the rigorous method used in Quantum Dynamics/Elastronics' Cryogenic Dielectric-to-Density Converter (CDDC): an instrument based on the application of the Lorentz macroscopic dielectric theory. With the CDDC, an accurate reading of density can be obtained directly at high resolution and with large signal levels in volts. The operation and calibration processes are simple; costly cryogenic calibration is not strictly necessary; and the output is an exact linear function of density. In addition, the same instrument provides data on the time-varying density phenomena (Fig. 11) of the fluid, which is often invaluable to the analysis and trouble shooting of cryogenic flow systems. In fact, the instrument even indicates solid or vapor phase formation in the system. Thus, with a single compact unit, many of the most difficult cryogenic measurement functions (density, phase change, temperature) can be performed with confidence.

### THEORY AND OPERATION

The sensor section of the CDDC — which can be a separate or an integral part of the flowmeter

<sup>1</sup>Liu, F. F., "Instrument for the Direct and Continuous Measurement of Liquid Hydrogen Density," *Rev. Sci. Instr.*, to be published in forthcoming issue; Stewart, J. W., *J. Chem. Phys.*, 40, 3297 (1964); Froelich, H., *Theory of Dielectrics*, Oxford (1958), pp. 108-111.

(Fig. 9) — is designed to provide stable, sensitive measurement of the dielectric properties of the cryogenic fluid. The electronic section (Fig. 10) then converts the sensed quantity into a direct indication of density by performing a rigorous — not approximate — on-line computation according to the Lorentz-Clausius-Mossotti formula. This formula is well known in macroscopic dielectric theory to be an exact representation of the dielectric-density relationship for cryogenic fluids and all nonpolar liquids and gases:

$$\rho = nM N = \bar{K}(\epsilon - 1)(\epsilon + 2)$$

where

$n$  is the number of molecules per unit volume,

$N$  is the Avogadro number,

$M$  is the molecular weight,

$\epsilon$  is the dielectric constant,

$\epsilon - 1/\epsilon + 2$  is the Clausius-Mossotti ratio,

$\bar{K} = 3M/4\pi N\alpha$  is a constant with  $\alpha$  as the molecular polarizability,

$\rho$  is the density of the cryogenic fluid.

Figure 12 is an illustrative block diagram of a CDDC circuit. It can be shown that when  $e_1$ ,  $e_2$ ,  $C_1$ ,  $C_2$ , and  $A$  are properly selected, an exact solution of the L-C-M formula can be effected, resulting directly in an accurate and linear indication of the density. It is also obvious from the equation that the present method is essentially one of counting the number of molecules per unit volume, which is valid for space flight as well as ground conditions.

For example, when the density of the fluid is 4.33 lb ft<sup>-3</sup>, the output of the CDDC is exactly 4.33 volts. In some models, the cable effect is eliminated by the use of a negative-capacitance compensation; and, an automatic reference check is provided that gives the zero-datum line once every five seconds. The density output can be continuously recorded by means of an oscillograph,

showing both the steady and transient pattern of density together with its zero (density) reference line. The CDDC is thus a unique high-resolution and accurate density-measurement device, capable of performing a variety of measurement functions with great simplicity and reliability. For instance, special instruments of this principle have been constructed to provide reading of cryogenic propellant-mass quantities in tank under "zero-g" conditions in substitution of conventional level gauges.

### SPECIFICATIONS, CDDC TYPE

**Applications:** a) density measurement of cryogenic fluids in liquid, vapor-gaseous, and solid phases and applicable to mixed-phase fluids; b) as an element of a cryogenic mass flow measurement system; c) as a system's abnormal and sub-normal operational warning-monitoring device; d) as an indirect cryogenic temperature-measurement device of high resolution; e) as an indicator for the amount of cryogenic fluid in the tank under "zero-g" space-flight conditions; and others.

**Accuracy:** within  $\pm 1\%$  (high-accuracy model also available).

**Input:** cryogenic fluids in still or flowing condition, either in single or mixed phase. Fluid may be of any of the following: liquid and or vapor phase hydrogen, helium, nitrogen, oxygen, fluorine, argon, or any other single component nonpolar fluid.

**Output:** 0 to 5 volts or emf, which is a direct and linear indication of the cryogenic density. An automatic "zero density reference" signal is provided once every 5 seconds to eliminate effects due to second-order change in the dielectric properties of the cable.

**Output impedance:** 10 ohms.

**Load allowable:** 3 ma maximum.

**Stability:** long-term drift,  $\pm 0.2\%$ .

## TANK, FREON

### PURPOSE & REQUIREMENTS

These tanks are to be used to store and supply Freon 11 and Freon 113 for the experiments. The requirements are:

<u>Experiment</u>	<u>Fluid</u>	<u>Quantity</u>
II	Freon 11	14.2 litre (0.5 ft <sup>3</sup> )
IV	Freon 113	23.8 litre (0.84 ft <sup>3</sup> )
Temperature:	21.1C (70F) nominal	
Operating Pressure:	101.4-137.9 kN/m <sup>2</sup> (14.7-20 psia) nominal	
Proof Pressure:	1034 kN/m <sup>2</sup> (150 psia)	

### HARDWARE STATUS

A capillary acquisition tank was described in our previous conceptual design study, Ref. 1 as applicable to Experiments I & II. This tank is assumed for use in these experiments here, as well as for the Liquid Orientation Experiment, No. IV.

### DESCRIPTION

A sketch of this spherical tank is shown Figure 4-3.

Weight, dry:	13.2 kg (29.1 lb) (Ref. 1)
Diameter:	29.2 cm (11.5 in) (Ref. 1)
Power:	0

### APPLICABLE EXPERIMENTS

<u>Experiment</u>	<u>No. Reqd.</u>
II	1
IV	1

## TANK, WATER

### PURPOSE & REQUIREMENTS

To store and introduce water into the water/air recirculation test loop for the Flow Pattern/Pressure Drop Experiment, No. I.

Storage Capacity:	3.28 litre (200 in <sup>3</sup> ) (0.87 gal.)
Type:	Positive expulsion by spring force
Expulsion Pressure:	34.5 kN/m <sup>2</sup> gauge ( ~5 psig)

### HARDWARE STATUS

Specially built based on existing designs.

### TECHNICAL DESCRIPTION

Estimated properties of this tank are:

Weight, dry :	0.91 kg (2 lb)
Volume:	4.25 litre (0.15 ft <sup>3</sup> )
Cost:	\$5,000

### APPLICABLE EXPERIMENTS

Experiment I, 1 reqd.

## THERMISTORS

### PURPOSE & REQUIREMENTS

To measure fluid temperatures in various experiments and transfer this data to the CDMS.

Range:	-3.3 - 37.8 C (26-100F)
Resolution:	0.01 C (0.2F)
Accuracy:	±0.1 C (± 0.2F)

### HARDWARE STATUS

Off-the-shelf sensors available. Specially made compact signal conditioners and a 2 volt dc regulated power supply will be required.

### TECHNICAL DESCRIPTION

Thermistor — Various probe configurations will be used to meet individual requirements. Several typical probe configurations are shown in the attached catalog sheet from Omega Engineering, Inc.

Typical Weight:	0.023 kg (0.05 lb)
Size:	Negl.
Power:	See signal conditioner
Cost:	\$50

#### Signal Conditioner (estimates)

Input Voltage:	2 volts dc
Weight:	0.023 kg (0.05 lb)
Size:	8.2 cm <sup>3</sup> (0.5 in <sup>3</sup> )
Power:	Negl.
Cost:	\$100

Power Supply — The estimated properties of a suitable power supply are:

Input Power:	115 volt, 400 Hz, < 5 watts
Output Power:	2 volt dc, < 1 watt
Weight:	0.91 kg (2 lbs)
Size:	819 cm <sup>3</sup> (50 in <sup>3</sup> )
Cost:	\$1K

THERMISTORS (CONT'D)

APPLICABLE EXPERIMENTS

<u>Experiment</u>	<u>Measurement</u>	<u>No. Required</u>		<u>Power Supply</u>
		<u>Thermistor</u>	<u>Signal Cond.</u>	
I & II	$T_1$ to $T_{14}$	14	14	}
IV	$T_1$ & $T_2$	2	2	
V	$T_1$	1	1	

# Linear Thermistor Components and Probes



## NEW! Linear Components

For applications requiring thermistors with linear response to temperature change, Omega offers linear components. These unique devices consist of a thermistor composite and resistor composite.

Thermistor composites 44018 and 44019 each contain two thermistors packaged in a single sensor (Figures 1A & 1B). Thermistor composite 44020 contains three thermistors packaged as a single sensor (Figure 1C).

Resistor composites for use with 44018 and 44019 thermistor composites consist of two metal film resistors of the size shown in Figure 2. Resistor composites for use with the 44020 thermistor composite consist of three of the same type metal film resistors.

Linear components are manufactured with different values for different temperature ranges. When they are connected in networks shown in Figures 3 and 4, they produce a varying voltage or resistance linear with temperature.

One of the basic network manifestations is a voltage divider as in Figure 3A for components other than #44212, and as shown in Figure 3B for component #44212. The area within the dashed lines represents the thermistor composite. The network hookup for linear resistance versus temperature is shown in Figure 4A for Linear components except #44212 and in Figure 4B for #44212.

Following is a description of why these networks produce linear information. The equation for a voltage divider network, consisting of R and R<sub>0</sub> in series is:

$$E_{out} = E_{in} \frac{R}{R + R_0}$$

where E<sub>out</sub> is the voltage drop across R. If R is a thermistor, E<sub>out</sub> is plotted versus temperature, the total curve will be essentially non-linear and of a general "S" shape with linear or nearly linear portions near the ends and in the center.

Figure 1A. Thermistor Composite 44018

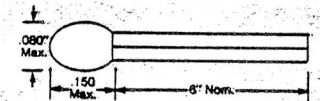


Figure 1B. Thermistor Composite 44019

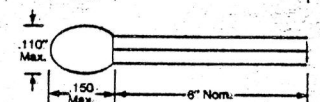


Figure 1C. Thermistor Composite 44020

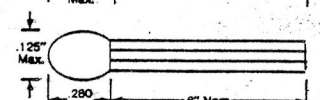
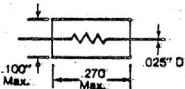


Figure 2. Metal Film Resistor



If R is modified by the addition of other thermistors and resistors, linearity of the center section of the curve, where sensitivity is greatest, can be extended to cover a wide range of temperatures. This section follows the general equation for a straight line, Y = mx + b or in terms of a linear component:

For Voltage Mode

$$E_{out} = \pm MT + b$$

where M is slope in volts/°T  
T is temperature in °C or °F  
b is the value of E<sub>out</sub> when T = 0°

For Resistance Mode

$$R_1 = MT + b$$

where M is slope in ohms/°T  
T is temperature in °C or °F  
b is the value of R in ohms when T = 0°

### Linear Voltage vs. Temperature

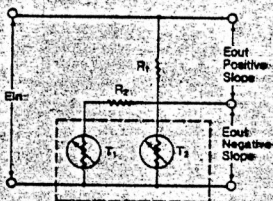


Figure 3A

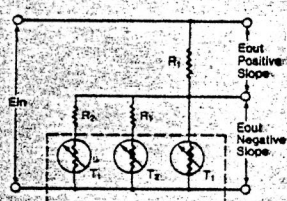


Figure 3B

### Linear Resistance vs. Temperature

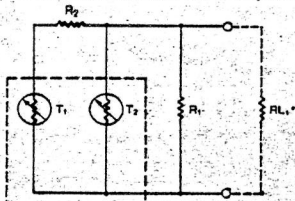


Figure 4A

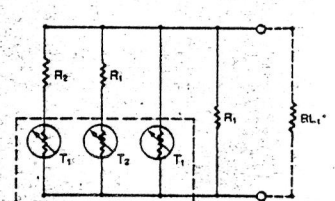


Figure 4B

\*RL<sub>1</sub> may be any value as long as a new R<sub>1</sub> value, R<sub>1A</sub> is selected to satisfy the relationship:  $R_{1A} = \frac{R_1 \times RL_1}{RL_1 - R_1}$

Sensitivity is 400 times greater than an IC thermocouple. Thermistor values as high as 30mV/°C are common. In addition, output voltage may be applied to a recorder or digital voltmeter to produce a precise, sensitive, direct reading thermometer.

### Multiplexing

The 44018 thermistor composite is used in four of the linear components. The part that changes in each component is the resistor composite, which determines the temperature range. Therefore, the 44018 thermistor composite can be used over the entire -30 to +100°C temperature range by simply changing resistor composites. Its accuracy and interchangeability over the full range is ±0.15°C.

It is not mandatory that Omega resistor composites be used with the 44018 thermistor composite. Any 0.1% resistors of the proper values and with a temperature coefficient of 30 PPM or less may be substituted.

In other situations it is frequently desirable to have thermistor composite temperature sensors at more than one location. When this is required, it is not necessary to have a

separate resistor composite for each thermistor composite. It is possible to multiplex any number of thermistor composites through a single resistor composite for greater design flexibility.

Linear Thermistor Components are manufactured under U.S. Patent #3316765 and Canadian Patent #782790.

### Thermistor Pricing

Part No.	List Price 1-9 units	Less 10% 11-24 units	Less 20% 25-100 units	Less 30% 101-500 units
44018	\$15.00	\$13.50	\$12.00	\$10.50
44019	15.00	13.50	12.00	10.50
44020	30.00	27.00	24.00	21.00
44201	20.00	18.00	16.00	14.00
44202	20.00	18.00	16.00	14.00
44203	20.00	18.00	16.00	14.00
44204	20.00	18.00	16.00	14.00
44211	20.00	18.00	16.00	14.00
44212	35.00	31.50	28.00	24.50

## Component Specifications

	°C	°F	°C	°F
Linear Component P/N	44201	44201	44202	44202
Range	0° to +100°C	+32° to +212°F	-5° to +45°C	+23° to +113°F
Thermistor Composite P/N	44018	44018	44018	44018
Resistor Composite Values	R <sub>1</sub> 3200 Ω, R <sub>2</sub> 6250 Ω	R <sub>1</sub> 3200 Ω, R <sub>2</sub> 6500 Ω	R <sub>1</sub> 5700 Ω, R <sub>2</sub> 12,000 Ω	R <sub>1</sub> 5700 Ω, R <sub>2</sub> 12,000 Ω
Thermistor Accuracy & Interchangeability	±0.15°C -30° to +100°C	±0.27°F -22° to +212°F	±0.15°C -30° to +100°C	±0.27°F -22° to +212°F
E <sub>0</sub> Positive Slope	E <sub>out</sub> = (+0.0053483 Ein) T + 0.13493 Ein	E <sub>out</sub> = (+0.00297127 Ein) T + 0.03985 Ein	E <sub>out</sub> = (+0.0056846 Ein) T + 0.194142 Ein	E <sub>out</sub> = (+0.0031581 Ein) T + 0.093083 Ein
E <sub>0</sub> Negative Slope	E <sub>out</sub> = (-0.0053483 Ein) T + 0.86507 Ein	E <sub>out</sub> = (-0.00297127 Ein) T + 0.96015 Ein	E <sub>out</sub> = (-0.0056846 Ein) T + 0.805858 Ein	E <sub>out</sub> = (-0.0031581 Ein) T + 0.906917 Ein
Resistance Mode	R <sub>T</sub> = (-17.115) T + 2768.23	R <sub>T</sub> = (-9.508) T + 3072.48	R <sub>T</sub> = (-32.402) T + 4593.39	R <sub>T</sub> = (-18.001) T + 5169.42
*E <sub>in</sub> MAX.	2.0 VOLTS	2.0 VOLTS	3.5 VOLTS	3.5 VOLTS
*I <sub>T</sub> MAX.	625 μA	625 μA	615 μA	615 μA
***Load Res. Min. RL	3 MEG Ω	3 MEG Ω	10 MEG Ω	10 MEG Ω
Linearity Deviation	±0.216°C	±0.388°F	±0.065°C	±.12°F
Linear Component P/N	44203	44203	44204	44204
Range	-30° to +50°C	-22° to +122°F	+30° to +100°F	
Thermistor Composite P/N	44018	44018	44018	
Resistor Composite Values	R <sub>1</sub> 18,700 Ω, R <sub>2</sub> 35,250 Ω	R <sub>1</sub> 18,700 Ω, R <sub>2</sub> 35,250 Ω	R <sub>1</sub> 5700 Ω, R <sub>2</sub> 12,400 Ω	
Thermistor Accuracy & Interchangeability	±0.15°C -30° to +100°C	±0.27°F -22° to +212°F	±.27°F -22° to +212°F	
E <sub>0</sub> Positive Slope	E <sub>out</sub> = (+0.0067966 Ein) T + 0.34893 Ein	E <sub>out</sub> = (+0.00377588 Ein) T + 0.228102 Ein	E <sub>out</sub> = (+0.0031289 Ein) T + 0.09232 Ein	
E <sub>0</sub> Negative Slope	E <sub>out</sub> = (-0.0067966 Ein) T + 0.65107 Ein	E <sub>out</sub> = (-0.00377588 Ein) T + 0.771898 Ein	E <sub>out</sub> = (-0.0031289 Ein) T + 0.90768 Ein	
Resistance Mode	R <sub>T</sub> = (-127.096) T + 12175	R <sub>T</sub> = (-70.608) T + 14435	R <sub>T</sub> = (-17.834) T - 5173.8	
*E <sub>in</sub> MAX.	3.0 VOLTS	3.0 VOLTS	4.0 VOLTS	
*I <sub>T</sub> MAX.	475 μA	475 μA	685 μA	
***Load Res. Min. RL	10 MEG Ω	10 MEG Ω	10 MEG Ω	
Linearity Deviation	±0.16°C	±0.29°F	±0.055°F	
Linear Component P/N	44211	44211	44212	44212
Range	-55° to +85°C	-67° to +185°F	-50° to +50°C	-58° to +122°F
Thermistor Composite P/N	44019	44019	44020	44020
Resistor Composite Values	R <sub>1</sub> 3525 Ω, R <sub>2</sub> 5825 Ω	R <sub>1</sub> 3525 Ω, R <sub>2</sub> 5825 Ω	R <sub>1</sub> 23,100 Ω, R <sub>2</sub> 88,200 Ω R <sub>3</sub> 38,000 Ω	R <sub>1</sub> 23,100 Ω, R <sub>2</sub> 88,200 Ω R <sub>3</sub> 38,000 Ω
Thermistor Accuracy & Interchangeability	±0.4°C 0 to +85°C ±0.8°C 0 to -55°C	±.72°F to 185°F ±1.44°F to -67°F	±0.1°C -50° to +50°C	±.18°F -58 to +122°F
E <sub>0</sub> Positive Slope	E <sub>out</sub> = (+0.005033 Ein) T + 0.34407 Ein	E <sub>out</sub> = (+0.0027961 Ein) T + 0.254595 Ein	E <sub>out</sub> = (+0.00559149 Ein) T + 0.40700 Ein	E <sub>out</sub> = (+0.00310638 Ein) T + 0.30760 Ein
E <sub>0</sub> Negative Slope	E <sub>out</sub> = (-0.005033 Ein) T + 0.65593 Ein	E <sub>out</sub> = (-0.0027961 Ein) T + 0.745405 Ein	E <sub>out</sub> = (-0.00559149 Ein) T + 0.59300 Ein	E <sub>out</sub> = (-0.00310638 Ein) T + 0.69240 Ein
Resistance Mode	R <sub>T</sub> = (-17.74) T + 2312	R <sub>T</sub> = (-9.855) T + 2627.36	R <sub>T</sub> = (-129.163) T + 13698.23	R <sub>T</sub> = (-71.757) T + 15994.5
E <sub>in</sub> Max.	2.0 VOLTS	2.0 VOLTS	3.5 VOLTS	3.5 VOLTS
I <sub>T</sub> MAX.	833 μA	833 μA	700 μA	700 μA
***Load Res. Min. RL	10 MEG Ω	10 MEG Ω	10 MEG Ω	10 MEG Ω
Linearity Deviation	±1.1°C	±2°F	±0.15°C (Condition "A")** ±0.08°C (Condition "B")**	±.27°F (A) ±.15°F (B)

\*E<sub>in</sub> Max and I<sub>T</sub> Max values have been assigned to control the thermistor self-heating errors so that they do not enlarge the component error band; i.e., the sum of the linearity deviation plus the probe tolerances. The values were assigned using a thermistor dissipation constant of 8mW/°C in stirred oil. If better heat-sink methods are used or if an enlargement of the error band is acceptable, E<sub>in</sub> Max and I<sub>T</sub> Max values may be exceeded without damage to the thermistor probe.

\*\*The maximum error at any point is the algebraic sum of the thermistor manufacturing tolerances, plus linearity deviation, a fixed network behavior. Condition "A" is the worst case linearity deviation of ±0.15°C and may occur with the ±0.1% resistors supplied. Condition "B" exists when the three resistors are within ±0.02% of nominal, which reduces linearity deviation to ±0.08°C.

\*\*\*See Figure 3, K-13

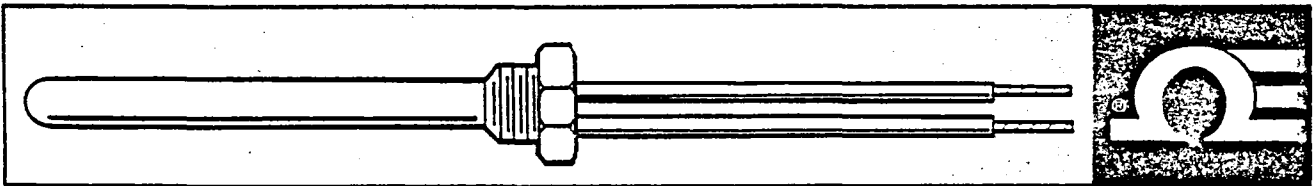
NOTE: The time required for a thermistor composite to indicate 63% of a newly impressed temperature is 1 second in air, 10 seconds in stirred oil, and 10 seconds in free still air.



UNIQUE DESIGN  
PRECISION MANUFACTURE  
CALIBRATION SERVICE

# THERMISTORS

<p><b>O-87</b></p>	<p><i>Vinyl Tip with Shielded-Jacketed Microphone Cable</i></p> <p><b>Biological:</b> Ideal for animal and biological applications in esophageal or rectal temperature measurement. It is also suitable for use in geographic and oceanographic applications. Design characteristics present an extremely rugged sensor assembly at a minimum cost.</p> <p>Leads: 12" Maximum temperature: 100°C Body Type <b>O-87</b></p> <p><b>All prices include sensor \$29</b></p>	<p>O-87-UUA-32J4 2,252.0</p> <p>O-87-UUA-33J4 3,000.0</p> <p>O-87-UUA-35J3 5,000.0</p>	
<p><b>O-88</b></p>	<p><b>Epoxy Encapsulated Thermistor Sensor in Stainless Steel Housing with Vinyl Insulated Leads:</b></p> <p>Surface temperature readings, or control and indication. Ideally suited for applications such as: heat loss or compressor efficiency measurement and control studies of piping systems; determining manifold wall and bearing surface temperatures. Construction facilitates easy attachment to skin or other flat surfaces.</p> <p>Leads: 12" Maximum temperature: 100°C Body Type <b>O-88</b></p> <p><b>All prices include sensor \$39</b></p>	<p>O-88-UUA-32J4 2,252.0</p> <p>O-88-UUA-33J4 3,000.0</p> <p>O-88-UUA-35J3 5,000.0</p>	
<p><b>O-90</b></p>	<p><b>Exposed Epoxy Coated Thermistor Sensor mounted in open-end Stainless Steel housing with vinyl shielded-jacketed Microphone cable.</b></p> <p>Air temperature measurement, control and indication; design characteristics offers a perfect sensor assembly for monitoring gas streams; ideal for temperature measurement and control of remote air readings.</p> <p>Leads: 12" Maximum temperature: 100°C Body Type <b>O-90</b></p> <p><b>All prices include sensor \$45</b></p>	<p>O-90-UUA-32J4 2,252.0</p> <p>O-90-UUA-33J4 3,000.0</p> <p>O-90-UUA-35J3 5,000.0</p>	
<p><b>O-91</b></p>	<p><b>Closed-End Stainless Steel Tube with Thermistor sensor Mounted in tip. 1/8" N.P.T. fitting with vinyl Shielded-Jacketed Microphone cable.</b></p> <p>Liquid immersion sensor assembly; rugged design and closed-end tube construction. Ideally suited for temperature measurement, control and indication in fluids. Also for use in a wide variety of pressurized systems applications.</p> <p>Leads: 12" Maximum temperature: 100°C Body Type <b>O-91</b></p> <p><b>All prices include sensor \$45</b></p>	<p>O-91-UUA-32J4 2,252.0</p> <p>O-91-UUA-33J4 3,000.0</p> <p>O-91-UUA-35J3 5,000.0</p>	
<p><b>O-92</b></p>	<p><b>Closed-End Stainless Steel tube with Thermistor sensor mounted in tip. 1/8" N.P.T. fitting with vinyl Shielded-Jacketed cable.</b></p> <p>Biological: tubular autoclavable immersion sensor assembly with detachable mating connector. Used in temperature measurement and control of animal operations. Also for use in closed vessels with pressurized systems where detachable leads are desirable.</p> <p>Leads: 12" Maximum temperature: 100°C Body Type <b>O-92</b></p> <p><b>All prices include sensor \$60</b></p>	<p>O-92-UUA-32J4 2,252.0</p> <p>O-92-UUA-33J4 3,000.0</p> <p>O-92-UUA-35J3 5,000.0</p>	



<p style="text-align: center;"><b>O-106</b></p>	<p>Epoxy Encapsulated Thermistor sensor in screw mounted aluminum housing with teflon insulated leads.</p> <p>Surface sensor assembly: designed for a variety of temperature measurement and control applications. It represents a low cost, fast response unit and lends itself to easy mounting on flat surfaces.</p> <p>Leads: 12"</p> <p>Maximum temperature: 100°C</p> <p>Body Type O-106</p> <p>All prices include sensor \$29</p>	<p>O-106-UUA-32J4</p> <p>O-106-UUA-33J4</p> <p>O-106-UUA-35J3</p>	<p>2,252.0</p> <p>3,000.0</p> <p>5,000.0</p>
<p style="text-align: center;"><b>O-107</b></p>	<p>Encapsulated Thermistor sensor in molded housing with teflon insulated leads.</p> <p>Insertion sensor assembly: specifically designed for high reliability, high volume and low cost applications where fast time response and small size are determining factors. The unit is easily affixed by inserting it into a small hole for mounting.</p> <p>Leads: 12"</p> <p>Maximum temperature: 100°C</p> <p>Body Type O-107</p> <p>All prices include sensor \$28</p>	<p>O-107-UUA-32J4</p> <p>O-107-UUA-33J4</p> <p>O-107-UUA-35J3</p>	<p>2,252.0</p> <p>3,000.0</p> <p>5,000.0</p>
<p style="text-align: center;"><b>O-108</b></p>	<p>Stainless steel housing with 1/4" hex head and #8-32 UNC-2A threaded body. Thermistor sensor epoxy encapsulated in housing with teflon insulated leads.</p> <p>Surface sensor assembly: for temperature measurement and control where design problems require stability against vibration and shock. The unit has been designed to meet many requirements of electronic classes, temperature control and measurement problems, where low cost and reliability is a proven factor.</p> <p>Leads: 12"</p> <p>Maximum temperature: 100°C</p> <p>Body Type O-108</p> <p>All prices include sensor \$30</p>	<p>O-108-UUA-32J4</p> <p>O-108-UUA-33J4</p> <p>O-108-UUA-35J3</p>	<p>2,252.0</p> <p>3,000.0</p> <p>5,000.0</p>
<p style="text-align: center;"><b>O-109</b></p>	<p>Closed-end Stainless Steel tube with thermistor sensor mounted in tip. Stainless steel mounting plate with (2) two mounting holes welded to tube. Teflon insulated leads.</p> <p>Air flow sensor assembly: designed to satisfy the many requirements of air temperature measurement and control in Air Conditioning systems and equipment cooling systems. The unit lends itself to easy mounting to standard metal ducting.</p> <p>Leads: 12"</p> <p>Maximum temperature: 100°C</p> <p>Body Type O-109</p> <p>All prices include sensor \$35</p>	<p>O-109-UUA-32J4</p> <p>O-109-UUA-33J4</p> <p>O-109-UUA-35J3</p>	<p>2,252.0</p> <p>3,000.0</p> <p>5,000.0</p>
<p style="text-align: center;"><b>O-110</b></p>	<p>Stainless Steel housing with 1/8" hex head and 1/8"-27 N.P.T. threaded body. Thermistor sensor epoxy encapsulated in housing with teflon insulated leads.</p> <p>Liquid immersion fluid sensor assembly: ideal for obtaining temperature measurement and control readings in pipes or closed vessels within pressurized systems. Threaded hex head design affords greater resistance to shock and vibration when mounted. Leads 12" standard, other lengths possible custom factory.</p> <p>Maximum temperature: 100°C</p> <p>Body Type O-110</p> <p>All prices include sensor \$39</p>	<p>O-110-UUA-32J4</p> <p>O-110-UUA-33J4</p> <p>O-110-UUA-35J3</p>	<p>2,252.0</p> <p>3,000.0</p> <p>5,000.0</p>

## THERMOCOUPLE REFERENCE JUNCTION

### PURPOSE/REQUIREMENTS

The purpose of this unit is to provide reference junctions for the thermocouples of the Pool Boiling Experiment No. III. The thermocouples are integral to the test cells and were specified by the P.I. to be chromel alumel.

No. of Channels:	9
Type of T.C.	Chromel Alumel (Type K)

### HARDWARE STATUS

Off-the-shelf equipment is available.

### TECHNICAL DESCRIPTION

#### Reference Junction

Model:	Omega Model OMI01, Ten Channel Modular Reference Junction
Weight:	0.45 kg (1 lb)
Size:	16.5 × 8.1 × 3.0 cm (6.5 × 3.2 × 1.2 in)
Power:	+14 to +16 volts, 19 mA max. -14 to -16 volts, 20 mA max. <.5 watts (use 28 volt dc supply to provide ±14 volt dc)
Cost:	\$395

### APPLICABLE EXPERIMENTS

Experiment III, 1 reqd. for monitoring test cell thermocouples. (1 also reqd. for use with heater controller, see Controller, Heater specification sheet.)

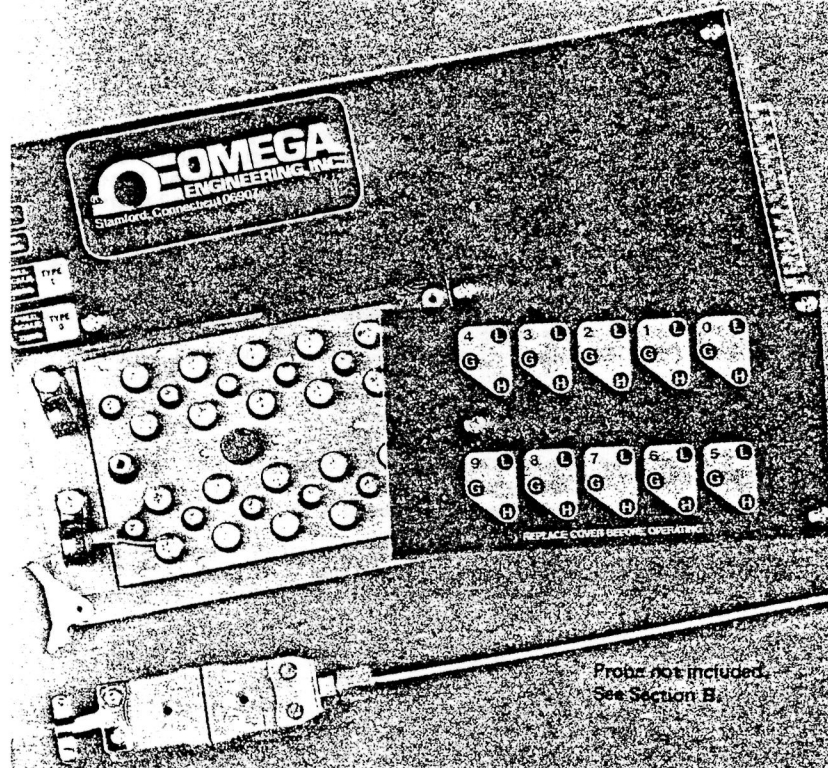
### NOTE

Omega Engineering, Inc., also makes a Ten Channel T.C. Scanner, Model OM 102, which provides automatic compensation and scanning at up to one T.C. per second. Catalog sheets on this unit are attached. It could be used in lieu of the reference junction and CDMS to provide the scanning function, depending upon CDMS interface considerations.

# A rugged thermocouple acquisition slave for your "Micro" or "Mini"

## OM102 Ten-Channel Thermocouple Scanner

**\$795**



Probe not included.  
See Section B.

- On-Board Reference Junction
- Automatic Break Detection
- Low-Thermal Scanner
- Low-Noise Amplifier
- AUTO-ICE™ Zero Stabilization
- Active Filter
- "Dead" Clock Eliminates EMI
- Full CMOS Control Logic
- Rugged Industrial Specs.
- DTL/TTL/CMOS Compatible
- Specifications Guaranteed by 100% Test
- NBS Traceable Calibration

A complete thermocouple acquisition module on a card, the OM102 Thermocouple Scanner solves all of the really hard data acquisition problems inherent in using thermocouples. Here in one compact module is everything you need to go from ten thermocouples directly into our OM110 A/D converter (figure 1) and with some of the best specifications in the industry.

Definitely NOT the usual fragile data acquisition module which must be pampered and buried inside your data system, the industrial-rated OM102 connects directly to input thermocouples, plugs into a standard 6.25" card slot, and extracts microvolt signals in the presence of common-mode voltages as high as 310 volts peak. Interchannel isolation is a remarkable 1000 megohms at 310 volts.

The unit receives grounded or ungrounded thermocouples (or mixed) and references, scans, amplifies, filters, and controls the selected signal. The control logic has been specially configured for bus operation with microprocessors and is fully DTL/TTL/CMOS compatible without buffering. Inside the unit a duplicate of OMEGA's popular OM100 precision reference junction automatically compensates all ten thermocouples and passes them to a low-thermal-read multiplexer (i.e. scanner). Strained leads in the "aux" area both the cumulative leakage effects and the "ply on" hazards often experienced with FET scanners in industrial environments. Strobe in your channel address and the multiplexer selects the channel — break before-make switching is guaranteed — and applies it to a low-noise amplifier. Our unique "AUTO-ICE" zero stabilizer provides zero referencing and eliminates time-based zero drift. After receiving precision amplification your signal is passed through an active filter which strips away the last remnants of 60-Hz noise. Then, for an encore, we even provide an output multiplexer; you can parallel bus the analog outputs of dozens of OM102's directly together.

The OM102 stands alone, complete on-board CMOS control logic obeys the single encode command, remembers current channel and mode selections, switches the multiplexer, cuts and status signals, and even provides three separate timing signals for filter settling, group digital outputs are parallel busable (1 to 20 units @ 200 channels).

**NEW!**

**OM102 PERFORMANCE SPECIFICATIONS**

**1. FUNCTIONAL**

- 1.1 **Functions Provided** Ten-channel automatic thermocouple reference junction, automatic break detection, low-thermal multiplexing, precision gain and filtering of thermocouple (and other low-level) signals, output multiplexing, and control logic including scanner identification.
- 1.2 **Compatibility** Can be commanded directly by OM110A/D Converter, microprocessors, digital logic, and switch closures. Logic is fully DTL/TTL/CMOS compatible.
- 1.3 **Channels** Ten switched channels with electrically isolated closures for HI, LO and GUARD of each channel.
- 1.4 **Amplification** Integral low-noise, low-drift amplifier provides gains from 20 to 2500 for selected channel.
- 1.5 **Input Configurations** Can be installed to function in guarded or shielded differential configurations. Note: the OM102 has noise guarding —not just leakage guarding.
- 1.6 **Calibration** Independent high resolution zero and span adjustments accessible through front cover.
- 1.7 **Control** Complete on-board logic. A single strobe signal (ENCODE) controls entry of channel and type select information. Internal logic guarantees break before make multiplexing and puts out FILTER ERROR flags for 1%, .1%, and .01% filter settling.
- 1.8 **Scan Rates** 16 channels/sec to 3 channels/sec depending on scan rate option ordered. Scan rate is largely determined by the settling time of the active filter; our (no-charge) standard is 6 channels/sec to 3 channels/sec. See also 4.4 and 4.5.
- 1.9 **Filter Active;** optimized for 60 Hz rejection.
- 1.10 **Zero Stabilization** AUTO-ICETM eliminates time-based zero drift.
- 1.11 **Wire Types** J, K, T, E, R, S, and B; others special order.
- 1.12 **Options** Special Gain, Dual Gain, Dual Wire Type, Fast Scan, and Very Fast Scan. See Section 4 "Options."
- 1.13 **Reliability** 8 years MTBF for electronics. 50 hour burn-in for unit 500 hour burn-in for selected parts.

**2. MECHANICAL**

- 2.1 **Overall Dimensions** ( $\pm .02"$ ) 6.25" (158.8mm) W x 9.50" (241.3mm) L x .97" (25.4mm) T, including card ejectors.
- 2.2 **Thermocouple Wire Attachment** Heavy-duty terminals accommodate up to 14 AWG thermocouple wire.
- 2.3 **Mechanical Mounting** Into standard 19" rack, spaced laterally on 1" centers and vertically for standard 6.25" width.

**3. ELECTRONIC**

- 3.1 **Calibrated Accuracy** (Includes all applicable items below, including allowances for 3.10, 3.13, 3.14, 3.15) Conservatively rated: after 1 hour stabilization and without AUTO-ICETM corrections applied within  $\pm .03\%$  RDG  $\pm 9$  microvolts for a period of 24 hours at 25C  $\pm 3C$  ambient variation at 15 volts  $\pm .5$  volt supply variation at 100% relay duty cycle. Guaranteed by factory temperature and time tests.
- 3.2 **Normal Mode Rejection** 60 db at 60 Hz with standard scan speed, plus A/D converter rejection.
- 3.3 **Common Mode Rejection** Greater than 100 db at 60 Hz with 1K input lead imbalance, plus normal mode rejection of A/D converter.
- 3.4 **Common Mode Range, Selected Channel** Typically 310 VDC or 220 VAC RMS when used in guarded configuration.  $\pm 12$  VDC or 8.5 VAC RMS in grounded configuration.
- 3.5 **Interchannel Common Mode Difference** 310 VDC difference or VAC peak difference.
- 3.6 **Input Signal Range** 100 mv or 10w/gain, whichever is less.
- 3.7 **Continuous Input Overload** 117 VAC RMS between HI & LO of any channel without damage or subsequent derating.
- 3.8 **Interchannel Dielectric Isolation** Greater than 1000 megohms at 310 VDC or VAC peak.
- 3.9 **Isolation to Ground** Depending on customer installation and guarding arrangements, typically 100 megohms for 310 VDC or VAC peak common-mode.

- 3.10 **Overall Noise** Less than 1.5 microvolts peak-to-peak (PTP) jitter from 1 Hz to 10 Hz, RTI.
- 3.11 **Zero Adjustment Range** Guaranteed settability to .1F or C for base metals and .2F or C for noble metals.
- 3.12 **Span Adjustment Range** The OM102 is internally trimmed at the factory to nominal gain. An additional customer span adjustment of  $\pm 1\%$  F.S. is provided.
- 3.13 **Ambient Temperature Effects**
  - 3.13.1 **Zero Reference Junction:** Within .04C/C for 25C  $\pm 20C$ , including wire nonlinearity.  
Input: Within .5 microvolts/C for 25C  $\pm 20C$  with AUTO-ICETM. Within 2.0 microvolts/C for 25C  $\pm 20C$  at standard gain without AUTO-ICETM.
  - 3.13.2 **Gain** .005% RDG/C for 25C  $\pm 20C$  with standard gain.
- 3.14 **Time Stability**
  - 3.14.1 **Zero** No drift with AUTO-ICETM activated. 10 microvolts/month typical without activation.
  - 3.14.2 **Gain** Within .02%/1000 hours. Within .04%/year.
- 3.15 **Thermoelectric Offsets in Multiplexer** Less than 6 microvolts at 100% duty cycle. Typically 2 microvolts.
- 3.16 **Relay Cycle Life** Designed for sequential scan of 10 channels at 4 channels/sec for 8 years.
- 3.17 **Analog Output Voltage Range**  $\pm 10$  volts min. at 1.6 mA delivery.
- 3.18 **Analog Output Protection** 30 VDC or VAC pk continuous, and static discharge protected.
- 3.19 **Analog Output Slew Rate** Tracks input thermocouple temperature gradients of 5 deg/sec with lag error less than .2 degree for any wire type.
- 3.20 **Analog Output Multiplexing** Internal output mux. switch allows parallel busing of up to 50 OM102's.
- 3.21 **Analog Output Impedance** Less than .1 ohm on-line. Greater than 100 megohms off-line.
- 3.22 **Power Required, Analog** + 15V  $\pm .5V$  at 40 mA max, -15V  $\pm .5V$  at 40 mA max.
- 3.23 **Power Required, Digital** +5V (Vcc or Vdd) or +10V to +15V (Vdd) at 130 mA max.
- 3.24 **Digital Inputs** Fully DTL/TTL/CMOS compatible. Inputs have additional protection for static discharge.
- 3.25 **Digital Outputs** Collector "ANDS" with internal pullups. Bus limit is 20 OM102's Fan-out: 5 normal loads unbussed, 1 normal load with 20 OM102's bussed.
- 3.26 **Self-Induced Digital Crosstalk Into Analog Circuitry** None. "Dead clock" synchronous logic.
- 3.27 **Input Impedance** Greater than 34 megohms.

**4. OPTIONS**

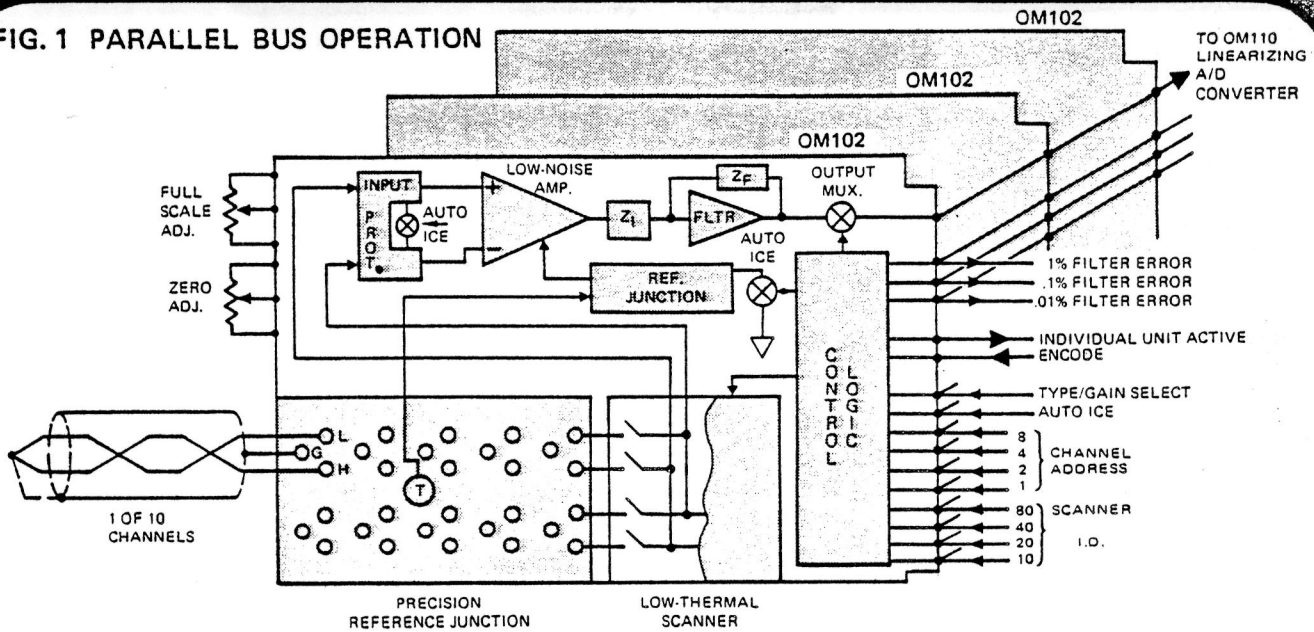
- 4.1 **Option 1 Single Special Gain** A D.C. gain of 100.0 is standard. \$80
- 4.2 **Option 2 Dual Type** The OM102 can be ordered to automatically compensate any combination of any two thermocouple wire types, or any wire type with "no" type (i.e. reference switched out), or two "no" types. Wire type is selected by type signal. \$70
- 4.3 **Option 3 Fast Scan** A faster settling filter with less noise rejection (-36db at 60 Hz) is substituted to achieve scan rates from 4.5 channels/sec to 9 channels/sec. All filter error flags are rescaled. \$25
- 4.4 **Option 4 Very Fast Scan** A "light" filter with -24 db rejection at 60 Hz is substituted to achieve scan rates from 8 ch/sec to 16 ch/sec. All filter error flags are rescaled. \$25
- 4.5 **Option Combinations** Allowable combinations are: 1-2, 1-3, 1-4, 1-2-3, 1-2-4, 2-3, 2-4.

**5. ACCESSORIES**

- 5.1 **Guard Plane OM901** Guard Plane. A 6.25"W x 9.75"L rack-mounted guard plane for driven guard applications. Guards OM102 units installed adjacent to lateral card rack faces.

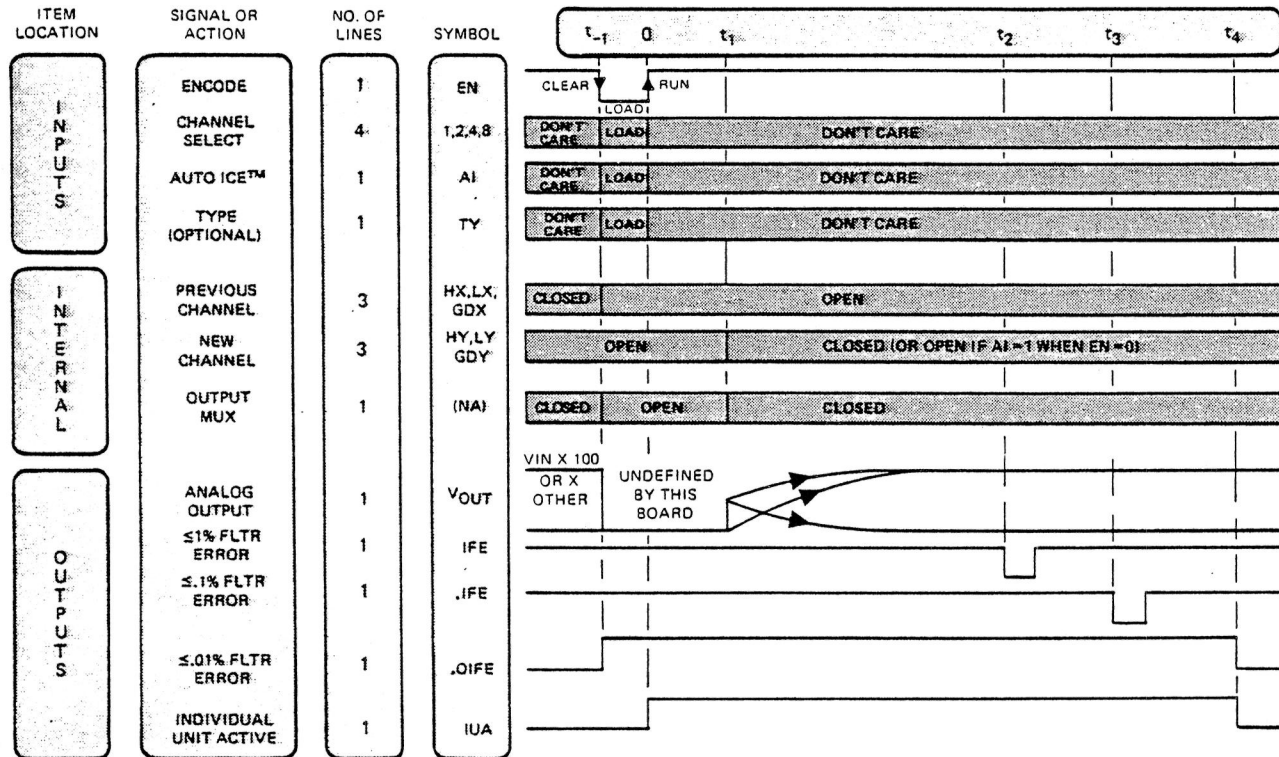
**NEW!**

FIG. 1 PARALLEL BUS OPERATION



OM102 TIMING DIAGRAM

NOTE:  $V_{OUT}$  and each digital output shown below except Individual Unit Active (IUA) can be directly bussed with up to 20 of its corresponding companions on other OM102 cards.



INTERVAL

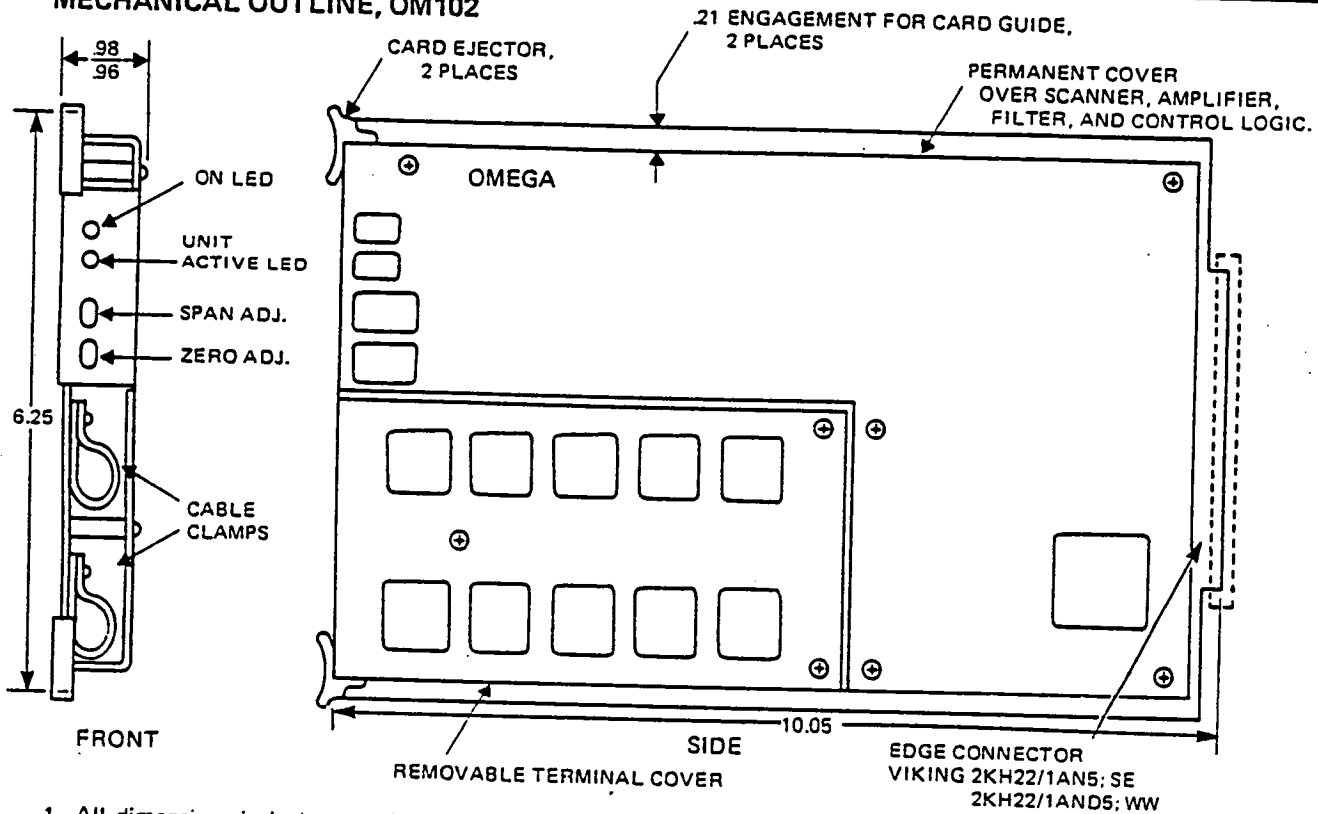
- $t_{-1}$  Interval  $t_{-1}$ , the load interval, is the elapsed time that EN is held low. Encoded channel selections may be interrupted or cancelled at any time and the unit initialized by taking EN low.  $t_{-1}$  can be as short as 5 microsec or indefinitely long, the later, holding the unit "off-line".
- $t_1$  Guaranteed break-before-make interval. 3.4 msec to 17.7 msec depending on scan speed option.

INTERVAL

- $t_2$  Marking edge for ≤1% filter error. 30.3 msec to 159 msec depending on scan speed option.
- $t_3$  Marking edge for ≤.1% filter error. 43.8 msec to 229 msec.
- $t_4$  Marking edge for ≤.01% filter error. 57.2 msec to 300 msec.

**NEW!**

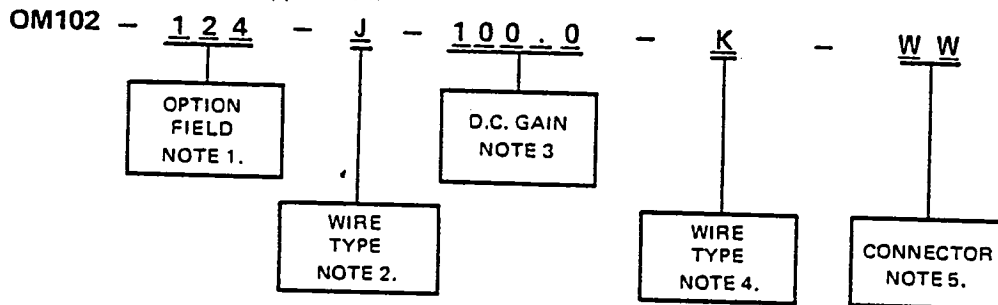
## MECHANICAL OUTLINE, OM102



1. All dimensions in inches and (rounded mm).
2. Tolerances unless otherwise noted are  $\pm 0.02$  inch ( $\pm 0.5$  mm).

## ORDERING YOUR OM102

Read the Options section in the Performance Specifications – the OM102 comes with so many options you can very likely tailor it to exactly your application.



- NOTES:
1. Specify all options desired in this three-space field. Consult table of allowable combinations in Option section. Put numbers in increasing order. Put "X" (no entry) where no numbers are used.
  2. This is the thermocouple wire type desired to which the reference junction will be configured. When ordering Option 2, Dual Type, this is the type that will be selected when TY signal is low. Specify J, K, T, E, R, S, B, X = no type, Z = special type per Remarks.
  3. This is the D.C. gain of the instrumentation amplifier associated with the wire type in Note 2. Gains may be anywhere from 10.00 to 1000. Include decimal point and four digits. "100.0" is the no-charge standard.
  4. Place an "X" here when ordering only one wire type, as already specified in Item 2. Specify as before when ordering Option 2, Dual Type. This is the reference junction compensation that will be activated when TY signal is high.
  5. Connector termination choice: WW = .025" x .056" wire wrap pins, SE = solder eyelets. SP designates special and specify in "Remarks".

APPENDIX B

LIQUID PROPELLANT REORIENTATION  
VELOCITY INCREMENTS

A CLOSED-FORM METHOD OF SOLUTION

Professor T. E. Bowman  
Florida Institute of Technology



The development below is based on the work of Irving E. Sumner published in NASA TM-78969, July 1978. It was prepared by Dr. Thomas E. Bowman to confirm the range of Bond numbers to be investigated in the experimental program. The closed-form solution confirmed the results of Sumner for similar fill conditions and fluid dynamic behavior.

### STEP 1

Express all times in terms of  $a_L$ , using

$$V'_L = \sqrt{2 (\ell_i + R_T) a_L} \quad \text{(A8) from TM-78969}$$

Then we have

$$t_1 = \frac{2\sqrt{\ell_i}}{\sqrt{2 a_L}} = \sqrt{2 \ell_i / a_L}$$

$$t_2 = \frac{2 (\ell_i + R_T) [\sqrt{\ell_i + R_T} - \sqrt{\ell_i}]}{\sqrt{2 (\ell_i + R_T) a_L} \sqrt{\ell_i + R_T}} = \sqrt{2} \left( \frac{\sqrt{\ell_i + R_T} - \sqrt{\ell_i}}{\sqrt{a_L}} \right)$$

$$t_1 + t_2 = \sqrt{\frac{2 (\ell_i + R_T)}{a_L}}$$

$$t_3 = 0.0516 \text{ Bo} \left( \frac{2 (\ell_i + R_T) a_L R_T}{\beta} \right) \sqrt{R_T^3 / \beta}$$

$$= 0.1032 \text{ Bo} (\ell_i + R_T) a_L \sqrt{R_T^5 / \beta^3}$$

$$t_4 = 2.76 \frac{\ell_c - \ell_i}{\sqrt{2 a_L R_T}}$$

using  $\ell_c = 2R_T (FR - 1)$  from (A1 of TM-78969) gives

$$t_4 = 3.90 \left( FR - 1 - \frac{\ell_i}{2 R_T} \right) \sqrt{R_T / a_L}$$

$$t_5 = 2 \left( \frac{l_i + R_T}{\sqrt{2 (l_i + R_T) a_L}} \right)$$

where  $l_j = l_i + (2/3) R_T$

$$\therefore t_5 = \sqrt{2} \left( \frac{l_i + (5/3) R_T}{\sqrt{(l_i + R_T) a_L}} \right)$$

All the above equations assume  $l_i > 0$  and  $V_L^2 R_T / \beta > 4$ . If  $l_i$  does not exist, then the following equations apply

$$t_1 + t_2 = 0$$

$$t_3 = 0.1032 B_0 R_T a_L \sqrt{R_T^5 / \beta^3}$$

$$t_4 = 5.51 \left( \frac{R_T FR - R_0}{\sqrt{2 R_T a_L}} \right) = 3.90 (FR - R_0/R_T) \sqrt{R_T/a_L}$$

$$t_5 = \sqrt{2} \left( \frac{l_i + (5/3) R_T}{\sqrt{R_T a_L}} \right)$$

(Note that in the last equation the numerator retains the negative value of  $l_i$  calculated from (A3 of TM-78969) -- see calculation of LJ and T5 in computer program, page 22, lower part, TM-78969).

The limit on  $t_3$  in terms of  $a_L$  is

$$a_L > \frac{2 \beta}{R_T (l_i + R_T)} \quad \text{if } l_i > 0$$

$$a_L > 2 \beta / R_T^2 \quad \text{otherwise}$$

and if  $a_L$  is smaller than this value,  $t_3 = 0$ .

## STEP 2

Write the equations for  $t_T$

$$t_1 + t_2 + t_3 = 1.414 \sqrt{(\ell_i/R_T) + 1} \sqrt{R_T/a_L} + 0.1032 \text{ Bo} \left( \frac{\ell_i}{R_T} + 1 \right) \\ \times \left( \frac{a_L}{R_T} \right) \left( \frac{R_T^3}{\beta} \right)^{3/2}$$

if  $\ell_i > 0$ , and  $a_L > 2\beta / [R_T(\ell_i + R_T)]$ .

$$t_1 + t_2 + t_3 = 0.1032 \text{ Bo} (a_L/R_T) (R_T^3/\beta)^{3/2}$$

if  $\ell_i < 0$ , and  $a_L < 2\beta/R_T^2$ .

$$t_1 + t_2 + t_3 = 1.414 \sqrt{(\ell_i/R_T) + 1} \sqrt{R_T/a_L}$$

if  $\ell_i > 0$ , and  $a_L < 2\beta/R_T (\ell_i + R_T)$

$$t_1 + t_2 + t_3 = 0$$

if  $\ell_i < 0$ , and  $a_L < 2\beta/R_T^2$ .

$$t_4 + t_5 = \left[ 3.90 \left( \text{FR} - 1 - \frac{\ell_i}{2R_T} \right) + \frac{\sqrt{2} [(\ell_i/R_T) + (5/3)]}{\sqrt{(\ell_i/R_T) + 1}} \right] \sqrt{R_T/a_L}$$

if  $\ell_i > 0$ .

$$t_4 + t_5 = \left[ 3.90 \left( \text{FR} - \frac{R_o}{R_T} \right) + \sqrt{2} \left( \frac{\ell_i}{R_T} + \frac{5}{3} \right) \right] \sqrt{R_T/a_L}$$

if  $\ell_i < 0$ .

## STEP 3

Define a settling Weber number

$$\text{We} \equiv \Delta V_T^2 R_T/\beta = a_T^2 t_T^2 R_T/\beta$$

where  $t_T$  is given by one of the six equations above.

Then

$$We_S = (a_T^2 R_T^2 / a_L \beta) f$$

where

$$f = \left[ \sqrt{2 (\ell_i / R_T) + 1} + 0.1032 Bo \left( \frac{\ell_i}{R_T} + 1 \right) \left( \frac{a_L R_T^2}{\beta} \right)^{3/2} \right]^2$$

or

$$f = 0.01065 Bo^2 (a_L R_T^2 / \beta)^3$$

or

$$f = 2 (\ell_i / R_T + 1)$$

or

$$f = 0$$

or

$$f = \left[ 3.90 \left( FR - 1 - \frac{\ell_i}{R_T} \right) + \sqrt{2} \left( \frac{(\ell_i / R_T) + (5/3)}{\sqrt{(\ell_i / R_T) + 1}} \right) \right]^2$$

or

$$f = \left[ 3.90 \left( FR - (R_o / R_T) \right) + \sqrt{2} \left( \frac{\ell_i}{R_T} + \frac{5}{3} \right) \right]^2$$

respectively.

#### STEP 4

Re-write (A22 from TM-78969) in terms of Bond number

$$V_o = 0.48 \sqrt{Bo \beta / R_T} \left[ 1 - (84/Bo)^{Bo/4.7} \right]$$

#### STEP 5

Combine this equation with (A13 from TM-78969) to get  $a_L$  in terms of Bo

$$a_L = 3.8 V_o^2 / R_T = 0.8755 (Bo \beta / R_T^2) \left[ 1 - (0.84/Bo)^{Bo/4.7} \right]^2$$

and substitute into the equations for  $We_s$

$$\begin{aligned} We_s &= (a_L^2 R_T^4 / 0.8755 Bo \beta^2) \left[ 1 - (0.84/Bo)^{Bo/4.7} \right]^{-2} f \\ &= (Bo/0.8755) \left[ 1 - (0.84/Bo)^{Bo/4.7} \right]^{-2} f \end{aligned}$$

where in the first two equations for  $f$  we now have

$$(a_L R_T^2 / \beta) = 0.8755 Bo \left[ 1 - (0.84/Bo)^{Bo/4.7} \right]^2$$

and the criterion on  $a_L$  becomes a Bond number criterion

$$a_L > \frac{2\beta}{R_T (\ell_i + R_T)} \implies Bo \left[ 1 - (0.84/Bo)^{Bo/4.7} \right]^2 > \frac{2.28}{[(\ell_i/R_T) + 1]}$$

$$a_L > \frac{2\beta}{R_T} \implies Bo \left[ 1 - (0.84/Bo)^{Bo/4.7} \right]^2 > 2.28$$

### SUMMATION

We can now look at two curves of  $We_s$  versus  $Bo$ , one corresponding to  $(t_1 + t_2 + t_3)$  (curve a), and one to  $(t_4 + t_5)$  (curve b), for each of the cases of interest, as follows:

If  $\ell_i > 0$

$$(We_s)_a = \left[ \sqrt{2} \sqrt{(\ell_i/R_T) + 1} + 0.0845 [(\ell_i/R_T) + 1] Bo^{5/2} B_1^3 \right] \left( \frac{Bo}{0.8755 B_1^2} \right)$$

if  $Bo B_1^2 > 2.28 / [(\ell_i/R_T) + 1]$ ,

or

$$(We_s)_a = 2.28 [(\ell_i/R_T) + 1] Bo B_1^{-2}$$

if  $Bo B_1^2 < 2.28 / [(\ell_i/R_T) + 1]$ ,

and

$$(We_s)_b = \left[ 3.90 \left( FR - 1 - \frac{\ell_i}{2R_T} \right) + \sqrt{2} \left( \frac{(\ell_i/R_T) + (5/3)}{\sqrt{(\ell_i/R_T) + 1}} \right) \right]^2 \left( \frac{Bo}{0.8755 B_1^2} \right)$$

If  $l_i < 0$

$$(We_s)_a = 0.00816 Bo^6 B_1^4$$

if  $Bo B_1^2 > 2.28$ , or

$$(We_s)_a = 0$$

if  $Bo B_1^2 < 2.28$ ,

and

$$(We_s)_b = \left[ 3.90 (FR - R_o/R_T) + \sqrt{2} \left( \frac{l_i}{R_T} + \frac{5}{3} \right) \right]^2 \left( \frac{Bo}{0.8755 B_1^2} \right)$$

where

$$B_1 = 1 - (0.84/Bo)^{Bo/4.7}$$

$$l_i/R_T = -4/3 \left[ 1 - (R_o/R_T)^3 \right]$$

in the last equation.

## RESULTS

These equations were solved on a programmable hand calculator to get sets of values of  $(We_s)_a$  and  $(We_s)_b$  for various values of the two parameters  $l_i$  and  $Bo$ , settling the fineness ratio  $FR = 2$  where necessary. Calculations for  $FR = 4$  have not been carried out yet. These results are valid for all values of fluid properties and tank diameters, and incorporate all of the various curves included in the back of TM-78969.

$l_i/R_T$	Bond Number								
	2	3	4	5	6	7	8	9	10
2.0	143.57	108.47	271.96	983.4	3178.0	8543	19,700	40,500	76,400
1.67	127.78	94.18	226.73	799.58	2555.0	6830	15,700	32,200	60,800
1.33	111.51	51.50	183.70	628.79	1981.5	5262	12,057	24,700	46,500
1.0	95.72	44.21	145.48	481.25	1492.0	3930	8,970	18,300	34,400
0.67	79.92	36.92	110.87	351.97	1069.5	2790	6,331	12,900	24,200
0.33	63.65	29.40	79.14	238.22	704.66	1813.5	4,085	8,279	15,500
0.0	47.86	22.10	16.88	147.21	420.0	1061	2,365	4,764	8,871

Settling Weber Number based on  $(t_1 + t_2 + t_3)$

	Bond Number								
	2	3	4	5	6	7	8	9	10
$l_i/R_T = 2.0$	214.89	99.25	75.79	70.83	72.77	78.17	85.55	94.13	103.44
1.67	298.98	138.09	105.45	98.55	101.25	108.76	119.03	130.97	143.91
1.33	399.66	184.60	140.96	131.74	135.35	145.38	159.11	175.07	192.38
1.0	511.00	236.02	180.23	168.44	173.05	185.88	203.44	223.85	245.97
0.67	636.04	293.78	224.33	209.66	215.40	231.37	253.22	278.62	306.16
0.33	780.31	360.42	275.22	257.22	264.26	283.85	310.66	341.82	375.60
$l_i/R_T = 0.0$ $R_o/R_T = 1.0$ }	938.64	433.55	331.06	309.41	317.88	341.44	373.69	411.18	451.81
0.8	897.05	414.34	316.39	295.70	303.79	326.31	357.14	392.96	431.79
0.6	963.30	444.94	339.76	317.54	326.23	350.41	383.51	421.98	463.68
0.4	1119	516.90	394.71	368.89	378.99	407.09	445.54	490.23	538.68
0.2	1351	624.0	476.48	445.32	457.51	491.42	537.8	591.8	650.3

Settling Weber Numbers based on  $(t_4 + t_5)$  for FR = 2

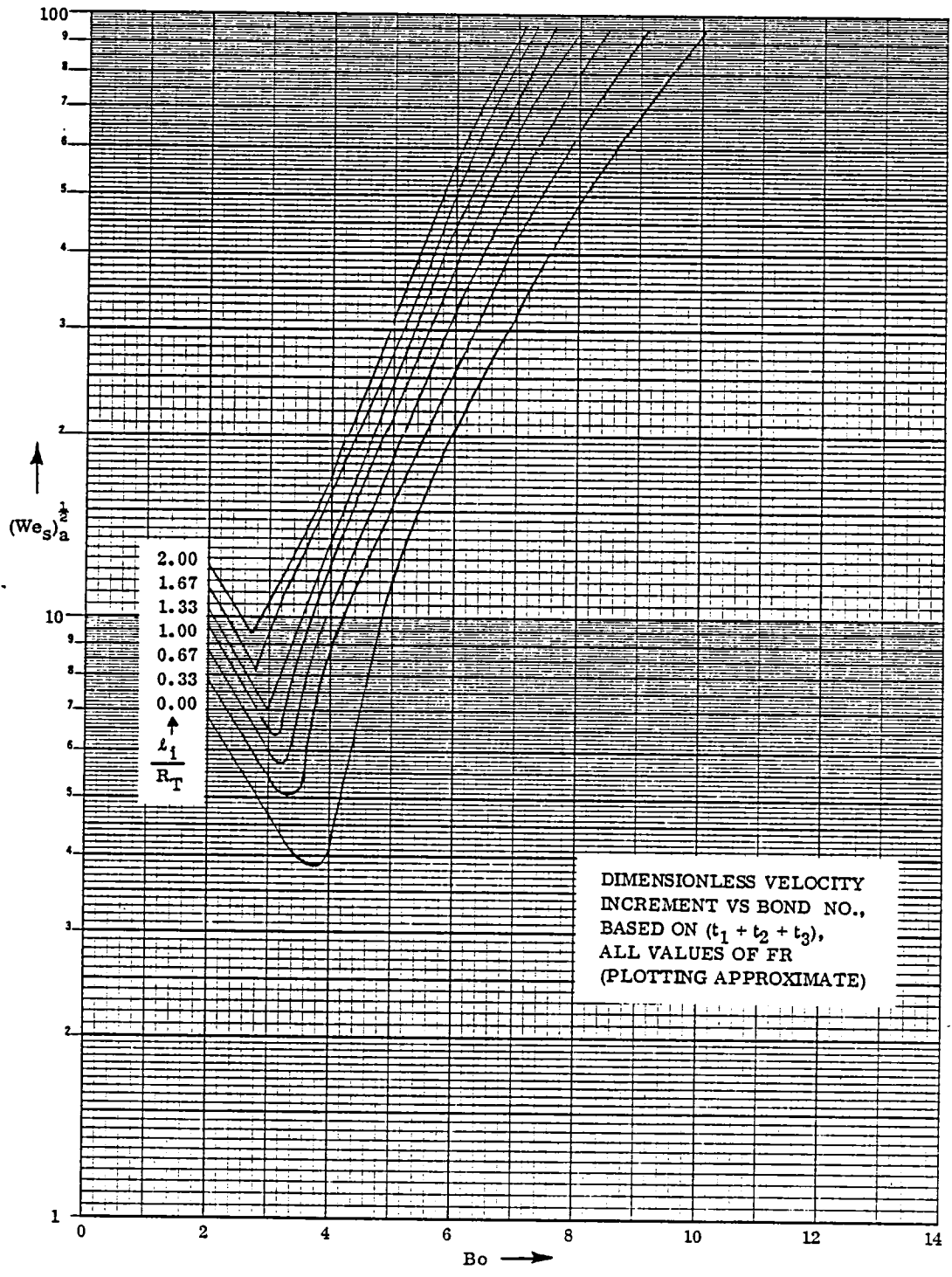
Note: The relationship between Fill Level (FL) and  $l_i$  for FR = 2 is:

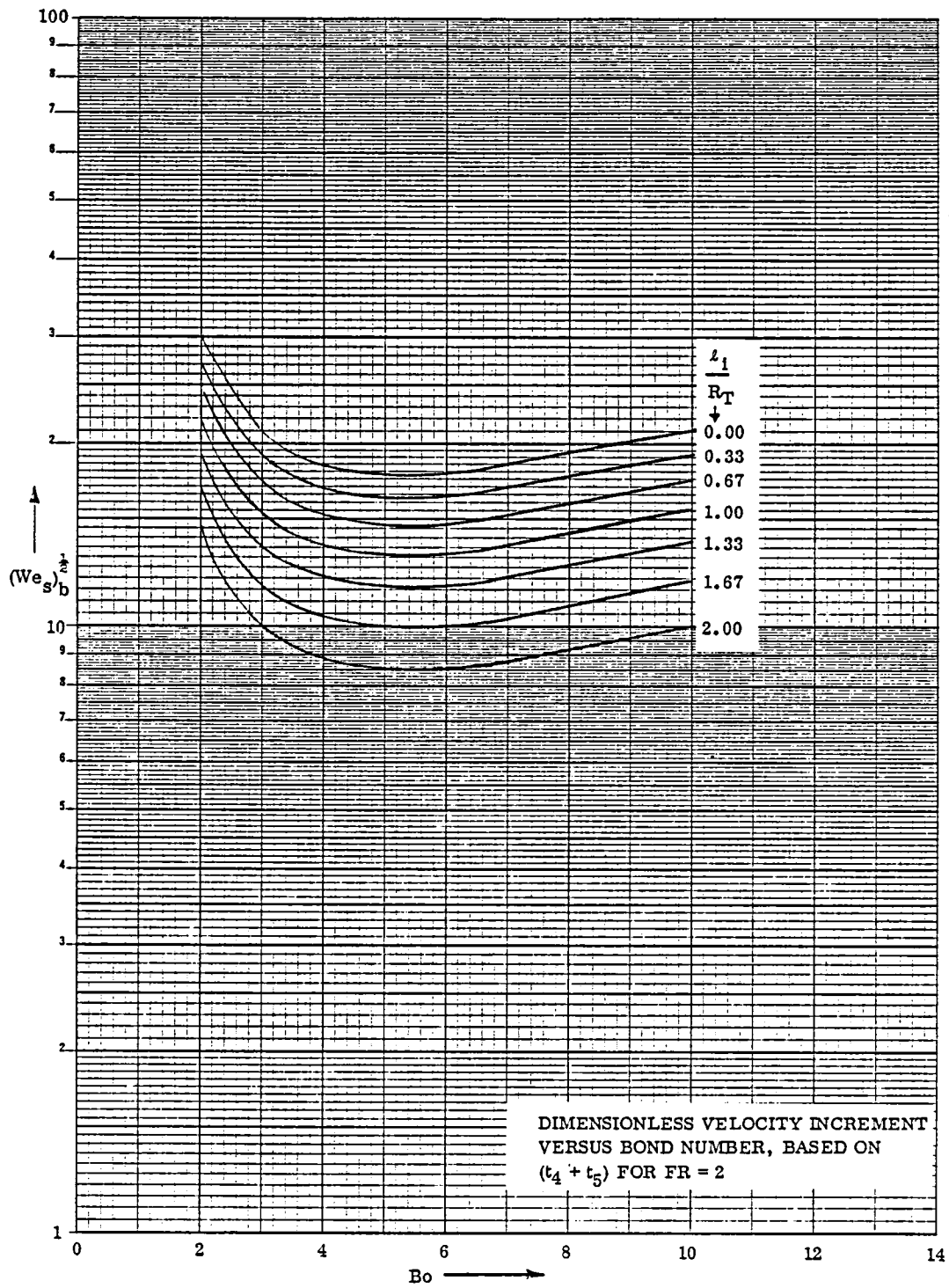
$l_i/R_T$	2.00	1.67	1.33	1.00	0.67	0.33	0.00
FL	0.0	0.1	0.2	0.3	0.4	0.5	0.6

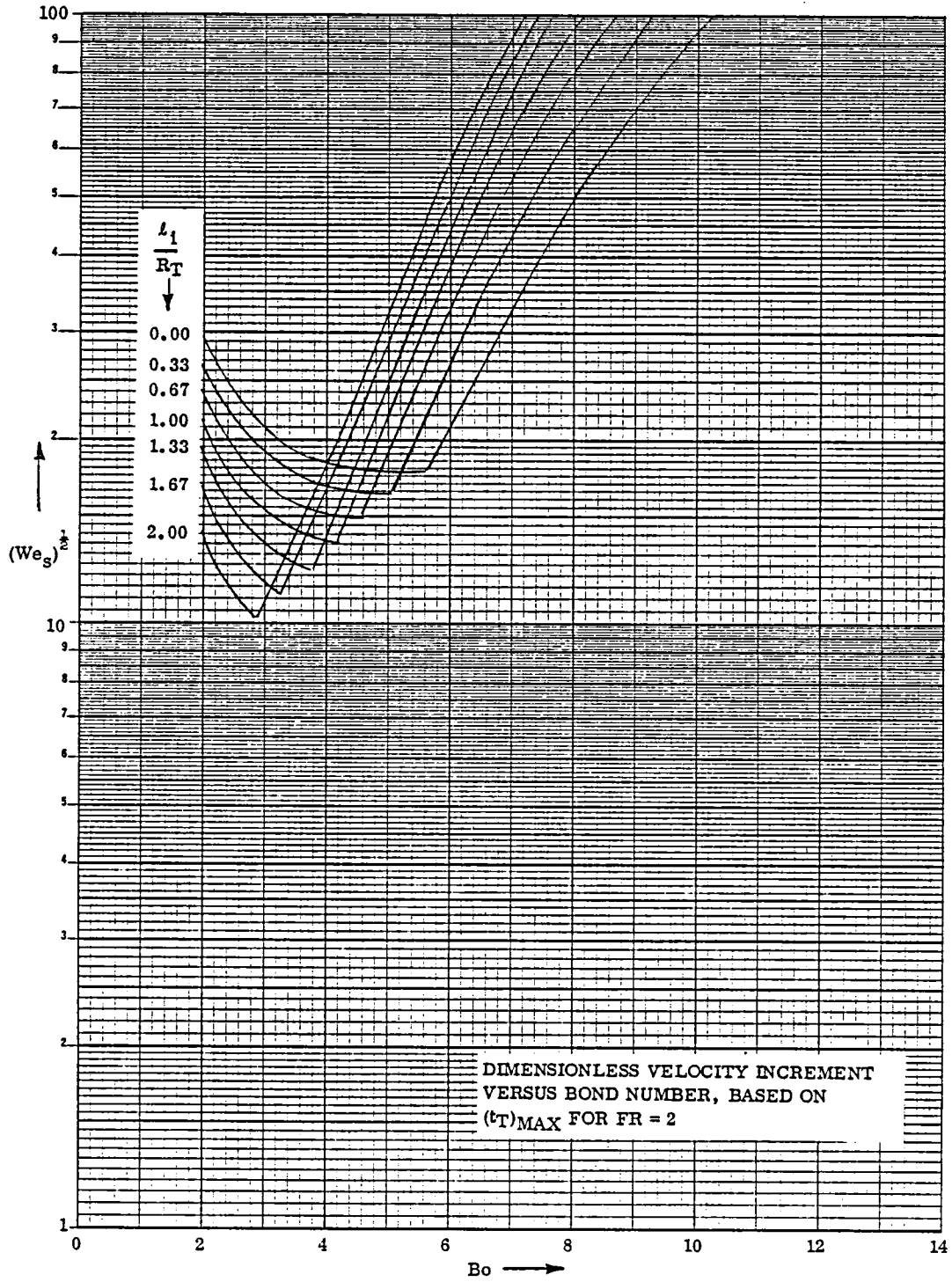
These curves are plotted on pages B-10 and B-11, and on Page B-12 they are combined to produce plots of the larger of the two values of  $We_s$ , comparable to Figures 6a, 6b, 6c, 8 and 13 of TM-78969. Note that all five of these sets of curves (and any others that might be generated for FR = 2) are all included in the single set of curves presented here on Page B-12. For the sake of the more direct comparison with the velocity-increment curves,  $We_s^{\frac{1}{2}}$  was plotted rather than Weber number itself.

## CONCLUSIONS

1. The optimum Bond number for "settling-to-clear-the-vent" (case b) is approximately 5.1 regardless of any other considerations: all values of fluid properties, tank diameter, fineness ratio, etc., and regardless of whether  $t_5$  is considered important or not. Values of velocity increment depend on these parameters, but not location of the minimum.
2. The optimum Bond number for "settling-to-flood-the-drain" (case a) varies between 2 and 4 for FR = 2, as fill level varies between zero (lowest optimum Bond number and highest minimum velocity increment) and 60 percent. Calculations for other FR values have not been carried out yet. This conclusion is strongly dependent on the relationship between  $t_3$  and  $Bo$ , since  $t_3$  is assumed to be a very strong function of  $Bo$  for small values of  $Bo$ ; further experimental data may change this conclusion significantly.







3. In cases where fill level is such that the ullage space is a large bubble (the liquid-vapor interface has no "leading edge,") settling-to-flood-the-drain amounts to simply moving the bubble away from the end of the tank. This case has not been studied yet, and certainly deserves further consideration.
4. If settling is defined as the accomplishment of all four of the following:
  - a. flooding the drain
  - b. subsidence of any geyser
  - c. clearing the vent
  - d. drying the walls

then the curves are closely similar to those of TM-78969, with optimum Bond numbers between 3 and 5.1, and again being strongly dependent on the tenuous assumption regarding  $t_3$ .

5. Regardless of all other considerations and uncertainties, I don't at the moment see any way that we could ever have an optimum Bond number greater than 5.1.



APPENDIX C

DISTRIBUTION LIST  
CONTRACT NAS3-21750

	<u>No. of Copies</u>		<u>No. of Copies</u>
National Aeronautics and Space Adm. Lewis Research Center 21000 Brookpark Road Cleveland, OH 44135		National Aeronautics and Space Adm. Johnson Space Center Houston, TX 77001	
Attn: Contracting Officer, MS 500-306	1	Attn: Library	1
E. A. Bourke, MS 501-5	2	EP2/Z. D. Kirkland	1
Technical Utilization Office, MS 7-3	1	EP5/W. Chandler	1
Technical Report Control Office, MS 5-5	1	EP4/Dale Connelly	1
AFSC Liaison Office, MS 501-3	2	PD13/James Thompson	1
Library, MS 60-3	2		
Office of Reliability & Quality Assurance, MS 500-211	1	National Aeronautics and Space Adm. George C. Marshall Space Flight Center Huntsville, AL 35812	
E. P. Symons, Project Mgr, MS 501-8	20	Attn: Library	1
T. H. Cochran, MS 501-8	1	EP43/L. Hastings	1
E. J. Domino, MS 501-8	1	EP43/A. L. Worlund	1
J. C. Aydelott, MS 501-8	1	EP45/Dr. Wayne Littles	1
E. W. Kroeger, MS 501-8	1	EP24/G. M. Chandler	1
Patent Counsel, MS 500-318	1	ES63/E. W. Urban	1
National Aeronautics and Space Adm. Headquarters Washington, DC 20546		Jet Propulsion Laboratory 4800 Oak Grove Drive Pasadena, CA 91103	
Attn: RS-5/Director, Space Systems Division	1	Attn: Library	1
RTS-6/Director, Research & Tech. Div.	1	Don Young, MS 125-224	1
RTP-6/F. W. Stephenson	1		
MHE-7/P. N. Herr	1	NASA Scientific & Technical Information Facility P.O. Box 8757 Baltimore/Washington International Airport, MD 21240	
RST-5/E. Gabris	1	Attn: Accessioning Department	10
National Aeronautics and Space Adm. Goddard Space Flight Center Greenbelt, MD 20771		Defense Documentation Center Cameron Station - Bldg. 5 5010 Duke Street Alexandria, VA 22314	
Attn: Library	1	Attn: TISIA	1
A. Sherman, MS 713	1		
National Aeronautics and Space Adm. John F. Kennedy Space Center Kennedy Space Center, FL 32899		National Aeronautics and Space Adm. Flight Research Center P.O. Box 273 Edwards, CA 93523	
Attn: Library	1	Attn: Library	1
DD-MED-41/F. S. Howard	1		
DE-A/W. H. Boggs	1		
National Aeronautics and Space Adm. Ames Research Center Moffett Field, CA 94035		Air Force Rocket Propulsion Laboratory Edwards, CA 93523	
Attn: Library	1	Attn: LKCC/J. E. Brannigan	1
J. Vorreiter, MS 244-7	1	LKDS/R. L. Wiswell	1
National Aeronautics and Space Adm. Langley Research Center Hampton, VA 23365		Aeronautical Systems Division Air Force Systems Command Wright Patterson Air Force Base Dayton, OH 45433	
Attn: Library	1	Attn: Library	1

	<u>No. of Copies</u>		<u>No. of Copies</u>
Air Force Office of Scientific Research Washington, DC 20333 Attn: Library	1	Martin-Marietta Corporation Denver Division P.O. Box 179 Denver, CO 80201 Attn: Library	1
Aerospace Corporation 2400 E. El Segundo Blvd. Los Angeles, CA 90045 Attn: Library - Documents	1	D. Fester	1
Beech Aircraft Corporation Boulder Facility Box 9631 Boulder, CO 80301 Attn: Library	1	J. Tegart	1
R. A. Mohling	1	R. Eberhardt	1
Bell Aerosystems, Inc. Box 1 Buffalo, NY 14240 Attn: Library	1	R. Dergance	1
J. Colt	1	Rockwell International Corp. Space Division 12214 Lakewood Blvd. Downey, CA 90241 Attn: Library	1
Boeing Company P.O. Box 3999 Seattle, WA 98124 Attn: Library	1	A. Jones	1
C. L. Wilkensen, MS 8K/31	1	Northrop Research and Technology Center 1 Research Park Palos Verdes Peninsula, CA 90274 Attn: Library	1
Chrysler Corporation Space Division P.O. Box 29200 New Orleans, LA 70129 Attn: Library	1	TRW Systems, Inc. 1 Space Park Redondo Beach, CA 90278 Attn: Tech. Lib. Doc. Acquisitions	1
McDonnell Douglas Astronautics Co. 5301 Balsa Avenue Huntington Beach, CA 92647 Attn: Library	1	National Science Foundation, Engr. Div. 1800 G. Street, NW Washington, DC 20540 Attn: Library	1
E. C. Cady	1	Florida Institute of Technology M. E. Department Melbourne, FL 32901 Attn: Dr. T. E. Bowmann	1
Missiles and Space Systems Center General Electric Company Valley Forge Space Technology Center P.O. Box 8555 Philadelphia, PA 19101 Attn: Library	1	RCA/AED P.O. Box 800 Princeton, NJ 08540 Attn: Mr. Daniel Balzer	1
IIT Research Institute Technology Center Chicago, IL 60616 Attn: Library	1	Southwest Research Institute Department of Mechanical Sciences P.O. Drawer 28510 San Antonio, TX 78284 Attn: H. Norman Abramson Franklin Dodge	1
Lockheed Missiles and Space Company P.O. Box 504 Sunnyvale, CA 94087 Attn: Library	1	Tufts University Mechanical Engineering Dept. Medford, MA 02155 Attn: Dr. Lloyd Trefethen	1
G. D. Bizzell	1	McDonnell Douglas Astronautics Co. - East P.O. Box 516 St. Louis, MO 63166 Attn: G. Orton	1
S. G. DeBrock	1	W. Regnier	1

No. of Copies

Xerox Electro-Optical Systems  
300 North Halstead  
Pasadena, CA 91107  
Attn: Robert Richter

1

Science Applications, Inc.  
1200 Prospect Street  
P.O. Box 2351  
La Jolla, CA 92037  
Attn: M. H. Blatt

1

University of Kentucky  
Mechanical Engineering Department  
Lexington, KY 40506  
Attn: Dr. John H. Lienhard  
Dr. Robert E. Peck

1

1

University of Tennessee Space Institute  
Atmospheric Science Division  
Tullahoma, TN 37388  
Attn: Dr. Walter Frost

1

University of Michigan  
Heat Transfer and Thermodynamics Lab.  
Ann Arbor, MI 48107  
Attn: Dr. John A. Clark

1





**GENERAL DYNAMICS**  
*Convair Division*